



<https://theses.gla.ac.uk/>

Theses Digitisation:

<https://www.gla.ac.uk/myglasgow/research/enlighten/theses/digitisation/>

This is a digitised version of the original print thesis.

Copyright and moral rights for this work are retained by the author

A copy can be downloaded for personal non-commercial research or study,
without prior permission or charge

This work cannot be reproduced or quoted extensively from without first
obtaining permission in writing from the author

The content must not be changed in any way or sold commercially in any
format or medium without the formal permission of the author

When referring to this work, full bibliographic details including the author,
title, awarding institution and date of the thesis must be given

Enlighten: Theses

<https://theses.gla.ac.uk/>
research-enlighten@glasgow.ac.uk

**APPROXIMATE ANALYSIS OF
THREE-DIMENSIONAL TALL BUILDING STRUCTURES**

by

WANG HAO

A thesis presented for the degree of
Master of Science

Department of Civil Engineering
University of Glasgow
October 1991

© WANG HAO October 1991

ProQuest Number: 11008057

All rights reserved

INFORMATION TO ALL USERS

The quality of this reproduction is dependent upon the quality of the copy submitted.

In the unlikely event that the author did not send a complete manuscript and there are missing pages, these will be noted. Also, if material had to be removed, a note will indicate the deletion.



ProQuest 11008057

Published by ProQuest LLC (2018). Copyright of the Dissertation is held by the Author.

All rights reserved.

This work is protected against unauthorized copying under Title 17, United States Code
Microform Edition © ProQuest LLC.

ProQuest LLC.
789 East Eisenhower Parkway
P.O. Box 1346
Ann Arbor, MI 48106 – 1346

ACKNOWLEDGEMENTS

The author wishes to express his grateful thanks to his research Supervisor, Professor A. Coull, FICE, FStructE, FRSE, Regius Professor of Civil Engineering at the University of Glasgow, for his guidance and constant encouragement throughout the research study. The author's special thanks are due to Professor D. R. Green, FStructE, ex-Head of Department, for his allowing the use of the facilities in the Department, and his guidance in the related computing analysis. Special thanks are also due to Dr I. McConnochie for all the arrangements and help he made for the author during the research study, and to Miss J. Sutherland for her patient help to familiarizing the use of the computing facilities in the Department.

The author is grateful to Taiyuan University of Technology for giving the opportunity to pursue higher study abroad, and to the Educational Commission of Shanxi Province for providing the necessary financial support throughout his stay and study in the U.K.

The author wishes to thank all those colleagues and friends, who gave great help and encouragement to enable him to complete this work, with special mention of Mrs Bai Xiaohong, Dr Wei Meijiu and his wife Mrs Xue Xiaonian, and Mrs Leng Xiaoling.

Finally, the author emotionally expresses his gratefulness to his newly-married-and-separated wife, Mrs Wang Chen, for her support and sacrifice, without which this study would not have been concluded.

S Y N O P S I S

Simplified approximate methods are presented in this thesis for the analysis of three-dimensional tall building structures subjected to lateral loads. The structures considered may consist of parallel uniform high-rise bents such as planar rigid frames, plane shear walls, coupled shear walls and structural cores. The intention is to establish generalized rapid hand methods which are suitable for the structural analysis in the early design stages, and which can be used as overall checking guides for more sophisticated methods such as finite element analysis.

Based on the continuum technique, studies are made to investigate the modes of load-deformation behaviour of individual assemblies, and analyses are presented for the interactions between wall-frame assemblies and coupled shear wall structures. Inspections show that these different structural bents can be classified as a general family of cantilevers, and a revised wall-frame method is presented to characterize the mode of lateral load-deformation behaviour of such assemblies.

On using the revised wall-frame method and a spring supported rigid beam model, a generalized method is presented for the analysis of complete three-dimensional wall-frame structures subjected to bending and torsion actions. Solutions can be obtained from formulae-based calculations based on several representative structural parameters.

An area influence coefficient method is presented for the analysis of three-dimensional tall building structures subjected bending to and torsion. The interaction forces between different assemblies in a structure are assumed to be

represented sufficiently accurately by a combination of three load components. Having determined the modes of force-deformation behaviour of individual assemblies, the horizontal compatibility conditions are achieved by means of equating the top deflections, the areas under the deflected diagrams, and the first moments of areas about the base of the deflected diagrams. Used in conjunction with the horizontal force equilibrium conditions, sufficient equations are obtained to solve for the force distributions on the assemblies. The simplicity of the structure of the equations makes it possible to achieve a solution by a hand calculation, using a pocket calculator.

A number of numerical examples are carried out using the methods presented. The accuracy and the validity of the methods are assessed by comparing the results with those obtained from a finite element analysis.

WAGNER ENGINEERING

100-111 East Annapolis and University Streets

College Park, Maryland 20740

Telephone: (301) 405-1111

100-111 East Annapolis and University Streets
College Park, Maryland 20740

Digress

100-111 East Annapolis and University Streets

C O N T E N T S

ACKNOWLEDGEMENTS	i	
SYNOPSIS	ii	
CHAPTER 1	INTRODUCTION	
1.1	Development of Tall Building Structures	1
1.2	Objective and Reason For Present Study	3
1.3	Methods of Analysis and Review of Previous Research	5
1.4	Scope of the Thesis	11
1.5	The Use of the "FLASH" Program	11
	Figures	13
CHAPTER 2	ANALYSIS OF WALL- FRAME STRUCTURES (PART ONE)	
2.1	Introduction	14
2.2	Shear Walls, Cores and Rigid Frames	14
2.2.1	Shear Walls and Structural Cores	14
2.2.2	Rigid Frames	16
2.3	Interaction Between Shear Wall and Rigid Frames – Simple Wall- Frame Theory	18
2.3.1	Basic Assumptions and Governing Equations	18
2.3.2	Solutions For Standare Load Cases	19
2.3.3	Numerical Examples of Wall- Frame Structures	22
2.4	Modification of GA Parameter For Low- Rise Rigid Frames at the Ground Storey Level	24
	Figures	26
CHAPTER 3	ANALYSIS OF COUPLED SHEAR WALL STRUCTURES	
3.1	Introduction	34
3.2	Continuum Theory of Coupled Shear Walls	35
3.2.1	Introduction	35

3.2.2	Basic Assumptions	36
3.2.3	Governing Differential Equations and General Solutions	37
3.2.4	Boundary Conditions	39
3.2.5	Solutions For Uniformly Distributed Lateral Load	40
3.2.6	Study of Significant Parameters	42
3.3	Analysis of Interactions Between Coupled Shear Walls and Other Cantilevers	44
3.3.1	Analysis of Interaction Between Coupled Shear Walls and Flexural Cantilevers	44
3.3.2	Analysis of Interaction Between Two Pairs of Linked Coupled Shear Walls	46
3.3.3	Analysis of Interaction Between Coupled Shear Walls and Shear Cantilevers	53
3.4	Numerical Examples	59
	Figures	64
CHAPTER 4	ANALYSIS OF WALL-FRAME STRUCTURES (PART TWO)	
	- REVISED WALL-FRAME STRUCTURES	
4.1	Introduction	79
4.2	Basic Mathematical Model and Governing Equations	79
4.3	Boundary Conditions and Solutions For Uniformly Distributed Lateral Load	82
4.4	Structural Rigidity Parameters EI , GA and EI_f	86
4.5	Numerical Examples	87
4.6	Design Curves	88
4.7	The Present Method and the Continuum Theory of Coupled Shear Walls - A General Family of Wall-Frame Cantilever Structures	90
	Figures	93

CHAPTER 5	SIMPLIFIED ANALYSIS OF REGULAR THREE – DIMENSIONAL WALL– FRAME STRUCTURES SUBJECTED TO BENDING AND TORSION	
5.1	Introduction	101
5.2	Basic Assumptions	102
5.3	Analysis of Regular Symmetric Three– Dimensional Wall– Frame Structures Subjected Pure Bending	103
5.4	Analysis of Regular Three– Dimensional Wall– Frame Structures Subjected Bending and Torsion	107
5.4.1	Method of Analysis	107
5.4.2	Effective Rigidities – Method of Rigid Beam on Spring Supports	110
5.4.3	Special Case of Symmetrical Structures Subjected to Pure Bending Action	113
5.5	Analysis Procedure	114
5.6	Numerical Examples	115
	Figures	139
CHAPTER 6	AREA INFLUENCE COEFFICIENT ANALYSIS OF THREE– DIMENSIONAL WALL– FRAME STRUCTURES	
6.1	Introduction	187
6.2	Basic Assumptions	188
6.3	General Method of Analysis	189
6.4	Analysis of Interaction Between Two Linked Components	191
6.4.1	Method of Analysis	191
6.4.2	Area Influence Coefficients For Individual Assemblies	194
6.4.3	Compatibility and Equilibrium Equations in Matrix Form	198
6.4.4	Numerical Example of the Interaction Between Two Linked Assemblies	198

6.5	Analysis of Symmetric Three– Dimensional Wall– Frame Structures Subjected to Pure Bending	201
6.5.1	Method of Analysis	201
6.5.2	Compatibility and Equilibrium Equations In Matrix Forms	203
6.5.3	Numerical Examples	205
6.6	Analysis of Three– Dimensional Wall– Frame Structures Subjected to Bending and Torsion Actions	211
6.6.1	Method of Analysis	211
6.6.2	Numerical Example of Three– Dimensional Structure Subjected to Bending and Torsion Actions	221
6.7	Hand Calculation For Load Distributions	224
6.8	Convergence of Solution	227
	Figures	228
CHAPTER 7	CONCLUSIONS AND RECOMMENDATIONS FOR FUTURE WORK	
7.1	Conclusions	271
7.2	Recommendations For Future Work	273
REFERENCES		276
APPENDIX 1	SIMPLE WALL– FRAME THEORY	
	Solutions For Other Two Standard Load Cases	279
APPENDIX 2	CONTINUUM THEORY OF COUPLED SHEAR WALLS	
	Solutions For Other Two Standard Load Cases	281
APPENDIX 3	REVISED WALL– FRAME THEORY	
	Solutions For Other Two Standard Load Cases	284

CHAPTER 1

INTRODUCTION

1.1 Development of Tall Building Structures

The presence of tall buildings relates closely to the concept of the city. The appearance of high-rise building structures has become the most significant symbols for many modern cities from East to West, such as Tokyo and New York. In this 20th century, the socioeconomic developments, the rapid growth of population, and the scarcity and hence the high cost of land in urban areas, have demanded a considerable amount of construction of tall building structures especially in the industrialised countries. But this would not have been possible without the development of new higher strength and structurally more efficient materials, innovations in structural forms, and the introduction of the elevator to facilitate vertical transportation.

There would not be a general agreement on what constitutes tallness in a building, because to a large extent it will reflect the particular environment concerned and the particular attitude or discipline of the professional questioned. But from the structural engineer's point of view, a tall building may be defined as one in which the structural design is affected by the need to provide adequate resistance to lateral loads due to wind or earthquake, whereas a low-rise building is generally designed predominantly to resist gravitational loads. However as buildings must be designed to resist both horizontal as well as vertical forces, any optimum system sought for tall buildings is to minimise the influence of the former.

Since tall buildings became popular, engineers have sought for new

structural forms to allow heights to be increased. The rigid-jointed frame was initially the most popular structural form of construction for multi-storey buildings after the development of new structural materials. These new materials, namely wrought iron and subsequently steel, and later, reinforced concrete, overcame the major disadvantages of the two earlier traditional basic building materials, timber and masonry. The former lacked the strength required and always presented a fire hazard; the latter also lacked tensile strength and suffered from its high weight. The development allowed lightweight frames or skeletal structures to be built to much greater heights and with larger openings. The lateral stiffness of frame structures is obtained by the rigidity of the beam-column connections. This form of structure is normally considered to be economic for residential buildings up to about 20 to 25 storeys in height. Above this height, it tends to be difficult for the frame structure to develop adequate lateral stiffness requirements when the wind forces begin to control the design. Therefore, other structural forms have been introduced and adopted in tall buildings as structural elements providing greater lateral stiffness. They have been classified as shear walls or cores, coupled shear walls, wall-frames and the more advanced braced or tube systems. These structural elements, either singly or in combination, in conjunction with the floor systems, form varieties of tall building structural systems. Fig. 1.1 shows typical planforms of various forms of tall buildings. Each of these different systems, from the economic point of view, tends to give a suitable solution to a particular range of building heights. The selection of an appropriate system for a specific height of building may enable an engineer to utilize the building materials more efficiently and hence reduce the building costs. Frame structures may be suitable for buildings up to around 25 storeys as mentioned above. A system of shear walls, which may be solid or perforated, may be adopted for structures up to about 40 storeys in height, whereas a choice of shear walls interacting with frames may be employed in a structure built up to

about 70 storeys. Even higher buildings will need other forms, such as framed tube, tube-in-tube or braced tube structural systems. General guidelines have been presented by Khan (Ref. 1) to indicate the range of heights over which the various structural systems are most economically feasible in the United State.

1.2 Objective and Reason for Present Study

The purpose of a structural analysis is to determine the strength requirement for a building structure to resist both vertical and horizontal loadings, the former being the gravitational loads deriving from the self-weight of the structural components and the superimposed floor loadings, and the latter including wind pressure as well as earthquakes.

Before the development and the considerable amount of construction of high-rise building structures, low-rise structures were traditionally designed mainly to resist the gravitational loads which are always present and form the reason for its very existence, and the influences of wind or earthquake loads only checked subsequently, since most Building Design Codes allow some overstress due to the transient nature of such loads. However, as the buildings increase in height, such influences become progressively more and more important and must be taken into consideration in the design. Nowadays, high-rise structures must be designed not only to be able to resist vertical loads, but to meet adequate requirements both in strength and stiffness to resist lateral loads. This demands analyses for the responses of different structural systems subjected to lateral loadings, which, however, are usually more difficult to deal with than that of vertically loaded structures. This thesis, thus, describes an effort to provide methods of analysis for the three-dimensional tall building structures subjected to lateral loadings.

Since the development of computers and the application of the finite element method in the field of building structural analysis and design, many general purpose computing programs or packages have been made commercially available in design office which have saved considerable laborious work for engineers. This, however, requires the use of digital computers, and the computational costs are usually high. It tends to limit their application to the later or final stage of design, since it would be expensive to carry out detailed analyses at the preliminary stages of planning and proportioning of the load resisting elements. On the other hand, when using the finite element method to analyze a complex building structure, an appropriate model for the structure is crucial for obtaining a correct solution. It is therefore essential for an engineer to have a good understanding of the true behaviour of the structure. A good simplified hand method may then be helpful to be used in the early stage of design and as a checking model for those more precise analyses.

Although numerous approximate methods for the analysis of tall building structures subjected to lateral loadings have been published in recent years, many of which have found application in the design office, methods available for rapid hand calculation have generally been restricted to certain limited classes of structure, and have not been applicable to structures comprising more complex combinations of structural forms.

Therefore, methods of analysis which require as little computational work as possible and which may apply to the analysis of more complex full three-dimensional structures are highly desirable.

The present study is also concerned with discovering and demonstrating the

fundamental structural element characteristics and the inherent relationships between structural elements with different structural behaviours.

1.3 Methods of Analysis and Review of Previous Research

During the major developments in tall building construction, mainly in the recent three or four decades, a large number of methods for the analysis of tall building structures have been presented by many investigators. Many of these methods have found application for structural designers in the design office. The most important methods of analysis, however, can be divided into three fields, which are, the frame analogy, the finite element method, and the continuous connection technique.

As the rigid frame is the most fundamental structural form adopted in tall building structures, the analysis of frame structures thus has become a major part in building structural design. The arrangement of the stiffness method of analysis in matrix form allows a concise and systematic approach to the analysis of rigid frames by digital computation. The method provides the most flexible and powerful technique for the analysis of frame and associated structures and programs are commercially available which demand little more of the engineer than the specification of the structural geometry, stiffness, and loading. However, before the wide use of large scale computers, which is still the case in many undeveloped countries, simplified methods suitable for hand calculation are still valuable for the use of the design office. Besides, these methods are particularly useful for preliminary design analyses. Approximate analyses of frames may be performed most conveniently by effectively reducing the degree of statical indeterminacy by suitable moment releases. By recognising the dominant mode of racking deformation of a laterally loaded structure, it is possible to make realistic

fundamental structural element characteristics and the inherent relationships between structural elements with different structural behaviours.

1.3 Methods of Analysis and Review of Previous Research

During the major developments in tall building construction, mainly in the recent three or four decades, a large number of methods for the analysis of tall building structures have been presented by many investigators. Many of these methods have found application for structural designers in the design office. The most important methods of analysis, however, can be divided into three fields, which are, the frame analogy, the finite element method, and the continuous connection technique.

As the rigid frame is the most fundamental structural form adopted in tall building structures, the analysis of frame structures thus has become a major part in building structural design. The arrangement of the stiffness method of analysis in matrix form allows a concise and systematic approach to the analysis of rigid frames by digital computation. The method provides the most flexible and powerful technique for the analysis of frame and associated structures and programs are commercially available which demand little more of the engineer than the specification of the structural geometry, stiffness, and loading. However, before the wide use of large scale computers, which is still the case in many undeveloped countries, simplified methods suitable for hand calculation are still valuable for the use of the design office. Besides, these methods are particularly useful for preliminary design analyses. Approximate analyses of frames may be performed most conveniently by effectively reducing the degree of statical indeterminacy by suitable moment releases. By recognising the dominant mode of racking deformation of a laterally loaded structure, it is possible to make realistic

predictions of the resulting points of contraflexure in both beams and columns. The degree of indeterminacy is reduced by the number of points of inflexion, or zero bending moment, assumed. As a result, the two main techniques which have been devised for the approximate analysis of multi-storey frames, the Cantilever and Portal methods, make use of the same assumption that points of contraflexure occur at the mid-height positions of all columns and at the mid-span positions of all beams (Ref. 2). Macleod has presented a simplified method for the calculation of deflections of multi-storey regular rigid jointed frames in which both bending and column axial deformation are taken into account (Ref. 3). Recently, an analysis of laterally loaded multi-storey frames, in which axial deformations of the columns are also included, has been presented by Chan, Heidebrecht and Tso (Ref. 4). In this analysis, in addition to the usual assumptions of points of contraflexure in the beams and columns, the alternative additional assumption made is that the axial deformations of the columns have a hyperbolic sine variation across the width of the building. An energy analysis yields a linear governing differential equation of the second order, which can be integrated to give closed-form solutions for any particular lateral load distribution. From the analysis, design curves have been presented to enable rapid assessments to be made of column axial forces and shears.

The presence of shear walls, either solid or perforated, in conjunction with frames in the structure, leads to the 'wide-column' frame analogy method, in which the finite widths of the shear walls are incorporated by stiff arms connecting the ends of the beams to the centroidal axes of the walls, and the structure then can be analyzed by the conventional frame analysis. The analogy appears to have been used first by Macleod (Refs. 5, 6), in the analysis of coupled shear wall structures. Further developments were due to Kratky and Puri (Ref. 7), who developed a subroutine to modify a standard framework program,

thereby achieving the same result, and Schwaighofer and Microys (Ref. 8) who used a framework analysis program that incorporates a variable member stiffness subroutine.

The finite element method of analysis has emerged with the development of large scale computer programming, and not only in the field of building structural design. It has been widely used in many other fields such as mechanical and aeronautical engineering. In the finite element analysis, the continuous structure is divided into a mesh of one, two or three-dimensional elements connected at their nodes. Simplified assumptions are made for the mode of deformation or stress distribution in each element, from which the stiffness matrix corresponding to the nodes is established. By combining these element stiffnesses, the total stiffness matrix for the structure is formed. On solving the usually very large matrix equation, a solution for the nodal displacements and forces can be achieved. The method is well established nowadays from which very detailed and accurate solutions can result. Since a digital computer and special programming are needed for the formation and solving of the huge matrix, the computational costs are usually high, and, depending on the scale of the structure analyzed, the method is often restricted to its use in the final detailed design of the structure.

The continuum technique is probably the most suitable method for hand calculations. The technique applies to those structures consisting of uniform members and consistent connections throughout their height so that these members can be approximately replaced by equivalent continua of effective stiffnesses and the connections replaced by equivalent continuous media. By considering the appropriate conditions of compatibility and equilibrium, differential equations can be derived, leading to simplified closed mathematical solutions to the problem. The simplest example of the technique is probably the replacement of uniform

multi-bay rigid frame structures by shear cantilevers. By considering the dominant mode of racking deformation of the laterally loaded rigid frame and by making use of the assumptions that points of contraflexure occur at the mid-height positions of all columns and at mid-span positions of all beams, a rigid frame can be represented by an equivalent uniform continuous medium which behaves essentially as a shear beam with a calculated shear rigidity GA . The replacement of frames has been used by Heidebrecht and Stafford Smith who presented a mathematical model for the interactions between a shear wall and a rigid frame subjected to lateral loads (Ref. 9). In their method, the shear wall, which is a flexural member represented by a flexural rigidity EI , interacts through an assumed continuous horizontal interaction force flow with the shear member—the frame. By considering the horizontal displacement compatibility and force equilibrium, a differential equation of the fourth order for the deflection is derived, and on using appropriate boundary conditions, a close-form solution is obtained. The method is appropriate for both static and dynamic analyses and can be used to analyze three-dimensional symmetric structures consisting of plane shear walls, cores and rigid frames, subjected to lateral loadings.

The analysis for coupled shear walls under lateral loads, using the continuum technique, was first introduced by Beck (Ref. 10) who used the shear forces in the connecting medium as the statically indeterminate function. He treated the single case of uniform coupled shear walls on a rigid foundation, subjected to a uniformly distributed lateral load. More comprehensive studies were followed by Rosman (Ref. 11) who derived solutions for a wall with two symmetric bands of openings, with various conditions of support at the lower end (piers on rigid basement, on separate foundations, and on various forms of column supports). Two loading cases, a uniformly distributed lateral load, and a point load at the top of the structure, were considered. A recent study has again

be made by Coull (Ref. 12) who re-examined the basic assumptions used in the continuum analysis of coupled walls, and established the general force relationships for a pair of unequal walls. A complete general solution was presented for a structure subjected to a uniformly distributed wind loading. Attention was focused on the top concentrated interactive force which is shown to exist in a continuum model, and its magnitude was investigated for the particular case of a pair of plane coupled walls. Discussion was made of the inconsistencies which can arise with other boundary conditions, such as a pair of walls on elastic foundations, or walls stiffened by a roof beam.

Based on the continuum theory of coupled shear walls, many simplified methods have been presented for the analyses of three-dimensional symmetric structures which may be replaced by equivalent plane systems. Coull presented a method for the analysis of regular symmetric structures consisting of coupled shear walls and cores (Ref. 13). The solution has also been given by Stafford Smith and Abergel (Ref. 14) for the same type of structures, but by treating the structure as a single pair of coupled shear walls, using modified parameters. Arvidsson presented a method (Ref. 15) for the analysis of the interactions between a pair of coupled shear walls and rigid frames, using the complementary energy theory, and a solution was obtained by Euler's formula. Khachatoorian presented an extended method (Ref. 16) for the analysis of the lateral load distributions between ~~between~~ coupled shear walls, cores and rigidly jointed frames. In this field of coupled shear wall continuum theory, a comprehensive approach was given by Stafford Smith, Kuster and Hoenderkamp who made a close study of the parameters in the coupled shear wall theory, and discovered the physical implications of these parameters. Having done so, they applied the coupled wall theory to uniform braced and rigid frames, considering that these types of structures, together with coupled shear wall structure, belong to a family

of cantilevers whose deflections can be defined by their bending and shearing characteristics (Ref. 17). In a later paper presented by the same investigators, an approximate method (Ref. 18) was presented for estimating the deflections of three-dimensional symmetric structures comprising any combination of shear walls, coupled shear walls, rigid frames and braced frames. Hoenderkamp and Stafford Smith also presented a simplified method of analysis (Ref. 19) for determining the internal forces between the assemblies in the same types of structures.

Although the continuum method has been used fairly extensively for the analysis of symmetrically-loaded symmetrical structures, few studies have been made of its use for three-dimensional asymmetric structures which twist as well as bend under the action of lateral loading. A method of analysis of three-dimensional structures including bending and torsional actions was presented by Coull and Adams (Ref. 20). In this method, the structures considered consisted essentially of parallel systems of shear wall assemblies and box-core elements. The assumption was made that the load distribution on each assembly could be represented by a polynomial in the height coordinate. The continuum technique was used to derive the deflected form of an individual assembly from which flexibility influence coefficients relating any given load term to the deflection at any reference level were obtained. By making use of the equilibrium and compatibility equations at the reference levels, a solution of the load distribution on each then could be determined. Due to ill-conditioning of the matrices involved, this assumption led to errors at higher and lower storey levels of the building. The method was later extended by Coull and Mohammed (Ref. 21), which included rigidly jointed frame assemblies in the structures; in order to obtain more accurate results, a top concentrated interactive force was added to the polynomial load distribution on each assembly to simulate the heavy interactions which occur at the topmost levels in such structures.

1.4 Scope of the Thesis

This thesis is concerned with the approximate linear elastic analysis of three-dimensional tall buildings subjected to bending as well as torsion. The analysis is based on the continuum technique. The buildings are assumed to consist of varieties of lateral load bearing assemblies which are uniform throughout the building height, constrained at every floor level by the rigid in-plane floor slabs, and rigidly built in at the base. These assemblies include most of the commonly adopted high-rise bents, namely rigid frames, coupled or uncoupled shear walls, and cores. In the first three chapters, studies are made of the different modes of force-deformation behaviour of these structural assemblies, either singly or coupled together. The important parameters which define the structural behaviour of these elements are examined. In the following two chapters, two approximate methods of analysis for three-dimensional high-rise wall-frame structures subjected to lateral loads are proposed: Chapter 5 presents a generalized method, using a revised wall-frame theory and a spring supporting rigid beam model, and Chapter 6 presents another simplified method, using an area influence coefficient approach. More accurate finite element studies are used to check the validity and the accuracy of the methods. Chapter 7 gives conclusions to the research, and suggestions for future work.

1.5 The Use of the "FLASH" Program

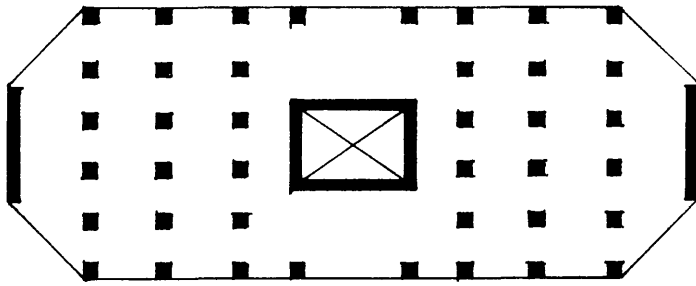
FLASH (Finite Element Analysis of SHells) is a general purpose finite element program for the analysis of beam structures, membranes, folded plates, plates, and shells. The program was originally developed at the Swiss Federal Institute of Technology and has been considerably enhanced and adjusted to the needs of practising engineers over the years. Due to modern hybrid elements,

high numerical efficiency, a simple and userfriendly input language, as well as comprehensive postprocessing of the results, FLASH is today a powerful and cost-effective tool of the engineer.

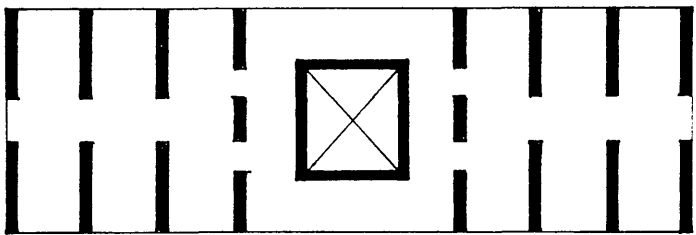
FLASH is used to solve numerous problems of the construction and the building industry. In particular the program is very well suited for

- linear static analysis
- stability analysis
- problems with second order effects
- structures on elastic foundations
- analysis of construction phases
- eigenvalue problems

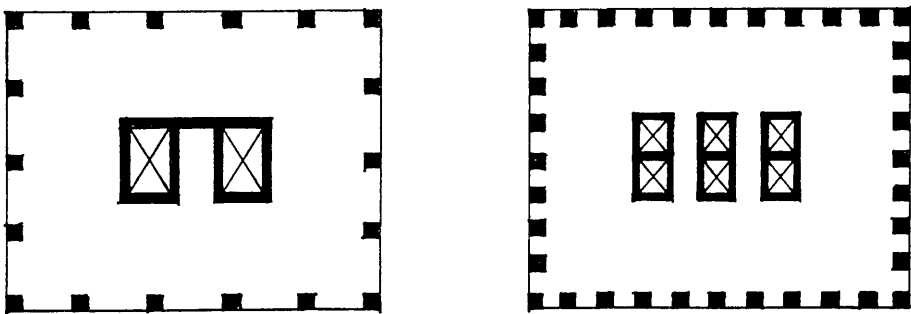
The FLASH program has been installed in the Department of Civil Engineering, and has been used to carry out numerical studies to examine the validity and accuracy of more approximate methods. All of the comparative curves throughout this thesis are obtained from the results of the FLASH program.



(a) Wall Frame Structure



(b) Coupled Shear Wall Structure



(c) Core Type Structures

Fig. 1.1 Typical Planforms of Tall Building Structures

CHAPTER 2

ANALYSIS OF WALL-FRAME STRUCTURES (PART ONE)

2.1 Introduction

Wall-frame structures refer to structures consisting of shear walls or structural cores, which perform as pure flexural cantilevers, acting in conjunction with rigid frames, which perform predominantly as shear cantilevers. When the two different types of cantilevers are combined in a high-rise structure, the differences in their free modes of load-deflection behaviour will cause them to interact horizontally through the connecting slabs. This horizontal interaction, as will be discussed later, will produce a much greater top stiffness and will strengthen the structure. Due to this characteristic, wall-frame structures are frequently adopted in high-rise residential and official blocks which can be built up to 40 to 60 storeys. Typical plans of such buildings are shown in Fig. 2.1.

2.2 Shear Walls, Cores And Rigid Frames

2.2.1 Shear Walls and Structural Cores

Shear walls and cores in a structure are usually designed to resist both gravitational and horizontal load. Structural cores can also provide the structure with large torsional stiffnesses, which resist any tendency to twist due to eccentric loading or structural asymmetry. Shear walls and cores in the structure can still be used to perform non-structural functions; shear walls can be used to divide and enclose space, provide fire and acoustic insulation between dwellings, and cores are usually used as elevator shafts, stair wells or other service ducts.

When subjected to lateral loads, shear walls and cores are usually considered to act as pure flexural cantilever beams. The load-deformation behaviour of such cantilever beam is described by the governing equation,

$$EI \frac{d^4 y}{dx^4} = w(x) \quad (2.1)$$

or,

$$EI \frac{d^2 y}{dx^2} = M(x) \quad (2.2)$$

in which EI is the flexural rigidity of the beam, y is the horizontal displacement, x is the height coordinate measured from the base and $w(x)$ and $M(x)$ are the distributed lateral load and moment applied to the beam, respectively. In the case of a uniformly distributed lateral load with intensity w_0 , the moment can be expressed as,

$$M(x) = \frac{1}{2} w_0 H^2 \left(1 - \frac{x}{H}\right)^2 \quad (2.3)$$

in which H is the total height.

By integrating Eq. 2.2, and using the appropriate boundary conditions for a structure which is rigidly built in at the base and free at the top, that is,

$$\text{At } x = 0, \quad y = \frac{dy}{dx} = 0 \quad (2.4)$$

the expression for the deflection then becomes,

$$y = \frac{w_0 H^4}{EI} \left\{ \left(\frac{x}{H}\right)^4 - 4\left(\frac{x}{H}\right)^3 + 6\left(\frac{x}{H}\right)^2 \right\} \quad (2.5)$$

This expression will give a flexural mode of deformation as shown in Fig. 2.2a, which is characterised by having a maximum slope at the top and concavity downwind.

The expressions for the deflection for other load cases can also be obtained

as, for example, in the case of a top concentrated horizontal load P ,

$$y = \frac{PH^3}{EI} \left\{ 3\left(\frac{x}{H}\right)^2 - \left(\frac{x}{H}\right)^3 \right\} \quad (2.6)$$

and in the case of a triangularly distributed lateral load with an intensity of q_0 at the top varying linearly down to zero at the base,

$$y = \frac{q_0 H^4}{EI} \left\{ \left(\frac{x}{H}\right)^5 - 10\left(\frac{x}{H}\right)^3 + 20\left(\frac{x}{H}\right)^2 \right\} \quad (2.7)$$

2.2.2 Rigid Frames

In many approximate analyses, planar rigid frames in tall building structures are considered to behave essentially as shear cantilevers, with their shear stiffness depending upon the member stiffnesses, the frame configuration, and the rigidity of the joints. The expression governing the load–deformation behaviour of a shear cantilever with effective rigidity GA may be written as,

$$GA \frac{dy}{dx} = S(x) \quad (2.8)$$

or,

$$GA \frac{d^2y}{dx^2} = w(x) \quad (2.9)$$

where $w(x)$ and $S(x)$ are the distributed lateral load and shear force applied to the cantilever, respectively. For a uniformly distributed lateral load of intensity w_0 , the expression for the shear force becomes,

$$S(x) = w_0 H \left(1 - \frac{x}{H}\right) \quad (2.10)$$

In this case, on integrating Eq. 2.8, with one boundary condition of $y(0)=0$, the expression for the deflection of the shear cantilever becomes,

$$y = \frac{w_0 H^2}{GA} \left[\frac{x}{H} - \frac{1}{2} \left(\frac{x}{H}\right)^2 \right] \quad (2.11)$$

The deflection profile, Fig. 2.2b, then takes up a characteristic shear mode,

with concavity upwind, and a maximum slope at the base.

Similarly, expressions for such cantilevers under the other two load cases can be obtained as:

Top concentrated horizontal force P ,

$$y = \frac{Px}{GA} \tag{2.12}$$

Triangularly distributed lateral load with maximum intensity q_0 :

$$y = \frac{q_0 H^2}{2GA} \left[\frac{x}{H} - \frac{1}{3} \left(\frac{x}{H} \right)^3 \right] \tag{2.13}$$

For a planar rigid frame, the value of the parameter GA can be determined by interpreting Eq. 2.8 for a one-storey segment of the frame. Such an interpretation defines the equivalent GA of the frame as the interstorey horizontal shear force required to give a unit horizontal shearing deformation over the one-storey height. A typical one-storey segment of a multi-bay frame (which is assumed regular through the height) is shown in Fig. 2.3a. As in most approximate analyses for multi-storey, multi-bay rigid frames, the assumption is made that points of contraflexure occur at the mid-height positions of all columns and at the mid-span positions of all beams. The restraining system for a single interior column is then shown in Fig. 2.3b. The horizontal force-deflection relationship for the column is given by,

$$P = \frac{12EI_C}{h^3} \frac{\Delta}{\left[1 + \frac{2I_C}{h(I_{b_1}/b_1 + I_{b_2}/b_2)} \right]} \tag{2.14}$$

in which I_C is the second moment of area of the column, h is the storey height, b_1 and b_2 are the total lengths of adjacent beams, I_{b_1} and I_{b_2} are second moments of area of corresponding beams, Δ is the lateral displacement of the one-storey column, and P is the lateral force. Eq. 2.14 is also applicable to

an exterior column by assuming a zero value for the second moment of area of the non-existing adjacent beam. If required, the effect of shear deformations within any of the frame components and the effect of the finite size of any beam-column joint corresponding to the free column height and beam span can be included by using a modified moment of inertia (Ref. 22) in Eq. 2.14. From Eq. 2.14, the contribution of the single column i to the GA parameter of the frame is given by,

$$GA_i = \frac{P}{\Delta/h} = \frac{12EI_c}{h^2} \frac{1}{\left[1 + \frac{2I_c}{h(I_{b_1}/b_1 + I_{b_2}/b_2)} \right]} \quad (2.15)$$

The total GA contribution of a planar frame is then the arithmetic sum of the GA terms for each of the columns in a typical storey of the frame.

2.3 Interaction Between Shear Walls and Rigid Frames

– Simple Wall-Frame Theory

2.3.1 Basic Assumptions and Governing Equations

The structure is considered to consist of a combination of uniform vertical flexural and shear cantilevers which are constrained to deflect equally when subjected to lateral loads. The representation of such a structure can be shown in Fig. 2.4a, in which the pin-ended links simulate the floor slabs which connect the two components. The links are then assumed smeared over the height of the structure to produce an equivalent continuous connecting medium. The discrete axial forces in the links may then be replaced by an axial force distribution of intensity n in the continuous medium.

The governing equations for flexural and shear cantilevers are given by Eqs. 2.1 and 2.8, respectively. So, referring to Fig. 2.4b, the governing equations

of the components of this composite cantilever, which may be referred to as a shear–flexural cantilever beam, are then given by,

$$EI \frac{d^4 y}{dx^4} = w(x) - n(x) \quad (2.16)$$

$$- GA \frac{d^2 y}{dx^2} = n(x) \quad (2.17)$$

Addition of Eq. 2.16 and 2.17, and dividing through by EI , yields,

$$\frac{d^4 y}{dx^4} - \alpha^2 \frac{d^2 y}{dx^2} = \frac{w(x)}{EI} \quad (2.18)$$

in which,

$$\alpha^2 = \frac{GA}{EI} \quad (2.19)$$

2.3.2 Solutions For Standard Load Cases

For a uniformly distributed load of intensity w_0 , the solution to Eq. 2.18 can be expressed as,

$$y(x) = C_1 + C_2 x + C_3 \cosh \alpha x + C_4 \sinh \alpha x - \frac{w_0 x^2}{2EI\alpha^2} \quad (2.20)$$

in which C_1 , C_2 , C_3 and C_4 are integration constants which must be determined from the appropriate boundary conditions. If the structure is rigidly built in at the base and free at the top, when the moment and total shear are zero, the four boundary conditions become,

$$y(0) = 0 \quad (2.21)$$

$$\frac{dy}{dx}(0) = 0 \quad (2.22)$$

$$M_b(H) = EI \frac{d^2 y}{dx^2} = 0 \quad (2.23)$$

$$S(H) = GA \frac{dy}{dx}(H) - EI \frac{d^3 y}{dx^3}(H) = 0 \quad (2.24)$$

It may be seen from Eq. 2.8 that the boundary condition in Eq. 2.22 is tantamount to considering that the shear in the frame is zero at the base, and the total shear is carried by the wall component.

The four constants can then be obtained from Eqs. 2.21 to 2.24, leading to the following expression for the deflection,

$$y = \frac{w_0 H^4}{EI} \left\{ \frac{1}{(\alpha H)^2} \left(\xi - \frac{\xi^2}{2} \right) + \frac{\cosh \alpha H \xi + \alpha H \sinh \alpha H (1 - \xi) - (\alpha H \sinh \alpha H + 1)}{(\alpha H)^4 \cosh \alpha H} \right\} \quad (2.25)$$

in which the deflection is expressed for convenience in the dimensionless height coordinate $\xi = x/H$.

The solution for the deflection leads to the resulting force distributions in the flexural and shear elements respectively as,

$$M_b = \frac{w_0 H^2}{(\alpha H)^2} \left\{ \frac{\cosh \alpha H \xi + \alpha H \sinh \alpha H (1 - \xi)}{\cosh \alpha H} - 1 \right\} \quad (2.26)$$

$$M_s = \frac{w_0 H^2}{2} (1 - \xi)^2 - M_b \quad (2.27)$$

$$S_b = w_0 H \left\{ \frac{\alpha H \cosh \alpha H (1 - \xi) - \sinh \alpha H \xi}{\alpha H \cosh \alpha H} \right\} \quad (2.28)$$

$$S_s = w_0 H \left\{ (1 - \xi) - \frac{\alpha H \cosh \alpha H (1 - \xi) - \sinh \alpha H \xi}{\alpha H \cosh \alpha H} \right\} \quad (2.29)$$

$$w_b = w_0 \left\{ \frac{\cosh \alpha H \xi + \alpha H \sinh \alpha H (1 - \xi)}{\cosh \alpha H} \right\} \quad (2.30)$$

$$w_s = w_0 \left\{ 1 - \frac{\cosh \alpha H \xi + \alpha H \sinh \alpha H (1 - \xi)}{\cosh \alpha H} \right\} \quad (2.31)$$

in which M_b and M_s are the moments applied to the flexural and shear cantilevers, respectively, S_b and S_s are the shears in the two components, and w_b and w_s are the load distributions to the two components.

It is worth noting that, when $x = H$ or $\xi = 1$, Eqs. 2.28 and 2.29 become,

$$S_s = -S_b = w_0H \left\{ \frac{\sinh\alpha H - \alpha H}{\alpha H \cosh\alpha H} \right\} \quad (2.32)$$

This shows that at the top of the structure, a shear exists in the two cantilevers, of magnitude,

$$Q = w_0H \left\{ \frac{\sinh\alpha H - \alpha H}{\alpha H \cosh\alpha H} \right\} \quad (2.33)$$

In the absence of any applied point loads, the existence of the shear force indicates the presence of a concentrated horizontal interactive force Q at the top of the structure. It is required to provide slope compatibility between the two components at the top of the structure, since, otherwise, a zero shear force in the frame would require a zero slope at the top (cf. Eq. 2.8).

The corresponding variation of Q/w_0H with the parameter αH is given in Fig. 2.5, from which it can be shown that this top interactive shear may reach a maximum of 23.34 percent of the total applied bottom shear w_0H when αH is near a value of 2.77. The concentrated force represents the heavy localised interactions which take place at the topmost levels in such composite structures. Their presence has been noted by other investigators using more sophisticated analyses, such as the finite element method.

The solutions for deflections and the force distributions for the other load cases, a triangularly distributed lateral of maximum intensity q_0 at the top varying linearly to zero at the base, and a concentrated horizontal load P at the top, are given in Appendix 1.

2.3.3 Numerical Examples of Wall-Frame Structures

An example of a regular symmetric building structure involving the interaction between flexural and shear members is considered. The floor plan is shown in Fig. 2.6 in which the flexural member includes one central core, and the shear member consists of four identical rigid frames. In order to test the rigid frame shear model, which may only be accurate for lower structures, two cases are considered; one is that the building is of 15-storeys with a total height of 42m, the other being of 40-storeys with a height of 112m. In each case, the following data are used:

Storey height $h = 2.8 \text{ m}$

Modulus of elasticity $E = 1.40 \times 10^7 \text{ kN/m}^2$

Applied floor point load $p_0 = 25 \text{ kN per floor,}$
or uniformly distributed load,

$$w_0 = 8.93 \text{ kN/m}$$

Flexural core component $I = 10.0 \text{ m}^4$

$$EI = 1.40 \times 10^8 \text{ N m}^2$$

Shear component (four identical rigid frames in total),

Spans $b_1 = b_2 = b_3 = 4.0 \text{ m}$

Inertias of the beams $I_{b1} = I_{b2} = I_{b3} = 1.042 \times 10^{-2} \text{ m}^4$

Inertias of the columns $I_{c1} = I_{c2} = I_{c3} = I_{c4} = 8.533 \times 10^{-3} \text{ m}^4$

Column sectional areas $A_{c1} = A_{c2} = A_{c3} = A_{c4} = 0.64 \text{ m}$

The total shear rigidity can be calculated from Eq. 2.15 as,

$$GA = 2.78 \times 10^5 \text{ kN}$$

The parameter $\alpha = 0.0446 \text{ m}^{-1}$.

And, in case 1 $\alpha H = 1.872$,

in case 2 $\alpha H = 4.991$

The resultant forces and deflections obtained by the present method for the two cases are compared with the results obtained from the 'FLASH' program. The curves are shown for case 1 in Figs. 2.7a to 2.7d, and for case 2 in Figs. 2.8a to 2.8d, in which, unless specified, the thicker lines refer to the present method, and the thinner lines refer to the 'FLASH' results. It can be seen that for the lower 15-storey structure, the results by this approximate method compare satisfactorily with those from the more exact finite element analysis. However, for the higher 40-storey structure, although the forces shown in Figs. 2.8b to 2.8d seem to be obtained reasonably well, the accuracy for the deflection shown in Fig. 2.8a is much poorer. For the purpose of examining this fact, one rigid frame in this example has been examined individually. Figs 2.9a and 2.9b show respectively the deflection curves of the individual laterally loaded 15-storey and 40-storey planar rigid frames obtained by the present method (Eq. 2.11), and from the 'FLASH' program. It can be seen that for the lower structure, the approximate method represents reasonably accurately the load-deformation behaviour of the frame, whereas it is no longer valid for the high-rise frame. The discrepancy is due to the axial deformations in the columns, which become progressively more important as the structure becomes taller, and produce an 'over-all bending action' for the frame. This factor will be discussed further in Chapter 4, when a revised method is introduced to improve the model.

2.4 Modification of the Parameter GA for Low-rise Rigid Frames at the Ground Storey Level

A number of different forms of frame structure, including frames with non-uniform bays, were analysed by both the shear cantilever and finite element (FLASH) methods. The effects of overall bending in the frame were suppressed by specifying large values of the cross-sectional areas of the columns in the FLASH program since these are not included in the shear cantilever model. It was generally found that the two deflection curves were of similar form in the upper levels, above first storey level, but with the two curves displaced horizontally at the first storey level, as shown in Fig. 2.10. It thus appeared that the uniform shear cantilever model was too flexible over the first storey only, and did not take account of the influence of the base rigidity.

Referring to Fig. 2.9a, it can be shown that the 'FLASH' result gives roughly a shear-deflected configuration for the laterally loaded 15-storey rigid frame. However, it also shows a reversal of curvature occurring at the ground storey level where the structure is stiffened by the rigid base. Referring to Figs. 2.3a and 2.3b, on attempting to improve the simple shear model, a modified shear stiffness at the ground storey level is obtained by introducing an alternative restraining system for a single interior column chosen from the first storey segment of a multibay frame, shown in Figs. 2.11a and 2.11b, in which the assumption is made that the points of contraflexure occur at the mid-spans for the adjacent beams and at the mid-column height for the upper column, but the lower column is rigidly built in at the base. The horizontal force-deflection relationship for the column is then given by,

$$P = \frac{12EI_c}{h^3} \frac{\Delta}{\left[1 + \frac{I_c}{h(I_{b_1}/b_1 + I_{b_2}/b_2 + I_c/6h)} \right]} \quad (2.34)$$

So the contribution of the single column to a modified shear stiffness GA_1 , is given by,

$$GA_{1i} = \frac{12EI_c}{h^2} \left[\frac{1}{1 + \frac{2I_c}{h(I_{b1}/b_1 + I_{b2}/b_2 + I_c/6h)}} \right] \quad (2.35)$$

The total GA_1 for the first storey level of the frame is given by the arithmetic sum of the GA_{1i} terms for each of the columns in the frame.

Referring to the deflection equation 2.11, when subjected to a uniformly distributed lateral load, the deflection for the rigid frame below the first storey level is given by,

$$y_1 = \frac{w_0 H^2}{GA_1} \left[\frac{x}{H} - \frac{1}{2} \left(\frac{x}{H} \right)^2 \right] \quad (2.36)$$

in which $x < h$, and the deflection above the first storey level can be approximately given by,

$$y = \frac{w_0 H^2}{GA} \left[\frac{x}{H} - \frac{1}{2} \left(\frac{x}{H} \right)^2 \right] + C \quad (2.37)$$

in which $x > h$, and,

$$C = - w_0 H^2 \left[\frac{h}{H} - \frac{1}{2} \left(\frac{h}{H} \right)^2 \right] \times \left[\frac{1}{GA} - \frac{1}{GA_1} \right] \quad (2.38)$$

Fig. 2.12 shows the deflected curve of the 15-storey rigid frame given by the modified method, compared with the result obtained by the FLASH program. It should be noted that the axial deformations in the columns of the frame are included in the FLASH analysis which produces bigger displacements at the higher levels of the structure.

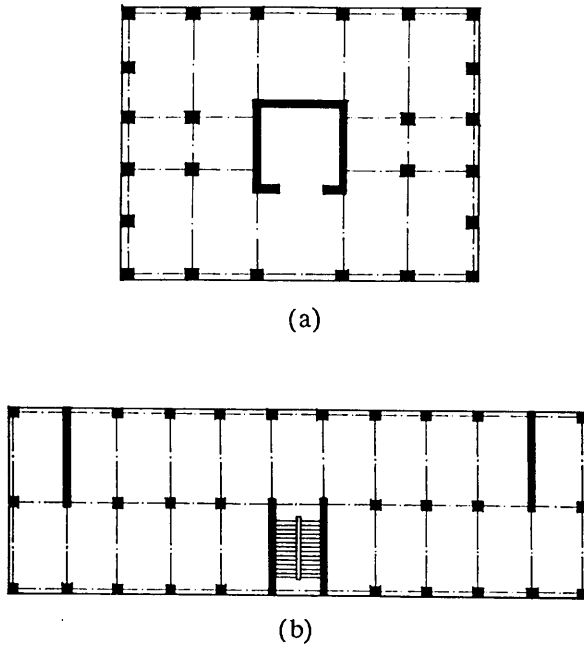


Fig. 2.1 Typical Planforms of Wall-Frame Structures

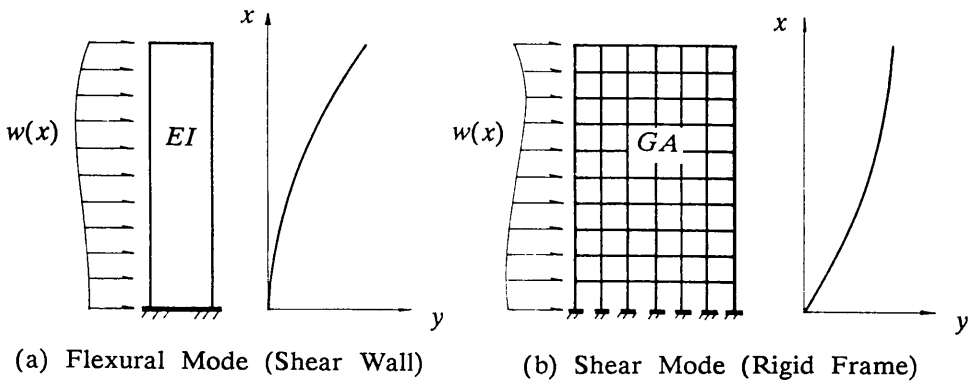


Fig. 2.2 Flexural and Shear Modes of Deflected Configurations

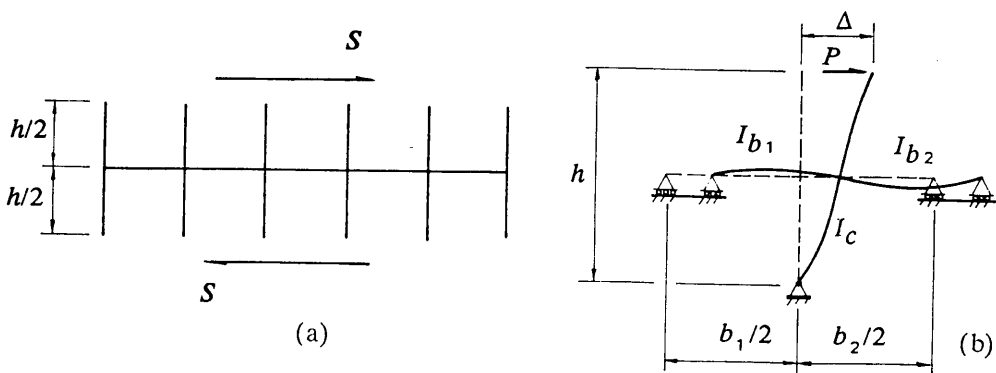


Fig. 2.3 Typical One-Storey Segment of Multibay Frame (a), and Restraining System of Interior Column (b)

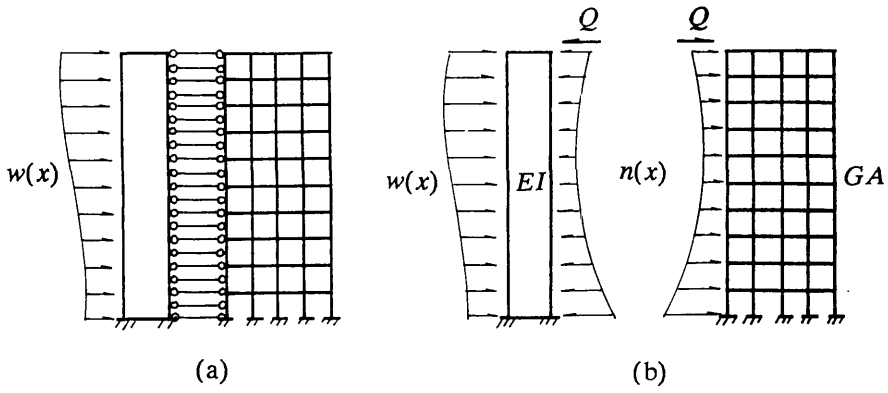


Fig. 2.4 Representation of Interacting Wall- Frame Structures

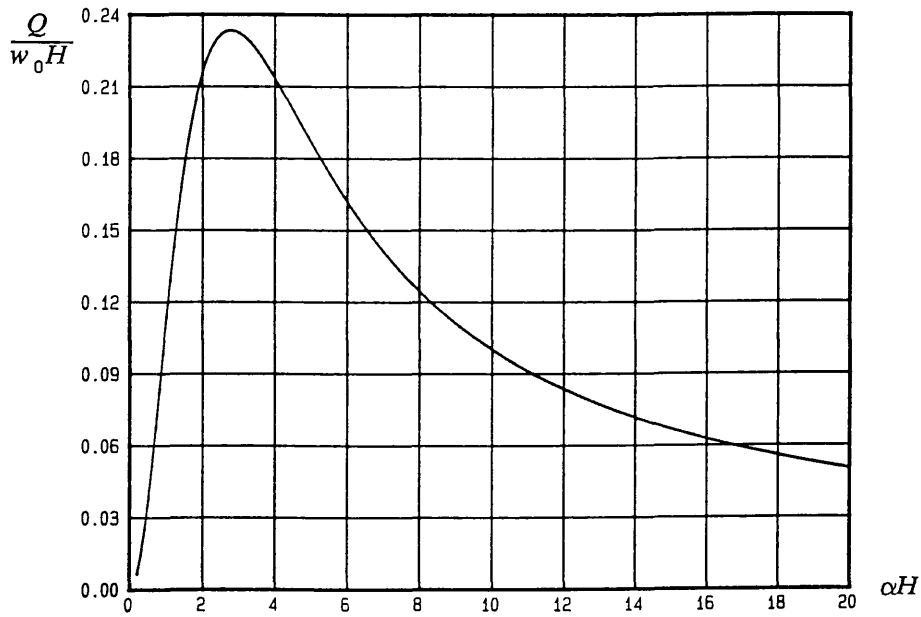


Fig. 2.5 Variation of Q/w_0H Versus αH

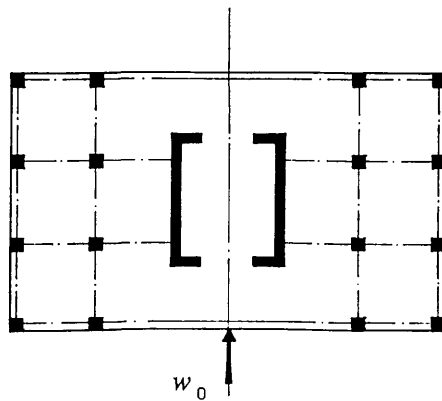
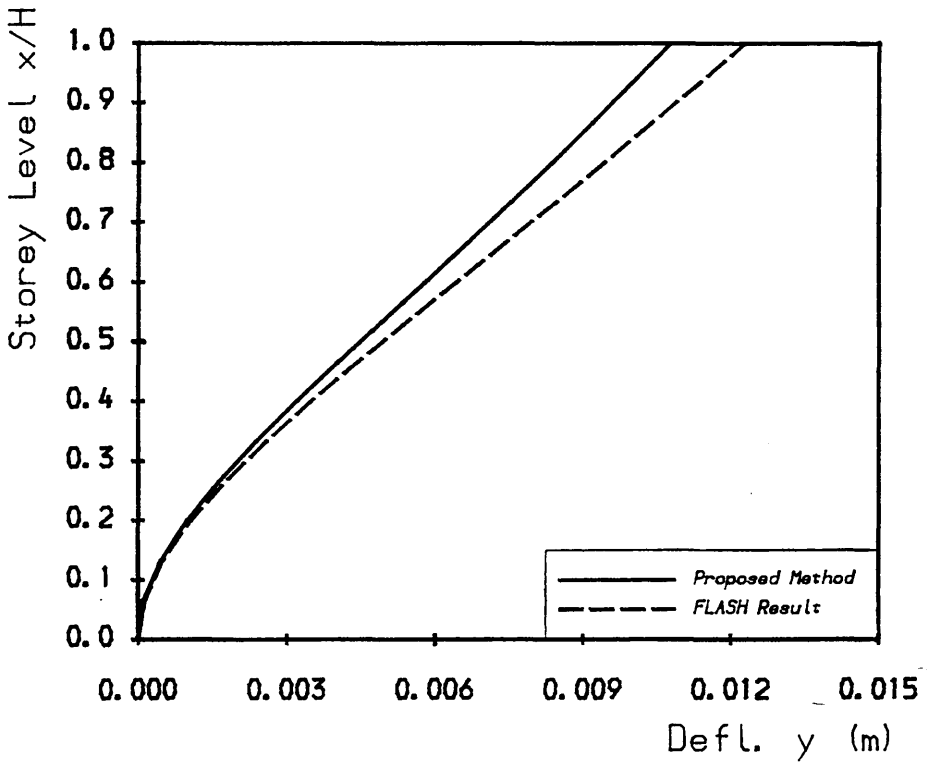


Fig. 2.6 Planform of Wall- Frame Structure Example



15-Storey Wall-Frame Example
Fig. 2.7a

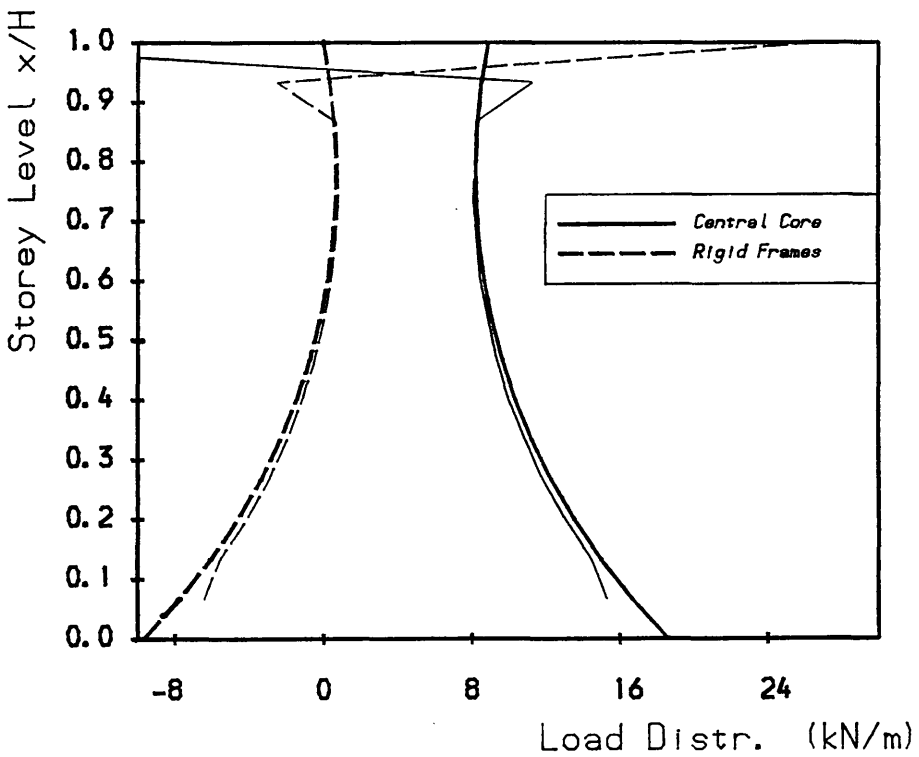


Fig. 2.7b

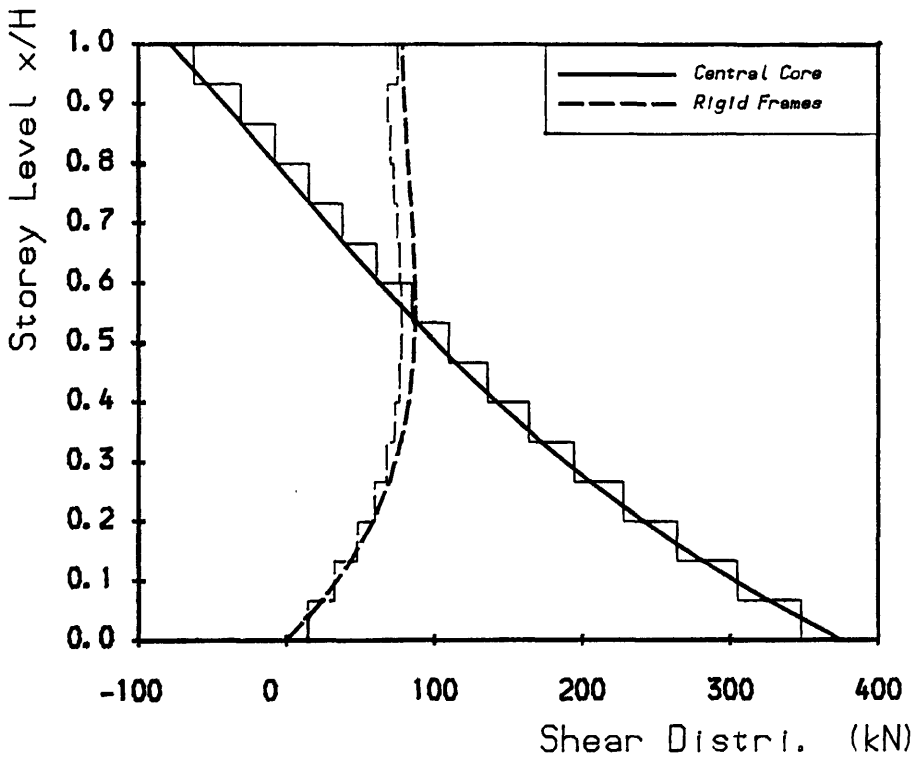


Fig. 2.7c

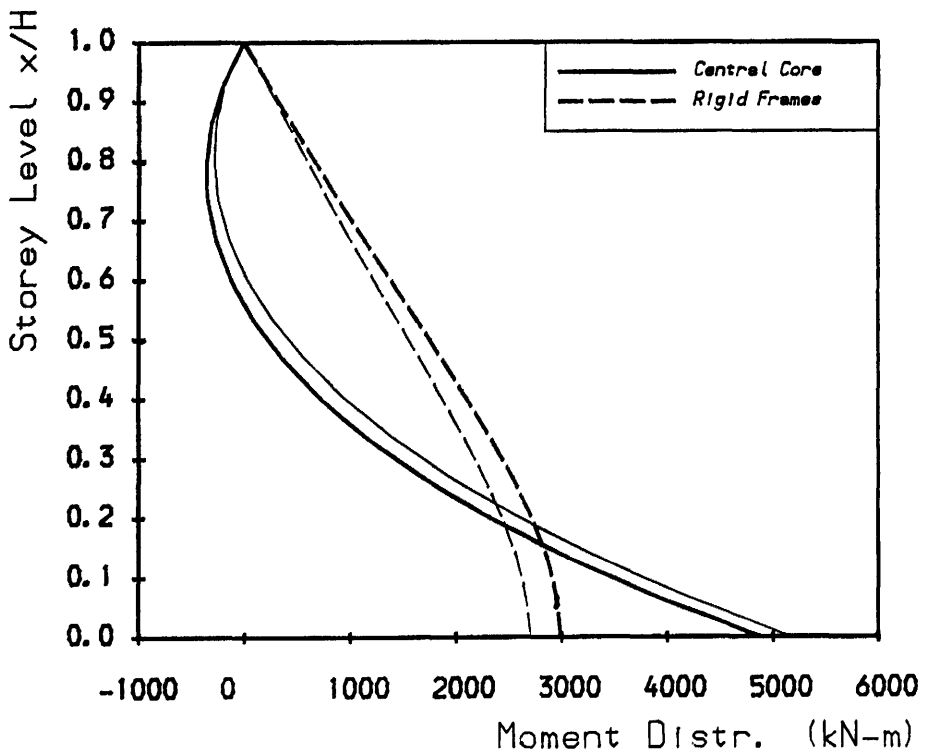
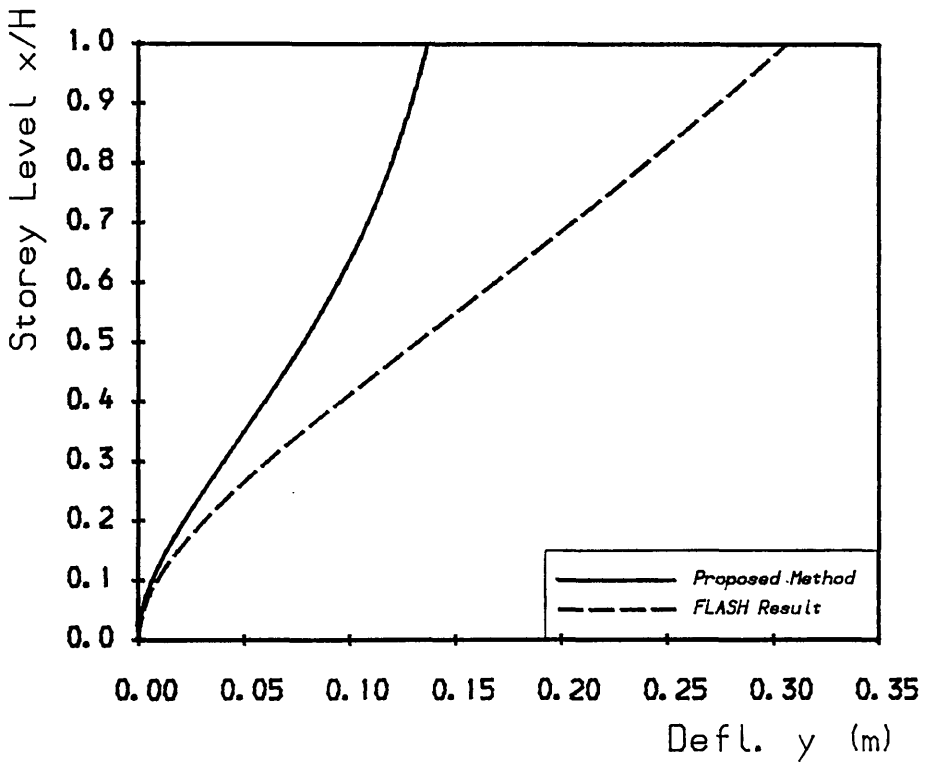


Fig. 2.7d



40-Storey Wall-Frame Example
Fig. 2.8a

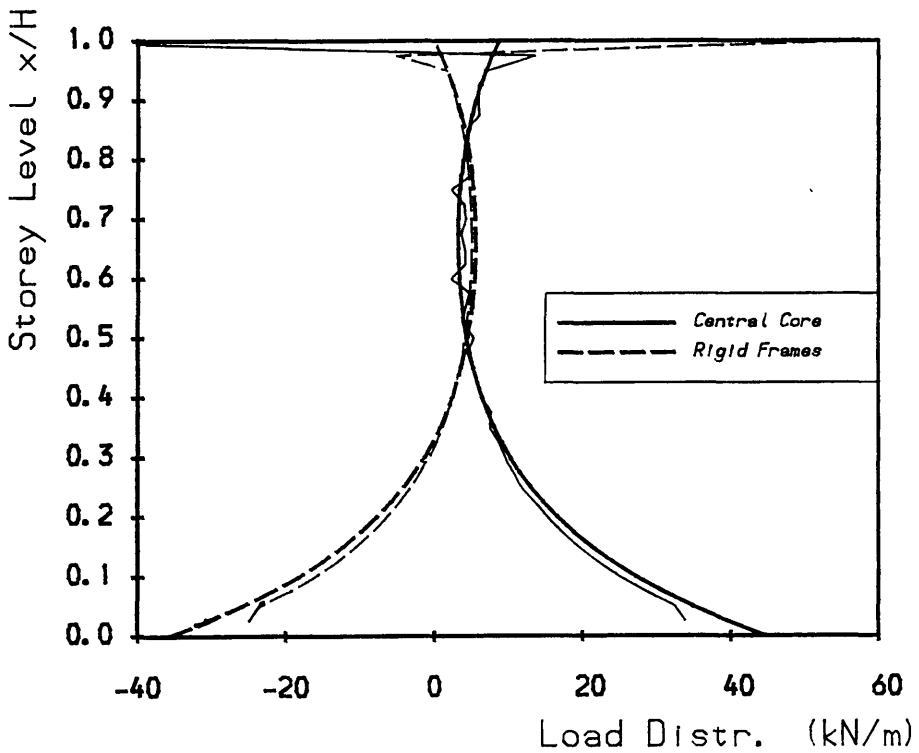


Fig. 2.8b

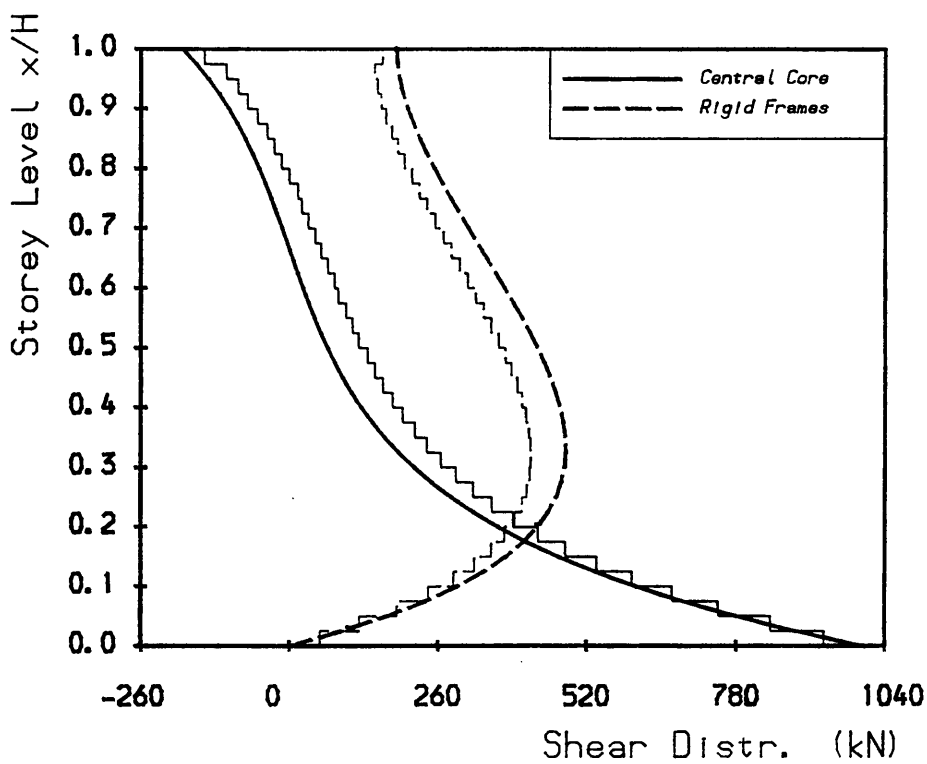


Fig. 2.8c

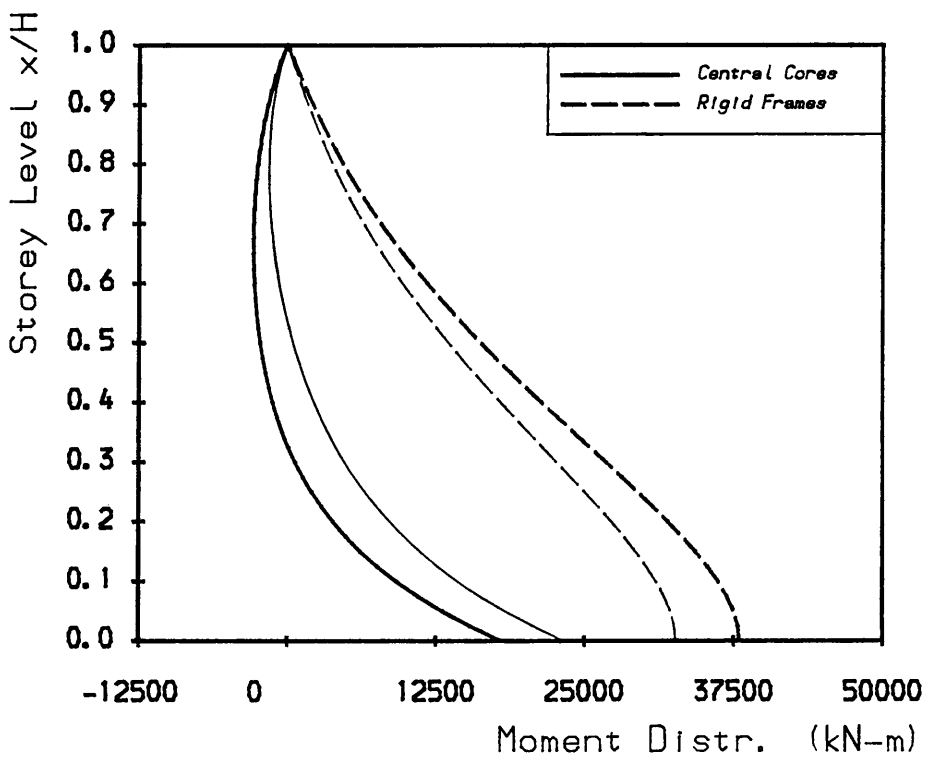
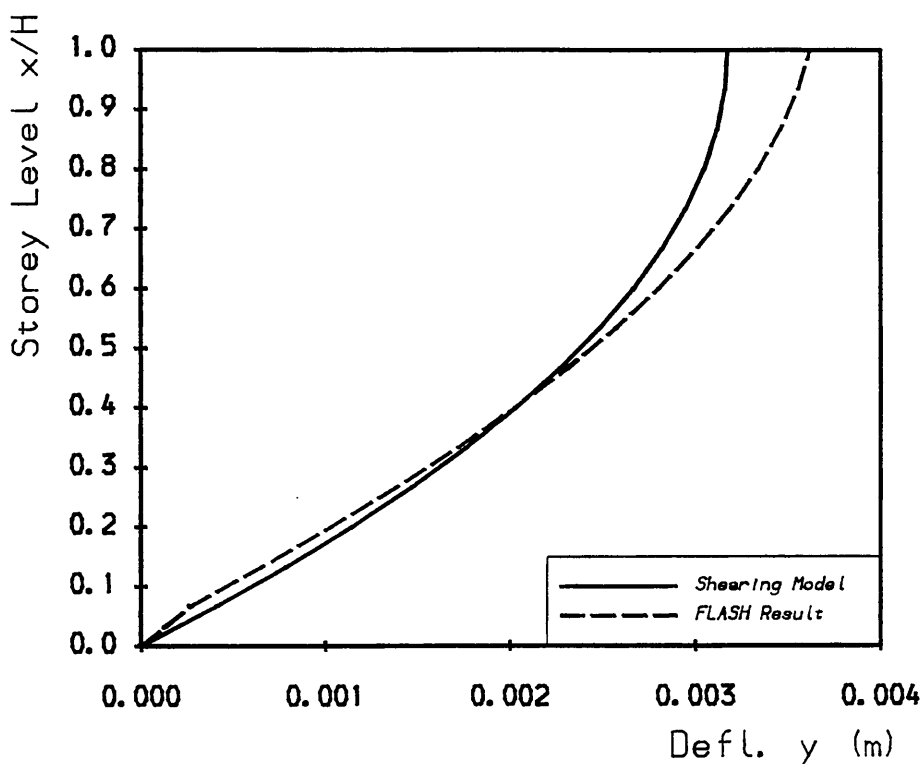
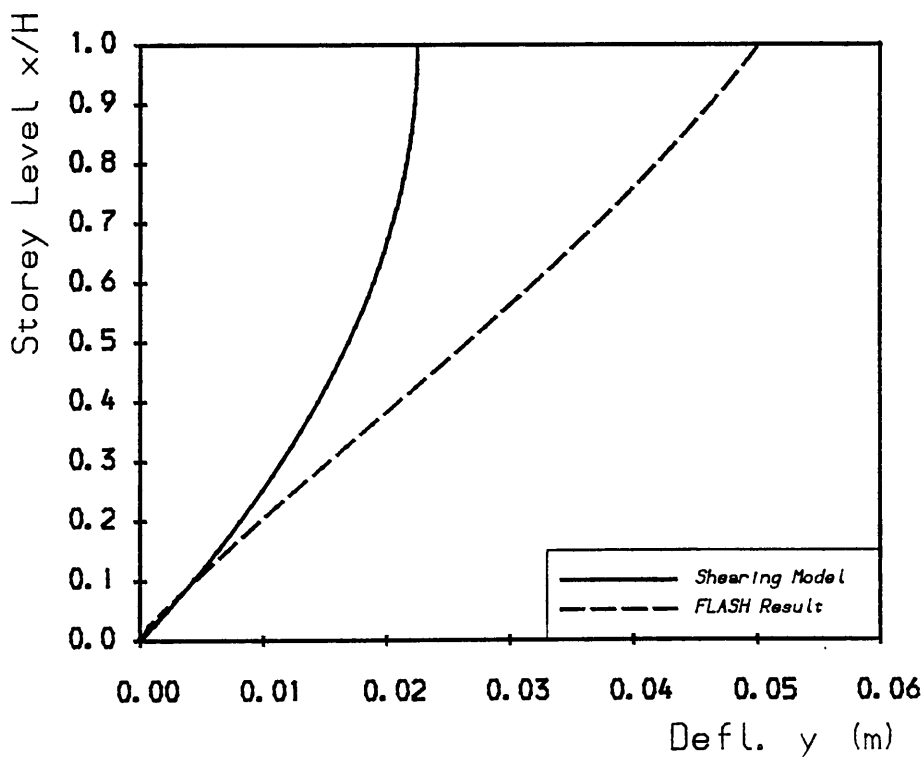


Fig. 2.8d



15-Storey Rigid Frame

Fig. 2.9a



40-Storey Rigid Frame

Fig. 2.9b

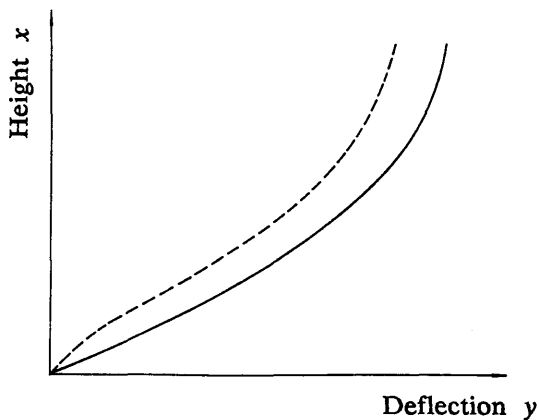


Fig. 2.10 Influence of the Base Rigidity of Rigid Frame

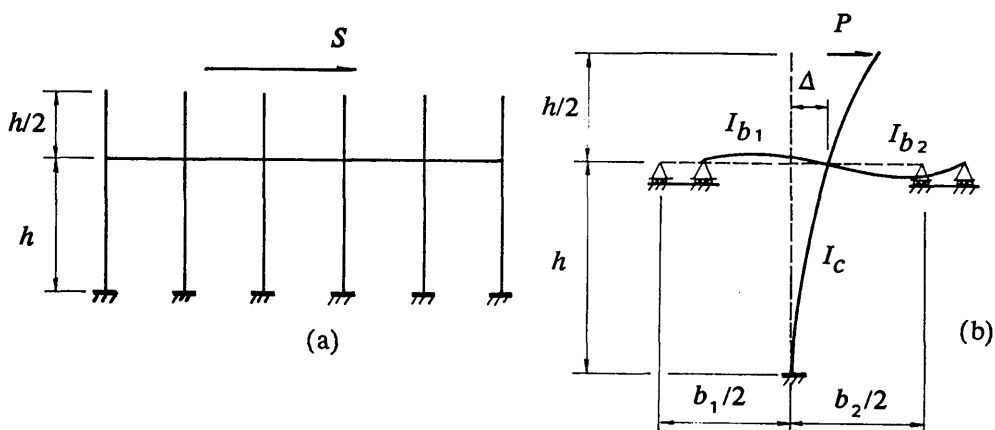


Fig. 2.11 Ground-Storey Segment of Multibay Frame (a), and Restraining System of Interior Column (b)

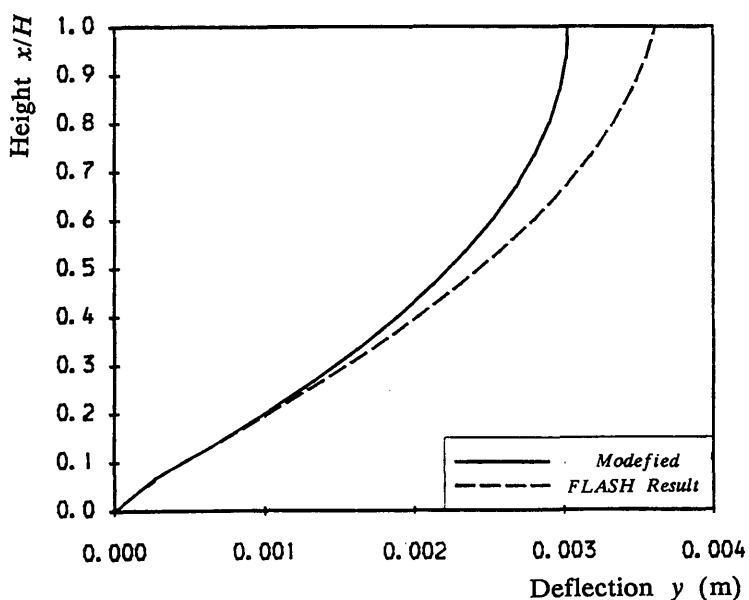


Fig. 2.12 Deflection of 15-Storey Rigid Frame of Modified Shear Model

CHAPTER 3

ANALYSIS OF COUPLED SHEAR WALL STRUCTURES

3.1 Introduction

Coupled shear walls, as indicated in Fig. 3.1, consist of a pair of shear walls connected at every floor level by lintel beams. Coupled shear walls are frequently used in tall building structures as efficient structural components because they not only effectively resist both gravitational and lateral loads, but also fulfil the non-structural functions of dividing and enclosing space, simultaneously providing fire and acoustic insulation between dwellings. The coupled shear wall system especially has an advantage in resisting lateral loads due to wind or earthquakes, because under such loads, the rigid-jointed connecting beams not only transfer horizontal forces from one wall to the other, but induce vertical forces as well as reversal moments in the two walls. The top stiffness of the system is significantly increased by such effects.

Coupled shear walls usually occur in cross-wall structures as main load-bearing elements, or in frame structures as end-wall systems. These structures normally also include one or more service cores which act as strong points in the building. In this chapter, structures which include one or more pairs of coupled shear walls, acting in conjunction with structural cores and/or rigid frames, are referred to as coupled shear wall structures. Typical planforms of symmetric coupled shear wall structures are shown in Fig. 3.2. In these structures, since different assemblies, coupled shear walls, structural cores and rigid frames, have vastly different modes of force-deformation behaviour, if they are constrained to act together by the floor slabs, considerable force redistributions may occur among them throughout the height. Analyses of interactions between

various combinations of these structural components are presented in this chapter. These methods can be applied to regular symmetric coupled shear wall structures in which the structural system may be replaced by equivalent plane systems. Such simplified replacements corresponding to those shown in Fig. 3.2 are illustrated in Fig. 3.3. The analyses are based on the continuum technique which is described in the next section.

3.2 Continuum Theory of Coupled Shear Walls

3.2.1 Introduction

There have been two main techniques developed to analyze individual coupled shear walls. One is the frame analogy in which the finite widths of the walls are incorporated by stiff arms connecting the two ends of the beams to the centroidal axes of the walls. By modifying the bending stiffnesses of the connecting beams, the structures can be analyzed by conventional framework methods, or, by formulating the stiffness matrix for displacements of the column nodes of the wide-column frame, a solution may be derived by standard matrix procedures using computer programs. The other uses the continuum technique, in which the discrete system of connecting beams is replaced by an equivalent continuous medium of the same effective stiffness. By assuming a fixed vertical line of contraflexure in the connecting medium, a governing linear differential equation of the second order is derived from the conditions of compatibility and equilibrium, and a closed-form solution to the problem is obtained mathematically for particular boundary conditions and prescribed standard load cases. The continuum technique is most appropriate for structures that are uniform throughout the height. The simplicity of the mathematical solutions enable rapid hand methods to be developed which can achieve an accurate analysis of

such structures, and which are suitable in use for design offices.

This thesis is concerned only with the continuum technique, and, to introduce the approach, the continuum analysis of a pair of regular coupled shear walls is presented in this section. It essentially follows the treatment given in Reference 12.

Three standard lateral load cases which are usually required in practice are those of a uniformly distributed lateral load of intensity w_0 , a concentrated horizontal load P at the top, and a triangularly distributed lateral load with a maximum of intensity w_1 at the top varying linearly to zero at the base. In this analysis, only the first load case is considered, but the solutions for the other two load cases are given in Appendix 2.

3.2.2 Basic Assumptions

- (1) The structure is uniform throughout the height, including material properties, wall and connecting beam sections and storey height, and is rigidly built in at the base.
- (2) Plane sections remain plane after bending, for all structural members.
- (3) Both walls deflect equally at every floor level. That is, the connecting beams are assumed axially stiff so that no axial deformations occur in the beams. This assumption is justified by the fact that the coupled shear walls are surrounded by floor slabs which are very stiff in plane, and lateral forces are distributed to each wall through the floor slabs, rather than through the connecting beams, regardless of the assumption of the analytical model. The discrete set of connecting beams,

each of flexural rigidity EI_b , are then replaced by an equivalent continuous axially-rigid connecting medium of stiffness EI_b/h per unit height as shown in Fig. 3.4a, where h is the storey height. From this assumption, it follows that the slopes of the two walls are everywhere equal along the height, and thus, from a straightforward application of the slope-deflection equations, it may be shown that every connecting beam deforms with a point of contraflexure at its mid-span position. It also follows that the two walls have identical curvatures along the height, so that the bending moments in the two walls are proportional to their flexural rigidities.

(4) The axial forces, shear forces and bending moments in the connecting beams are then replaced by equivalent continuous distributions of intensity n , q and m per unit height, respectively. In particular, if the connecting medium is assumed cut along the vertical line of contraflexure, only a shear flow of intensity q and an axial force flow of intensity n exist, as shown in Fig. 3.4b.

3.2.3 Governing Differential Equations and General Solutions

In the structure which is assumed cut at the line of contraflexure, as shown in Fig. 3.4b, the relative vertical displacements at the cut ends of the connecting medium must be zero, and the condition of vertical displacement compatibility becomes,

$$l \frac{dy}{dx} - \frac{b^3 h}{12EI_b} q - \frac{1}{E} \left(\frac{1}{A_1} + \frac{1}{A_2} \right) \int_0^x N dx = 0 \quad (3.1)$$

in which N is the axial force in each wall, q is the shear flow at the cut ends of the connecting medium, y is the lateral displacement, l is the distance between the centroidal axes of the two walls, and A_1 and A_2 are the cross-sectional areas of the two walls. In the compatibility equation, the three

terms represent respectively the relative displacements due to the slopes of the walls, the displacements of the cut ends of the connecting medium due to the shears acting as concentrated forces on the ends of cantilever beams, and the displacements due to the axial deformations of the walls.

Considering the vertical equilibrium condition for a small element of wall subjected to the set of stress resultants shown in Fig. 3.5, it follows that,

$$\frac{dN}{dx} + q = 0 \quad (3.2)$$

The moment-curvature relationships for the walls are,

$$EI_1 \frac{d^2y}{dx^2} = M_1 = M - \left[\frac{b}{2} + d_1 \right] \int_x^H q(\lambda) d\lambda - M_a \quad (3.3)$$

$$EI_2 \frac{d^2y}{dx^2} = M_2 = - \left[\frac{b}{2} + d_2 \right] \int_x^H q(\lambda) d\lambda + M_a \quad (3.4)$$

in which EI_1 and EI_2 are the flexural rigidities of the two walls, M_1 and M_2 are the bending moments in the two walls, M is the applied external bending moment, λ is a dummy variable, and M_a is the moment due to the axial forces in the connecting medium.

The axial force N in each wall at any level is given by,

$$N = \int_x^H q(\lambda) d\lambda \quad (3.5)$$

The addition of Eqs. 3.3 and 3.4 yields the overall moment-curvature relationship,

$$EI \frac{d^2y}{dx^2} = M - I \int_x^H q(\lambda) d\lambda = M - IN \quad (3.6)$$

in which $I = I_1 + I_2$

On substituting q from Eq. 3.2 into Eq. 3.1 and differentiating once, the

equation becomes,

$$l \frac{d^2y}{dx^2} + \frac{b^3 h}{12EI_b} \frac{d^2N}{dx^2} - \frac{1}{E} \left(\frac{1}{A_1} + \frac{1}{A_2} \right) N = 0 \quad (3.7)$$

On either eliminating N or y from Eqs. 3.6 and 3.7, the governing differential equations either in terms of the axial force or the deflection can be obtained as follows,

$$\frac{d^2N}{dx^2} - k^2 \alpha^2 N = - \frac{\alpha^2}{l} M \quad (3.8)$$

$$\frac{d^4y}{dx^4} - k^2 \alpha^2 \frac{d^2y}{dx^2} = \frac{1}{EI} \left(\frac{d^2M}{dx^2} - (k^2 - 1) \alpha^2 M \right) \quad (3.9)$$

where

$$\alpha^2 = \frac{12I_b l^2}{b^3 h I} \quad (3.10)$$

$$k^2 = 1 + \frac{(A_1 + A_2) I}{A_1 A_2 l^2} \quad (3.11)$$

The general solutions of Eqs. 3.8 and 3.9 will be of the form,

$$N = K_1 \cosh k \alpha x + K_2 \sinh k \alpha x - \frac{1}{k^2 l} \left[1 + \frac{D^2}{k^2 \alpha^2} + \frac{D^4}{k^4 \alpha^4} + \dots \right] M \quad (3.12)$$

$$y = C_1 + C_2 x + C_3 \cosh k \alpha x + C_4 \sinh k \alpha x - \frac{1}{EI k^2 \alpha^2} \times \left[\frac{1}{D^2} + \frac{1}{k^2 \alpha^2} + \frac{D^2}{k^4 \alpha^4} + \frac{D^4}{k^6 \alpha^6} + \dots \right] \left[\frac{d^2 M}{dx^2} - (k^2 - 1) \alpha^2 M \right] \quad (3.13)$$

in which D is the operator d/dx , K_1 , K_2 and C_1 to C_4 are integration constants which must be determined from the appropriate boundary conditions.

3.2.4 Boundary Conditions

If the structure is rigidly built in at the base and free at the top, the boundary conditions can be deduced from the conditions of compatibility and the

equilibrium at the top and bottom of the structure as, in terms of axial force N ,

$$\text{At } x = 0, \quad \frac{dN}{dx} = 0 \quad (3.14)$$

$$\text{At } x = H, \quad N = 0 \quad (3.15)$$

and in terms of deflection y ,

$$\text{At } x = 0, \quad y = 0 \quad (3.16)$$

$$\text{At } x = 0, \quad dy/dx = 0 \quad (3.17)$$

$$\text{At } x = H, \quad d^2y/dx^2 = 0 \quad (3.18)$$

At $x = 0$, from Eq. 3.1, $q = 0$, and hence, from Eq. 3.2, $dN/dx = 0$, so that, on differentiating Eq. 3.6, the final boundary condition needed in term of y is derived as,

$$\text{At } x = 0, \quad EI \frac{d^3y}{dx^3} = \frac{dM}{dx} = -S_0 \quad (3.19)$$

in which S_0 is the total applied shear at the base.

3.2.5 Solution For Uniformly Distributed Lateral Load

For the case of a uniformly distributed load of intensity w_0 , the applied bending moment will be,

$$M = \frac{1}{2}w_0H^2\left(1 - \frac{x}{H}\right)^2 \quad (3.20)$$

The solutions of Eqs. 3.12 and 3.13, subjected to the boundary conditions of Eqs. 3.14 to 3.19 then become,

$$N = \frac{w_0H^2}{l} \left\{ \frac{1}{2k^2}(1 - \xi)^2 - \frac{\cosh k\alpha H \xi + k\alpha H \sinh k\alpha H (1-\xi) - \cosh k\alpha H}{k^2(k\alpha H)^2 \cosh k\alpha H} \right\} \quad (3.21)$$

$$y = \frac{w_0H^4}{EI} \left\{ \frac{k^2-1}{24k^2}(\xi^4 - 4\xi^3 + 6\xi^2) + \frac{1}{k^2(k\alpha H)^2}(\xi - \frac{\xi^2}{2}) + \frac{\cosh k\alpha H \xi + k\alpha H \sinh k\alpha H (1-\xi) - k\alpha H \sinh k\alpha H - 1}{k^2(k\alpha H)^4 \cosh k\alpha H} \right\} \quad (3.22)$$

in which $\xi = x/H$ is a non-dimensional height coordinate.

On differentiating Eq. 3.21, the shear flow q can be obtained as, from Eq. 3.2,

$$q = \frac{w_0 H}{k^2 I} \left\{ (1 - \xi) + \frac{\sinh k\alpha H \xi - k\alpha H \cosh k\alpha H (1 - \xi)}{k\alpha H \cosh k\alpha H} \right\} \quad (3.23)$$

Following the moment-curvature relationships for the two walls given by Eqs. 3.3 and 3.4, the moments in the two walls become, on differentiating Eq. 3.22,

$$M_1 = \frac{EI_1 w_0 H^2 F_M}{EI} \quad \text{and} \quad M_2 = \frac{EI_2 w_0 H^2 F_M}{EI} \quad (3.24)$$

in which

$$F_M = \frac{k^2 - 1}{2k^2} (1 - \xi)^2 - \frac{1}{k^2 (k\alpha H)^2} + \frac{\cosh k\alpha H \xi + \sinh k\alpha H (1 - \xi)}{k^2 (k\alpha H)^2 \cosh k\alpha H} \quad (3.25)$$

Considering the conditions of rotational equilibrium for the small vertical wall elements subjected to the set of stress resultants shown in Fig. 3.5, the shears in the two walls can be deduced as,

$$S_1 = - \frac{dM_1}{dx} + \left[\frac{b}{2} + d_1 \right] q \quad (3.26)$$

$$S_2 = - \frac{dM_2}{dx} + \left[\frac{b}{2} + d_2 \right] q \quad (3.27)$$

or,

$$S_1 = \frac{EI_1 w_0 H F_S}{EI} + \left[\frac{b}{2} + d_1 \right] q \quad (3.28)$$

$$S_2 = \frac{EI_2 w_0 H F_S}{EI} + \left[\frac{b}{2} + d_2 \right] q \quad (3.29)$$

in which,

$$F_S = \frac{k^2 - 1}{k^2} (1 - \xi) - \frac{\sinh k\alpha H \xi - \cosh k\alpha H (1 - \xi)}{k^2 (k\alpha H) \cosh k\alpha H} \quad (3.30)$$

and thus the axial force flow in the connecting medium can be obtained

by,

$$n = - \frac{dS_2}{dx} \quad (3.31)$$

or,

$$n = w_0 \left\{ \frac{EI}{EI} 2F_n - \frac{1}{l} \left[\frac{b}{2} + d_2 \right] (F_n - 1) \right\} \quad (3.32)$$

in which,

$$F_n = \frac{k^2 - 1}{k^2} + \frac{\cosh k\alpha H \xi + \sinh k\alpha H (1 - \xi)}{k^2 \cosh k\alpha H} \quad (3.33)$$

3.2.6 Study of Significant Parameters

It has been shown that the deflection of a pair of uniform coupled shear walls subjected to a uniformly distributed lateral load is described by Eq. 3.22. The equation is written in terms of two dimensionless parameters k and $k\alpha H$. These two parameters govern the deflected configuration of the structure. The value of k is expressed in Eq. 3.11. It is shown that for a given pair of shear walls, k is determined by the wall centroidal spacing l , and is greater than 1. It is usually in the range of 1.02 to 1.1 in practical structures. The parameter $k\alpha H$ involves the parameter α , which, defined by Eq. 3.10, is fundamental to the differential equations 3.8 and 3.9. This parameter α also depends on the centroidal distance l , but more important, it may be considered to define the flexural rigidity (I_b/h) or the stiffness of the connecting medium. In practice, $k\alpha H$ tends to lie between 1 and 8. Two extreme cases may be identified. When the connecting beams are very stiff, the structure will deflect like a single composite vertical cantilever, with the connecting beams acting effectively as dowels (Fig. 3.6a). On the other hand, when the connecting beams are very flexible, the shear walls will act as if they are pin-connected, and will deflect as independent flexural cantilevers (Fig. 3.6b). For beams of intermediate stiffnesses,

the induced shears give rise to restraining moments in the walls, Fig. 3.6c, which tend to produce a reverse bending action in the upper levels where the applied moments are least. The resulting deflection profile then takes the form shown in Fig. 3.7; the profile may be regarded as a combination of a bending mode in the lower levels, and a shearing mode in the upper levels.

The deflection profile of any particular structure will depend significantly on the relative values of the parameters k and $k\alpha H$. Fig. 3.8 shows a series of configurations, expressed in terms of the top deflection Y , for different values of the two parameters. The curves indicate that a coupled shear wall structure can take up a profile which may range between the two extremes of a pure flexural and a pure shearing mode. Because of the base boundary condition of zero vertical slope, it can never take up a pure shearing mode, although the deflection curve will approach it closely if k is very close to unity, say less than about 1.0001, and $k\alpha H$ is very large, say over 100. In Fig. 3.8, the curves corresponding to a particular value of k may be regarded as 'lower bounds' on the deflected shape, since the profile for any value of $k\alpha H$ will always lie on or above that particular curve; that is, the particular value of k defines how closely the deflection profile will approach the pure shearing mode. The corresponding curves of Fig. 3.9 show the value of $k\alpha H$ corresponding to the particular value of k for which the deflected profile will approach most closely a shearing mode. Unless k is less than about 1.01, the predominant mode of deformation will be flexure rather than shear.

It may be noted here that in a further study described in Chapter 4, it will be shown that the continuum theory reveals that coupled shear walls and wall-frame structure can be classified as a general family of cantilever structures, whose behaviour depends on the relative primary modes of lateral-load resisting

behaviour – flexure, shear and axial flexure. These primary modes depend on the relative value of two basic parameters k and $k\alpha H$.

3.3 Analysis of Interactions Between Coupled Shear Walls and Other Cantilevers

3.3.1 Interaction Between Coupled Shear Walls and Flexural Cantilevers

Consider a plane system consisting of a pair of coupled shear walls interacting with pure flexural cantilevers through a pin-ended connecting medium (Fig. 3.3a). Any number of linked cantilevers may be included, with the sum of their flexural rigidities represented by EI_B . In the analysis, most of the terms for coupled shear walls are still used, except that the axial force flow in the connecting medium and the top concentrated horizontal interactive force in the coupled shear walls are expressed respectively by n_1 and Q_1 , whilst n_2 and Q_2 are used to denote the axial force flow in the pin-ended connecting medium, and another top concentrated interactive horizontal force between the coupled shear walls and the flexural component (shown in Fig. 3.10).

The condition of compatibility for the coupled shear walls can be written in the same form as that of Eq. 3.7, which is,

$$l \frac{d^2 y}{dx^2} + \frac{b^3 h}{12EI_B} \frac{d^2 N}{dx^2} - \frac{1}{E} \left(\frac{1}{A_1} + \frac{1}{A_2} \right) N = 0 \quad (3.34)$$

The moment–curvature relationship for the coupled shear walls, (c.f. Eq. 3.6) is given by,

$$EI_C \frac{dy^2}{dx^2} = M_C - lN \quad (3.35)$$

in which $EI_C = EI_1 + EI_2$ is the sum of the flexural stiffnesses of the coupled shear walls, and M_C is the bending moment in the coupled shear walls.

The moment–curvature relationship for the flexural component is given by,

$$EI_B \frac{d^2 y}{dx^2} = M_B \quad (3.36)$$

in which M_B is the bending moment in the flexural component.

The addition of Eqs. 3.35 and 3.36 yields the overall moment–curvature relationship,

$$EI \frac{dy^2}{dx^2} = M - lN \quad (3.37)$$

in which $EI = EI_C + EI_B$ is the total flexural rigidity of the three walls, and M is the applied bending moment, $M = M_C + M_B$.

Following the same procedure as in Section 3.2.3, and differentiating either N or y from Eqs. 3.34 and 3.37, it may be shown that the governing equations take the same forms as those for coupled shear walls (Eqs. 3.8 and 3.9), with the parameters k and α now defined as,

$$\alpha^2 = \frac{12I_b l^2}{b^3 h I} \quad (3.38)$$

$$k^2 = 1 + \frac{(A_1 + A_2) I}{A_1 A_2 l^2} \quad (3.39)$$

where $I = I_C + I_B$ is now defined as the total flexural rigidity of the three components.

It may also be shown that, when subjected to a uniformly distributed lateral load with intensity of w_0 , the solutions for the axial force N in the coupled shear walls, the lateral deflection y , and the shear flow q_1 , the axial force flow n in the connecting medium take the same forms as that given by Eqs. 3.21, 3.22, 3.23 and 3.32 with α^2 and k^2 now redefined as in Eqs. 3.38 and 3.39.

After substituting from Eq. 3.22, differentiating Eq. 3.36, and dividing through by $-EI$, the shear force in the flexural component S_2 can be obtained as,

$$S_2 = \frac{EI_B w_0}{EI} H \left\{ \frac{k^2-1}{k^2} (1-\xi) - \frac{\sinh k\alpha H \xi - k\alpha H \cosh k\alpha H (1-\xi)}{k^2 k\alpha H \cosh k\alpha H} \right\} \quad (3.40)$$

When $x = H$, since a shear force again exists, a concentrated horizontal force must exist at the top, interacting between the coupled shear walls and the flexural component, of magnitude,

$$Q_2 = \frac{EI_B w_0}{EI} H \left\{ \frac{k\alpha H - \sinh k\alpha H}{k^2 k\alpha H \cosh k\alpha H} \right\} \quad (3.41)$$

The force-deflection relationship for the flexural cantilever can be expressed by,

$$EI_B \frac{d^4 y}{dx^4} = w_B = n_2 \quad (3.42)$$

On differentiating Eq. 3.22, and multiplying by EI_B , the axial force flow n_2 is then obtained from Eq. 3.42 as,

$$n_2 = \frac{EI_B w_0}{EI} \left\{ \frac{k^2-1}{k^2} + \frac{\cosh k\alpha H \xi + k\alpha H \sinh k\alpha H (1-\xi)}{k^2 \cosh k\alpha H} \right\} \quad (3.43)$$

3.3.2 Interaction Between Two Pairs of Linked Coupled Walls

The structure considered is a plane system consisting of two pairs of coupled shear walls interacting through pin-ended links, as shown in Figs. 3.3b and 3.11. In addition, for generality, following the discussions in the two earlier sections, the structure is assumed to include any number of linked independent flexural cantilevers of total flexural rigidity EI_B . The case of a pair of linked coupled shear walls is then obtained simply by putting EI_B equal to zero.

Referring to Eq. 3.7, the conditions of compatibility for the pair of coupled

shear walls can be expressed respectively as,

$$l_1 \frac{d^2y}{dx^2} + \frac{b_1^3 h_1}{12EI_{b_1}} \frac{d^2N_1}{dx^2} - \frac{1}{E} \left(\frac{1}{A_{11}} + \frac{1}{A_{12}} \right) N_1 = 0 \quad (3.44)$$

$$l_2 \frac{d^2y}{dx^2} + \frac{b_2^3 h_2}{12EI_{b_2}} \frac{d^2N_2}{dx^2} - \frac{1}{E} \left(\frac{1}{A_{21}} + \frac{1}{A_{22}} \right) N_2 = 0 \quad (3.45)$$

in which the same terms for coupled shear walls are still used as in the earlier section, the subscripts 1 and 2 being added to indicate the pair of the coupled shear walls considered.

From Eq. 3.6, the moment-curvature relationships for the two coupled shear walls are,

$$EI_{C_1} \frac{d^2y}{dx^2} = M_1 - l_1 N_1 \quad (3.46)$$

$$EI_{C_2} \frac{d^2y}{dx^2} = M_2 - l_2 N_2 \quad (3.47)$$

in which EI_{C_1} and EI_{C_2} are respectively the total flexural rigidities for the two pairs of the coupled shear walls, and M_1 and M_2 are the bending moments in the two coupled walls, respectively.

The moment-curvature relationship for any additional flexural cantilever carrying a moment M_B is given by,

$$EI_B \frac{d^2y}{dx^2} = M_B \quad (3.48)$$

Addition of Eqs. 3.46, 3.47 and 3.48 yields the overall moment-curvature relationship as,

$$EI \frac{d^2y}{dx^2} = M - l_1 N_1 - l_2 N_2 \quad (3.49)$$

in which $EI = EI_{C_1} + EI_{C_2} + EI_B$ is the total flexural rigidity of all the members, and the applied bending moment, which equals to the sum of the bending moments in all members is, $M = M_1 + M_2 + M_B$.

On eliminating any two of the three unknowns N_1 , N_2 and y from Eqs. 3.44, 3.45 and 3.49, the governing differential equations can be derived as:

For the axial forces N_1 and N_2 ,

$$\frac{d^4 N_1}{dx^4} - p_1 \frac{d^2 N_1}{dx^2} + p_2 N_1 = -r_1 \frac{d^2 M}{dx^2} + r_1 \alpha_2^2 (k_2^2 - 1) M \quad (3.50)$$

$$\frac{d^4 N_2}{dx^4} - p_1 \frac{d^2 N_2}{dx^2} + p_2 N_2 = -r_2 \frac{d^2 M}{dx^2} + r_2 \alpha_1^2 (k_1^2 - 1) M \quad (3.51)$$

For the deflection,

$$\frac{d^6 y}{dx^6} - p_1 \frac{d^4 y}{dx^4} + p_2 \frac{d^2 y}{dx^2} = \frac{1}{EI} \left\{ \frac{d^4 M}{dx^4} - p_3 \frac{d^2 M}{dx^2} + p_4 M \right\} \quad (3.52)$$

in which,

$$\alpha_1^2 = \frac{12 I_{b_1} l_1^2}{b_1^3 h_1 I_{C_1}} \quad (3.53)$$

$$k_1^2 = \left(\frac{A_1 I_{C_1}}{A_{11} A_{12} l_1^2} + 1 \right) \quad (3.54)$$

$$\alpha_2^2 = \frac{12 I_{b_2} l_2^2}{b_2^3 h_2 I_{C_2}} \quad (3.55)$$

$$k_2^2 = \left(\frac{A_2 I_{C_2}}{A_{21} A_{22} l_2^2} + 1 \right) \quad (3.56)$$

$$p_1 = (k_1^2 - \frac{I_{C_2}}{I}) \alpha_1^2 + (k_2^2 - \frac{I_{C_1}}{I}) \alpha_2^2 \quad (3.57)$$

$$p_2 = \alpha_1^2 \alpha_2^2 (k_1^2 k_2^2 - \frac{I_{C_1} k_1^2}{I} - \frac{I_{C_2} k_2^2}{I}) \quad (3.58)$$

$$p_3 = \alpha_1^2 (k_1^2 - 1) + \alpha_2^2 (k_2^2 - 1) \quad (3.59)$$

$$p_4 = \alpha_1^2 \alpha_2^2 (k_1^2 - 1) (k_2^2 - 1) \quad (3.60)$$

$$r_1 = \frac{I_{C_1}}{I} \frac{\alpha_1^2}{l_1} \quad (3.61)$$

$$r_2 = \frac{I_{C_2}}{I} \frac{\alpha_2^2}{l_2} \quad (3.62)$$

The solutions of Eqs. 3.50, 3.51 and 3.52, will be of the form,

$$N_1 = C_1 \cosh \lambda_1 x + C_2 \sinh \lambda_1 x + C_3 \cosh \lambda_2 x + C_4 \sinh \lambda_2 x + N_1^* \quad (3.63)$$

$$N_2 = D_1 \cosh \lambda_1 x + D_2 \sinh \lambda_1 x + D_3 \cosh \lambda_2 x + D_4 \sinh \lambda_2 x + N_2^* \quad (3.64)$$

$$y = K_1 + K_2 x + K_3 \cosh \lambda_1 x + K_4 \sinh \lambda_1 x + K_5 \cosh \lambda_2 x + K_6 \sinh \lambda_2 x + y^* \quad (3.65)$$

in which C_1 to C_4 , D_1 to D_4 and K_1 to K_6 are integration constants which must be determined from the appropriate boundary conditions, N_1^* , N_2^* and y^* are particular integral solutions for specific load cases, and $\pm \lambda_1$ and $\pm \lambda_2$, are the four roots of the homogeneous equation for the differential equations 3.50, 3.51 and 3.52, which is,

$$\lambda^4 - p_1 \lambda^2 + p_2 = 0 \quad (3.66)$$

The four roots are then given by,

$$\lambda^2 = \frac{1}{2}(p_1 \pm \sqrt{p_1^2 - 4p_2}) \quad (3.67)$$

As it is known that, $I \gg IC_1 + IC_2$, it is not difficult to prove from Eq. 3.57 and 3.48 that both p_1 and $p_2 \gg 0$, and it can be shown that,

$$p_1^2 - 4p_2 = \left[(k_1 - \frac{IC_2}{I})\alpha_1^2 - (k_2 - \frac{IC_1}{I})\alpha_2^2 \right]^2 + 4\alpha_1^2 \alpha_2^2 \frac{IC_1 IC_2}{I^2} \quad (3.68)$$

Hence, $p_1^2 - 4p_2 \gg 0$, so,

$$\frac{1}{2}(p_1 + \sqrt{p_1^2 - 4p_2}) \gg 0 \quad (3.69a)$$

and,

$$\frac{1}{2}(p_1 - \sqrt{p_1^2 - 4p_2}) \gg \frac{1}{2}(p_1 - \sqrt{p_1^2}) = 0 \quad (3.69b)$$

From the expression 3.69, the right side of Eq. 3.67 must have real and non-negative values. The four roots determined by Eq. 3.67 must then have real values, which is necessary for the solutions given by Eqs. 3.63, 3.64 and 3.65 to exist in those forms.

By considering the conditions of compatibility and equilibrium at the top and bottom of the structure, appropriate boundary conditions may be deduced in terms of the axial forces or the deflection. If the structure is rigidly built in at the base and free at the top, the boundary conditions in both cases can be shown to be,

Case 1. In terms of the axial forces N_1 or N_2 ,

$$(a) \text{ At } x = H, \quad N_i = 0 \quad (i = 1, 2) \quad (3.70)$$

$$(b) \text{ At } x = 0, \quad \frac{dN_i}{dx} = 0 \quad (3.71)$$

As it is known that at $x = H$, $N_i = 0$, and $d^2y/dx^2 = 0$, so from Eqs. 3.44 and 3.45, it is shown that,

$$(c) \text{ At } x = H, \quad \frac{d^2N_i}{dx^2} = 0 \quad (3.72)$$

On differentiating Eq. 3.44 or 3.45, it can be shown that,

$$EI_i \alpha_i^2 \frac{d^3y}{dx^3} + l_i \frac{d^3N_i}{dx^3} - (k_i^2 - 1) \alpha_i^2 l_i \frac{dN_i}{dx} = 0 \quad (3.73)$$

On differentiating Eq. 3.49, it is found that,

$$EI \frac{d^3y}{dx^3} = \frac{dM}{dx} - l_1 \frac{dN_1}{dx} - l_2 \frac{dN_2}{dx} \quad (3.74)$$

Since, at $x = 0$, $dN_i/dx = 0$, the final base boundary conditions needed can be deduced as,

$$(d) \text{ At } x = 0, \quad \frac{d^3N_i}{dx^3} = - \frac{I_i \alpha_i^2}{I l_i} \frac{dM}{dx} \quad (3.75)$$

Case 2. In terms of the deflection y ,

$$(a) \text{ At } x = 0, \quad y = 0 \quad (3.76)$$

$$(b) \text{ At } x = 0, \quad \frac{dy}{dx} = 0 \quad (3.77)$$

$$(c) \text{ At } x = H, \quad \frac{d^2y}{dx^2} = 0 \quad (3.78)$$

and from Eqs. 3.71 and 3.74

$$(d) \text{ At } x = 0, \quad EI \frac{d^3y}{dx^3} = \frac{dM}{dx} \quad (3.79)$$

Since from Eq. 3.72, at $x = H$, $d^2N/dx^2 = 0$, on differentiating Eq. 3.74, the fifth boundary condition becomes,

$$(e) \text{ At } x = H, \quad EI \frac{d^4y}{dx^4} = \frac{d^2M}{dx^2} \quad (3.80)$$

Further, on differentiating Eq. 3.74 twice, and using Eq. 3.75 to obtain the third derivative of N , the final boundary condition becomes,

$$(f) \text{ At } x = 0, \quad EI \frac{d^5y}{dx^5} = \frac{d^3M}{dx^3} - \left(\frac{IC_1}{I} \alpha_1^2 + \frac{IC_2}{I} \alpha_2^2 \right) \frac{dM}{dx} \quad (3.81)$$

For the case of a uniformly distributed lateral load of intensity w_0 , the particular solutions can be chosen to be,

$$N_1^* = \frac{\alpha_2^2(k_2^2-1)w_0r_1H^2}{\lambda_1^2\lambda_2^2} \left\{ \frac{1}{(\lambda_1H)^2} + \frac{1}{(\lambda_2H)^2} + \frac{(1-\xi)^2}{2} \right\} + \frac{r_1w_0}{\lambda_1^2\lambda_2^2} \quad (3.82)$$

$$N_2^* = \frac{\alpha_1^2(k_1^2-1)w_0r_2H^2}{\lambda_1^2\lambda_2^2} \left\{ \frac{1}{(\lambda_1H)^2} + \frac{1}{(\lambda_2H)^2} + \frac{(1-\xi)^2}{2} \right\} + \frac{r_2w_0}{\lambda_1^2\lambda_2^2} \quad (3.83)$$

$$y^* = \frac{w_0H^4}{EI} \frac{\alpha_1^2(k_1^2-1)\alpha_2^2(k_2^2-1)}{\lambda_1^2\lambda_2^2} \left\{ \frac{1}{2} \left(\frac{1}{(\lambda_1H)^2} + \frac{1}{(\lambda_2H)^2} \right) + \frac{\xi^4 - 4\xi^3 + 6\xi^2}{24} \right\} - \frac{w_0H^2}{2EI} \frac{\alpha_1^2(k_1^2-1) + \alpha_2^2(k_2^2-1)}{\lambda_1^2\lambda_2^2} \quad (3.84)$$

The four constants C_1 to C_4 then can be determined from the boundary conditions of Eqs. 3.70, 3.71, 3.72 and 3.75, leading to the following expressions,

$$C_1 = r_1 w_0 H^2 \frac{[\alpha_2^2(k_2^2-1) - \lambda_1^2](\lambda_1 H \sinh \lambda_1 H + 1)}{\lambda_1^2(\lambda_1^2 - \lambda_2^2)(\lambda_1 H)^2 \cosh \lambda_1 H} \quad (3.85)$$

$$C_2 = -r_1 w_0 H^2 \frac{\alpha_2^2(k_2^2-1) - \lambda_1^2}{\lambda_1^2(\lambda_1^2 - \lambda_2^2)\lambda_1 H} \quad (3.86)$$

$$C_3 = -r_1 w_0 H^2 \frac{[\alpha_2^2(k_2^2-1) - \lambda_2^2](\lambda_2 H \sinh \lambda_2 H + 1)}{\lambda_2^2(\lambda_1^2 - \lambda_2^2)(\lambda_2 H)^2 \cosh \lambda_2 H} \quad (3.87)$$

$$C_4 = r_1 w_0 H^2 \frac{\alpha_2^2(k_2^2-1) - \lambda_2^2}{\lambda_2^2(\lambda_1^2 - \lambda_2^2)\lambda_2 H} \quad (3.88)$$

The expressions for the constants D_1 to D_4 can be obtained simply by changing the subscripts of r , α and k from 1 to 2. The constants K_1 to K_6 in Eq. 3.65 can also be determined from the boundary conditions in terms of the deflection y provided by Eqs. 3.76 to 3.81. However, instead of solving 6 equations to determine 6 constants, the solution for the deflection can also be obtained by integrating Eq. 3.49, in which the two axial forces are already known. In this case, only two boundary conditions in terms of the deflection y are required to determine the two integration constants. Then,

$$EIy = K_a + K_b x - l_1 \iint N_1 dx dx - l_2 \iint N_2 dx dx + \iint M dx dx \quad (3.89)$$

in which K_a and K_b are the two integration constants concerned.

On eliminating the deflection y from Eqs. 3.46 to 3.49, the resultant bending moments in the three components can be obtained as,

$$M_1 = \frac{IC_1}{I}(M - l_1 N_1 - l_2 N_2) + l_1 N_1 \quad (3.90)$$

$$M_2 = \frac{IC_2}{I}(M - l_1 N_1 - l_2 N_2) + l_2 N_2 \quad (3.91)$$

$$M_B = \frac{IB}{I}(M - l_1 N_1 - l_2 N_2) \quad (3.92)$$

On differentiating Eqs. 3.90 to 3.92, the resultant shears in the three components can be obtained as,

$$S_1 = \frac{I_{C1}}{I} \left(-\frac{dM}{dx} + l_1 \frac{dN_1}{dx} + l_2 \frac{dN_2}{dx} \right) - l_1 \frac{dN_1}{dx} \quad (3.93)$$

$$S_2 = \frac{I_{C2}}{I} \left(-\frac{dM}{dx} + l_1 \frac{dN_1}{dx} + l_2 \frac{dN_2}{dx} \right) - l_2 \frac{dN_2}{dx} \quad (3.94)$$

$$S_B = \frac{I_B}{I} \left(-\frac{dM}{dx} + l_1 \frac{dN_1}{dx} + l_2 \frac{dN_2}{dx} \right) \quad (3.95)$$

in which S_1 , S_2 and S_B are the resultant shears exerted on the two pairs of coupled shear walls and the flexural cantilever, respectively.

The differentiation of Eqs. 3.93 to 3.94 will yield the expressions for the resultant distributed forces on the three components, respectively as,

$$w_1 = \frac{I_{C1}}{I} \left(\frac{d^2M}{dx^2} - l_1 \frac{d^2N_1}{dx^2} - l_2 \frac{d^2N_2}{dx^2} \right) + l_1 \frac{d^2N_1}{dx^2} \quad (3.96)$$

$$w_2 = \frac{I_{C2}}{I} \left(\frac{d^2M}{dx^2} - l_1 \frac{d^2N_1}{dx^2} - l_2 \frac{d^2N_2}{dx^2} \right) + l_2 \frac{d^2N_2}{dx^2} \quad (3.97)$$

$$w_B = \frac{I_B}{I} \left(\frac{d^2M}{dx^2} - l_1 \frac{d^2N_1}{dx^2} - l_2 \frac{d^2N_2}{dx^2} \right) \quad (3.98)$$

3.3.3 Interaction Between Coupled Shear Walls and Shear Cantilevers

The structural system considered consists of a pair of coupled shear walls interacting with a shear cantilever. For generality, the structure is also assumed to include a flexural cantilever of flexural rigidity EI_B , which is linked to the other two components, as shown in Figs. 3.3c and 3.12.

The compatibility equation, Eq. 3.7, again applies for the coupled shear walls. That is,

$$l \frac{d^2y}{dx^2} + \frac{b^3 h}{12EI_b} \frac{d^2N}{dx^2} - \frac{1}{E} \left(\frac{1}{A_1} + \frac{1}{A_2} \right) N = 0 \quad (3.99)$$

The force-deformation relationships for the three components in the structure will be:

Coupled shear walls,

$$EI_C \frac{d^2y}{dx^2} = M_C - lN \quad (3.100)$$

in which M_C is the moment in the coupled shear walls, and $EI_C = EI_1 + EI_2$ is the sum of the flexural stiffnesses of the coupled shear walls.

Shear cantilever,

$$GA \frac{dy}{dx} = S_S = - \frac{dM_S}{dx} \quad (3.101)$$

in which S_S and M_S are the shear and moment in the shear cantilever.

Flexural cantilever,

$$EI_B \frac{d^2y}{dx^2} = M_B \quad (3.102)$$

in which M_B is the bending moment in the flexural cantilever.

The addition of above equations 3.100, 3.101 and 3.102 yields the overall force-deformation relationship,

$$\frac{d^3y}{dx^3} - \beta^2 \frac{dy}{dx} = \frac{1}{EI} \left\{ \frac{dM}{dx} - l \frac{dN}{dx} \right\} \quad (3.103)$$

in which $M = M_C + M_S + M_B$ is the applied bending moment, and,

$$\beta^2 = \frac{GA}{EI} \quad (3.104)$$

where $EI = EI_C + EI_B$.

On eliminating either N or y from Eqs. 3.99 and 3.103, the governing differential equations for the deflection and the axial force are obtained as,

$$\frac{d^5y}{dx^5} - (k^2\alpha^2 + \beta^2)\frac{d^3y}{dx^3} + (k^2 - 1)\alpha^2\beta^2\frac{dy}{dx} = \frac{1}{EI}\left\{\frac{d^3M}{dx^3} - (k^2 - 1)\alpha^2\frac{dM}{dx}\right\} \quad (3.105)$$

$$\frac{d^4N}{dx^4} - (k^2\alpha^2 + \beta^2)\frac{d^2N}{dx^2} + (k^2 - 1)\alpha^2\beta^2N = -\frac{\alpha^2}{I}\frac{d^2M}{dx^2} \quad (3.106)$$

in which k and α are defined in Eqs. 3.38 and 3.39 in which I is now defined as, $I = I_C + I_B$.

The general solutions of Eqs. 3.105 and 3.106 will be of the forms:

For the deflection y ,

$$y = C_1 \cosh \lambda_1 x + C_2 \sinh \lambda_1 x + C_3 \cosh \lambda_2 x + C_4 \sinh \lambda_2 x + C_5 + y^* \quad (3.107)$$

For the axial force N ,

$$N = D_1 \cosh \lambda_1 x + D_2 \sinh \lambda_1 x + D_3 \cosh \lambda_2 x + D_4 \sinh \lambda_2 x + N^* \quad (3.108)$$

in which y^* and N^* are particular integral solutions for specific load cases, C_1 to C_5 , and D_1 to D_4 are integration constants which must be determined from the appropriate boundary conditions, and $\pm\lambda_1$ and $\pm\lambda_2$ are again the four roots of the homogeneous polynomial equation which is given by,

$$\lambda^4 - (k^2\alpha^2 + \beta^2)\lambda^2 + (k^2 - 1)\alpha^2\beta^2 = 0 \quad (3.109)$$

The four roots are obtained from,

$$\lambda^2 = \frac{k^2\alpha^2 + \beta^2 \pm \sqrt{(k^2\alpha^2 + \beta^2)^2 - 4(k^2 - 1)\alpha^2\beta^2}}{2} \quad (3.110)$$

The roots may again be readily proved to be real.

For the structure which is rigidly built in at the base and free at the top, by considering the conditions of compatibility and equilibrium, the boundary conditions in the two cases become,

Case 1. In terms of deflection y ,

$$\text{At } x = 0, \quad y = 0 \quad (3.111)$$

$$\text{At } x = 0, \quad \frac{dy}{dx} = 0 \quad (3.112)$$

$$\text{At } x = H, \quad \frac{d^2y}{dx^2} = 0 \quad (3.113)$$

Referring to Eq. 3.79,

$$\text{At } x = 0, \quad EI \frac{d^3y}{dx^3} = \frac{dM}{dx} \quad (3.114)$$

And referring to Eq. 3.80

$$\text{At } x = H, \quad EI \frac{d^4y}{dx^4} = \frac{d^2M}{dx^2} \quad (3.115)$$

Case 2. In terms of axial forces N ,

$$\text{At } x = H, \quad N = 0 \quad (3.116)$$

$$\text{At } x = 0, \quad \frac{dN}{dx} = 0 \quad (3.117)$$

$$\text{At } x = H, \quad \frac{d^2N}{dx^2} = 0 \quad (3.118)$$

On differentiating Eq. 3.99, it can be shown that,

$$EI\alpha^2 \frac{d^3y}{dx^3} + l \frac{d^3N}{dx^3} - (k^2-1)\alpha^2 l \frac{dN}{dx} = 0 \quad (3.119)$$

It then follows from Eqs. 3.114 and 2.117 that,

$$\text{At } x = 0, \quad \frac{d^3N}{dx^3} = - \frac{\alpha^2}{l} \frac{dM}{dx} \quad (3.120)$$

In the case of a uniformly distributed distributed lateral load with an intensity of w_0 , the expression for the applied moment is given by Eq. 3.20, and

the particular solutions in Eqs. 3.107 and 3.108 may be chosen to be,

$$y^* = - \frac{w_0 H^2}{2EI\beta^2} \left(1 - \frac{x}{H}\right)^2 \quad (3.121)$$

and,

$$N^* = - \frac{w_0}{(k^2-1)\beta^2 l} \quad (3.122)$$

The constants in Eqs. 3.107 and 3.108, are then determined from the boundary conditions of Eqs. 3.111 to 3.120 as,

$$C_1 = \frac{w_0 H^2}{EI\beta^2} \frac{\beta^2 - \lambda_2^2}{\lambda_1^2 - \lambda_2^2} \frac{1 + \lambda_1 H \sinh \lambda_1 H}{(\lambda_1 H)^2 \cosh \lambda_1 H} \quad (3.123)$$

$$C_2 = - \frac{w_0 H^2}{EI\beta^2} \frac{\beta^2 - \lambda_2^2}{\lambda_1^2 - \lambda_2^2} \frac{1}{\lambda_1 H} \quad (3.124)$$

$$C_3 = - \frac{w_0 H^2}{EI\beta^2} \frac{\beta^2 - \lambda_1^2}{\lambda_1^2 - \lambda_2^2} \frac{1 + \lambda_2 H \sinh \lambda_2 H}{(\lambda_2 H)^2 \cosh \lambda_2 H} \quad (3.125)$$

$$C_4 = \frac{w_0 H^2}{EI\beta^2} \frac{\beta^2 - \lambda_1^2}{\lambda_1^2 - \lambda_2^2} \frac{1}{\lambda_2 H} \quad (3.126)$$

$$C_5 = \frac{w_0 H^2}{EI\beta^2} \left\{ \frac{1}{2} - \frac{1}{\lambda_1^2 - \lambda_2^2} \left[\frac{(\beta^2 - \lambda_2^2)(1 + \lambda_1 H \sinh \lambda_1 H)}{(\lambda_1 H)^2 \cosh \lambda_1 H} - \frac{(\beta^2 - \lambda_1^2)(1 + \lambda_2 H \sinh \lambda_2 H)}{(\lambda_2 H)^2 \cosh \lambda_2 H} \right] \right\} \quad (3.127)$$

$$D_1 = - \frac{w_0 H^2 \alpha^2}{l(\lambda_1^2 - \lambda_2^2)} \frac{1 + \lambda_1 H \sinh \lambda_1 H}{(\lambda_1 H)^2 \cosh \lambda_1 H} \quad (3.128)$$

$$D_2 = \frac{w_0 H^2 \alpha^2}{l(\lambda_1^2 - \lambda_2^2)} \frac{1}{\lambda_1 H} \quad (3.129)$$

$$D_3 = \frac{w_0 H^2 \alpha^2}{l(\lambda_1^2 - \lambda_2^2)} \frac{1 + \lambda_2 H \sinh \lambda_2 H}{(\lambda_2 H)^2 \cosh \lambda_2 H} \quad (3.130)$$

$$D_4 = - \frac{w_0 H^2 \alpha^2}{l(\lambda_1^2 - \lambda_2^2)} \frac{1}{\lambda_2 H} \quad (3.131)$$

By eliminating y from Eq. 3.99, 3.100 and 3.102, the expressions for the resultant bending moments in the coupled shear walls and the flexural cantilever, in terms of N , are obtained as,

$$M_C = - \frac{I_C l}{I} \left\{ \frac{1}{\alpha^2} \frac{d^2 N}{dx^2} - (k^2 - 1)N \right\} + lN \quad (3.132)$$

$$M_B = - \frac{I_B l}{I} \left\{ \frac{1}{\alpha^2} \frac{d^2 N}{dx^2} - (k^2 - 1)N \right\} \quad (3.133)$$

The moment in the shear cantilever then can be obtained by subtracting M_C and M_B from the applied moment, which yields,

$$M_S = M + l \left\{ \frac{1}{\alpha^2} \frac{d^2 N}{dx^2} - k^2 N \right\} \quad (3.134)$$

On differentiating Eqs. 3.132, 3.133 and 3.134, the resultant shear in the three components are then obtained respectively as,

$$S_C = \frac{I_C l}{I} \left\{ \frac{1}{\alpha^2} \frac{d^3 N}{dx^3} - (k^2 - 1) \frac{dN}{dx} \right\} - l \frac{dN}{dx} \quad (3.135)$$

$$S_B = \frac{I_B l}{I} \left\{ \frac{1}{\alpha^2} \frac{d^3 N}{dx^3} - (k^2 - 1) \frac{dN}{dx} \right\} \quad (3.136)$$

$$S_S = w_0 H \left(1 - \frac{x}{H} \right) - l \left\{ \frac{1}{\alpha^2} \frac{d^3 N}{dx^3} - k^2 \frac{dN}{dx} \right\} \quad (3.137)$$

On further differentiating the shears from Eqs. 3.135, 3.136 and 3.137, the resultant distributed forces in the three components are obtained as,

$$w_C = - \frac{I_C l}{I} \left\{ \frac{1}{\alpha^2} \frac{d^4 N}{dx^4} - (k^2 - 1) \frac{d^2 N}{dx^2} \right\} + l \frac{d^2 N}{dx^2} \quad (3.138)$$

$$w_B = - \frac{I_B l}{I} \left\{ \frac{1}{\alpha^2} \frac{d^4 N}{dx^4} - (k^2 - 1) \frac{d^2 N}{dx^2} \right\} \quad (3.139)$$

and,

$$w_S = w_0 + l \left\{ \frac{1}{\alpha^2} \frac{d^4 N}{dx^4} - k^2 \frac{d^2 N}{dx^2} \right\} \quad (3.140)$$

In Eqs. 3.132 to 3.140, the subscripts C , B and S refer to coupled shear walls, the flexural cantilever and the shear cantilever, respectively.

3.4 Numerical Examples

Example 1. Coupled shear walls subjected to lateral load

In order to examine the continuum theory of coupled shear walls presented in Section 3.2, two representative examples of coupled shear walls individually subjected to uniformly distributed lateral loads are considered as follows:

The original data for the examples are,

Storey height h	2.8 m
Number of storeys	30
Total height H	84 m
Modulus of elasticity E	1.40×10^7 kN/m ²
Uniformly distributed load w_0	10 kN/m

Coupled shear walls 1:

Depths of the two walls	$D_1 = 5.5$ m, $D_2 = 4.5$ m
Clear span of the beams b	2.0 m
Depths of the connecting beams D_b	0.4 m
Thickness of the walls and beams t	0.3 m

Coupled shear walls 2:

Depths of the two walls	$D_1 = 4.5$ m, $D_2 = 4.0$ m
Clear span of the beams b	3.5 m
Depths of the connecting beams D_b	0.4 m
Thickness of the walls and beams t	0.3 m

The calculated parameters are:

Coupled shear wall 1:

$$EI = 9.0125 \times 10^7 \text{ kN m}^2$$

$$k = 1.084868$$

$$\alpha = 0.076652 \text{ m}^{-1}$$

$$k\alpha H = 6.9853$$

Coupled shear wall 2:

$$EI = 5.4294 \times 10^7 \text{ kN m}^2$$

$$k = 1.049588$$

$$\alpha = 0.048896 \text{ m}^{-1}$$

$$k\alpha H = 4.3109$$

The solutions of the present method are compared with the results obtained from the FLASH program using the wide-column frame analogy. The result curves are shown in Figs. 3.13 to 3.20 for the two examples, in which, unless specified, the thicker (smooth) lines refer to the results obtained from the present method, and the thinner (discontinuous) lines refer to the results obtained from the FLASH program. Fig. 3.13 shows the deflection curves for the two pairs of coupled shear walls from which it can be seen that both the continuum method and the FLASH program produce almost exactly the same results so that the two pairs of the curves are almost identical. Figs. 3.14 to 3.16 show respectively the axial forces in the walls, the shear flows in the connecting beams, and the axial force flows in the connecting beams, for the two examples. Figs. 3.17 and 3.19 show the moments and the shears in the two walls of the first pair of coupled shear walls, and Figs. 3.18 and 3.20 show the same curves for the second pair of coupled shear walls. From these two examples, it can be seen that compared with

the more exact finite element method the continuum hand method gives extremely accurate results for coupled shear wall structures. It is worth noting that both examples are unequal-wall coupled shear wall structures.

Example 2. Interaction Between Two Pairs of Coupled Shear Walls

This example considers the analysis of two pairs of linked coupled shear walls subjected to a uniformly distributed lateral load, $w_0 = 20$ kN/m, using the method presented in Section 3.3.2. The two pairs of coupled walls in Example 1 are still used in this example with the same original data and parameters presented in Example 1. The additional parameters needed in this analysis are as follows:

New parameters:

$$\lambda_1 = 0.0739465 \text{ m}^{-1}, \quad \lambda_1 H = 6.173553$$

$$\lambda_2 = 0.0194942 \text{ m}^{-1}, \quad \lambda_2 H = 1.637511$$

Integration constants:

$$C_1 = -111.8205 \text{ kN}, \quad D_1 = -20.9830 \text{ kN}$$

$$C_2 = 111.7492 \text{ kN}, \quad D_2 = 20.9696 \text{ kN}$$

$$C_3 = 184.9143 \text{ kN}, \quad D_3 = -197.0646 \text{ kN}$$

$$C_4 = -159.9632 \text{ kN}, \quad D_4 = 170.4740 \text{ kN}$$

$$K_a = 2.98623 \times 10^{-5} \text{ m} \times EI$$

$$K_b = 7.41286 \times 10^{-2} \text{ m} \times EI$$

The solution of the analysis is then compared with the 'FLASH' results, shown in Fig. 3.21, for the deflection, Fig. 3.22, for the axial forces, and Figs. 3.23, 3.24 and 3.25, for the load distributions, the shear distributions and

the moment distributions, respectively, for the two pairs of coupled shear walls.

From all the curves, it can be concluded that the analysis produces very good results compared with those obtained from the more 'exact' computer finite element method, the FLASH program.

Example 3. Interaction Between Coupled Shear Walls and Shear Cantilever

This example considers the analysis of the interaction between a pair of coupled shear walls and a shear cantilever — a 5-span lumped rigid frame, subjected to a uniformly distributed lateral load, $w_0 = 20 \text{ kN/m}$, using the method presented in Section 3.3.3. The coupled shear walls used in this example is Coupled Shear Walls 1 in Example 1. The lumped rigid frame which represents three identical frames is described as follows:

Lumped rigid frame (total stiffnesses):

Beam spans b_i ($i = 1$ to 5) 2.5, 3.0, 2.0, 2.5, 2.0 m

Inertias of beams I_{bi} $4.0000 \times 10^{-3} \text{ m}^4$

Column storey heights h_c 2.80 m

Inertias of columns I_{ci} ($i = 1$ to 6) $1.5625 \times 10^{-2} \text{ m}^4$

From Eq. 2.15,

$$GA = 4.0287 \times 10^5 \text{ kN}$$

Calculated parameters:

$$\alpha = 0.076652 \text{ m}^{-1}$$

$$k = 1.084868$$

$$\beta = 0.066859 \text{ m}^{-1}$$

$$\lambda_1 = 0.1046967 \text{ m}^{-1}, \quad \lambda_1 H = 8.794520$$

$$\lambda_2 = 0.0205904 \text{ m}^{-1}, \quad \lambda_2 H = 1.729597$$

Integration constants:

$$C_1 = 0.0152945 \text{ m}$$

$$C_2 = -0.0152940 \text{ m}$$

$$C_3 = 0.1419560 \text{ m}$$

$$C_4 = -0.1247595 \text{ m}$$

$$C_5 = 0.0178928 \text{ m}$$

$$D_1 = -1278.2374 \text{ kN}$$

$$D_2 = 1278.1934 \text{ kN}$$

$$D_3 = 7395.0996 \text{ kN}$$

$$D_4 = -6499.2578 \text{ kN}$$

The solution of the analysis is compared with the FLASH results, noting that, in the FLASH analysis, the influence of the axial deformations in the columns of the frames, or the overall axial bending effect is suppressed by specifying large values of the cross-sectional areas of the columns since it is not included in the shear cantilever model.

The comparison curves are shown in Fig. 3.26 for the deflection, in Fig. 3.27 for the axial forces in the coupled shear walls, and in Figs. 3.27, 3.28 and 3.29 for the load distribution, the shear distribution and the moment distribution between the two elements, respectively. It can be seen that very accurate results are obtained from the present method when compared with the FLASH analysis.

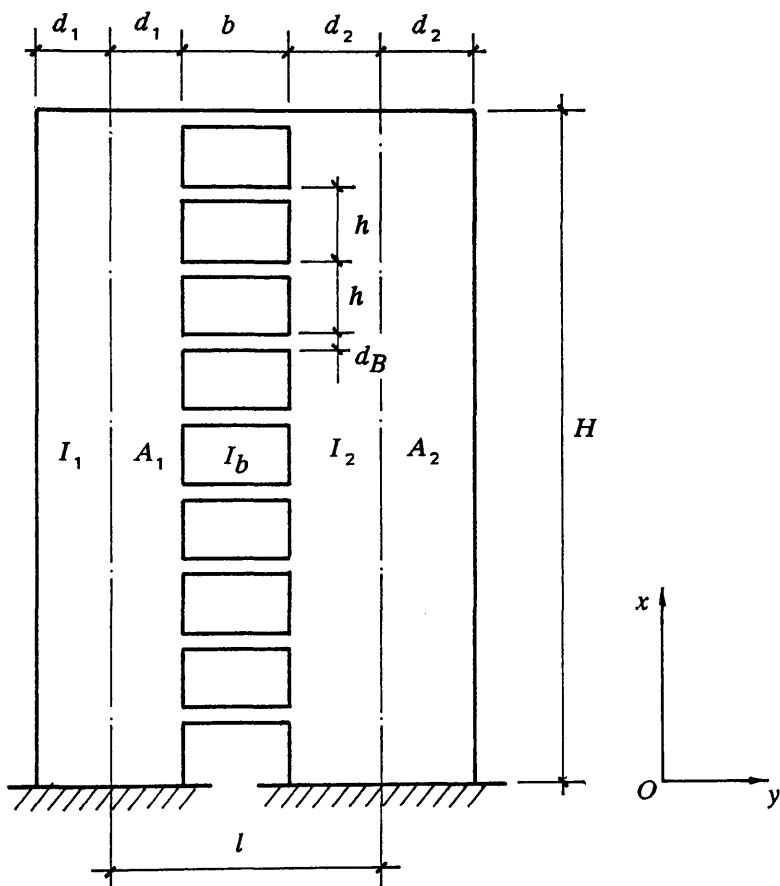


Fig. 3.1 Coupled Shear Walls

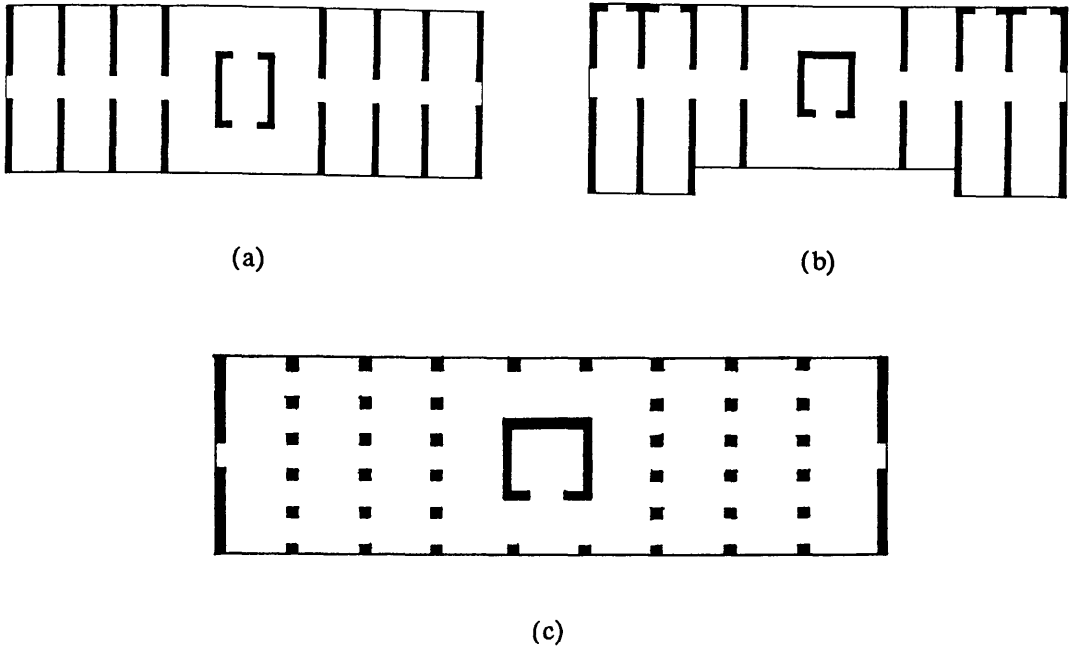


Fig. 3.2 Coupled Shear Wall Structures

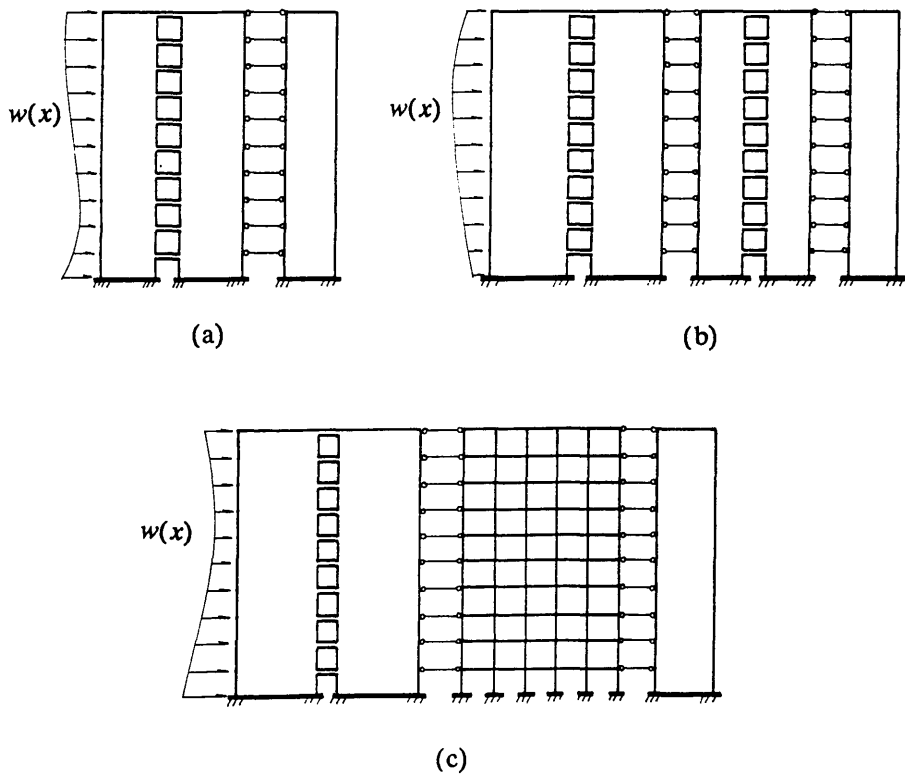


Fig. 3.3 Representation of Symmetric Coupled Shear Wall Structures

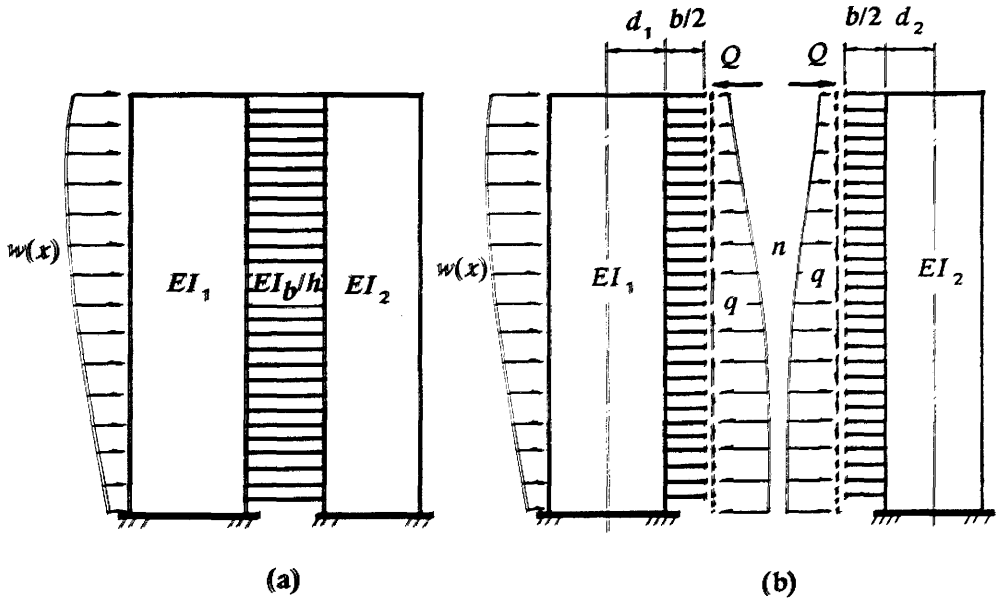


Fig. 3.4 Continuum Model of Coupled Shear Walls

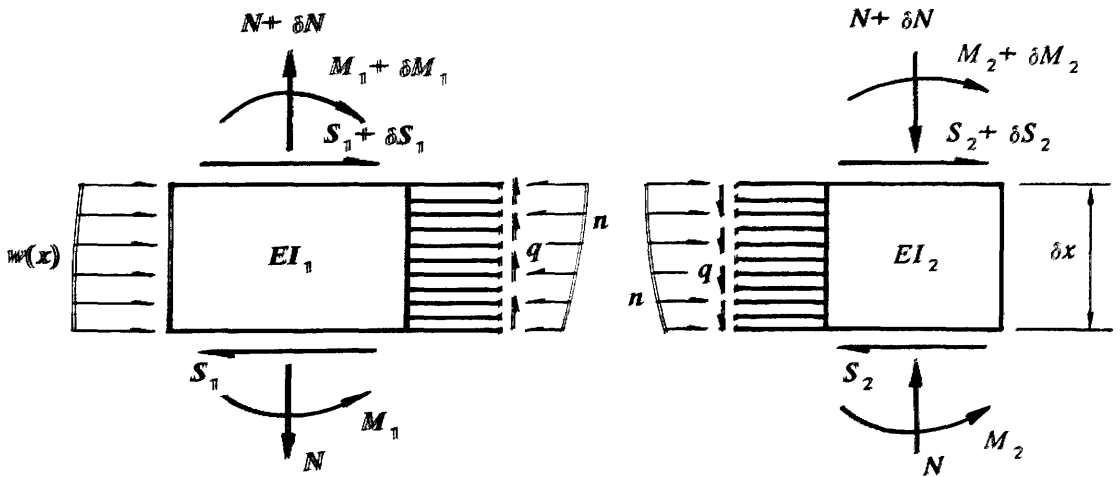


Fig. 3.5 Stress Resultants on Wall Elements

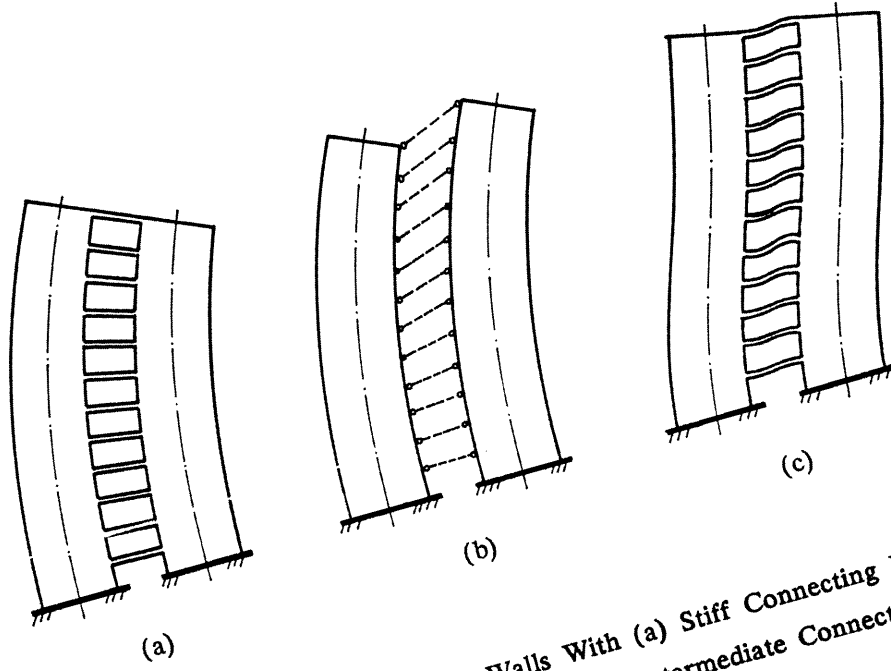


Fig. 3.6 Coupled Shear Walls With (a) Stiff Connecting Beams, (b) Flexible Connecting Beams and (c) Intermediate Connecting Beams

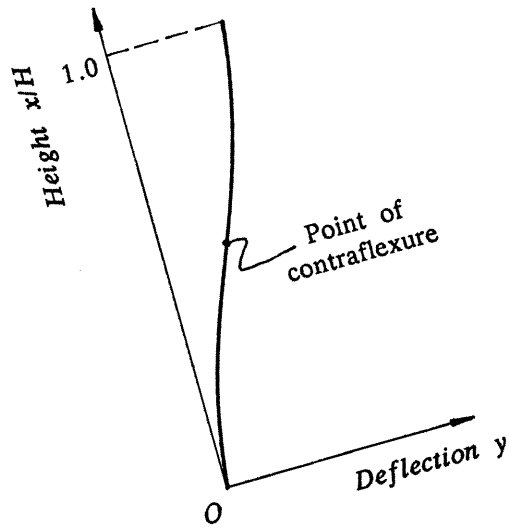


Fig. 3.7 Deflected Profile of Coupled Shear Walls

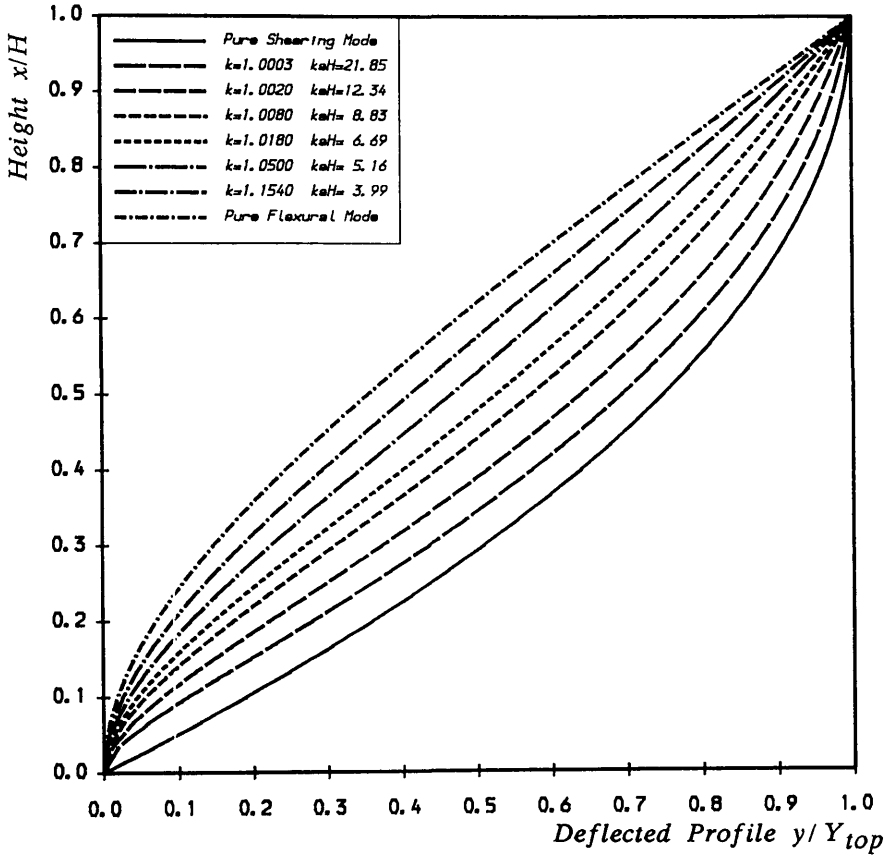


Fig. 3.8 Deflected Configurations of Coupled Shear Walls

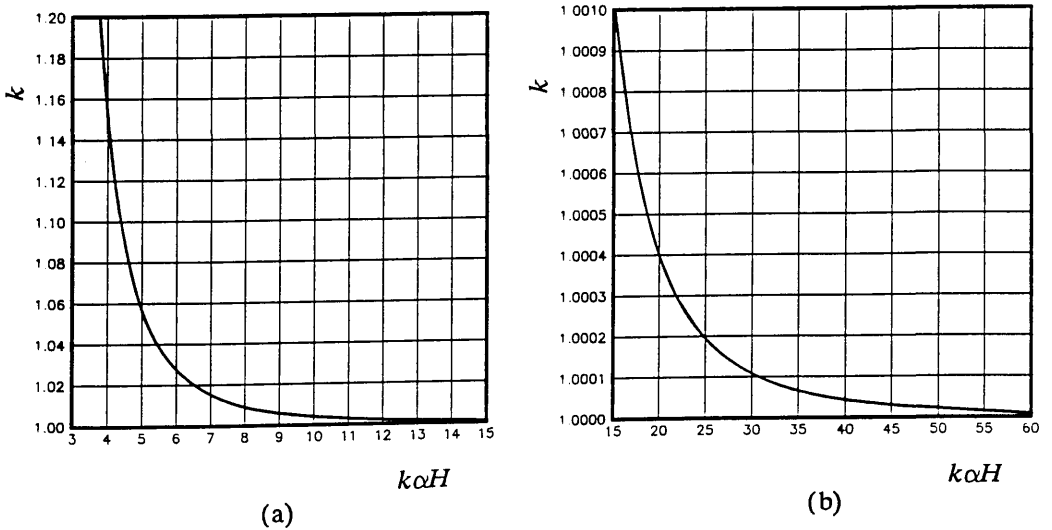


Fig. 3.9 Corresponding $k\alpha H$ curve

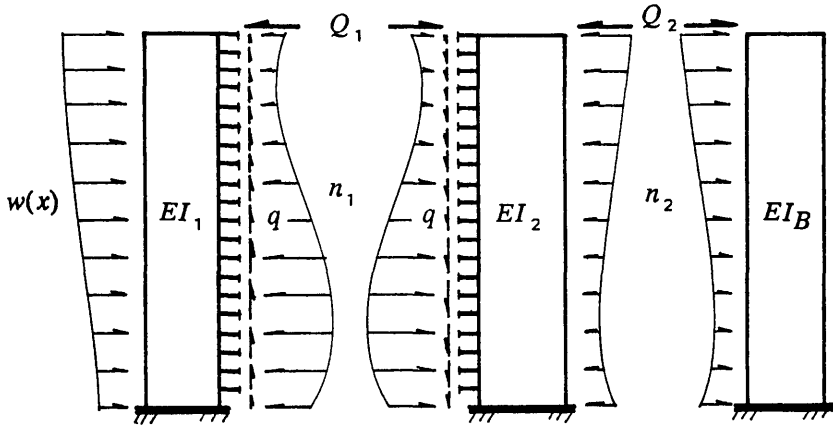


Fig. 3.10 Interacting Coupled Shear Walls and Plane Shear Wall

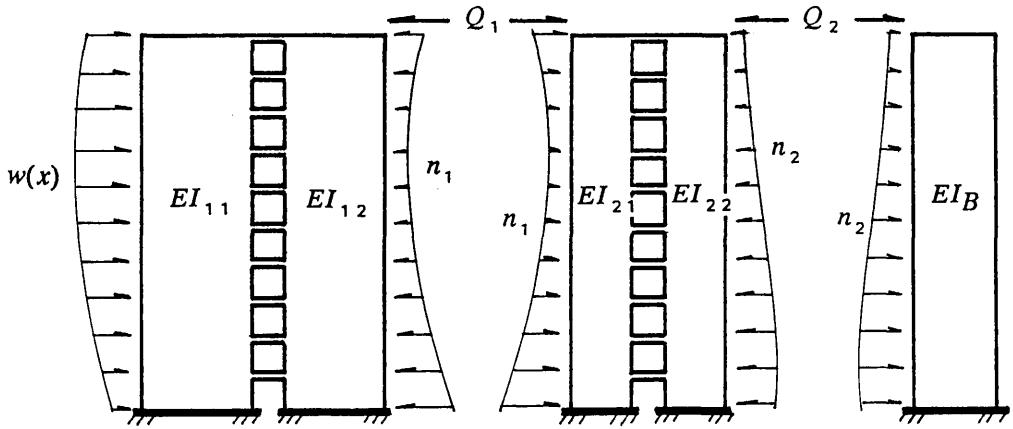


Fig. 3.11 Interaction Between Two Pairs of Coupled Shear Walls

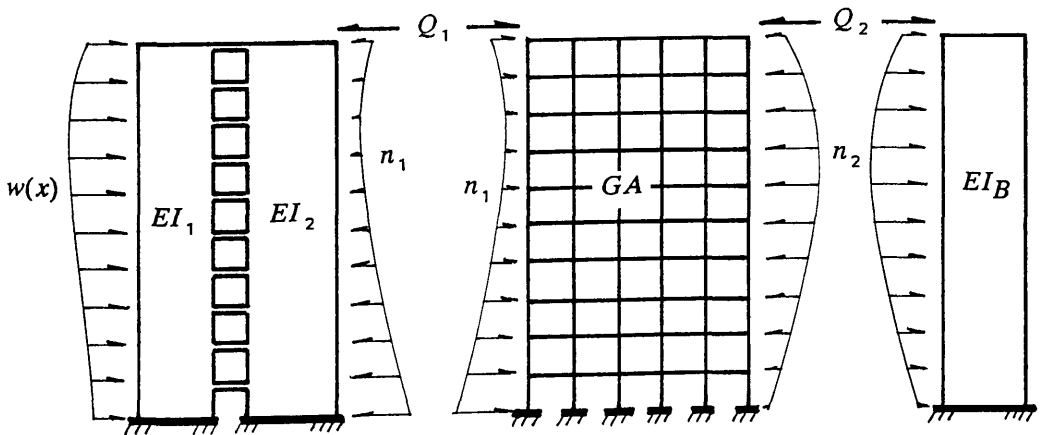


Fig. 3.12 Interaction Between Coupled Shear Walls and Shear Cantilevers

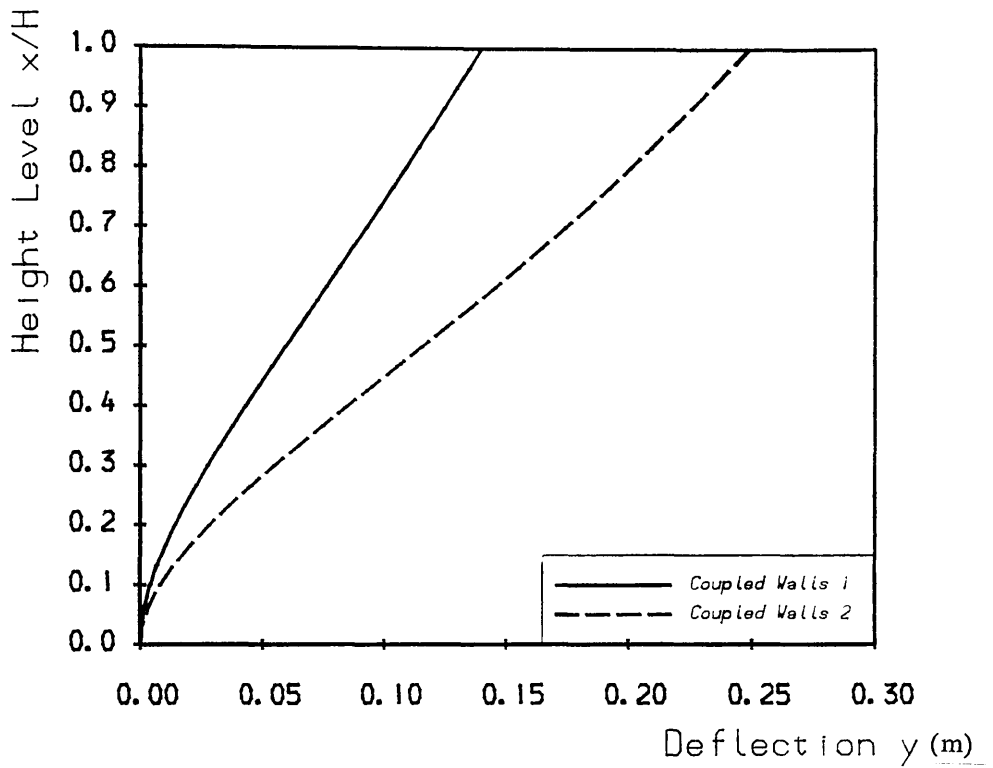


Fig. 3.13 Deflections
Coupled Walls 1 and 2

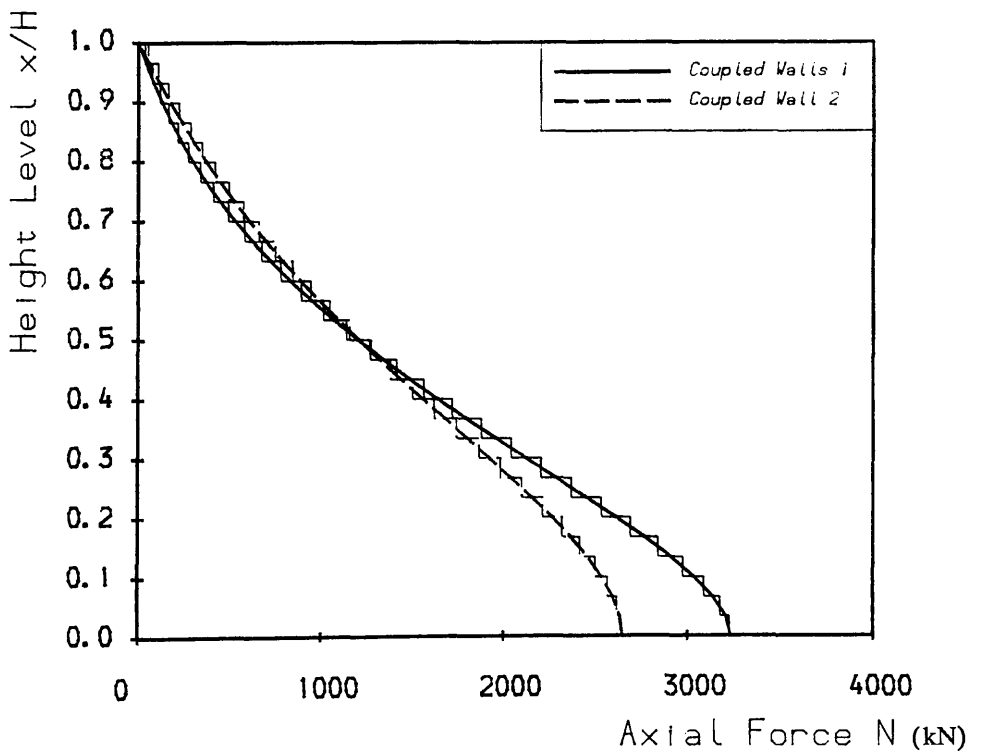


Fig. 3.14 Axial Forces
Coupled Shear Walls 1 and 2

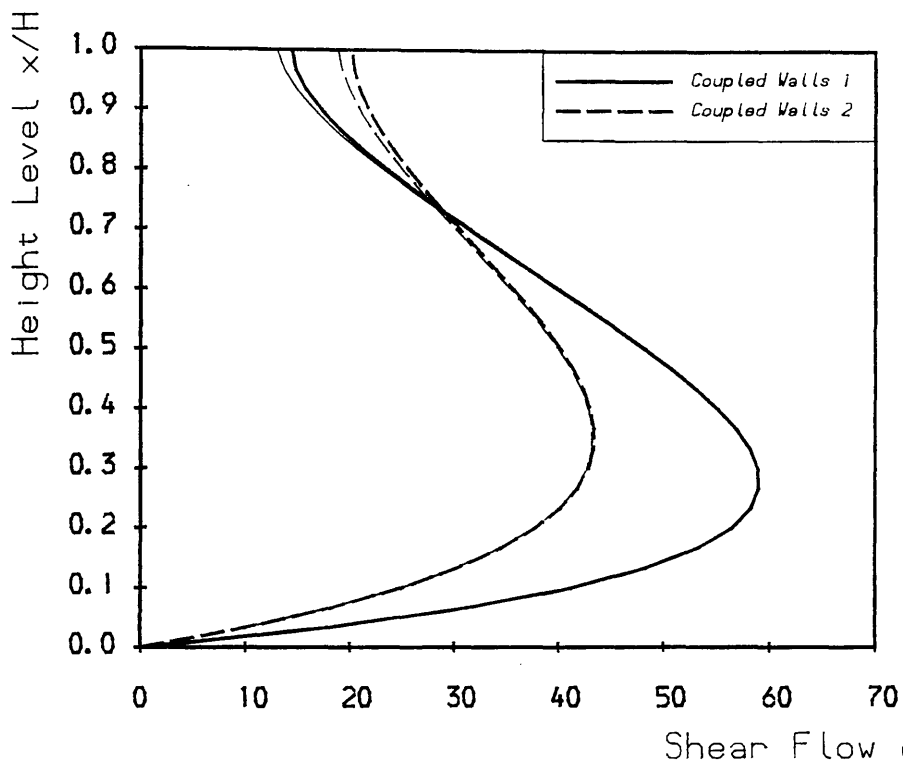


Fig. 3.15 Shear Flows In Connecting Beams
Coupled Shear Walls 1 and 2

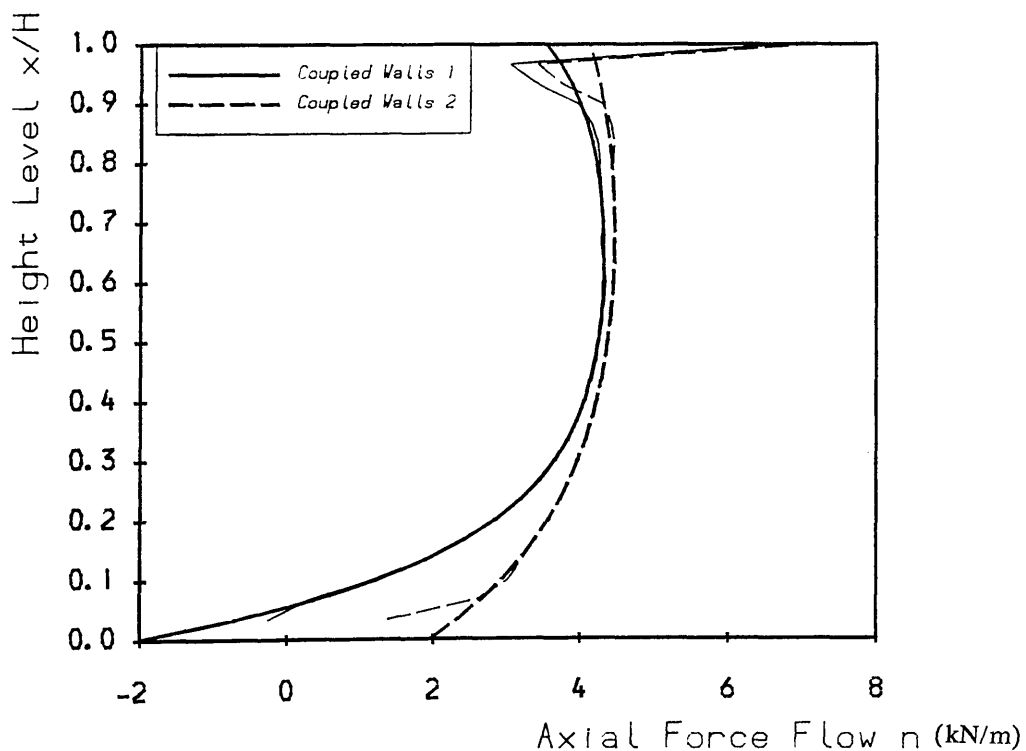


Fig. 3.16 Axial Forces In Connecting Beams
Coupled Shear Walls 1 and 2

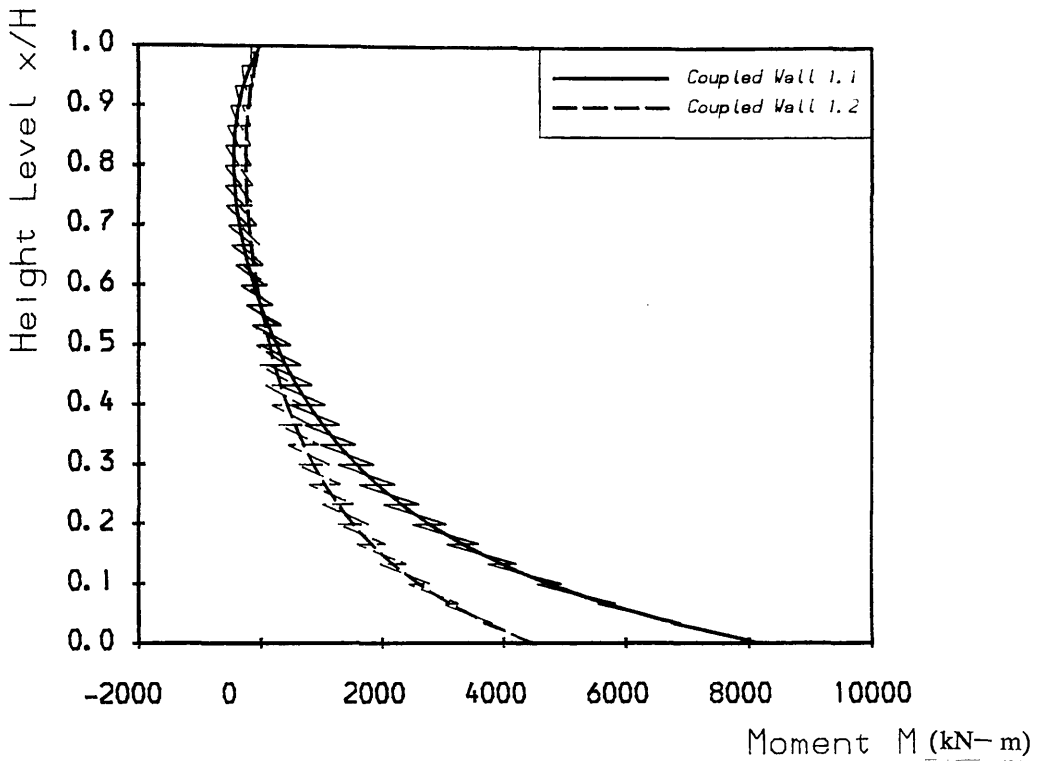


Fig. 3.17 Moments In Two Walls
Coupled Shear Walls 1

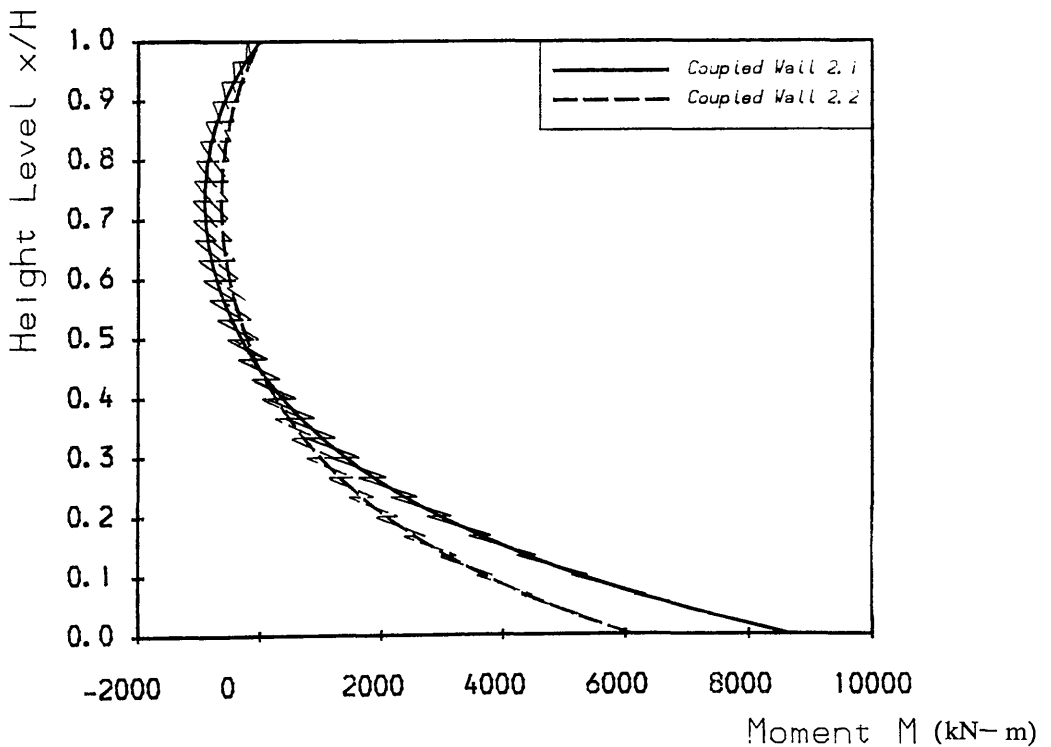


Fig. 3.18 Moment In Two Walls
Coupled Shear Walls 2

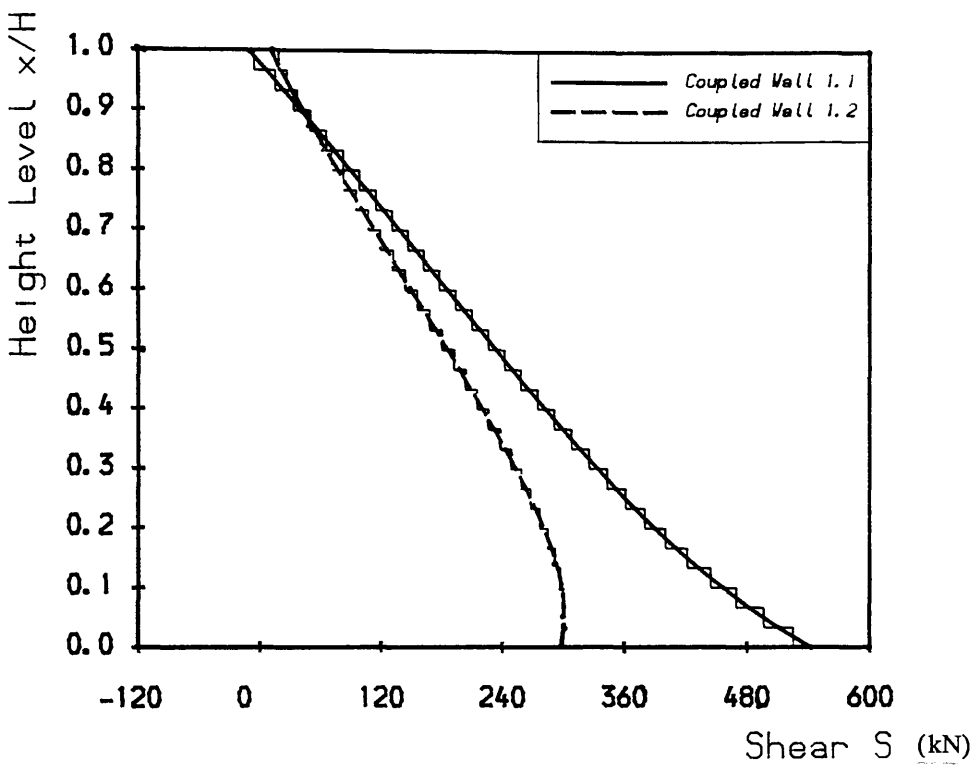


Fig. 3.19 Shears In Two Walls
Coupled Shear Walls 1

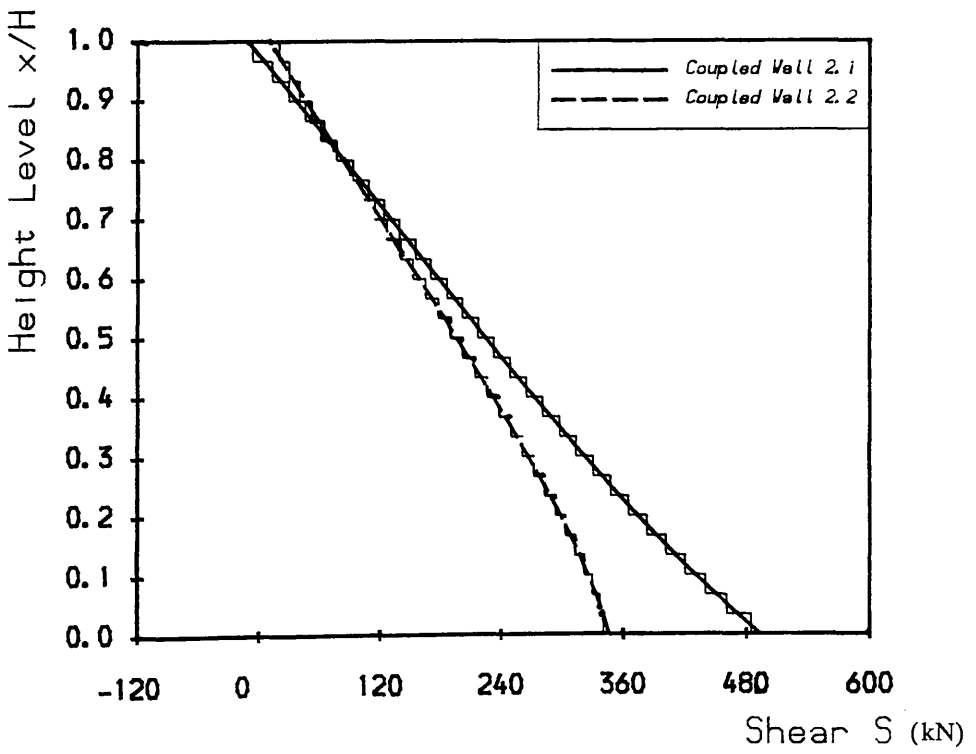


Fig. 3.20 Shears In Two Walls
Coupled Shear Walls 2

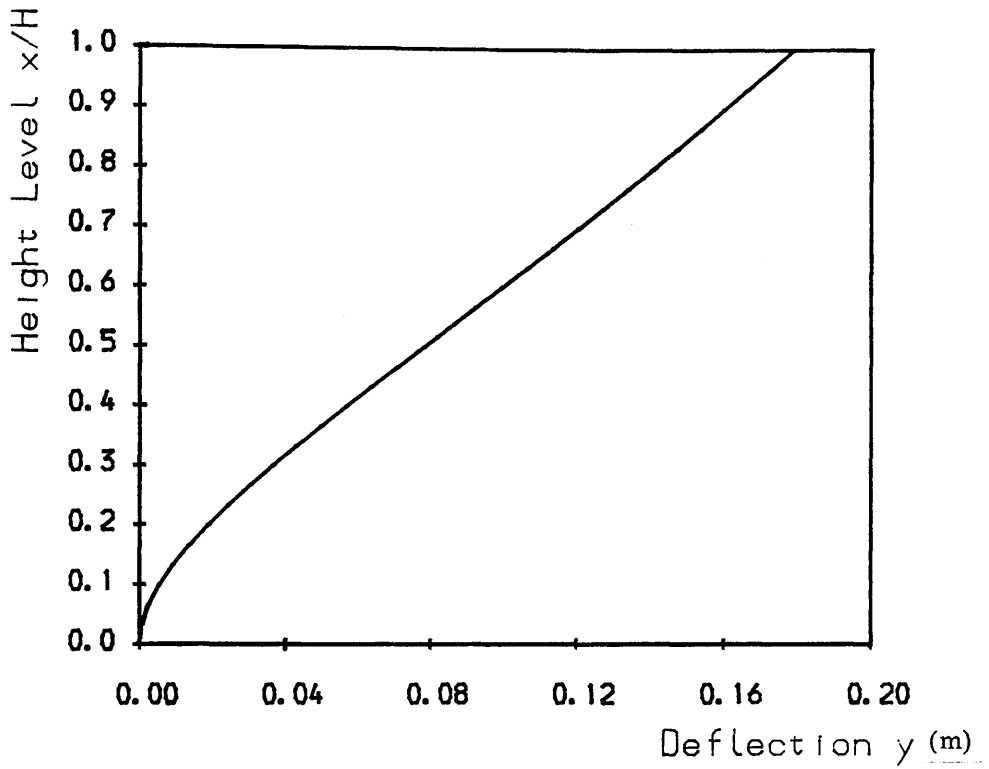


Fig. 3.21 Deflection
Two Pairs of Linked Coupled Walls

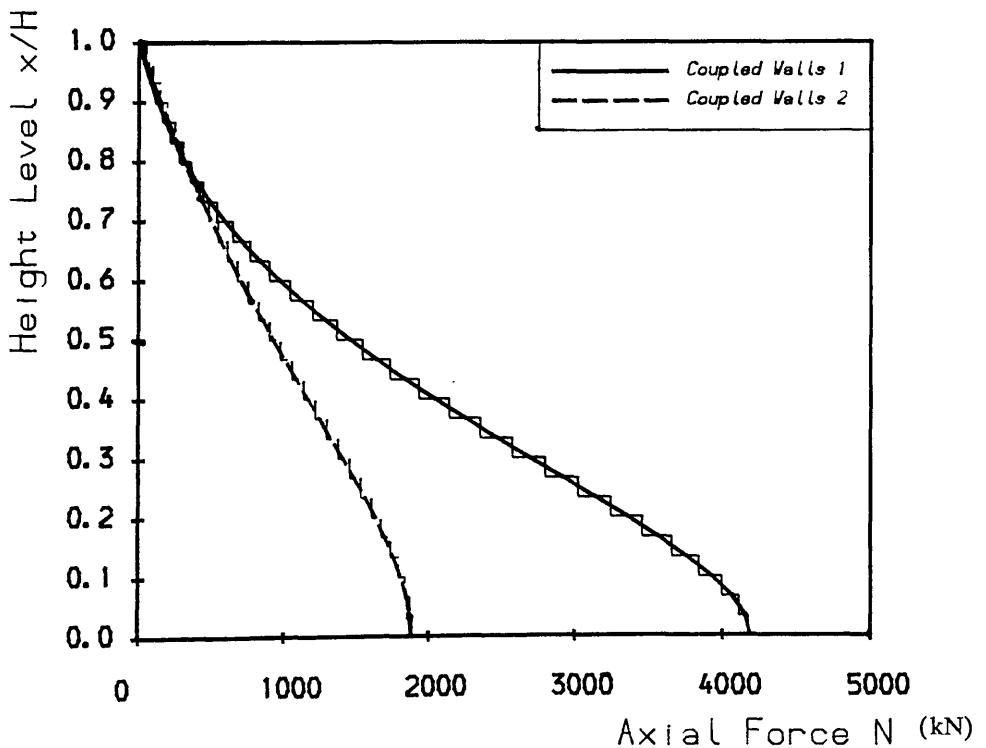


Fig. 3.22 Axial Forces
Two Pairs of Linked Coupled Walls

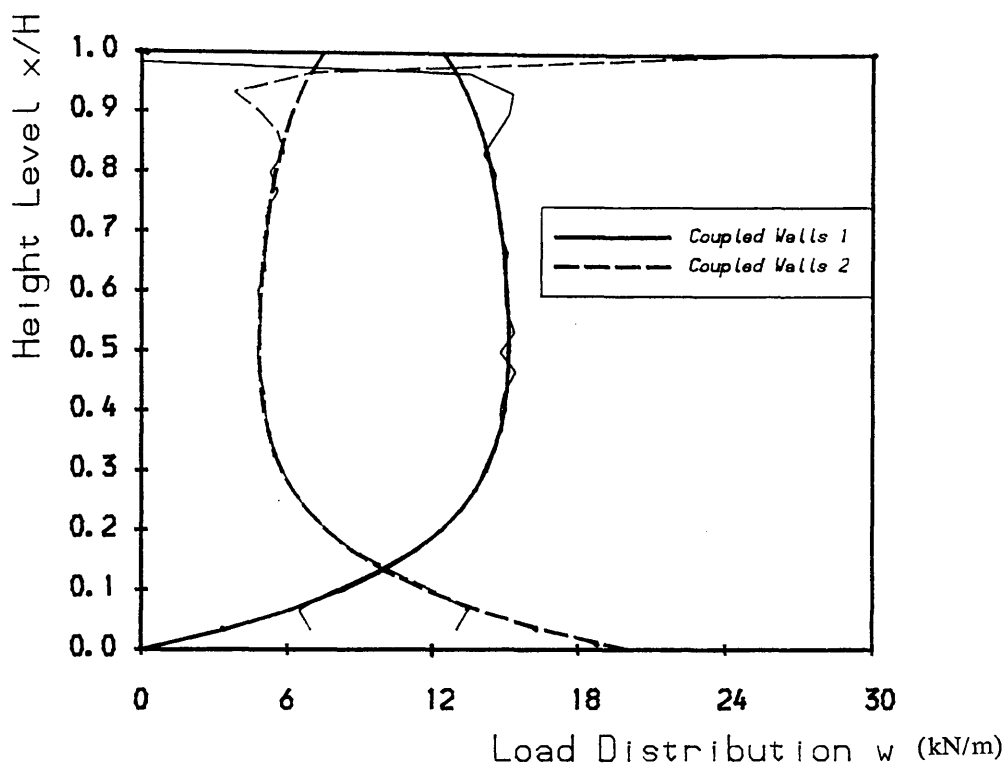


Fig. 3.23 Load Distributions
Two Pairs of Linked Coupled Walls

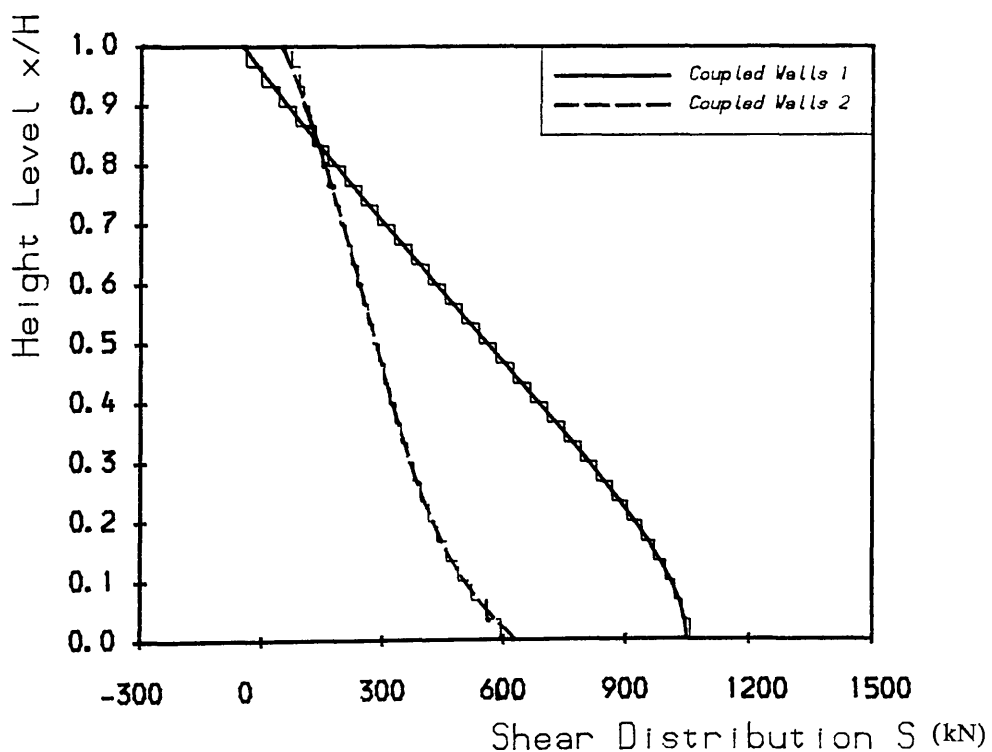


Fig. 3.24 Shear Distributions
Two Pairs of Linked Coupled Walls

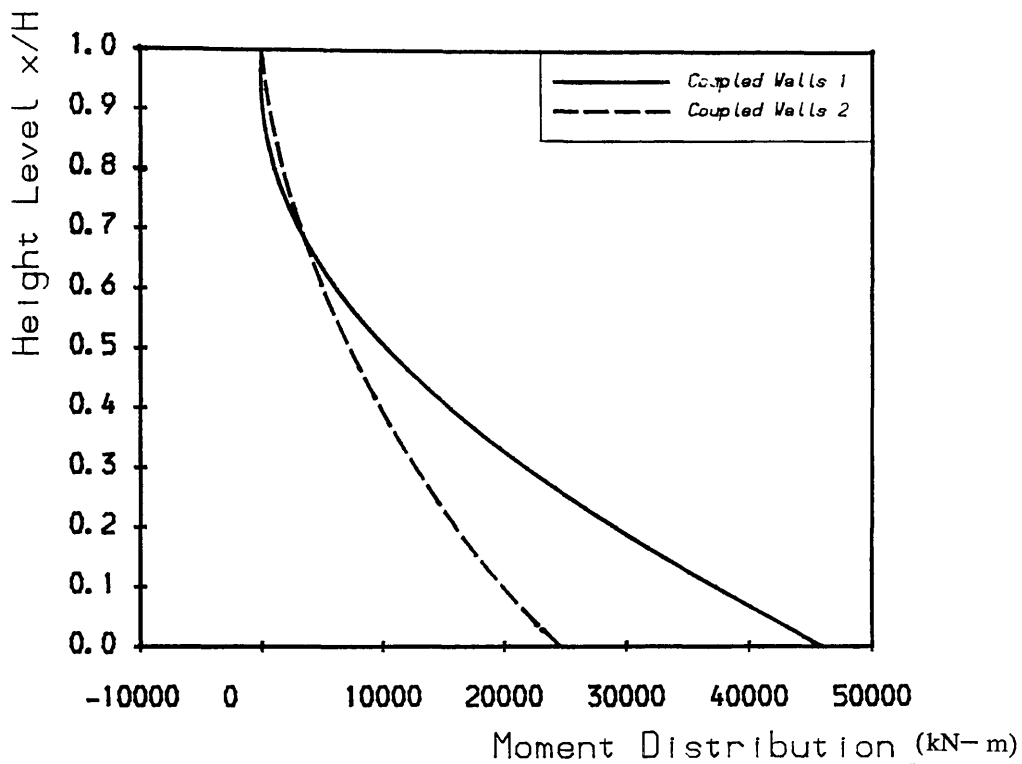


Fig. 3.25 Moment Distributions
Two Pairs of Linked Coupled Walls

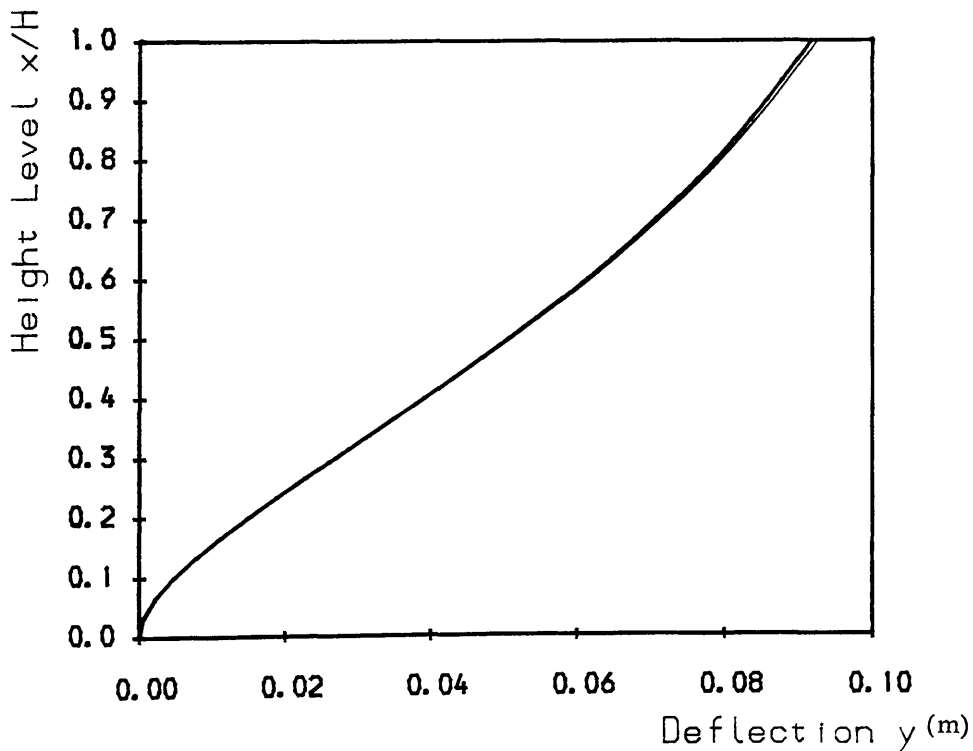


Fig. 3.26 Deflection
Linked Coupled Walls and Rigid Frame

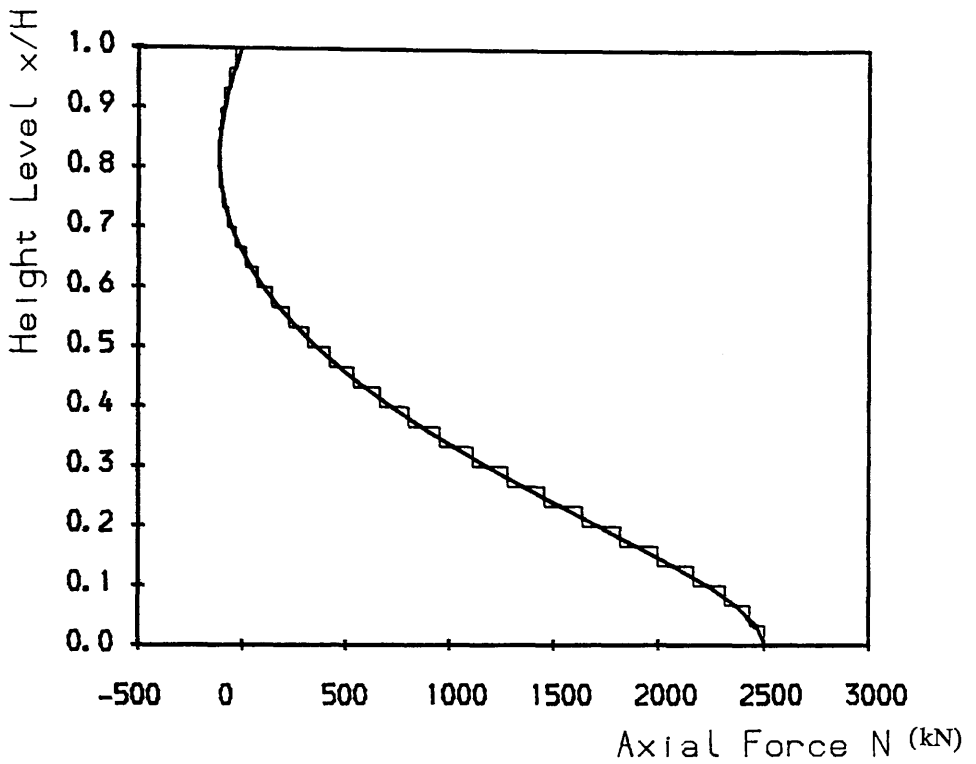


Fig. 3.27 Axial Forces In Coupled Walls
Linked Coupled Walls and Rigid Frame

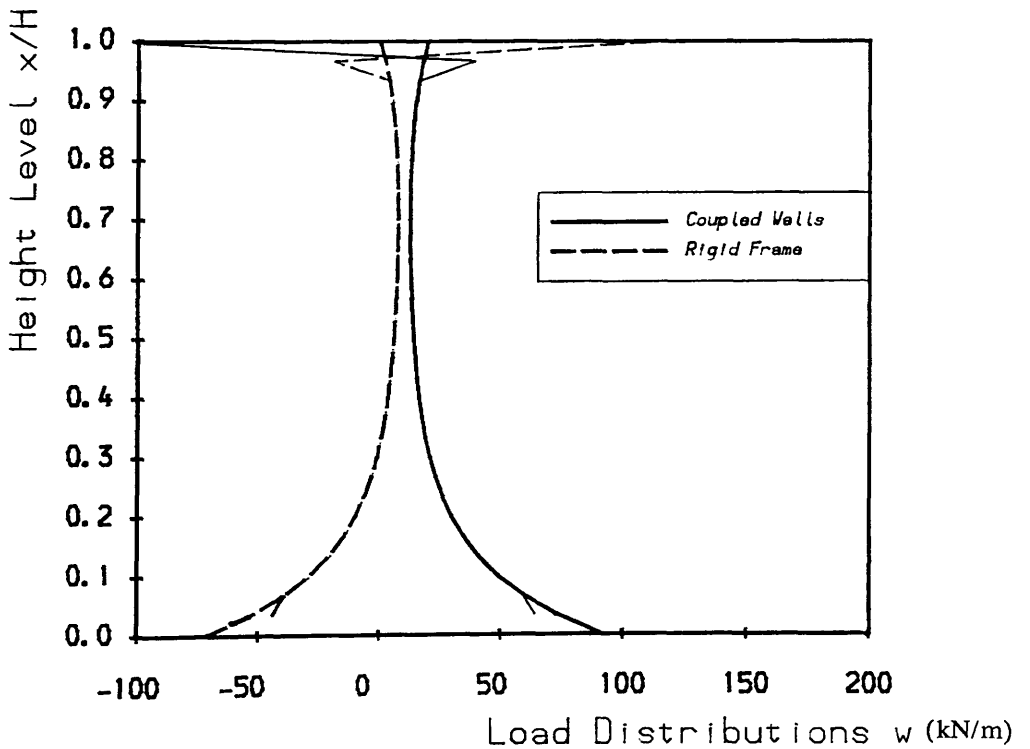


Fig. 3.28 Load Distribution
Linked Coupled Walls and Rigid Frame

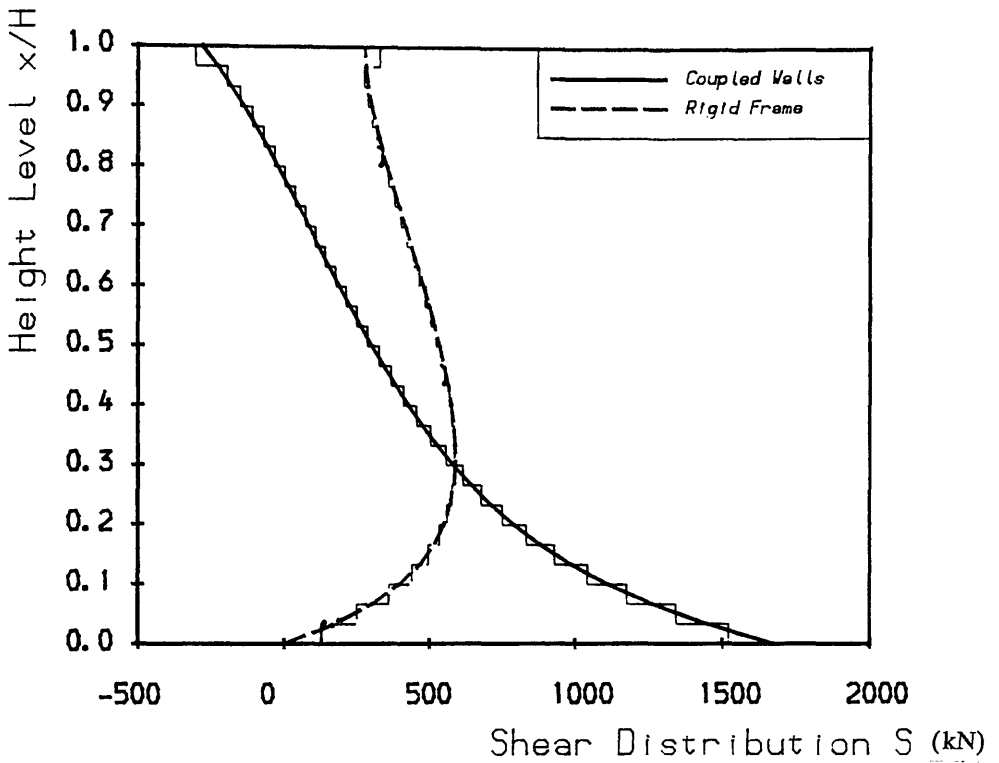


Fig. 3.29 Shear Distributions
Linked Coupled Walls and Rigid Frame

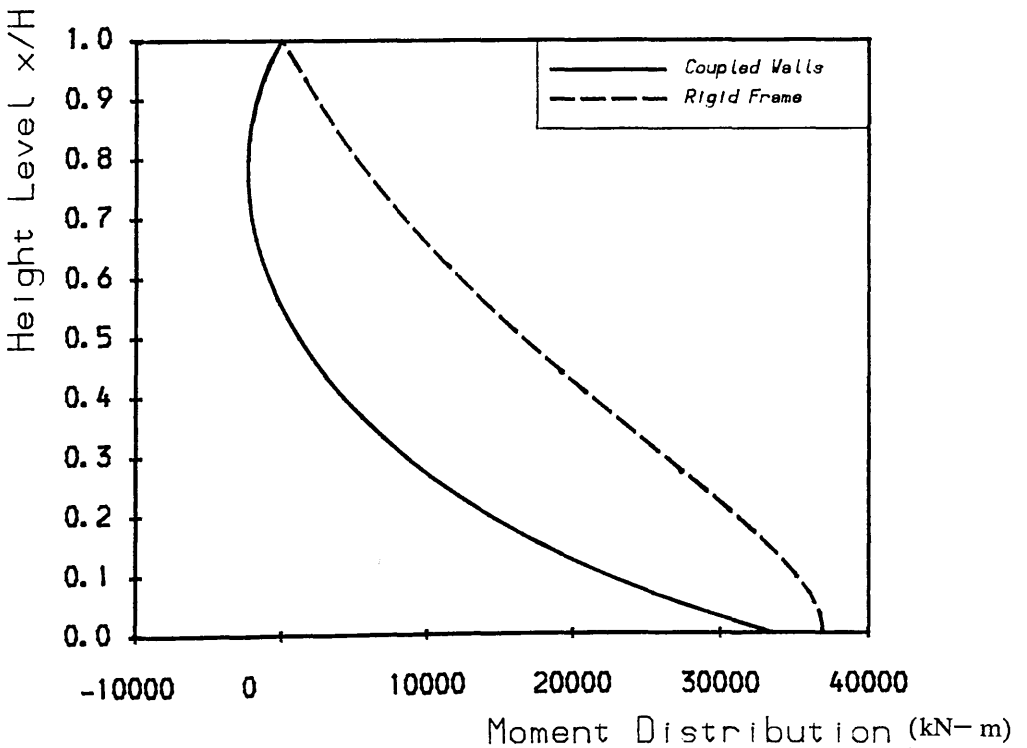


Fig. 3.30 Moment Distributions
Linked Coupled Walls and Rigid Frame

CHAPTER 4
ANALYSIS OF WALL-FRAME STRUCTURES (PART TWO)
- REVISED WALL-FRAME THEORY

4.1 Introduction

The modes of load-deformation behaviour of plane shear walls, cores and planar rigid frames have been discussed in Chapter 2. A simplified method of analysis of interacting shear walls and rigid frames was presented, corresponding to that presented by Heidebrecht and Stafford Smith (cf. Ref. 9). It has been shown that this wall-frame theory tends to give incorrect results, especially for the deflections, when the structure is very high, say over 20 storeys. The discrepancy is due to the influence of the axial deformations in the columns of the frames, giving rise to an overall bending effect which is neglected for low-rise structures. In this chapter, a revised wall-frame theory is presented to take into account of such effects in the frames, leading to a generalized method of analysis for wall-frame structures. In the analysis, only a uniformly distributed lateral load is considered. The solutions for the other two standard load cases are presented in Appendix 3.

4.2 Basic Mathematical Model and Governing Equations

The structure is assumed to consist of two types of vertical cantilever beams, one of which is a flexural cantilever, whose mode of load-deformation behaviour is governed by Eqs. 2.1 or 2.2, the other being a 'shear-flexural' cantilever whose mode of load-deformation behaviour is defined as such that, when subjected to a lateral load, two independent deformations occur. One is a shearing deformation y_{s1} which depends on the shearing rigidity GA , and the

other is an overall bending deformation y_{s2} depending on the overall bending rigidity, EI_f . The equations governing the behaviour of the two types of beam, referring to Figs. 4.1a and 4.1b, are:

For the flexural cantilever,

$$EI \frac{d^4 y_B}{dx^4} = w_B(x) \quad (4.1)$$

For the composite shear-flexural cantilever,

$$- GA \frac{d^2 y_{S1}}{dx^2} = w_S(x) \quad (4.2)$$

and,

$$EI_f \frac{d^4 y_{S2}}{dx^4} = w_S(x) \quad (4.3)$$

$$\text{and, } y_S = y_{S1} + y_{S2} \quad (4.4)$$

in which $y_B(x)$ is the deflection of the flexural beam, $w_B(x)$ and $w_S(x)$ are the distributed lateral loads acting on the flexural and shear-flexural cantilevers, respectively, EI_B is the flexural rigidity of the flexural cantilever, and the subscripts, B and S , refer to the flexural and the shear-flexural cantilevers, respectively.

Consider now the case in which the shear-flexural and the flexural beams are linked to deflect identically throughout their height, subjected together to an external applied distributed lateral load $w(x)$, as shown in Fig. 4.2a. A distributed horizontal interactive force of magnitude $q(x)$, and a concentrated top interaction force of magnitude Q are then required to maintain this compatibility, as shown in Fig. 4.2b.

The equations governing the flexural and the shear-flexural cantilever beams, referring to Fig. 4.2b, are then given by,

$$EI \frac{d^4 y}{dx^4} = w - q \quad (4.5)$$

$$- GA \frac{d^2 y_1}{dx^2} = q \quad (4.6)$$

and,

$$EI_f \frac{d^4 y_2}{dx^4} = q \quad (4.7)$$

in which y_1 and y_2 are the two types of deflection occurring in the shear-flexural cantilever, the sum of which is the total lateral deflection y . That is,

$$y = y_1 + y_2 \quad (4.8)$$

In addition, the equations for the shears and moments in the two types of cantilever beam are,

$$M_B = EI \frac{d^2 y}{dx^2} \quad (4.9)$$

$$S_B = - \frac{dM_B}{dx} = -EI \frac{d^3 y}{dx^3} \quad (4.10)$$

$$M_S = EI_f \frac{d^2 y_2}{dx^2} \quad (4.11)$$

$$S_S = GA \frac{dy_1}{dx} = -EI_f \frac{d^3 y_2}{dx^3} \quad (4.12)$$

On differentiating Eq. 4.6 twice, dividing through by $-GA$, and dividing Eq. 4.7 by EI_f , subject to Eq. 4.8, the equation governing the load-deformation behaviour of the shear-flexural cantilever becomes,

$$\frac{d^4 y}{dx^4} = - \frac{1}{GA} \frac{d^2 q}{dx^2} + \frac{1}{EI_f} q \quad (4.13)$$

On eliminating either y or q from Eqs. 4.12 and 4.13, the governing differential equations for the combined cantilever beam, in terms of q or y can be derived as,

$$\frac{d^2 q}{dx^2} - k^2 \alpha^2 q = - \alpha^2 w \quad (4.14)$$

and,

$$\frac{d^6y}{dx^6} - k^2\alpha^2 \frac{d^4y}{dx^4} = \frac{1}{EI} \frac{d^2w}{dx^2} - \alpha^2 \frac{1}{EI_f} w \quad (4.15)$$

in which,

$$\alpha^2 = \frac{GA}{EI} \quad (4.16)$$

$$k^2 = 1 + \frac{EI}{EI_f} \quad (4.17)$$

The general solutions of Eqs. 4.8 and 4.9 can be written in the form,

$$q = C_1 \cosh k\alpha x + C_2 \sinh k\alpha x + q^* \quad (4.18)$$

$$y = D_1 + D_2 x + D_3 x^2 + D_4 x^3 + D_5 \cosh k\alpha x + D_6 \sinh k\alpha x + y^* \quad (4.19)$$

in which C_1 and C_2 , and D_1 to D_6 are integration constants which must be determined from the appropriate boundary conditions, and q^* and y^* are particular integral solutions for specific load cases.

4.3 Boundary Conditions and Solutions for Uniformly Distributed Lateral Load

The structure is regarded as a vertical cantilever beam which is rigidly built in at the base and free at the top. By considering the conditions of zero deflection and rotation at the base, and zero moment at the top, the appropriate boundary conditions in terms of the interactive force flow, q , can be deduced as follows:

(a) At $x = H$, $M_B = M_S = 0$, and hence from Eqs. 4.9 and 4.11, $d^2y/dx^2 = d^2y_2/dx^2 = 0$. It then can be deduced from Eq. 4.8 that, $d^2y_1/dx^2 = 0$, and from Eq. 4.6, it follows that,

$$q(H) = 0 \quad (4.20)$$

(b) At $x = 0$, $dy/dx = 0$. Since y_2 represents a flexural deformation, from the nature of the flexural beam, it can be assumed that at $x = 0$, $dy_2/dx = 0$. It follows that $dy_1/dx = 0$, and from Eq. 4.12, $S_S = 0$. It then follows that $d^3y_2/dx^3 = 0$. This indicates that at the base of the structure, the flexural cantilever carries the total applied shear, which is, from Eq. 4.10,

At $x = 0$,

$$S_B = -EI \frac{d^3y}{dx^3} = -EI \left\{ \frac{d^3y_1}{dx^3} + \frac{d^3y_2}{dx^3} \right\} = -EI \frac{d^3y_1}{dx^3} = S_0 \quad (4.21)$$

in which S_0 is the total applied shear at the base. For a uniformly distributed lateral load of intensity w_0 , $S_0 = w_0H$.

On differentiating Eq. 4.6, and using Eqs. 4.16 and 4.21, it follows that,

$$\frac{dq}{dx}(0) = \alpha^2 S_0 \quad (4.22)$$

For the case of a uniformly distributed lateral load of intensity w_0 , the particular solution $q^*(x)$ of Eq. 4.14 can be chosen to be,

$$q^* = \frac{w_0}{k^2} \quad (4.23)$$

The two constants in Eq. 4.18 are then determined from the boundary conditions given by Eqs. 4.20 and 4.22 as,

$$C_1 = - \frac{1 + k\alpha H \sinh k\alpha H}{k^2 \cosh k\alpha H} w_0 \quad (4.24)$$

$$C_2 = \frac{\alpha}{k} w_0 H \quad (4.25)$$

The expression for the interactive force intensity q then can be written as,

$$q(\xi) = \frac{w_0}{k^2} \left\{ 1 - \frac{\cosh k\alpha H \xi + k\alpha H \sinh k\alpha H (1-\xi)}{\cosh k\alpha H} \right\} \quad (4.26)$$

in which $\xi = x/H$ is the dimensionless height coordinate.

The resultant distributed forces carried by the two components, referring to Fig. 4.2b, are obtained as,

$$q_B = w_0 - q$$

$$= \left\{ \frac{k^2 - 1}{k^2} + \frac{\cosh k\alpha H \xi + k\alpha H \sinh k\alpha H (1 - \xi)}{k^2 \cosh k\alpha H} \right\} w_0 \quad (4.27)$$

and,

$$q_S = q = \left\{ \frac{1}{k^2} - \frac{\cosh k\alpha H \xi + k\alpha H \sinh k\alpha H (1 - \xi)}{k^2 \cosh k\alpha H} \right\} w_0 \quad (4.28)$$

Instead of solving for the deflection in Eq. 4.19, in which six integration constants must be determined from six boundary conditions, the deflection can alternatively be obtained from Eq. 4.5, in which $q_B = w_0 - q$ is known from Eq. 4.27. On integrating Eq. 4.5 four times and dividing through by EI , the expression for the deflection y can be written as,

$$y(\xi) = \frac{w_0 H^4}{EI} \left\{ \frac{k^2 - 1}{24k^2} \xi^4 + \frac{\cosh k\alpha H \xi + k\alpha H \sinh k\alpha H (1 - \xi)}{k^2 (k\alpha H)^4 \cosh k\alpha H} \right.$$

$$\left. + K_1 + K_2 \xi + K_3 \xi^2 + K_4 \xi^3 \right\} \quad (4.29)$$

in which K_1 to K_4 are integration constants which also must be determined from the appropriate boundary conditions.

By considering the structure as described above for obtaining the boundary conditions in terms of q in Eqs. 4.20 to 4.22, the four boundary conditions in terms of y can be shown to be,

$$(a) \quad y(0) = 0 \quad (4.30)$$

$$(b) \quad \frac{dy}{dx}(0) = 0 \quad (4.31)$$

$$(c) \quad M_B(H) = EI \frac{d^2 y}{dx^2}(H) = 0 \quad (4.32)$$

and,

$$(d) \quad S_B(0) = -EI \frac{d^3y}{dx^3}(0) = S_0 = w_0 H \quad (4.33)$$

Determining the four constants in Eq. 4.29 from the above boundary conditions leads to the following expression for the deflection,

$$y = \frac{w_0 H^4}{EI} \left\{ \frac{k^2-1}{24k^2} (\xi^4 - 4\xi^3 + 6\xi^2) + \frac{1}{k^2(k\alpha H)^2} \left(\xi - \frac{\xi^2}{2} \right) + \frac{\cosh k\alpha H \xi + k\alpha H \sinh k\alpha H (1-\xi) - k\alpha H \sinh k\alpha H - 1}{k^2(k\alpha H)^4 \cosh k\alpha H} \right\} \quad (4.34)$$

On differentiating the deflection twice, and multiplying by EI (Eq. 4.9), the moment in the flexural cantilever is obtained as,

$$M_B = w_0 H^2 \left\{ \frac{k^2-1}{2k^2} (1-\xi)^2 + \frac{\cosh k\alpha H \xi + k\alpha H \sinh k\alpha H (1-\xi) - \cosh k\alpha H}{k^2(k\alpha H)^2 \cosh k\alpha H} \right\} \quad (4.35)$$

By subtracting Eq. 4.35 from the total applied moment ($\frac{1}{2}w_0 H^2(1-\xi)^2$), the moment in the shear-flexural cantilever is obtained as,

$$M_S = w_0 H^2 \left\{ \frac{1}{2k^2} (1-\xi)^2 - \frac{\cosh k\alpha H \xi + k\alpha H \sinh k\alpha H (1-\xi) - \cosh k\alpha H}{k^2(k\alpha H)^2 \cosh k\alpha H} \right\} \quad (4.36)$$

On differentiating Eqs. 4.35 and 4.36, and changing the signs, the shears in the two components are obtained as,

$$S_B = w_0 H \left\{ \frac{k^2-1}{k^2} (1-\xi) - \frac{\sinh k\alpha H \xi - k\alpha H \cosh k\alpha H (1-\xi)}{k^2(k\alpha H) \cosh k\alpha H} \right\} \quad (4.37)$$

and,

$$S_S = w_0 H \left\{ \frac{1}{k^2} (1-\xi) + \frac{\sinh k\alpha H \xi - k\alpha H \cosh k\alpha H (1-\xi)}{k^2(k\alpha H) \cosh k\alpha H} \right\} \quad (4.38)$$

4.4 Structural Rigidity Parameters, EI , GA and EI_f

It has been shown that the two components which comprise the structure involve three distinct structural rigidity parameters, EI , GA and EI_f , representing three different modes of deformation behaviour. The three rigidities can be defined as follows:

(1) EI , as described in Chapter 2, expresses the flexural rigidity of any flexural components, such as shear walls or cores which are continuous up the height of the structure.

(2) GA is an equivalent shear rigidity for planar rigid frames defined by Eq. 2.15 in Chapter 2.

(3) EI_f , as introduced in this chapter, is another flexural rigidity which represents the overall bending action for a rigid frame. By considering the total moment resistance from the axial stiffness of the columns, this rigidity can be obtained from the second moment of area of the column sections about the common centroidal axis of all the columns, assuming that the horizontal beams connecting the columns are rigid. That is, referring to Fig. 4.3,

$$EI_f = \sum^n EA_i Z_i^2 \quad (4.39)$$

in which A_i is the cross-sectional area of the column i , and Z_i is the distance from the column i to the common centroidal axis of all the columns in the frame.

4.5 Numerical Examples

For a comparison of the revised and the original simple wall-frame methods, the example wall-frame structure used in Chapter 2 is again considered.

In addition to the original data provided in Section 2.3.3, the overall flexural rigidity EI_f for the four frames is now determined from Eq. 4.39 as,

$$EI_f = 7.168 \times 10^8 \text{ N m}^2$$

The parameters are then:

$$\alpha = 0.0446 \text{ m}^{-1}$$

$$k = 1.0933$$

$$\text{For case 1 } k\alpha H = 2.0462,$$

$$\text{For case 2 } k\alpha H = 5.4564$$

On using the present revised wall-frame method, and comparing with the results of the finite element method from the 'FLASH' program, the resulting curves are shown for case 1 in Figs. 4.4a to 4.4d, and for case 2 in Figs. 4.5a to 4.5d. In the Figures, unless specified, the thicker lines refer to the present method, and the thinner lines to the 'FLASH' results. It can be seen from these curves that the present method, which takes into account the effects of the axial deformations of the columns in the frames, improves significantly the accuracy for high-rise wall-frame structures.

4.6 Design Curves

On inspecting the resulting force equations 4.27, 4.28 and 4.35 to 4.36, it can be seen that all these equations contain two significant parts. The first part of every equation always consists of an external force term with a multiplier of $(k^2-1)/k^2$ for the flexural component and $1/k^2$ for the composite shear-flexure component. The second part of every equation is always a function of hyperbolic sines and cosines involving the parameters $k\alpha H$ and k . If the parameter k^2 is taken out of the overall bracket, this part only involves $k\alpha H$. In considering this, the equations can be re-written in the following forms:

For the loads distributed in the two components:

$$q_B = \frac{w_0}{k^2} \left\{ (k^2 - 1) + F_1 \right\} \quad (4.40)$$

$$q_S = \frac{w_0}{k^2} \left\{ 1 - F_1 \right\} \quad (4.41)$$

in which,

$$F_1 = \frac{\cosh k\alpha H \xi + k\alpha H \sinh k\alpha H (1-\xi)}{\cosh k\alpha H} \quad (4.42)$$

For the shears in the two components:

$$S_B = \frac{w_0 H}{k^2} \left\{ (k^2 - 1)(1 - \xi) - F_2 \right\} \quad (4.43)$$

$$S_S = \frac{w_0 H}{k^2} \left\{ (1 - \xi) + F_2 \right\} \quad (4.44)$$

in which,

$$F_2 = \frac{\sinh k\alpha H \xi - k\alpha H \cosh k\alpha H (1-\xi)}{k\alpha H \cosh k\alpha H} \quad (4.45)$$

and,

$$F_2 = \frac{1}{(k\alpha H)^2} \frac{dF_1}{d\xi} \quad (4.46)$$

For the moments in the two components:

$$M_B = \frac{w_0 H^2}{k^2} \left\{ (k^2 - 1) \frac{(1 - \xi)^2}{2} + F_3 \right\} \quad (4.47)$$

and,

$$M_S = \frac{w_0 H^2}{k^2} \left\{ \frac{1}{2} (1 - \xi)^2 + F_3 \right\} \quad (4.48)$$

in which,

$$F_3 = \frac{\cosh k\alpha H \xi + k\alpha H \sinh k\alpha H (1 - \xi) - \cosh k\alpha H}{(k\alpha H)^2 \cosh k\alpha H} \quad (4.49)$$

Similarly, the expression for the deflection can be re-written as,

$$y = \frac{w_0 H^4}{EI k^2} \left\{ \frac{k^2 - 1}{24} (\xi^4 - 4\xi^3 + 6\xi^2) + \frac{1}{(k\alpha H)^2} \left(\xi - \frac{\xi^2}{2} \right) + \frac{F_4}{(k\alpha H)^4} \right\} \quad (4.50)$$

in which,

$$F_4 = \frac{\cosh k\alpha H \xi + k\alpha H \sinh k\alpha H (1 - \xi) - k\alpha H \sinh k\alpha H - 1}{\cosh k\alpha H} \quad (4.51)$$

It can be seen in Eq. 4.50 that the first part can be recognized as the deflection equation for a flexural cantilever subjected to a uniformly distributed lateral load of intensity w_0 , multiplied by $(k^2 - 1)/k^2$, or,

$$y_a = \frac{k^2 - 1}{k^2} \frac{w_0 H^4}{24 EI} (\xi^4 - 4\xi^3 + 6\xi^2) \quad (4.52)$$

The second part, by substituting for α^2 from Eq. 4.16, becomes the deflection equation of a shear cantilever of shear rigidity GA , subjected to a uniformly distributed lateral load of intensity w_0 , multiplied by $1/k^4$, or,

$$y_b = \frac{1}{k^4} \frac{w_0 H^2}{GA} \left(\xi - \frac{\xi^2}{2} \right) \quad (4.53)$$

The complete solution of wall-frame structures can thus be expressed in terms of four relatively simple functions F_1 , F_2 , F_3 and F_4 of the basic structural parameters $k\alpha H$, and the height coordinate ξ .

The variations of the functions F_1 , F_2 , F_3 and F_4 with height, for different values of $k\alpha H$ covering a wide range of practical situations for wall-frame structures, are shown in Figs. 4.6a, 4.6b, 4.6c and 4.6d. These figures can be used directly as design curves for calculating the the deflections and forces in practical structures, and especially in applying the method to three-dimensional structural analysis which will be discussed in Chapter 5.

4.7 The Present Method and The Continuum Theory of Coupled Shear Walls – A General Family of Wall-Frame Cantilever Structures

It can be seen from Eqs. 4.26 and 4.34 that the equations for the interactive forces and the deflection are written in terms of two dimensionless parameters k and $k\alpha H$, in which α and k are defined respectively by Eqs. 4.16 and 4.17. By comparing the present method with the simple wall-frame theory given in Chapter 2, it can be shown that the presentation of the additional overall bending deformation in the shear cantilever leads to the appearance of the parameter k in the interaction analysis. This parameter k relates closely to the overall bending rigidity of the shear-flexure cantilever. In the case of $k = 1$, the shear-flexure cantilever becomes a pure shear cantilever because of the implied infinite value of EI_f and hence the non-existence of the overall bending deformation. The present method then reverts to the same equations as that of the simple wall-frame theory. Thus the parameter k may be regarded as the parameter which governs the effect of the overall bending of the shear-flexural cantilever, or the influence of axial deformations in the columns of the frame.

It can be recognized that the expression for the deflection given by Eq. 4.34 is of exactly the same form as that for coupled shear walls in Eq. 3.22 which is also written in terms of two parameters α and k . By considering the

definitions of the two parameters α and k from Eqs. 4.16 and 4.17, and comparing them with those defined for coupled shear walls in Eqs. 3.10 and 3.11, it can be seen that the coupled shear walls can be interpreted also as having three structural rigidities which represent three primary modes of deformation behaviour. These are, the flexural rigidity EI , the racking shear rigidity GA and the overall bending rigidity EI_f . For a pair of coupled shear walls, the three rigidities can be characterized and determined as follows:

(1) The flexural rigidity EI is sum of the flexural rigidities of the two shear walls, $EI = EI_1 + EI_2$.

(2) The racking shear rigidity of a coupled shear wall structure depends on the flexural rigidity of the connecting beams, and the width and spacing of the walls. Referring to the storey-height module shown in Fig. 4.7, the equivalent shear rigidity of the coupled shear wall system is given by,

$$GA = \frac{Ph}{\delta} = \frac{12EI_b l^2}{b^3 h} \quad (4.54)$$

From Eq. 4.16, the parameter α for the coupled shear wall structure is then,

$$\alpha = \frac{GA}{EI} = \frac{12I_b l^2}{b^3 h I} \quad (4.55)$$

This equation corroborates Eq. 3.10.

(3) The overall bending rigidity EI_f , similar to that for rigid frames in Eq. 4.39, can be obtained from the second moment of area of the wall sections about the common centroidal axis. Referring to Fig. 4.8, that is,

$$EI_f = E(A_1 Z_1^2 + A_2 Z_2^2) \quad (4.56)$$

in which A_1 and A_2 are the cross-sectional areas of the two walls, and

Z_1 and Z_2 are the distances from the wall centroidal axes to the common centroidal axis of the two walls, which can be determined by, $Z_1 + Z_2 = l$, and $Z_1 A_1 = Z_2 A_2$, where l is the distance between the wall axes. Eq. 4.42 then becomes,

$$EI_f = E \frac{A_1 A_2 l^2}{A_1 + A_2} \quad (4.57)$$

From Eq. 4.17, the parameter k for the coupled shear wall structure is,

$$k = 1 + \frac{EI}{EI_f} = 1 + \frac{(A_1 + A_2) I}{A_1 A_2 l^2} \quad (4.58)$$

This equation also corroborates Eq. 3.11.

From the above discussion, it can be concluded that the revised wall-frame method presented can be considered as a generalized method for a class of cantilever structures, provided that the structure can be regarded as an equivalent assembly with three appropriate structural stiffnesses representing three distinct modes of load-deformation behaviour. These structures, including interacting wall-frame structures, coupled shear walls, planar rigid and braced frames, can be regarded as a general family of wall-frame structures. It should be noted that, when applying the method to a rigid frame structure without interacting shear walls, the flexural rigidities of the individual columns contribute to the total flexural rigidity EI , although they may generally be neglected when interacting shear walls are involved, since their flexural rigidities are very small when compared to those from the shear walls. Braced frames and rigidly jointed wall-frame assemblies, which also can be considered as the members of the wall-frame structure family, are not included in this thesis, but are treated in Ref. 18.

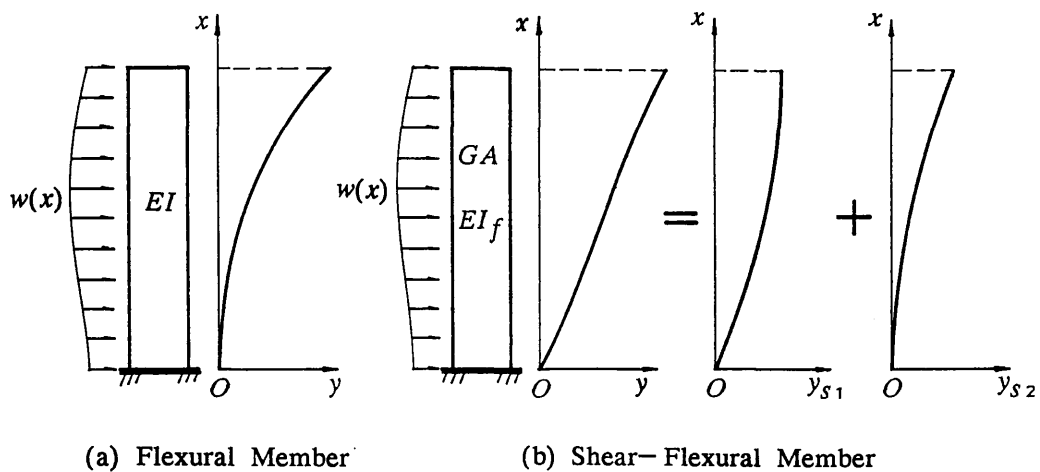


Fig. 4.1 Modes of Deflection Behaviour of Two Types of Beam

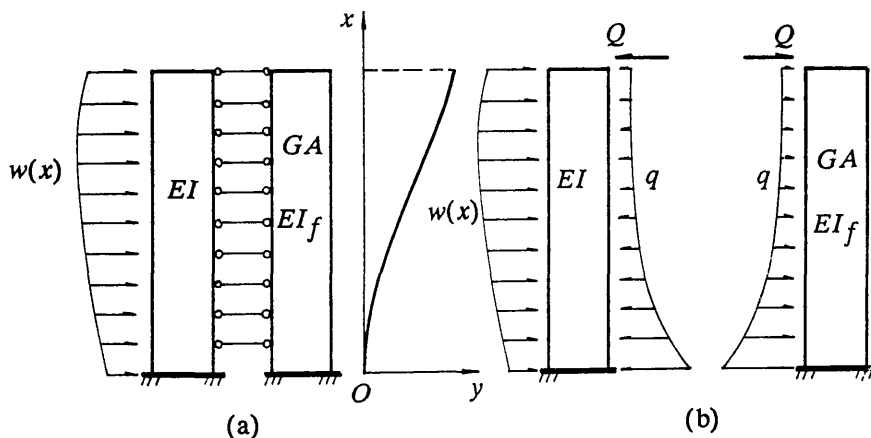


Fig. 4.2 Interaction Between Flexural and Shear-Flexural Beams

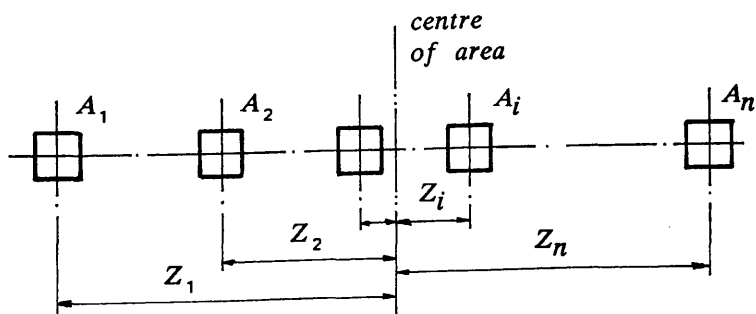


Fig. 4.3 Column Section of Multibay Rigid Frame

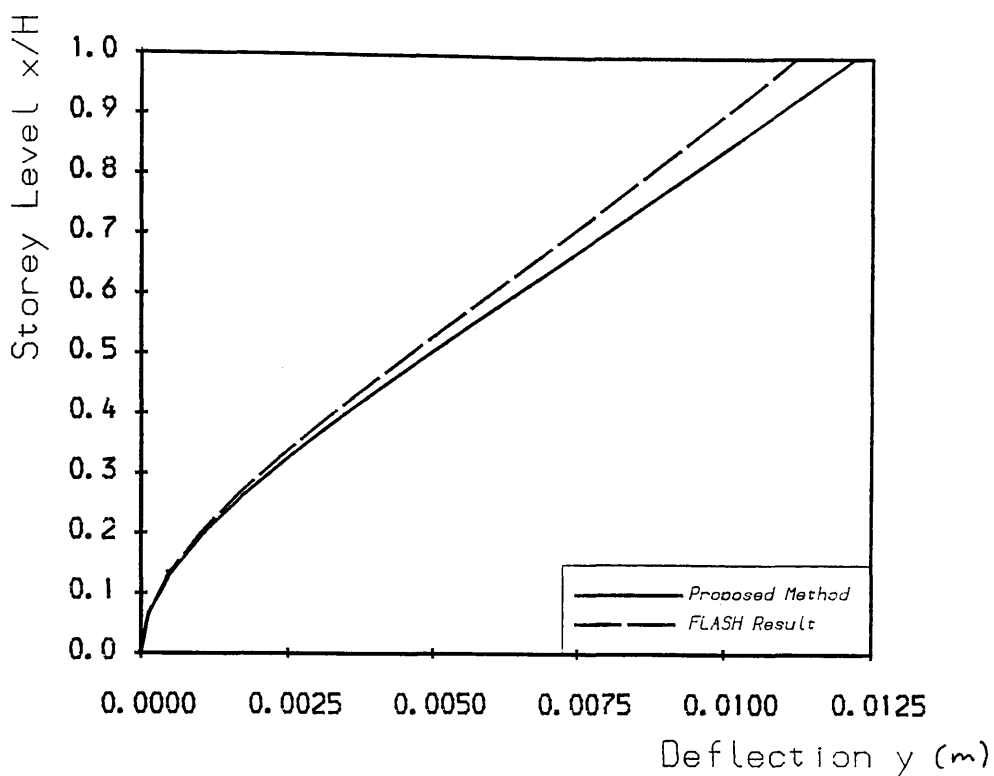


Fig. 4.4a 15-Storey Wall-Frame Example
Revised Wall-Frame Theory

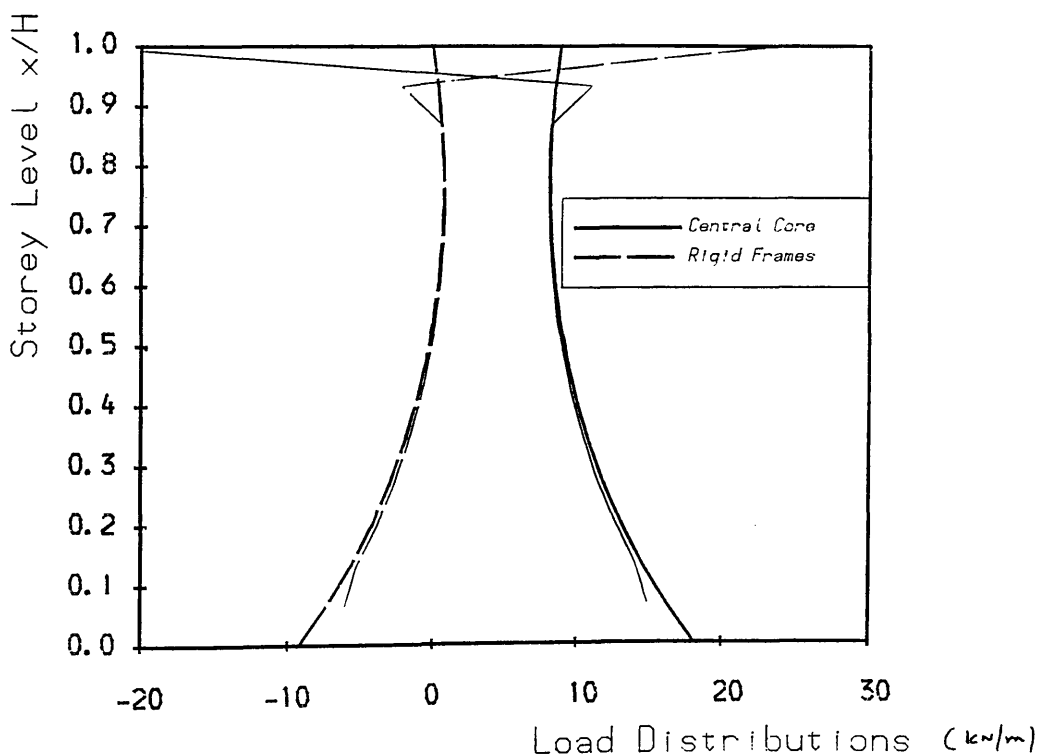


Fig. 4.4b 15-Storey Wall-Frame Example
Revised Wall-Frame Theory

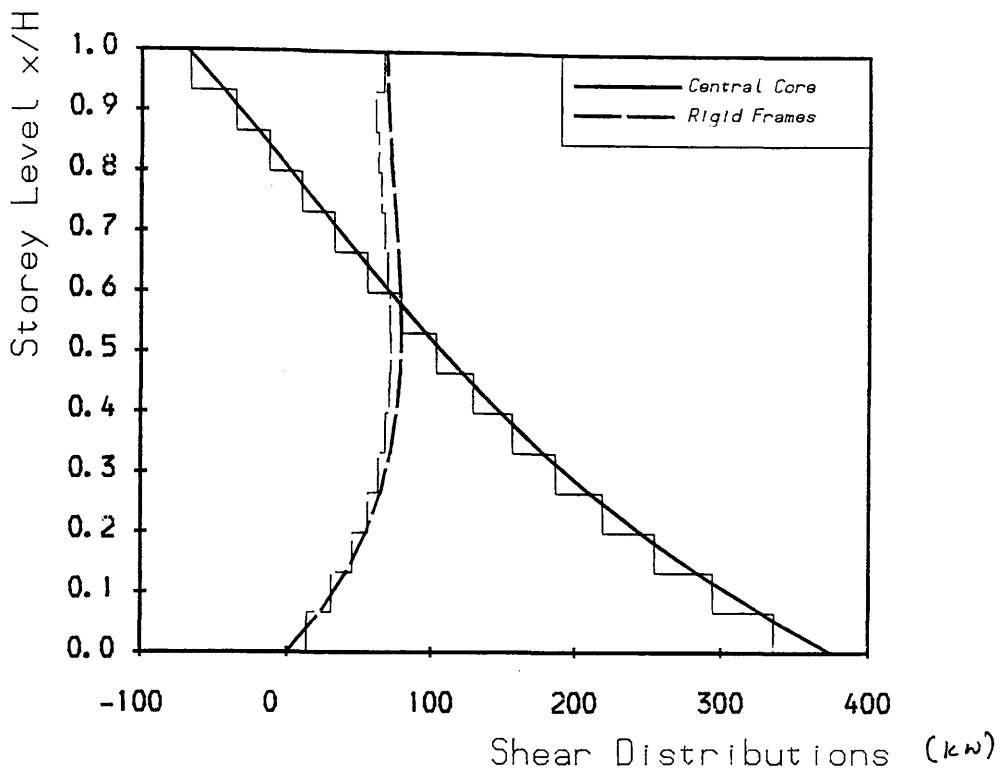


Fig. 4.4c 15-Storey Wall-Frame Example
Revised Wall-Frame Theory

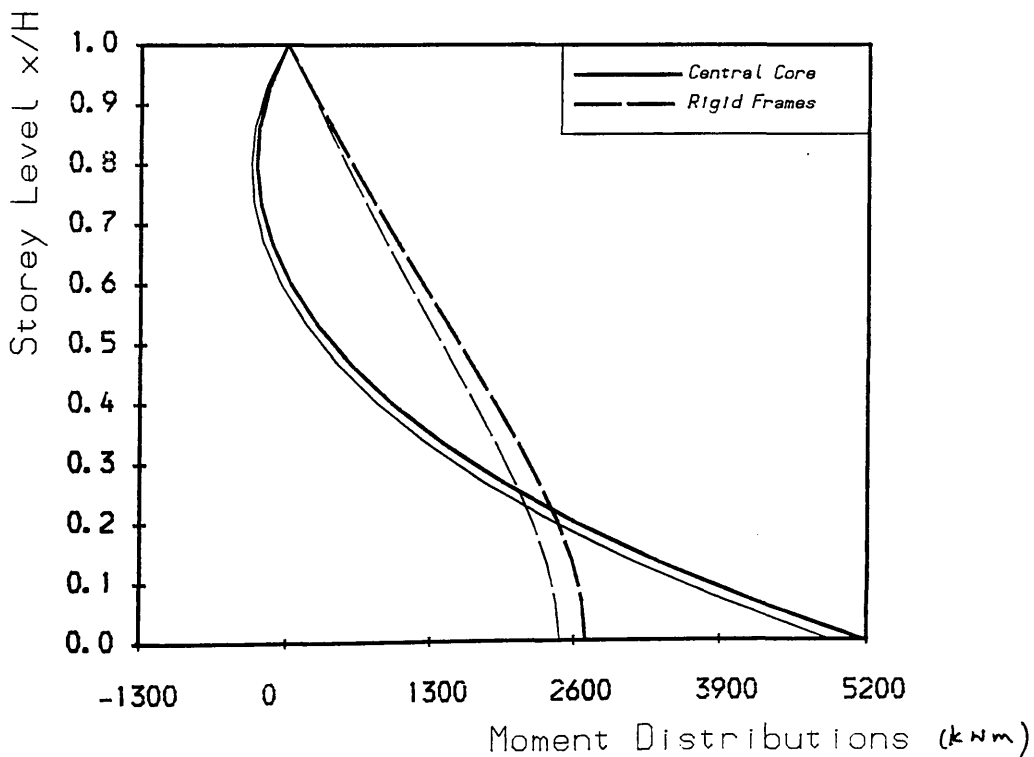


Fig. 4.4d 15-Storey Wall-Frame Example
Revised Wall-Frame Theory

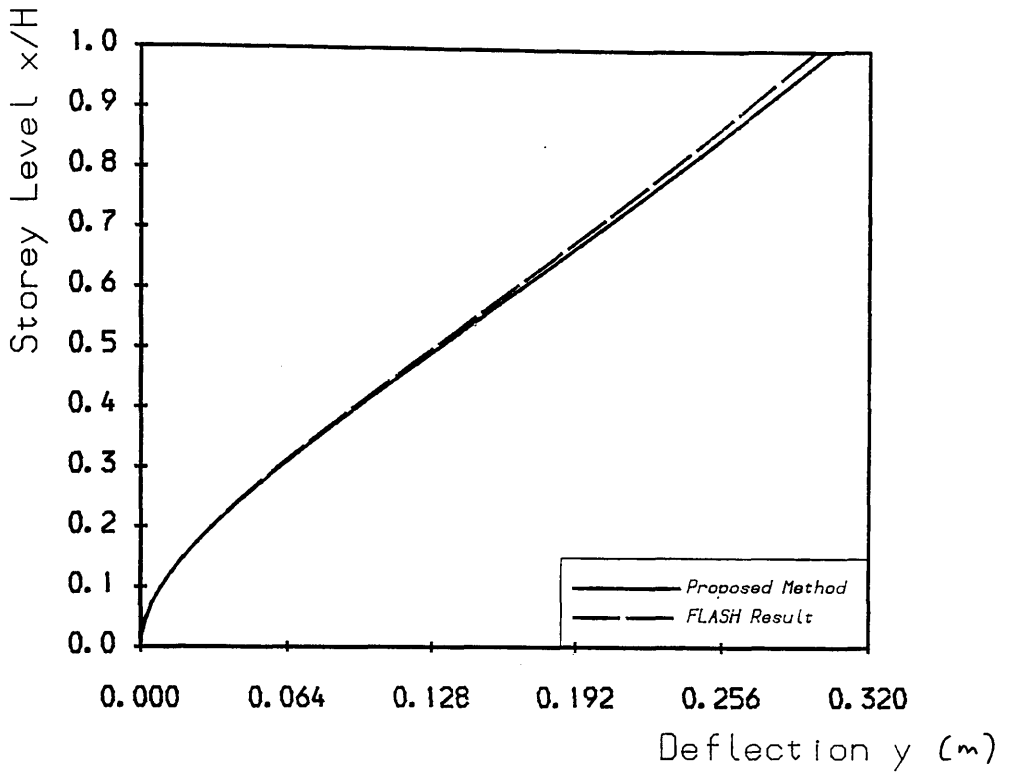


Fig. 4.5a 40-Storey Wall-Frame Example
Revised Wall-Frame Theory

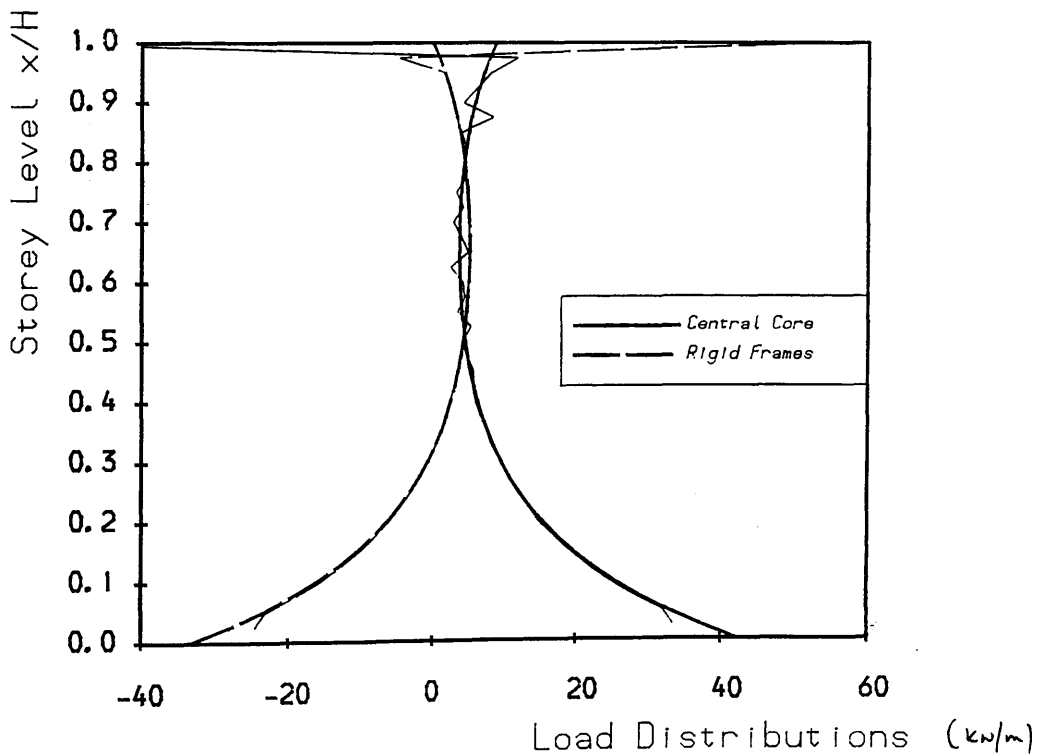


Fig. 4.5b 40-Storey Wall-Frame Example
Revised Wall-Frame Theory

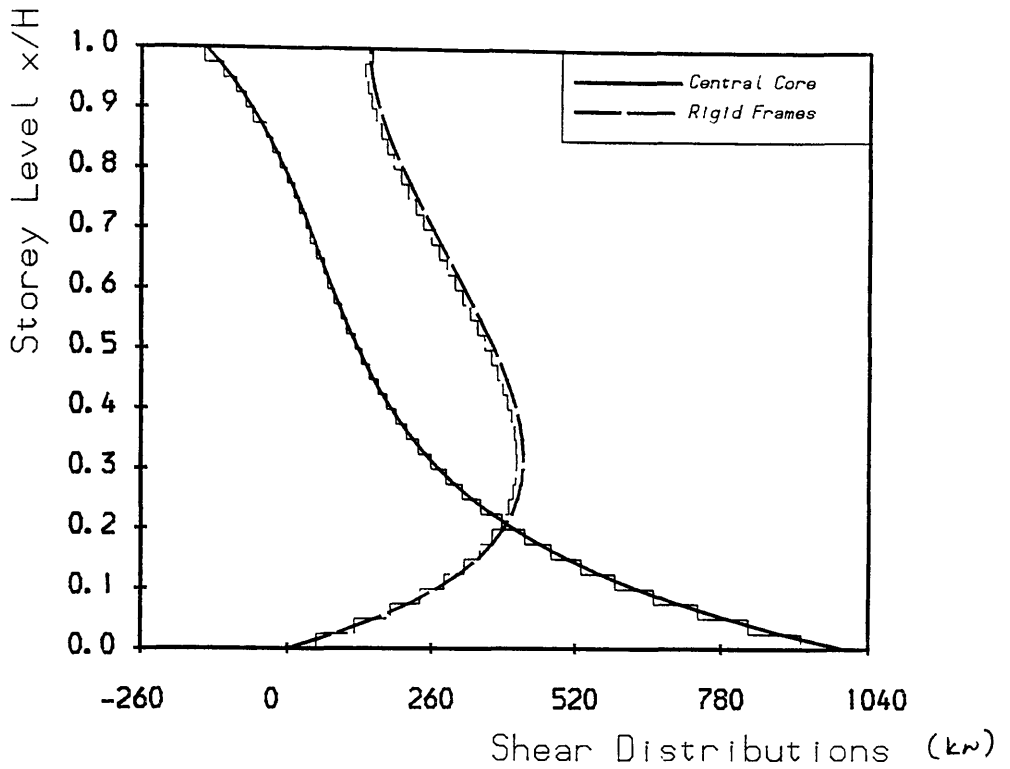


Fig. 4.5c 40-Storey Wall-Frame Example
Revised Wall-Frame Theory

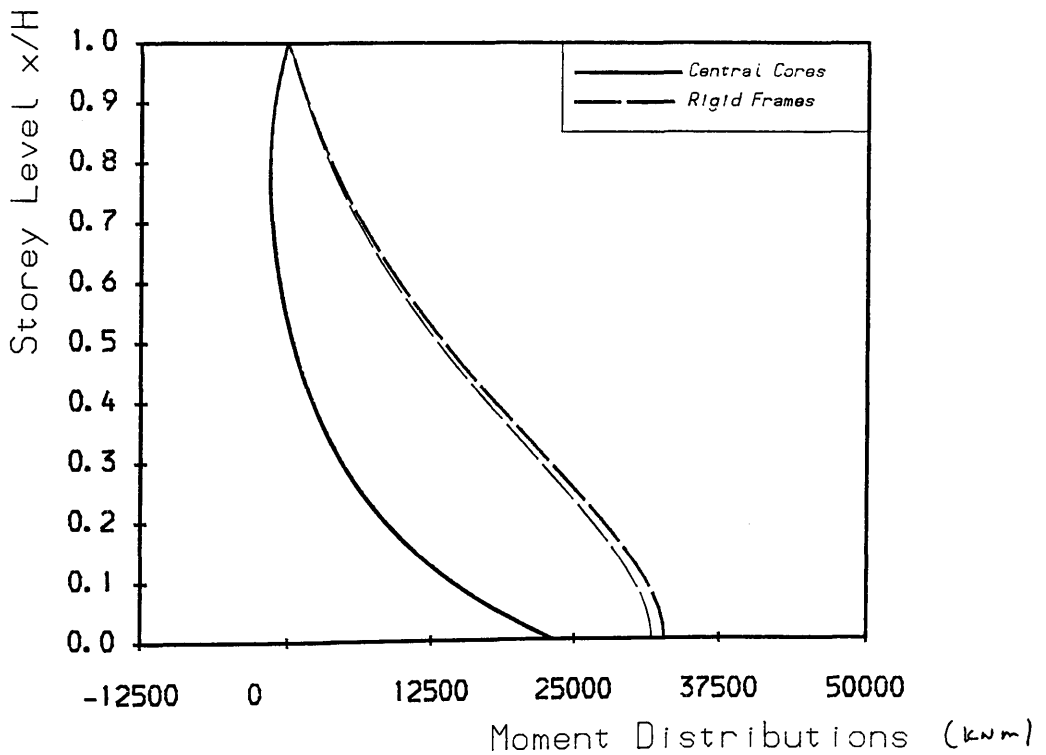
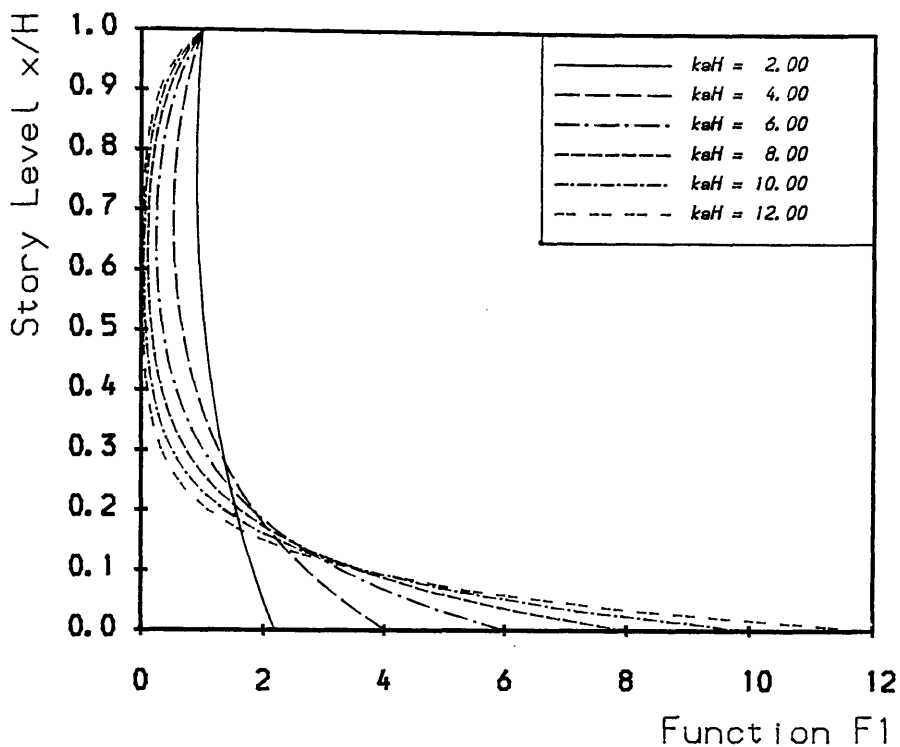
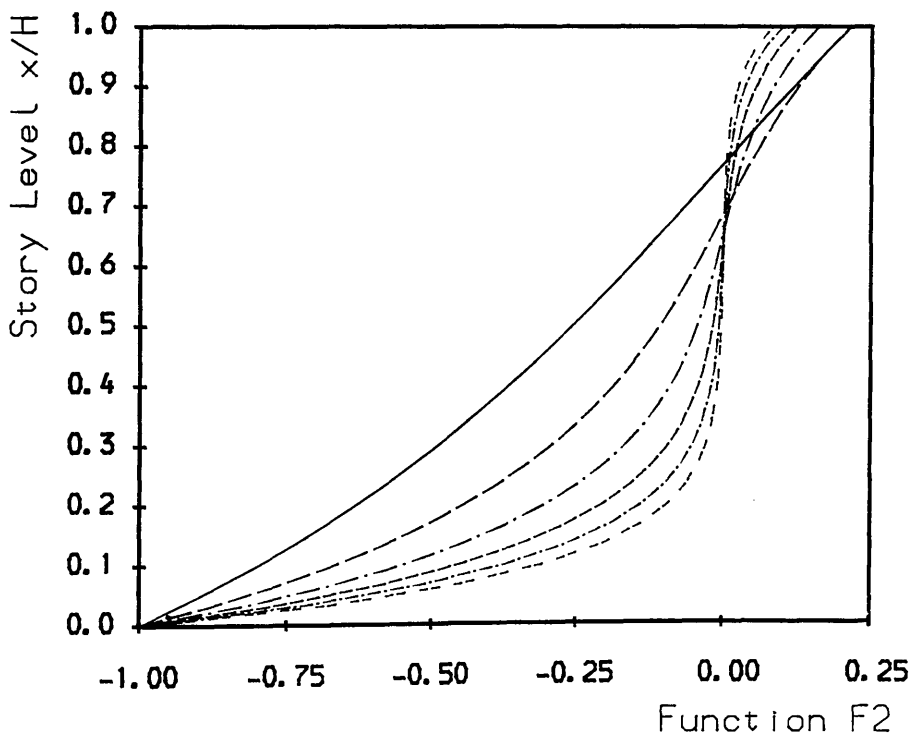


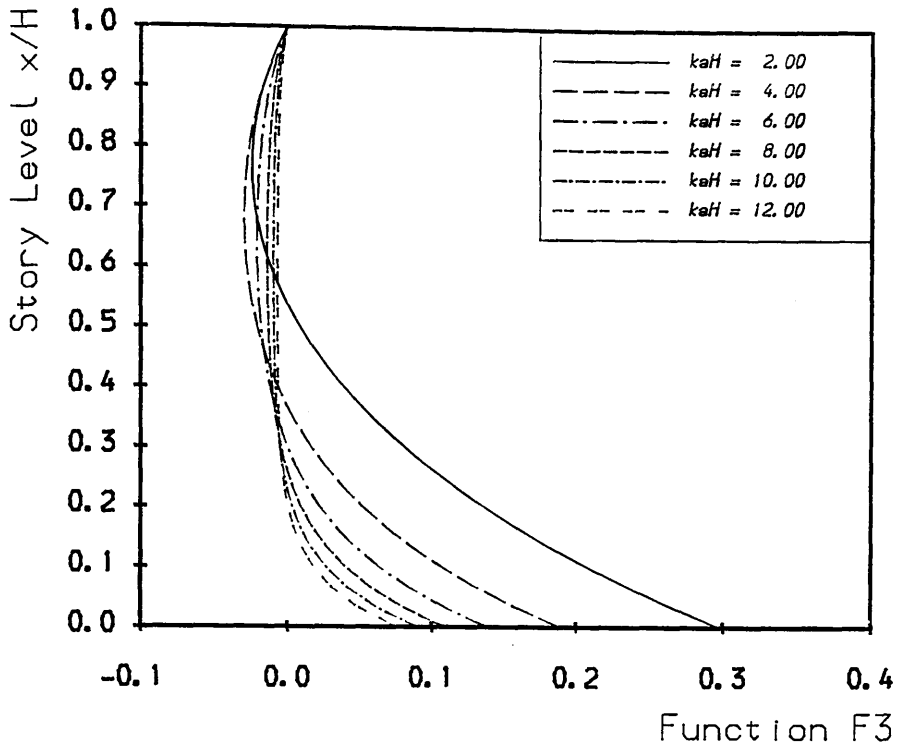
Fig. 4.5d 40-Storey Wall-Frame Example
Revised Wall-Frame Theory



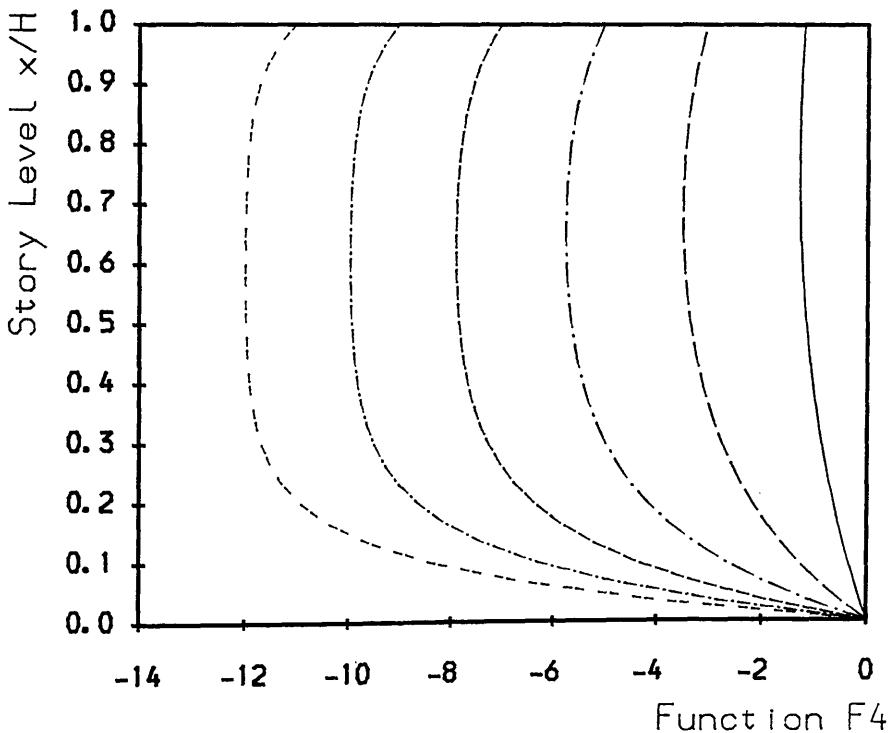
Variation of Function F1
Fig. 4.6a Design Curves



Variation of Function F2
Fig. 4.6b Design Curves



Variation of Function F3
Fig. 4.6c Design Curves



Variation of Function F4
Fig. 4.6d Design Curves

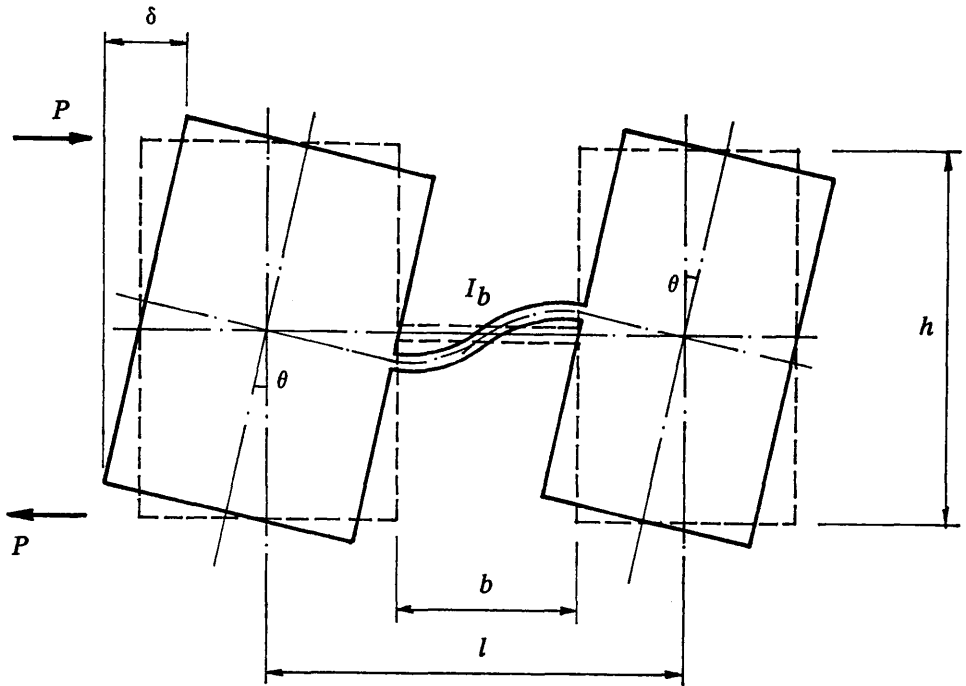


Fig. 4.7 Deflection of Coupled Shear Walls
Related to Effective Shear Stiffness

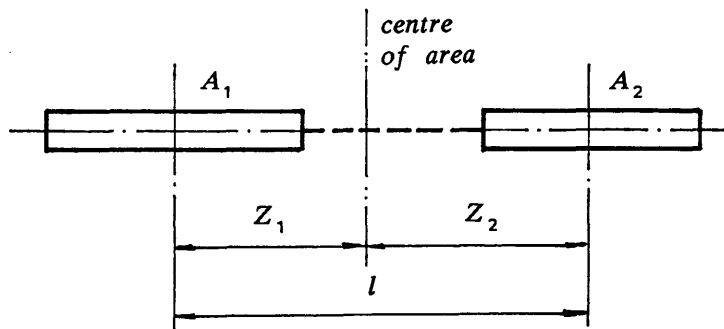


Fig. 4.8 Wall Section with Centre of Area

CHAPTER 5
SIMPLIFIED ANALYSIS OF REGULAR THREE-DIMENSIONAL
WALL-FRAME STRUCTURES SUBJECTED TO BENDING AND TORSION

5.1 Introduction

In the previous chapters, the modes of load-deformation behaviour of various high-rise structural cantilevers and their interactions have been discussed. These structural cantilevers, plane shear walls, cores, rigid frames and coupled shear walls, represent almost all types of high-rise structural bents which, individually or in combination, are usually employed in tall building structures to resist both horizontal and gravitational loads. It has been shown that, when these various types of cantilevers are combined in a tall building structure and subjected to lateral loads, the differences in their modes of load-deformation behaviour will cause them to interact horizontally through the connecting slabs and hence significant lateral force redistributions will occur in these elements. The analyses of the interactions for a combination of any two types of cantilevers, in addition to a pure flexural cantilever, have been presented in the previous chapters. The analyses can be applied directly to regular symmetric tall building structures which consist of combinations of two types of cantilevers only, combined with any number of pure flexural cantilevers, subjected to pure bending action. However, most tall building structures are composed of many types of high-rise bents in order to meet different architectural requirement as well as satisfactory structural performance. For the reason that it has not been found possible to achieve a general closed-form mathematical solution for a complex three-dimensional structure which involves more than three interactive assemblies, and even more difficult when torsion takes place due to either asymmetry of building plan or eccentricity of external loading, an approximate method is now developed for the

analysis of regular symmetric three-dimensional high-rise wall-frame structures subjected to pure bending action, based on the revised wall-frame theory. The method is then extended to the analysis of more complex three-dimensional asymmetric structures subjected to bending and torsion. The structures considered may consist of any number of parallel cantilever bents, including flexural cantilevers such as plane shear walls and cores, and shear-flexural cantilevers such as coupled shear walls and rigid frames. Other types of cantilevers such as braced frames and rigid jointed wall-frame assemblies can also be included, but are not included in the chapter. Typical planforms for such structures are shown in Fig. 5.1.

Although the majority of structures contain bents which are parallel or orthogonal, occasionally some exist at an angle to the main axes. If the structure includes any inclined bents, the same techniques may be used provided that the appropriate stiffness components of the inclined bents are used.

5.2 Basic Assumptions

(1) The structure is considered to be uniform with all the components having constant properties throughout their height.

(2) The structure is considered to consist of parallel assemblies which can be divided into two types. The first type is the flexural cantilever which is characterized by its flexural rigidity EI . This includes plane shear walls and any cores which undergo pure flexural deformation. The second type is a group of cantilevers which have been classified as a family of shear-flexure cantilevers including coupled shear walls, and rigid and braced frames. Such cantilevers can be represented by equivalent interacting wall-frame assemblies, each having three

effective rigidities, representing their three primary modes of load-deformation behaviour.

(3) The floor slabs connecting all the assemblies at every storey level are considered to have such large in-plane stiffnesses that they are assumed to be rigid in their own plane. It follows that all the assemblies undergo a rigid body movement at every floor level, and, consequently, there is a linear displacement relationship for all the assemblies at every floor level.

(4) The basic equations for the method given in this chapter is that for a uniformly distributed lateral load of intensity w_0 . The equations for the other two standard load cases, which are of a concentrated horizontal load P at the top of the structure and a triangularly distributed lateral load of maximum intensity q_0 at the top, are given in Appendix 3. On using these equations, the other two load cases can also be considered.

5.3 Analysis of Regular Symmetric Three-Dimensional Wall-Frame Structure Subjected to Pure Bending

Consider a symmetrical structure subjected to a uniformly distributed lateral load of intensity w_0 at the centre of the structure, as shown in Fig. 5.2a. Following Assumption (3), all the assemblies in the structure will have identical horizontal deflections, so that the structure can be replaced by an equivalent plane system in which the assemblies are connected at every storey level by axially-stiff pin-ended links. Since the analysis uses the continuum technique, these pin-ended links are incorporated by equivalent continuous pin-connected media, as shown in Fig. 5.2b. Suppose the assemblies in the structure in the first instance are all shear-flexure cantilevers which are represented by 'wall-frame'

assemblies, each having a 'wall' member, which is a pure flexural member of flexural rigidities EI representing its flexural mode of behaviour, interacting with a 'frame' member, which is a combined racking shear and overall bending cantilever with two corresponding shear and overall-bending rigidities GA and EI_f representing its two combined modes of deformation behaviour, respectively. The structure then can be further replaced by a plane system of interacting wall-frame assemblies, as shown in Fig. 5.2c. It is now assumed that the corresponding members which have the same load-deformation behaviour in all the assemblies can be lumped together, so that the structure can be represented by a single wall-frame structure, as shown in Fig. 5.2d, in which the lumped wall represents all the 'wall' members, having a overall flexural rigidity EI_t , which is the sum of all the flexural rigidities, and the lumped frame consisting of all the 'frame' members, having a total shear rigidity GA_t and a total overall-bending rigidity EI_{ft} , each being the sum of the corresponding components in the structure. A flexural cantilever of flexural rigidity EI then may be considered as a special case of a wall-frame assembly with zero values of GA and EI_f .

For a structure which consists of n wall-frame assemblies as shown in Figs. 5.2a to 5.2c, the three overall rigidities for the structure are obtained as,

$$EI_t = \sum^n EI_i, \quad GA_t = \sum^n GA_i \quad \text{and} \quad EI_{ft} = \sum^n EI_{fi} \quad (5.1)$$

By making use of the revised wall-frame theory in chapter 4, the deflection of the structure is determined by,

$$y = \frac{w_0 H^4}{EI_t} \left\{ \frac{k^2-1}{24k^2} (\xi^4 - 4\xi^3 + 6\xi^2) + \frac{1}{k^2(k\alpha H)^2} \left(\xi - \frac{\xi^2}{2} \right) + \frac{\cosh k\alpha H \xi + k\alpha H \sinh k\alpha H (1-\xi) - k\alpha H \sinh k\alpha H - 1}{k^2(k\alpha H)^4 \cosh k\alpha H} \right\} \quad (5.2)$$

As a single interacting wall-frame structure, the resultant loads and forces distributed into the two lumped components can also be obtained by:

Distributions of load,

$$q_W = \left\{ \frac{k^2-1}{k^2} + \frac{\cosh k\alpha H \xi + k\alpha H \sinh k\alpha H (1-\xi)}{k^2 \cosh k\alpha H} \right\} w_0 \quad (5.3)$$

$$q_F = \left\{ \frac{1}{k^2} - \frac{\cosh k\alpha H \xi + k\alpha H \sinh k\alpha H (1-\xi)}{k^2 \cosh k\alpha H} \right\} w_0 \quad (5.4)$$

Distributions of shear,

$$S_W = w_0 H \left\{ \frac{k^2-1}{k^2} (1-\xi) - \frac{\sinh k\alpha H \xi - k\alpha H \cosh k\alpha H (1-\xi)}{k^2 (k\alpha H) \cosh k\alpha H} \right\} \quad (5.5)$$

$$S_F = w_0 H \left\{ \frac{1}{k^2} (1-\xi) + \frac{\sinh k\alpha H \xi - k\alpha H \cosh k\alpha H (1-\xi)}{k^2 (k\alpha H) \cosh k\alpha H} \right\} \quad (5.6)$$

Distributions of bending moment,

$$M_W = w_0 H^2 \left\{ \frac{k^2-1}{2k^2} (1-\xi)^2 - \frac{1}{k^2 (k\alpha H)^2} + \frac{\cosh k\alpha H \xi + k\alpha H \sinh k\alpha H (1-\xi)}{k^2 (k\alpha H)^2 \cosh k\alpha H} \right\} \quad (5.7)$$

$$M_F = w_0 H^2 \left\{ \frac{1}{2k^2} (1-\xi)^2 + \frac{1}{k^2 (k\alpha H)^2} - \frac{\cosh k\alpha H \xi + k\alpha H \sinh k\alpha H (1-\xi)}{k^2 (k\alpha H)^2 \cosh k\alpha H} \right\} \quad (5.8)$$

In above equations, the subscript W and F refer to the two lumped components, the wall and the frame, respectively, $\xi = x/H$ is the non-dimensional height coordinate, H is the total height, and the parameters α and k in the equations are defined by,

$$\alpha^2 = \frac{GA_t}{EI_t} \quad (5.9)$$

$$k^2 = 1 + \frac{EI_t}{EI_{ft}} \quad (5.10)$$

These force distributions in the two lumped components, Eqs. 5.3 to 5.10, can be considered as the overall force distribution for the structure. That is, the force distribution in the lumped wall, referred to as F_W , is considered to be carried by all the flexural members of the components, with the force distribution in the lumped frame, referred to as F_F , to be carried by all the shear-overall-bending members of all the components. By apportioning F_W and F_F to each individual wall-frame assembly, the actual force distributions in the assembly, referring to as F_i , can be obtained, assuming that the force distributions in the assembly are divided into two parts; one carried by the flexural member, the other carried by the shear-overall-bending member, of the individual wall-frame assembly. On doing this, F_W is considered to be distributed in proportion to the individual flexural rigidity EI_i of the overall flexural rigidity EI_t . In the absence of any more fundamental basis for distributing the second force component, F_F is assumed to be apportioned by taking the average proportions of the individual shear rigidity GA_i and the individual overall-bending rigidity EI_{fi} to the total shear rigidity GA_t and the overall-bending rigidity EI_{ft} . This was regarded as being the simplest way of achieving the required distribution. That is,

$$F_i = v_{fi}F_W + v_{ci}F_F \quad (5.11)$$

in which v_{fi} and v_{ci} are the force distribution factors for each assembly i , given by,

$$v_{fi} = \frac{EI_i}{EI_t} \quad \text{and,} \quad v_{ci} = \frac{1}{2} \left(\frac{GA_i}{GA_t} + \frac{EI_{fi}}{EI_{ft}} \right) \quad (5.12)$$

Eq. 5.11 includes the distributions of load, shear and moment in each assembly, referring to Eqs. 5.3 to 5.8, that is,

$$w_i = v_{fi}w_W + v_{ci}w_F \quad (5.13)$$

$$S_i = v_{fi}S_W + v_{ci}S_F \quad (5.14)$$

$$M_i = v_{fi}M_W + v_{ci}M_F \quad (5.15)$$

in which w_i , M_i and S_i are the distributions of load, shear and moment in component i , respectively.

5.4 Analysis of Regular Three-Dimensional Wall-Frame Structures Subjected to Bending and Torsion

Following the approximate method presented in Section 5.3 for the analysis of symmetrical structures subjected to symmetrical loading, a generalized approximate method of analysis is developed for more complex three-dimensional wall-frame structures subjected to bending and torsion actions.

5.4.1 Method of Analysis

Consider a structure which consists of a number of wall-frame assemblies, either symmetrical or not, subjected to a known resultant lateral load at any position, as shown in Fig. 5.3a. Any asymmetry of the structural plan or eccentricity of the external loading will give rise to torsional actions in the structure, and the building will hence tend to twist as well as bend. Due to the constraint of the in-plane rigid connecting floor slabs, the assemblies will deform in a series of linearly related lateral deflections, and thus considerable force redistributions may take place among the assemblies due to their different modes of deformation behaviour.

Suppose that the structure consists of n wall-frame assemblies, subjected to a uniformly distributed lateral load of intensity w_0 at any particular position as shown in Fig. 5.3a. The structure will tend to bend as well as twist, and the related deflection configurations for the assemblies will be as shown in Fig. 5.3b.

For each assembly i in the structure, which is represented by its three rigidities, EI_i , GA_i and EI_{fi} , under the action of the interactive forces, its deflection is assumed to be y_i as shown in Fig. 5.4a. The proposed method assumes that for such an assembly i , an equivalent assembly ei can be found by defining three 'effective' rigidities, EI_{ei} , GA_{ei} and EI_{fei} , such that under the action of the applied load, which is now assumed to be a uniformly distributed lateral load w_0 , the equivalent assembly will have a deflection which is the same as y_i (Fig. 5.4b). That is, if the 'effective' rigidities for the assembly are obtained, the deflection y_i can be determined by the deflection equation, Eq.5.2, that is,

$$y_i = \frac{w_0 H^4}{EI_{ei}} \left\{ \frac{k_{ei}^2 - 1}{\cosh k_{ei} \alpha_{ei} H \xi + k_{ei} \alpha_{ei} H \sinh k_{ei} \alpha_{ei} H (1 - \xi)} (\xi^4 - 4\xi^3 + 6\xi^2) + \frac{1}{k_{ei} \alpha_{ei} H \sinh k_{ei} \alpha_{ei} H (1 - \xi) - k_{ei} \alpha_{ei} H \sinh k_{ei} \alpha_{ei} H - 1} (\xi - \xi^2) \right. \\ \left. + \frac{\cosh k_{ei} \alpha_{ei} H \xi + k_{ei} \alpha_{ei} H \sinh k_{ei} \alpha_{ei} H (1 - \xi) - k_{ei} \alpha_{ei} H \sinh k_{ei} \alpha_{ei} H - 1}{k_{ei}^2 (k_{ei} \alpha_{ei} H)^4 \cosh k_{ei} \alpha_{ei} H} \right\} \quad (5.16)$$

in which the parameters are defined as,

$$\alpha_{ei}^2 = \frac{GA_{ei}}{EI_{ei}} \quad (5.17)$$

$$k_{ei}^2 = 1 + \frac{EI_{ei}}{EI_{fei}} \quad (5.18)$$

Also, on considering this equivalent assembly ei as an interactive wall-frame structure as discussed in Chapter 4, subjected to the uniformly distributed lateral load w_0 , a series of resulting distributions of forces in the two kinds of cantilever beams, referred to as F_{Wei} and F_{Fei} respectively, can also be obtained from Eqs. 5.3 to 5.8 as:

Distributions of load,

$$q_{Wei} = \left\{ \frac{k_{ei}^2 - 1}{k_{ei}^2} + \frac{\cosh k_{ei} \alpha_{ei} H \xi + k_{ei} \alpha_{ei} H \sinh k_{ei} \alpha_{ei} H (1 - \xi)}{k_{ei}^2 \cosh k_{ei} \alpha_{ei} H} \right\} w_0 \quad (5.19)$$

$$q_{Fei} = \left\{ \frac{1}{k_{ei}^2} - \frac{\cosh k_{ei}\alpha_{ei}H\xi + k_{ei}\alpha_{ei}H \sinh k_{ei}\alpha_{ei}H(1-\xi)}{k_{ei}^2 \cosh k_{ei}\alpha_{ei}H} \right\} w_0 \quad (5.20)$$

Distributions of shear,

$$S_{Wei} = w_0 H \left\{ \frac{k_{ei}^2 - 1}{k_{ei}^2} (1 - \xi) - \frac{\sinh k_{ei}\alpha_{ei}H\xi - k_{ei}\alpha_{ei}H \cosh k_{ei}\alpha_{ei}H(1-\xi)}{k_{ei}^2 (k_{ei}\alpha_{ei}H) \cosh k_{ei}\alpha_{ei}H} \right\} \quad (5.21)$$

$$S_{Fei} = w_0 H \left\{ \frac{1}{k_{ei}^2} (1 - \xi) + \frac{\sinh k_{ei}\alpha_{ei}H\xi - k_{ei}\alpha_{ei}H \cosh k_{ei}\alpha_{ei}H(1-\xi)}{k_{ei}^2 (k_{ei}\alpha_{ei}H) \cosh k_{ei}\alpha_{ei}H} \right\} \quad (5.22)$$

Distributions of moment,

$$M_{Wei} = w_0 H^2 \left\{ \frac{k_{ei}^2 - 1}{2k_{ei}^2} (1 - \xi)^2 - \frac{1}{k_{ei}^2 (k_{ei}\alpha_{ei}H)^2} + \frac{\cosh k_{ei}\alpha_{ei}H\xi + k_{ei}\alpha_{ei}H \sinh k_{ei}\alpha_{ei}H(1-\xi)}{k_{ei}^2 (k_{ei}\alpha_{ei}H)^2 \cosh k_{ei}\alpha_{ei}H} \right\} \quad (5.23)$$

$$M_{Fei} = w_0 H^2 \left\{ \frac{1}{2k_{ei}^2} (1 - \xi)^2 + \frac{1}{k_{ei}^2 (k_{ei}\alpha_{ei}H)^2} - \frac{\cosh k_{ei}\alpha_{ei}H\xi + k_{ei}\alpha_{ei}H \sinh k_{ei}\alpha_{ei}H(1-\xi)}{k_{ei}^2 (k_{ei}\alpha_{ei}H)^2 \cosh k_{ei}\alpha_{ei}H} \right\} \quad (5.24)$$

in which the subscript W and F refer to the fictitious 'wall' and 'frame' components of the equivalent assembly ei .

When these loads and forces in the 'wall' and 'frame' are obtained from Eqs. 5.19 to 5.24, the method then assumes that the true forces in the original assembly i can be derived, referring to the method presented in Section 5.3, Eqs. 5.11 and 5.12, from,

$$F_i = v_{fi} F_{Wei} + v_{ci} F_{Fei} \quad (5.25)$$

in which, as before, the force distribution factors for each assembly i are given by,

$$v_{fi} = \frac{EI_i}{EI_{ei}} \quad \text{and,} \quad v_{ci} = \frac{1}{2} \left(\frac{GA_i}{GA_{ei}} + \frac{EI_{fi}}{EI_{fei}} \right) \quad (5.26)$$

Eq. 5.25 also includes the distributions of load, shear and moment, referring to Eqs. 5.13 to 5.15, that is,

$$w_i = v_{fi}w_{Wei} + v_{ci}w_{Fei} \quad (5.27)$$

$$S_i = v_{fi}S_{Wei} + v_{ci}S_{Fei} \quad (5.28)$$

$$M_i = v_{fi}M_{Wei} + v_{ci}M_{Fei} \quad (5.29)$$

The following section presents a method, referred to as 'Method of Rigid Beam on Spring Supports', which is used to determine the effective rigidities for all the assemblies in a complete structure.

5.4.2 Effective Rigidities – Method of Rigid Beam on Spring Supports

As the structure is deformed by the lateral load, the three equivalent rigidities of every assembly may be determined by considering that the deformations of the building cross-sections may be represented by a rigid body (representing the floor slabs), supported on a series of springs (representing the different rigidities of the various assemblies in the structure). The equivalent rigidities will depend on the resultant load position, as well as the relative rigidities of the different assemblies.

In order to illustrate the rigid beam method, consider as an example the special case of a structure which consists of parallel plane shear walls as shown in Fig. 5.5; that is, all the assemblies are flexural cantilevers, each having a flexural rigidity EI_i . The similarity of the load-deformation profiles of the assemblies causes the structure to have a uniform distribution of lateral resisting

rigidity throughout the height, and consequently a shear centre exists, so that under the action of the lateral load $w(x)$, the structure will tend to bend and twist about the shear centre. It follows that there are no force redistributions among the assemblies, that is; the applied load will be distributed to the assemblies in similar forms. In particular, if the applied load acts through the shear centre, the structure will bend without twisting, and the applied load will be distributed to the assemblies in proportion to their rigidities.

On considering the simplicity of the load and force distributions among the assemblies, the rigid bodies of the floor slabs of the structure are represented by a spring-supported rigid beam as shown in Fig. 5.6a, in which each supporting spring, its position, and its spring rigidity k_i correspond to the position and the flexural rigidity of the assembly in the structure. On referring to Fig. 5.5, $k_i = EI_i$, and a unit load P is located at the same position as the resultant applied lateral load w_0 . On choosing a point O as a datum, a simple calculation determines the deformation profile of the beam, as shown in Fig. 5.6b. The rotation of the beam θ can be determined by,

$$\theta = \frac{(d_p - d_0)P}{\sum k_i d_i^2 - d_0 \sum k_i d_i} \quad (5.30)$$

in which, referring to Fig. 5.6a, d_i is the distance between the assembly i and the chosen datum, d_p is the load position about the datum, and d_0 , which defines the position of the shear centre respecting the datum, is determined by,

$$d_0 = \frac{\sum k_i d_i}{\sum k_i} \quad (5.31)$$

The displacement at each spring position on the beam, δ_i , is then given by,

$$\delta_i = \delta_0 + \theta(d_i - d_p) \quad (5.32)$$

where δ_0 is the displacement at the shear centre position on the beam, given by,

$$\delta_0 = \frac{P}{\sum k_i} \quad (5.33)$$

The reacting force in each spring, R_i , then becomes,

$$R_i = k_i \delta_i \quad (5.34)$$

An effective rigidity k_{ei} for the spring k_i is now introduced, defined as,

$$k_{ei} = \frac{P}{\delta_i} \quad (5.35)$$

On using the effective rigidity, the displacement and the reacting force in the spring k_i can be obtained as,

$$\delta_i = \frac{P}{k_{ei}} = \frac{P}{P/\delta_i} = \delta_i \quad (5.36)$$

$$R_i = \frac{k_i}{k_{ei}} P = \frac{k_i}{P/\delta_i} P = k_i \delta_i \quad (5.37)$$

On applying such a method to the real structure, each flexural element of rigidity EI_i in the structure is assumed to be replaced by an equivalent flexural assembly of rigidity $EI_{ei} = k_{ei}$ (as $EI_i = k_i$). If the applied load is a uniformly distributed lateral load of intensity w_0 , on using the effective rigidity EI_{ei} for assembly i , the deflection y_i and the load distribution w_i can be obtained by,

$$y_i(x) = \frac{w_0 H^4}{EI_{ei}} \left\{ \left(\frac{x}{H}\right)^4 - 4\left(\frac{x}{H}\right)^3 + 6\left(\frac{x}{H}\right)^2 \right\} \quad (5.38)$$

and,

$$w_i(x) = \frac{EI_i}{EI_{ei}} w_0 \quad (5.39)$$

It can be shown that through this simple rigid beam method, exact solutions can be obtained for a structure which consists of similar types of assemblies. However, if the structure considered consists of wall-frame assemblies

which have different modes of load–deformation behaviour, each of these assemblies usually has originally three distinct structural rigidities representing the three primary modes of lateral load deformation. The rigid beam system for the structure then will be as shown in Fig. 5.7, in which each supporting spring i represents three rigidities, EI_i , GA_i and EI_{fi} . As the method of analysis requires that three equivalent rigidities for each assembly be determined, an approximation is made in the analysis by assuming that the spring system in Fig. 5.7 can be uncoupled into three corresponding rigid beams, as shown in Figs. 5.8a, 5.8b and 5.8c. On using Eqs. 5.30 to 5.33, three deformation profiles of the beams are then determined which give the results for the three equivalent rigidities for each assembly from Eq. 5.35; that is,

$$EI_{ei} = P/\delta_i \quad (5.40)$$

$$GA_{ei} = P/\lambda_i \quad (5.41)$$

$$EI_{fei} = P/\varepsilon_i \quad (5.42)$$

in which, referring to Figs. 5.8a to 5.8c, δ_i , λ_i and ε_i are the displacements of the corresponding springs in the three rigid beam models.

5.4.3 Special Case of Symmetrical Structures Subjected to Pure Bending Action

If the structure is symmetric in plan and laterally loaded at the centre of the structure as discussed in Section 5.3, the structure then has a shear centre in the middle throughout the height, through which the applied load acts. The three beams in Figs. 5.8a to 5.8c, with the load P acting at the centres, will all have translational displacements only. This can be shown from Eq. 5.30, with $d_p = d_0$, $\theta = 0$. It then follows from Eqs. 5.34 and 5.35 that,

$$\delta_i = \delta_0 = \frac{P}{\sum k_i} \quad (5.43)$$

From Eqs. 5.35 and 5.43, the equivalent rigidity becomes,

$$k_{ei} = \frac{P}{\delta_i} = \sum_i^n k_i \quad (5.44)$$

The conclusion from Eq. 5.44 implies that the equivalent rigidities k_{ei} for all assemblies are the same, being the sum of the rigidities of all the assemblies. This applies to the three types of structural rigidities, EI_{ei} , GA_{ei} and EI_{fei} ; that is,

$$EI_{ei} = \sum_i^n EI_i, \quad GA_{ei} = \sum_i^n GA_i \text{ and } EI_{fei} = \sum_i^n EI_{fi} \quad (5.45)$$

Comparing Eq. 5.45 with Eq. 5.1, it can be seen that in this special case, the method gives exactly the same solution as that in Section 5.3. It therefore can be concluded that the proposed method is a generalized method for three-dimensional wall-frame structures, either symmetric or asymmetric, subjected to bending and torsion actions.

5.5 Analysis Procedure

The following procedure describes how to use the present method to analyze three-dimensional tall wall-frame structures subjected to lateral loads.

(1). Calculate the three structural rigidities, EI_i , GA_i and EI_{fi} , for the individual assemblies. This has been described in Section 4.4 and 4.7 for coupled shear walls and rigid frames. For pure flexural assemblies of flexural rigidities EI_i , they are considered as having zero values of GA_i and EI_{fi} .

(2). Calculate the three effective rigidities, EI_{ei} , GA_{ei} and EI_{fei} for each

assembly, using the method described in Section 5.4.2, Eqs. 5.30 to 5.37 and Eqs. 5.40 to 5.42 (Figs. 5.8a to 5.8c)

(3). For a resultant external uniformly distributed lateral load, on obtaining the effective structural parameters for each assembly, k_{ei} and α_{ei} , the deflection of the assembly is then determined by Eq. 5.16. Following Eqs. 5.19 to 5.29, the distributions of load, shear and moment on the assembly are then obtained. For the other two standard load cases, other than using Eqs. 5.16, and 5.19 to 5.24a, solutions can be obtained by using the alternative equations in Appendix 3.

In the particular case of symmetrical structures subjected to pure bending action, the three effective rigidities of each assembly can be obtained from Eqs. 5.1, noting that the effective rigidities of each assembly are the same for all the assemblies, being the overall rigidities for the structure, EI_t , GA_t and EI_{ft} . The solutions for the deflection and the distributions of load, shear and moment can then be determined using Eqs. 5.2 to 5.15.

5.6 Numerical Examples

A number of examples have been worked out using the present methods, and the results have been compared with those obtained from the FLASH program in order to examine the validity and the accuracy of the present methods. The following sections present four representative examples, the first two being symmetric structures subjected to pure bending actions, using the method presented in Section 5.3, and the last two being asymmetric structures subjected to bending and torsional actions, using the method presented in Section 5.4.

Symmetric Structure Example 1.

The planform of a 30-storey symmetric structure is as shown in Fig. 5.9, subjected to a uniformly distributed lateral load of intensity 20 kN/m. Due to symmetry, only half of the structure is considered, which consists of a flexural element (half of the central core), three identical 7-span rigid frames and a pair of coupled shear walls, subjected to half of the applied load, $w_0 = 10$ kN/m. The three identical rigid frames, due to their similar structural behaviour, are lumped together as a single element with a summed rigidity. The total resulting forces on the lumped frame then can be divided equally into each frames afterwards.

The original data for the structure are,

Storey height h	2.8 m
Number of storeys	30
Total height H	84.0 m
Modulus of elasticity E	1.40×10^7 kN/m ²
Uniformly distributed load w_0	10 kN/m

Coupled Shear Walls:

Depths of the two walls	$D_1 = D_2 = 6.0$ m
Clear span of the beams b	6.0 m
Depths of the connecting beams D_b	0.50 m
Thickness of the walls and beams t	0.30 m

Lumped rigid frame (total stiffnesses):

Beam spans b_i ($i = 1$ to 7)	4.0 m
Inertias of beams I_{bi}	$1.563 \times 10^{-2} \text{ m}^4$
Inertias of columns I_{ci} ($i=1$ to 8)	$3.125 \times 10^{-2} \text{ m}^4$
Column sectional areas A_{ci}	1.500 m^2

Core assembly:

Flexural rigidity EI	$1.660 \times 10^8 \text{ kN m}^2$
------------------------	------------------------------------

The structural rigidities for the assemblies are,

Coupled shear walls:

$$EI_1 = 1.512 \times 10^8 \text{ kN m}^2$$

$$GA_1 = 1.226 \times 10^5 \text{ kN}$$

$$EI_{f1} = 1.814 \times 10^9 \text{ kN m}^2$$

Lumped rigid frame:

$$EI_2 = 3.500 \times 10^6 \text{ kN m}^2$$

$$GA_2 = 1.241 \times 10^6 \text{ kN}$$

$$EI_{f2} = 1.411 \times 10^{10} \text{ kN m}^2$$

Flexural assembly:

$$EI_3 = 1.660 \times 10^8 \text{ kN m}^2$$

Overall rigidities:

$$EI_t = 3.207 \times 10^8 \text{ kN m}^2$$

$$GA_t = 1.364 \times 10^6 \text{ kN}$$

$$EI_{ft} = 1.592 \times 10^{10} \text{ kN m}^2$$

The structural parameters for the structure are,

$$EI = 3.207 \times 10^8 \text{ kN m}^2$$

$$\alpha = 0.06521 \text{ m}^{-1}, \quad k = 1.01002$$

Force distribution factors:

$$v_{f_1} = 0.4715, \quad v_{c_1} = 0.1019$$

$$v_{f_2} = 0.0109, \quad v_{c_2} = 0.8981$$

$$v_{f_3} = 0.5176, \quad v_{c_3} = 0$$

The results obtained from the present method and from the FLASH analysis are shown in Figs. 5.10a to 5.10d, including the deflection of the structure, the load distribution, the shear distribution and the moment distribution between the assemblies. In these figures, the thicker lines represent the present method, and thinner lines represent the results from the FLASH program. It can be seen that the present method gives very accurate results when compared with the FLASH analysis.

Symmetric Structure Example 2.

The planform of a 40-storey symmetric structure is shown in Fig. 5.11, subjected to a uniformly distributed lateral load of intensity 20 kN/m. The half of the structure considered consists of two pairs of coupled shear walls, two identical rigid frames and the half of the central core as a flexural assembly. As before, the two rigid frames are considered to be a lumped rigid frame with their summed rigidities. The applied lateral load is then $w_0 = 10$ kN/m.

The original data for the structure are as follows,

Storey height h	2.8 m
Number of storeys	40
Total height H	112.0 m
Modulus of elasticity E	1.40×10^7 kN/m ²
Uniformly distributed load w_0	10 kN/m

Coupled Shear Walls A:

Depths of the two walls D_1, D_2	5.5, 4.5 m
Clear span of the beams b	2.0 m
Depths of the connecting beams D_b	0.40 m
Thickness of the walls and beams t	0.30 m

Coupled Shear Walls B:

Depths of the two walls D_1, D_2	4.5, 4.0 m
Clear span of the beams b	3.0 m
Depths of the connecting beams D_b	0.40 m
Thickness of the walls and beams t	0.30 m

Lumped 5-span rigid frame (total stiffnesses):

Beam spans b_i ($i = 1$ to 5)	2.5, 2.5, 2.0, 2.5, 2.5 m
Inertias of beams I_{bi}	$5.2083 \times 10^{-3} \text{ m}^4$
Inertias of columns I_{ci} ($i=1$ to 8)	$1.0417 \times 10^{-2} \text{ m}^4$
Column sectional areas A_{ci}	0.2500 m^2

Core assembly:

Flexural rigidity EI	$1.660 \times 10^8 \text{ kN m}^2$
------------------------	------------------------------------

The structural rigidities for the assemblies are,

Coupled shear walls A:

$$EI_1 = 9.012 \times 10^7 \text{ kN m}^2$$

$$GA_1 = 5.295 \times 10^5 \text{ kN}$$

$$EI_{f1} = 5.094 \times 10^8 \text{ kN m}^2$$

Coupled shear walls B:

$$EI_2 = 5.429 \times 10^7 \text{ kN m}^2$$

$$GA_2 = 1.781 \times 10^5 \text{ kN}$$

$$EI_{f_2} = 4.675 \times 10^8 \text{ kN m}^2$$

Lumped rigid frame:

$$EI_3 = 8.750 \times 10^5 \text{ kN m}^2$$

$$GA_3 = 4.304 \times 10^5 \text{ kN}$$

$$EI_{f_3} = 6.894 \times 10^8 \text{ kN m}^2$$

Flexural assembly:

$$EI_4 = 1.660 \times 10^8 \text{ kN m}^2$$

Overall rigidities:

$$EI_t = 3.113 \times 10^8 \text{ kN m}^2$$

$$GA_t = 1.138 \times 10^6 \text{ kN}$$

$$EI_{ft} = 1.666 \times 10^9 \text{ kN m}^2$$

The structural parameters for the structure are,

$$EI = 3.113 \times 10^8 \text{ kN m}^2$$

$$\alpha = 0.06042 \text{ m}^{-1}$$

$$k = 1.08941$$

Force distribution factors:

$$v_{f_1} = 0.2895, \quad v_{c_1} = 0.3855$$

$$v_{f_2} = 0.1744, \quad v_{c_2} = 0.2185$$

$$v_{f_3} = 0.0028, \quad v_{c_3} = 0.3960$$

$$v_{f_4} = 0.5333, \quad v_{c_4} = 0$$

Figs. 5.12a to 5.12d show the resulting curves obtained from the present method, compared with the results from the FLASH program. It can be seen that for this relatively complicated structure, the solution of the present approximate method still compares reasonably accurately with the results from the FLASH analysis.

Asymmetric Structure Example 1.

The 30-storey structure, as shown in Fig. 5.13, consists of two pairs of coupled shear walls and three unequal rigid frames. The applied lateral load considered is a uniformly distributed load, $w_0 = 10 \text{ kN/m}$, acting respectively at three load positions as shown in Fig. 5.13. The results, thus, are given for three load cases.

The original data for the structure are as follows,

Storey height h	2.8 m
Number of storeys	30
Total height H	84.0 m
Modulus of elasticity E	$1.40 \times 10^7 \text{ kN/m}^2$
Uniformly distributed load w_0	10 kN/m

Coupled Shear Walls A:

Depths of the two walls D_1, D_2	6.0, 8.0 m
Clear span of the beams b	3.0 m
Depths of the connecting beams D_b	0.40 m
Thickness of the walls and beams t	0.30 m

Rigid frame 1 (3-span):

Beam spans b_i ($i = 1$ to 3)	6.0, 3.0, 4.5 m
Inertias of beams	$I_{b_1} = 4.5000 \times 10^{-3} \text{ m}^4,$ $I_{b_2} = 1.3333 \times 10^{-3} \text{ m}^4,$ $I_{b_3} = 2.6042 \times 10^{-3} \text{ m}^4$
Inertias of columns I_{c_i} ($i=1$ to 4)	$1.0800 \times 10^{-2} \text{ m}^4$
Column sectional areas A_{c_i}	0.3600 m^2

Rigid frame 2 (4-span):

Beam spans b_i ($i = 1$ to 4)	3.0, 4.5, 5.0, 2.5 m
Inertias of beams	$I_{b_1} = 1.3333 \times 10^{-3} \text{ m}^4,$ $I_{b_2} = 2.6042 \times 10^{-3} \text{ m}^4,$ $I_{b_3} = 2.6042 \times 10^{-3} \text{ m}^4,$ $I_{b_4} = 5.6250 \times 10^{-4} \text{ m}^4$
Inertias of columns I_{c_i} ($i=1$ to 5)	$1.0800 \times 10^{-2} \text{ m}^4$
Column sectional areas A_{c_i}	0.3600 m^2

Rigid frame 3 (6-span):

Beam spans b_i ($i = 1$ to 6)	3.5, 3.0, 2.5, 2.5, 2.5 2.5 m
Inertias of beams	$I_{b_1} = 1.3333 \times 10^{-4} \text{ m}^4,$ $I_{b_i} (i=2 \text{ to } 6) = 5.6250 \times 10^{-4} \text{ m}^4$
Inertias of columns I_{c_i} ($i=1$ to 7)	$5.2083 \times 10^{-3} \text{ m}^4$
Column sectional areas A_{c_i}	0.2500 m^2

Coupled Shear Walls B:

Depths of the two walls D_1, D_2	6.0, 4.0 m
Clear span of the beams b	4.0 m
Depths of the connecting beams D_b	0.40 m
Thickness of the walls and beams t	0.30 m

The original structural rigidities and the calculated parameters for all individual assemblies are listed as follows,

Assembly 1 - Coupled shear walls A:

$$EI = 2.54800\text{E}+08 \quad GA = 3.38926\text{E}+05 \quad EI_f = 1.44000\text{E}+09$$

$$k = 1.08487034\text{E}+00 \quad \alpha = 3.64714228\text{E}-02$$

Assembly 2 - Rigid frame 1:

$$EI = 6.04800E+05 \quad GA = 9.47854E+04 \quad EI_f = 4.84785E+08$$

$$k = 1.00062370E+00 \quad \alpha = 3.95881057E-01$$

Assembly 3 - Rigid frame 2:

$$EI = 7.56000E+05 \quad GA = 9.55400E+04 \quad EI_f = 7.94808E+08$$

$$k = 1.00047493E+00 \quad \alpha = 3.55493486E-01$$

Assembly 4 - Rigid frame 3:

$$EI = 5.10413E+05 \quad GA = 7.87943E+04 \quad EI_f = 7.15500E+08$$

$$k = 1.00035667E+00 \quad \alpha = 3.92904043E-01$$

Assembly 5 - Coupled shear walls B:

$$EI = 9.80000E+07 \quad GA = 1.18237E+05 \quad EI_f = 8.16480E+08$$

$$k = 1.05831337E+00 \quad \alpha = 3.47347073E-02$$

On using the Rigid Beam method presented in Section 5.4.2, the effective rigidities, the effective parameters and the force distribution factors for all the assemblies employed in the structure are obtained as follows,

For load position 1,

Assembly: 1

$$EI_e = 3.40939E+08 \quad GA_e = 5.97785E+05 \quad EI_{fe} = 2.70686E+09$$

$$k_e = 1.06110954E+00 \quad \alpha_e = 4.18730043E-02$$

$$v_f = 7.47348E-01 \quad v_c = 5.49476E-01$$

Assembly: 2

$$EI_e = 3.53198E+08 \quad GA_e = 6.86413E+05 \quad EI_{fe} = 3.41053E+09$$

$$k_e = 1.05050468E+00 \quad \alpha_e = 4.40842621E-02$$

$$v_f = 1.71235E-03 \quad v_c = 1.40116E-01$$

Assembly: 3

$$EI_e = 3.66372E+08 \quad GA_e = 8.05897E+05 \quad EI_{fe} = 4.60859E+09$$

$$k_e = 1.03898907E+00 \quad \alpha_e = 4.69006188E-02$$

$$v_f = 2.06348E-03 \quad v_c = 1.45507E-01$$

Assembly: 4

$$EI_e = 3.80566E+08 \quad GA_e = 9.75744E+05 \quad EI_{fe} = 7.10413E+09$$

$$k_e = 1.02643490E+00 \quad \alpha_e = 5.06352484E-02$$

$$v_f = 1.34119E-03 \quad v_c = 9.07345E-02$$

Assembly: 5

$$EI_e = 3.95905E+08 \quad GA_e = 1.23630E+06 \quad EI_{fe} = 1.54942E+10$$

$$k_e = 1.01269531E+00 \quad \alpha_e = 5.58812879E-02$$

$$v_f = 2.47534E-01 \quad v_c = 7.41668E-02$$

For load position 2,

Assembly: 1

$$EI_e = 5.12791E+08 \quad GA_e = 1.14483E+06 \quad EI_{fe} = 5.18024E+09$$

$$k_e = 1.04832745E+00 \quad \alpha_e = 4.72498313E-02$$

$$v_f = 4.96889E-01 \quad v_c = 2.87014E-01$$

Assembly: 2

$$EI_e = 3.66372E+08 \quad GA_e = 8.05897E+05 \quad EI_{fe} = 4.60859E+09$$

$$k_e = 1.03898907E+00 \quad \alpha_e = 4.69006188E-02$$

$$v_f = 1.65078E-03 \quad v_c = 1.11403E-01$$

Assembly: 3

$$EI_e = 2.84995E+08 \quad GA_e = 6.21806E+05 \quad EI_{fe} = 4.15057E+09$$

$$k_e = 1.03376198E+00 \quad \alpha_e = 4.67098840E-02$$

$$v_f = 2.65268E-03 \quad v_c = 1.72571E-01$$

Assembly: 4

$$EI_e = 2.33199E+08 \quad GA_e = 5.06180E+05 \quad EI_{fe} = 3.77535E+09$$

$$k_e = 1.03042126E+00 \quad \alpha_e = 4.65896167E-02$$

$$v_f = 2.18874E-03 \quad v_c = 1.72592E-01$$

Assembly: 5

$$\begin{aligned} EI_e &= 1.97334E+08 & GA_e &= 4.26813E+05 & EI_{fe} &= 3.46236E+09 \\ k_e &= 1.02810192E+00 & \alpha_e &= 4.65069488E-02 \\ v_f &= 4.96620E-01 & v_c &= 2.56419E-01 \end{aligned}$$

For load position 3,

Assembly: 1

$$\begin{aligned} EI_e &= 1.03397E+09 & GA_e &= 1.34890E+07 & EI_{fe} &= 6.00573E+10 \\ k_e &= 1.00857067E+00 & \alpha_e &= 1.14218354E-01 \\ v_f &= 2.46429E-01 & v_c &= 2.45516E-02 \end{aligned}$$

Assembly: 2

$$\begin{aligned} EI_e &= 3.80566E+08 & GA_e &= 9.75744E+05 & EI_{fe} &= 7.10413E+09 \\ k_e &= 1.02643490E+00 & \alpha_e &= 5.06352484E-02 \\ v_f &= 1.58921E-03 & v_c &= 8.26907E-02 \end{aligned}$$

Assembly: 3

$$\begin{aligned} EI_e &= 2.33199E+08 & GA_e &= 5.06180E+05 & EI_{fe} &= 3.77535E+09 \\ k_e &= 1.03042126E+00 & \alpha_e &= 4.65896167E-02 \\ v_f &= 3.24187E-03 & v_c &= 1.99636E-01 \end{aligned}$$

Assembly: 4

$$\begin{aligned} EI_e &= 1.68104E+08 & GA_e &= 3.41728E+05 & EI_{fe} &= 2.57077E+09 \\ k_e &= 1.03217697E+00 & \alpha_e &= 4.50869910E-02 \\ v_f &= 3.03629E-03 & v_c &= 2.54449E-01 \end{aligned}$$

Assembly: 5

$$\begin{aligned} EI_e &= 1.31419E+08 & GA_e &= 2.57929E+05 & EI_{fe} &= 1.94893E+09 \\ k_e &= 1.03316498E+00 & \alpha_e &= 4.43017595E-02 \\ v_f &= 7.45706E-01 & v_c &= 4.38673E-01 \end{aligned}$$

The resulting deflections, the load distribution, and the shear and moment

distributions between the assemblies are shown in Figs. 5.14a to 5.14d for load position 1, in Figs. 5.15a to 5.15d for load position 2, and in Figs. 5.16a to 5.16d for load position 3. In comparing with the curves obtained from the FLASH analysis, it can be seen that the present method produces very accurate results.

Asymmetric Structure Example 2.

This example is a 30-storey structure consisting of two pairs of identical coupled shear walls, 5 rigid frames of two different types, and a central core. The planform of the structure is as shown in Fig. 5.17. The applied lateral load considered is a uniformly distributed load, $w_0 = 15 \text{ kN/m}$. Eight load positions are considered.

The original data for the structure are as follows,

Storey height h	2.8 m
Number of storeys	30
Total height H	84.0 m
Modulus of elasticity E	$1.40 \times 10^7 \text{ kN/m}^2$
Uniformly distributed load w_0	15 kN/m

Coupled Shear Walls A and B:

Depths of the two walls D_1, D_2	7.25, 7.25 m
Clear span of the beams b	4.0 m
Depths of the connecting beams D_b	0.50 m
Thickness of the walls and beams t	0.30 m

Rigid frame 1, 2 and 3 (3-span):

Beam spans b_i ($i = 1$ to 3)	6.0 m
Inertias of beams I_{b_i} ($i=1$ to 3)	$5.7214 \times 10^{-3} \text{ m}^4$
Inertias of columns I_{c_i} ($i=1$ to 4)	$7.6255 \times 10^{-3} \text{ m}^4$
Column sectional areas A_{c_i}	0.3025 m^2

Rigid frame 4 and 5 (5-span):

Beam spans b_i ($i=1$ to 4)	3.0, 3.0, 6.0, 3.0, 3.0 m
Inertias of beams $I_{b_{1,2,4,5}}$	$1.3333 \times 10^{-3} \text{ m}^4$,
I_{b_2}	$7.1458 \times 10^{-3} \text{ m}^4$
Inertias of columns I_{c_i} ($i=1$ to 6)	$5.2083 \times 10^{-3} \text{ m}^4$
Column sectional areas A_{c_i}	0.2500 m^2

The structural rigidities and parameters for all individual assemblies are listed as follows,

Assembly 1 - Coupled shear walls A:

$$EI = 2.66755\text{E}+08 \quad GA = 3.55459\text{E}+05 \quad EI_f = 1.92691\text{E}+09$$

$$k = 1.06697559\text{E}+00 \quad \alpha = 3.65038291\text{E}-02$$

Assembly 2 - Rigid frame 1:

$$EI = 4.27028\text{E}+05 \quad GA = 1.33443\text{E}+05 \quad EI_f = 7.62300\text{E}+08$$

$$k = 1.00027943\text{E}+00 \quad \alpha = 5.59010148\text{E}-01$$

Assembly 3 - Central core:

$$EI = 4.36410\text{E}+08 \quad GA = 0.00000\text{E}+00 \quad EI_f = 0.00000\text{E}+00$$

Assembly 4 - Rigid frame 2:

$$EI = 4.27028\text{E}+05 \quad GA = 1.33433\text{E}+05 \quad EI_f = 7.62300\text{E}+08$$

$$k = 1.00027943\text{E}+00 \quad \alpha = 5.58989227\text{E}-01$$

Assembly 5 - Rigid frame 3:

$$EI = 4.27028E+05 \quad GA = 1.33433E+05 \quad EI_f = 7.62300E+08$$

$$k = 1.00027943E+00 \quad \alpha = 5.58989227E-01$$

Assembly 6 - Rigid frame 4:

$$EI = 4.37497E+05 \quad GA = 1.35028E+05 \quad EI_f = 8.82000E+08$$

$$k = 1.00024796E+00 \quad \alpha = 5.55551529E-01$$

Assembly 7 - Rigid frame 5:

$$EI = 4.37497E+05 \quad GA = 1.35028E+05 \quad EI_f = 8.82000E+08$$

$$k = 1.00024796E+00 \quad \alpha = 5.55551529E-01$$

Assembly 8 - Coupled shear wall B:

$$EI = 2.66755E+08 \quad GA = 3.55459E+05 \quad EI_f = 1.92691E+09$$

$$k = 1.06697559E+00 \quad \alpha = 3.65038291E-02$$

The effective rigidities, the effective parameters and the force distribution factors for all the assemblies in the structure, under different load cases are obtained as follows,

For load position 1,

Assembly 1

$$EI_e = 4.44986E+08 \quad GA_e = 4.97424E+05 \quad EI_{fe} = 2.73538E+09$$

$$k_e = 1.07827568E+00 \quad \alpha_e = 3.34341377E-02$$

$$v_f = 5.99468E-01 \quad v_c = 7.09519E-01$$

Assembly 2

$$EI_e = 5.31601E+08 \quad GA_e = 5.84492E+05 \quad EI_{fe} = 3.21740E+09$$

$$k_e = 1.07945633E+00 \quad \alpha_e = 3.31586152E-02$$

$$v_f = 8.03287E-04 \quad v_c = 2.32618E-01$$

Assembly 3

$$EI_e = 7.50817E+08 \quad GA_e = 7.92594E+05 \quad EI_{fe} = 4.37341E+09$$

$$k_e = 1.08244038E+00 \quad \alpha_e = 3.24906409E-02$$

$$v_f = 5.81247E-01 \quad v_c = 0.00000E+00$$

Assembly 4

$$EI_e = 1.27770E+09 \quad GA_e = 1.23081E+06 \quad EI_{fe} = 6.82598E+09$$

$$k_e = 1.08957863E+00 \quad \alpha_e = 3.10370922E-02$$

$$v_f = 3.34216E-04 \quad v_c = 1.10043E-01$$

Assembly 5

$$EI_e = 2.40094E+09 \quad GA_e = 1.94930E+06 \quad EI_{fe} = 1.09017E+10$$

$$k_e = 1.10464287E+00 \quad \alpha_e = 2.84936875E-02$$

$$v_f = 1.77859E-04 \quad v_c = 6.91882E-02$$

Assembly 6

$$EI_e = 1.98603E+10 \quad GA_e = 4.68312E+06 \quad EI_{fe} = 2.70574E+10$$

$$k_e = 1.31681633E+00 \quad \alpha_e = 1.53558813E-02$$

$$v_f = 2.20287E-05 \quad v_c = 3.07151E-02$$

Assembly 7

$$EI_e = -3.16656E+09 \quad GA_e = -1.16363E+07 \quad EI_{fe} = -5.61425E+10$$

$$k_e = 1.02781391E+00 \quad \alpha_e = 6.06196709E-02$$

$$v_f = -1.38162E-04 \quad v_c = -1.36570E-02$$

Assembly 8

$$EI_e = -1.46638E+09 \quad GA_e = -2.59465E+06 \quad EI_{fe} = -1.37775E+10$$

$$k_e = 1.05187130E+00 \quad \alpha_e = 4.20645364E-02$$

$$v_f = -1.81914E-01 \quad v_c = -1.38428E-01$$

For load position 2,

Assembly 1

$$EI_e = 5.31601E+08 \quad GA_e = 5.84492E+05 \quad EI_{fe} = 3.21740E+09$$

$$k_e = 1.07945633E+00 \quad \alpha_e = 3.31586152E-02$$

$$v_f = 5.01796E-01 \quad v_c = 6.03526E-01$$

Assembly 2

$$\begin{aligned} EI_e &= 6.15392E+08 & GA_e &= 6.75159E+05 & EI_{fe} &= 3.72319E+09 \\ k_e &= 1.07948399E+00 & \alpha_e &= 3.31228040E-02 \\ v_f &= 6.93912E-04 & v_c &= 2.01195E-01 \end{aligned}$$

Assembly 3

$$\begin{aligned} EI_e &= 8.05939E+08 & GA_e &= 8.79894E+05 & EI_{fe} &= 4.87203E+09 \\ k_e &= 1.07954693E+00 & \alpha_e &= 3.30418274E-02 \\ v_f &= 5.41493E-01 & v_c &= 0.00000E+00 \end{aligned}$$

Assembly 4

$$\begin{aligned} EI_e &= 1.16741E+09 & GA_e &= 1.26283E+06 & EI_{fe} &= 7.04628E+09 \\ k_e &= 1.07966518E+00 & \alpha_e &= 3.28897648E-02 \\ v_f &= 3.65791E-04 & v_c &= 1.06923E-01 \end{aligned}$$

Assembly 5

$$\begin{aligned} EI_e &= 1.66537E+09 & GA_e &= 1.77900E+06 & EI_{fe} &= 1.00305E+10 \\ k_e &= 1.07982826E+00 & \alpha_e &= 3.26838009E-02 \\ v_f &= 2.56416E-04 & v_c &= 7.55013E-02 \end{aligned}$$

Assembly 6

$$\begin{aligned} EI_e &= 2.90412E+09 & GA_e &= 3.00878E+06 & EI_{fe} &= 1.73993E+10 \\ k_e &= 1.08023548E+00 & \alpha_e &= 3.21875513E-02 \\ v_f &= 1.50647E-04 & v_c &= 4.77848E-02 \end{aligned}$$

Assembly 7

$$\begin{aligned} EI_e &= 1.13366E+10 & GA_e &= 9.74599E+06 & EI_{fe} &= 6.55709E+10 \\ k_e &= 1.08300114E+00 & \alpha_e &= 2.93205082E-02 \\ v_f &= 3.85915E-05 & v_c &= 1.36529E-02 \end{aligned}$$

Assembly 8

$$\begin{aligned} EI_e &= -5.95528E+09 & GA_e &= -7.86485E+06 & EI_{fe} &= -3.70754E+10 \\ k_e &= 1.07732296E+00 & \alpha_e &= 3.63407657E-02 \\ v_f &= -4.47930E-02 & v_c &= -4.85843E-02 \end{aligned}$$

For load position 3,

Assembly 1

$$EI_e = 7.50817E+08 \quad GA_e = 7.92594E+05 \quad EI_{fe} = 4.37341E+09$$

$$k_e = 1.08244038E+00 \quad \alpha_e = 3.24906409E-02$$

$$v_f = 3.55286E-01 \quad v_c = 4.44536E-01$$

Assembly 2

$$EI_e = 8.05939E+08 \quad GA_e = 8.79894E+05 \quad EI_{fe} = 4.87203E+09$$

$$k_e = 1.07954693E+00 \quad \alpha_e = 3.30418274E-02$$

$$v_f = 5.29852E-04 \quad v_c = 1.54061E-01$$

Assembly 3

$$EI_e = 9.05676E+08 \quad GA_e = 1.05404E+06 \quad EI_{fe} = 5.87714E+09$$

$$k_e = 1.07429123E+00 \quad \alpha_e = 3.41147408E-02$$

$$v_f = 4.81861E-01 \quad v_c = 0.00000E+00$$

Assembly 4

$$EI_e = 1.03358E+09 \quad GA_e = 1.31413E+06 \quad EI_{fe} = 7.40473E+09$$

$$k_e = 1.06751251E+00 \quad \alpha_e = 3.56571898E-02$$

$$v_f = 4.13154E-04 \quad v_c = 1.02242E-01$$

Assembly 5

$$EI_e = 1.14101E+09 \quad GA_e = 1.57287E+06 \quad EI_{fe} = 8.95678E+09$$

$$k_e = 1.06178665E+00 \quad \alpha_e = 3.71280126E-02$$

$$v_f = 3.74254E-04 \quad v_c = 8.49713E-02$$

Assembly 6

$$EI_e = 1.27337E+09 \quad GA_e = 1.95847E+06 \quad EI_{fe} = 1.13320E+10$$

$$k_e = 1.05468845E+00 \quad \alpha_e = 3.92176099E-02$$

$$v_f = 3.43574E-04 \quad v_c = 7.33891E-02$$

Assembly 7

$$EI_e = 1.44045E+09 \quad GA_e = 2.59455E+06 \quad EI_{fe} = 1.54215E+10$$

$$k_e = 1.04566002E+00 \quad \alpha_e = 4.24406379E-02$$

$$v_f = 3.03722E-04 \quad v_c = 5.46179E-02$$

Assembly 8

$$EI_e = 1.65801E+09 \quad GA_e = 3.84256E+06 \quad EI_{fe} = 2.41296E+10$$

$$k_e = 1.03378582E+00 \quad \alpha_e = 4.81411815E-02$$

$$v_f = 1.60889E-01 \quad v_c = 8.61812E-02$$

For load position 4,

Assembly 1

$$EI_e = 1.27770E+09 \quad GA_e = 1.23081E+06 \quad EI_{fe} = 6.82598E+09$$

$$k_e = 1.08957863E+00 \quad \alpha_e = 3.10370922E-02$$

$$v_f = 2.08777E-01 \quad v_c = 2.85546E-01$$

Assembly 2

$$EI_e = 1.16741E+09 \quad GA_e = 1.26283E+06 \quad EI_{fe} = 7.04628E+09$$

$$k_e = 1.07966518E+00 \quad \alpha_e = 3.28897648E-02$$

$$v_f = 3.65791E-04 \quad v_c = 1.06927E-01$$

Assembly 3

$$EI_e = 1.03358E+09 \quad GA_e = 1.31413E+06 \quad EI_{fe} = 7.40473E+09$$

$$k_e = 1.06751251E+00 \quad \alpha_e = 3.56571898E-02$$

$$v_f = 4.22232E-01 \quad v_c = 0.00000E+00$$

Assembly 4

$$EI_e = 9.27284E+08 \quad GA_e = 1.36976E+06 \quad EI_{fe} = 7.80162E+09$$

$$k_e = 1.05776024E+00 \quad \alpha_e = 3.84340249E-02$$

$$v_f = 4.60515E-04 \quad v_c = 9.75619E-02$$

Assembly 5

$$EI_e = 8.67785E+08 \quad GA_e = 1.40954E+06 \quad EI_{fe} = 8.09072E+09$$

$$k_e = 1.05226231E+00 \quad \alpha_e = 4.03025597E-02$$

$$v_f = 4.92089E-04 \quad v_c = 9.44416E-02$$

Assembly 6

$EI_e = 8.15462E+08$ $GA_e = 1.45171E+06$ $EI_{fe} = 8.40207E+09$
 $k_e = 1.04740334E+00$ $\alpha_e = 4.21927758E-02$
 $v_f = 5.36502E-04$ $v_c = 9.89935E-02$

Assembly 7

$EI_e = 7.69089E+08$ $GA_e = 1.49647E+06$ $EI_{fe} = 8.73835E+09$
 $k_e = 1.04307842E+00$ $\alpha_e = 4.41108756E-02$
 $v_f = 5.68851E-04$ $v_c = 9.55827E-02$

Assembly 8

$EI_e = 7.27706E+08$ $GA_e = 1.54408E+06$ $EI_{fe} = 9.10266E+09$
 $k_e = 1.03920364E+00$ $\alpha_e = 4.60634939E-02$
 $v_f = 3.66570E-01$ $v_c = 2.20947E-01$

For load position 5,

Assembly 1

$EI_e = 2.40094E+09$ $GA_e = 1.94930E+06$ $EI_{fe} = 1.09017E+10$
 $k_e = 1.10464287E+00$ $\alpha_e = 2.84936875E-02$
 $v_f = 1.11104E-01$ $v_c = 1.79553E-01$

Assembly 2

$EI_e = 1.66537E+09$ $GA_e = 1.77900E+06$ $EI_{fe} = 1.00305E+10$
 $k_e = 1.07982826E+00$ $\alpha_e = 3.26838009E-02$
 $v_f = 2.56416E-04$ $v_c = 7.55041E-02$

Assembly 3

$EI_e = 1.14101E+09$ $GA_e = 1.57287E+06$ $EI_{fe} = 8.95678E+09$
 $k_e = 1.06178665E+00$ $\alpha_e = 3.71280126E-02$
 $v_f = 3.82477E-01$ $v_c = 0.00000E+00$

Assembly 4

$EI_e = 8.67785E+08$ $GA_e = 1.40954E+06$ $EI_{fe} = 8.09072E+09$

$$k_e = 1.05226231E+00 \quad \alpha_e = 4.03025597E-02$$

$$v_f = 4.92089E-04 \quad v_c = 9.44416E-02$$

Assembly 5

$$EI_e = 7.48322E+08 \quad GA_e = 1.31829E+06 \quad EI_{fe} = 7.60076E+09$$

$$k_e = 1.04807091E+00 \quad \alpha_e = 4.19721454E-02$$

$$v_f = 5.70647E-04 \quad v_c = 1.00755E-01$$

Assembly 6

$$EI_e = 6.57771E+08 \quad GA_e = 1.23813E+06 \quad EI_{fe} = 7.16675E+09$$

$$k_e = 1.04488277E+00 \quad \alpha_e = 4.33856137E-02$$

$$v_f = 6.65120E-04 \quad v_c = 1.16063E-01$$

Assembly 7

$$EI_e = 5.86768E+08 \quad GA_e = 1.16716E+06 \quad EI_{fe} = 6.77963E+09$$

$$k_e = 1.04237652E+00 \quad \alpha_e = 4.45997007E-02$$

$$v_f = 7.45605E-04 \quad v_c = 1.22892E-01$$

Assembly 8

$$EI_e = 5.29601E+08 \quad GA_e = 1.10388E+06 \quad EI_{fe} = 6.43219E+09$$

$$k_e = 1.04035378E+00 \quad \alpha_e = 4.56548072E-02$$

$$v_f = 5.03690E-01 \quad v_c = 3.10791E-01$$

For load position 6,

Assembly 1

$$EI_e = 1.98603E+10 \quad GA_e = 4.68312E+06 \quad EI_{fe} = 2.70574E+10$$

$$k_e = 1.31681633E+00 \quad \alpha_e = 1.53558813E-02$$

$$v_f = 1.34316E-02 \quad v_c = 7.35589E-02$$

Assembly 2

$$EI_e = 2.90412E+09 \quad GA_e = 3.00878E+06 \quad EI_{fe} = 1.73993E+10$$

$$k_e = 1.08023548E+00 \quad \alpha_e = 3.21875513E-02$$

$$v_f = 1.47042E-04 \quad v_c = 4.40816E-02$$

Assembly 3

$$\begin{aligned} EI_e &= 1.27337E+09 & GA_e &= 1.95847E+06 & EI_{fe} &= 1.13320E+10 \\ k_e &= 1.05468845E+00 & \alpha_e &= 3.92176099E-02 \\ v_f &= 3.42721E-01 & v_c &= 0.00000E+00 \end{aligned}$$

Assembly 4

$$\begin{aligned} EI_e &= 8.15462E+08 & GA_e &= 1.45171E+06 & EI_{fe} &= 8.40207E+09 \\ k_e &= 1.04740334E+00 & \alpha_e &= 4.21927758E-02 \\ v_f &= 5.23664E-04 & v_c &= 9.13209E-02 \end{aligned}$$

Assembly 5

$$\begin{aligned} EI_e &= 6.57771E+08 & GA_e &= 1.23813E+06 & EI_{fe} &= 7.16675E+09 \\ k_e &= 1.04488277E+00 & \alpha_e &= 4.33856137E-02 \\ v_f &= 6.49204E-04 & v_c &= 1.07068E-01 \end{aligned}$$

Assembly 6

$$\begin{aligned} EI_e &= 5.51185E+08 & GA_e &= 1.07933E+06 & EI_{fe} &= 6.24812E+09 \\ k_e &= 1.04317570E+00 & \alpha_e &= 4.42515463E-02 \\ v_f &= 7.93739E-04 & v_c &= 1.33133E-01 \end{aligned}$$

Assembly 7

$$\begin{aligned} EI_e &= 4.74325E+08 & GA_e &= 9.56637E+05 & EI_{fe} &= 5.53823E+09 \\ k_e &= 1.04194260E+00 & \alpha_e &= 4.49092276E-02 \\ v_f &= 9.22357E-04 & v_c &= 1.50203E-01 \end{aligned}$$

Assembly 8

$$\begin{aligned} EI_e &= 4.16277E+08 & GA_e &= 8.58991E+05 & EI_{fe} &= 4.97319E+09 \\ k_e &= 1.04101086E+00 & \alpha_e &= 4.54258546E-02 \\ v_f &= 6.40811E-01 & v_c &= 4.00635E-01 \end{aligned}$$

For load position 7,

Assembly 1

$$EI_e = -3.16656E+09 \quad GA_e = -1.16363E+07 \quad EI_{fe} = -5.61425E+10$$

$$k_e = 1.02781391E+00 \quad \alpha_e = 6.06196709E-02$$

$$v_f = -8.42412E-02 \quad v_c = -3.24346E-02$$

Assembly 2

$$EI_e = 1.13366E+10 \quad GA_e = 9.74599E+06 \quad EI_{fe} = 6.55709E+10$$

$$k_e = 1.08300114E+00 \quad \alpha_e = 2.93205082E-02$$

$$v_f = 3.76681E-05 \quad v_c = 1.26588E-02$$

Assembly 3

$$EI_e = 1.44045E+09 \quad GA_e = 2.59455E+06 \quad EI_{fe} = 1.54215E+10$$

$$k_e = 1.04566002E+00 \quad \alpha_e = 4.24406379E-02$$

$$v_f = 3.02968E-01 \quad v_c = 0.00000E+00$$

Assembly 4

$$EI_e = 7.69089E+08 \quad GA_e = 1.49647E+06 \quad EI_{fe} = 8.73835E+09$$

$$k_e = 1.04307842E+00 \quad \alpha_e = 4.41108756E-02$$

$$v_f = 5.55239E-04 \quad v_c = 8.82006E-02$$

Assembly 5

$$EI_e = 5.86768E+08 \quad GA_e = 1.16716E+06 \quad EI_{fe} = 6.77963E+09$$

$$k_e = 1.04237652E+00 \quad \alpha_e = 4.45997007E-02$$

$$v_f = 7.27763E-04 \quad v_c = 1.13381E-01$$

Assembly 6

$$EI_e = 4.74325E+08 \quad GA_e = 9.56637E+05 \quad EI_{fe} = 5.53823E+09$$

$$k_e = 1.04194260E+00 \quad \alpha_e = 4.49092276E-02$$

$$v_f = 9.22357E-04 \quad v_c = 1.50203E-01$$

Assembly 7

$$EI_e = 3.98046E+08 \quad GA_e = 8.10456E+05 \quad EI_{fe} = 4.68109E+09$$

$$k_e = 1.04164886E+00 \quad \alpha_e = 4.51230146E-02$$

$$v_f = 1.09911E-03 \quad v_c = 1.77513E-01$$

Assembly 8

$$EI_e = 3.42903E+08 \quad GA_e = 7.03029E+05 \quad EI_{fe} = 4.05370E+09$$

$$k_e = 1.04143620E+00 \quad \alpha_e = 4.52794284E-02$$

$$v_f = 7.77931E-01 \quad v_c = 4.90478E-01$$

For load position 8,

Assembly 1

$$EI_e = -1.46638E+09 \quad GA_e = -2.59465E+06 \quad EI_{fe} = -1.37775E+10$$

$$k_e = 1.05187130E+00 \quad \alpha_e = 4.20645364E-02$$

$$v_f = -1.81914E-01 \quad v_c = -1.38428E-01$$

Assembly 2

$$EI_e = -5.95528E+09 \quad GA_e = -7.86485E+06 \quad EI_{fe} = -3.70754E+10$$

$$k_e = 1.07732296E+00 \quad \alpha_e = 3.63407657E-02$$

$$v_f = -7.17058E-05 \quad v_c = -1.87639E-02$$

Assembly 3

$$EI_e = 1.65801E+09 \quad GA_e = 3.84256E+06 \quad EI_{fe} = 2.41296E+10$$

$$k_e = 1.03378582E+00 \quad \alpha_e = 4.81411815E-02$$

$$v_f = 2.63213E-01 \quad v_c = 0.00000E+00$$

Assembly 4

$$EI_e = 7.27706E+08 \quad GA_e = 1.54408E+06 \quad EI_{fe} = 9.10266E+09$$

$$k_e = 1.03920364E+00 \quad \alpha_e = 4.60634939E-02$$

$$v_f = 5.86814E-04 \quad v_c = 8.50803E-02$$

Assembly 5

$$EI_e = 5.29601E+08 \quad GA_e = 1.10388E+06 \quad EI_{fe} = 6.43219E+09$$

$$k_e = 1.04035378E+00 \quad \alpha_e = 4.56548072E-02$$

$$v_f = 8.06320E-04 \quad v_c = 1.19695E-01$$

Assembly 6

$$EI_e = 4.16277E+08 \quad GA_e = 8.58991E+05 \quad EI_{fe} = 4.97319E+09$$

$$k_e = 1.04101086E+00 \quad \alpha_e = 4.54258546E-02$$

$$v_f = 1.05098E-03 \quad v_c = 1.67272E-01$$

Assembly 7

$$EI_e = 3.42903E+08 \quad GA_e = 7.03029E+05 \quad EI_{fe} = 4.05370E+09$$

$$k_e = 1.04143620E+00 \quad \alpha_e = 4.52794284E-02$$

$$v_f = 1.27586E-03 \quad v_c = 2.04822E-01$$

Assembly 8

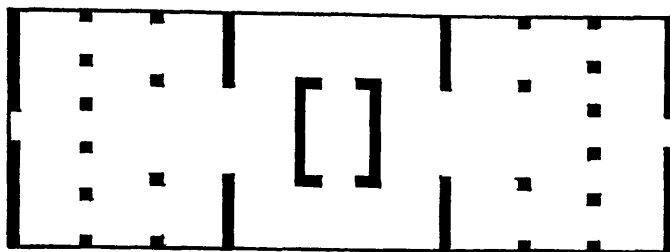
$$EI_e = 2.91519E+08 \quad GA_e = 5.94998E+05 \quad EI_{fe} = 3.42116E+09$$

$$k_e = 1.04173374E+00 \quad \alpha_e = 4.51777205E-02$$

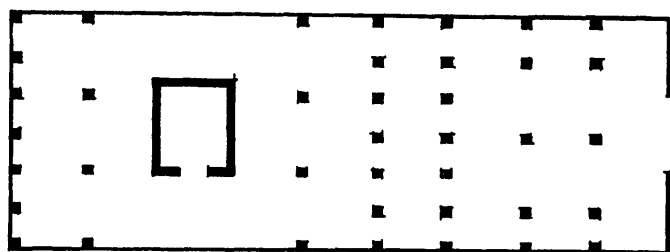
$$v_f = 9.15052E-01 \quad v_c = 5.80322E-01$$

The resulting deflections, the load distributions and the shear and moment distributions for all the assemblies, from both the present method and the FLASH analysis, are shown in Figs. 5.18 to 5.25, respectively for the eight load cases. It can again be seen that the method produces satisfactorily accurate results when compared with the more 'exact' finite element analysis.

From these numerical examples representing three-dimensional symmetric or asymmetric structures subjected to bending and torsion, it appears that this simplified method can be used to analyze relatively complicated three-dimensional structures consisting of parallel uniform wall-frame assemblies. A solution can be achieved on merely solving a few formulae, using a pocket calculator or making use of design curves. Most other methods, however, usually require the solution of a large numbers of equations, using particular computing programs. As an approximate method, it can be effectively employed to analyze structures at the preliminary stages of design, and to determine the basic lateral-load-resisting behaviour of the structural elements.

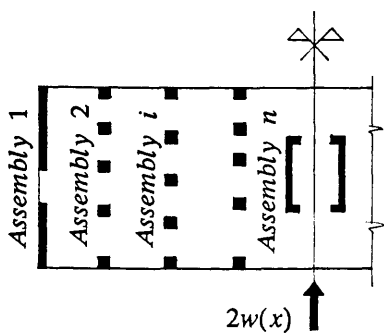


(a)

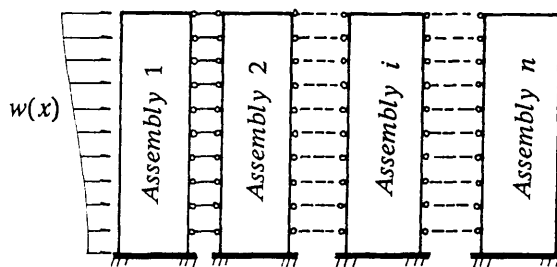


(b)

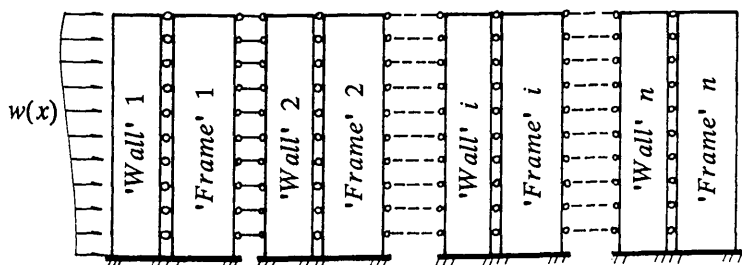
Fig. 5.1 Typical Planforms of Three-Dimensional High-Rise Wall-Frame Structures



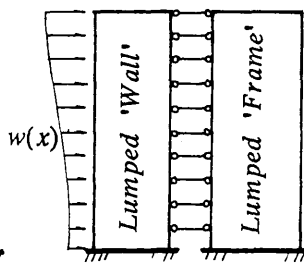
(a) Representative Structure



(b) Equivalent Plane System

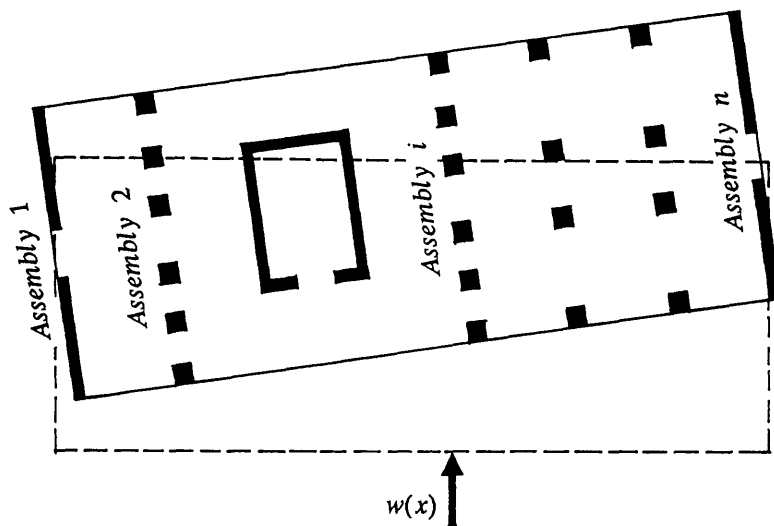


(c) Replacement of Wall-Frame Plane System

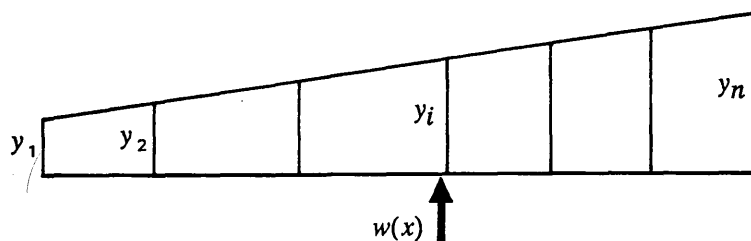


(d) Lumped Wall-Frame Structure

Fig. 5.2 Illustration for Analysis of Symmetric Structure

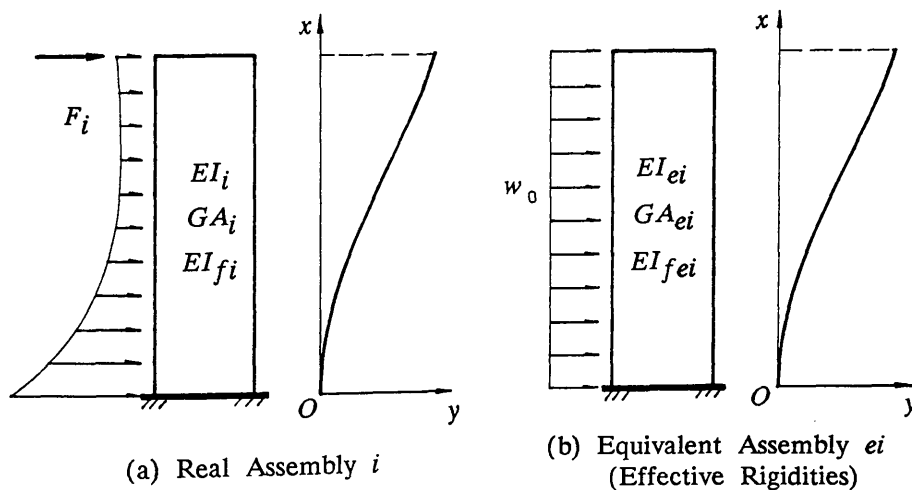


(a) Rigid Body Movement of Floor Slab



(b) Displacement Diagram of Assemblies

Fig. 5.3 Three-Dimensional Structure Subjected to Bending and Torsion



(a) Real Assembly i

(b) Equivalent Assembly ei
(Effective Rigidities)

Fig. 5.4 Illustration of Equivalent Assembly

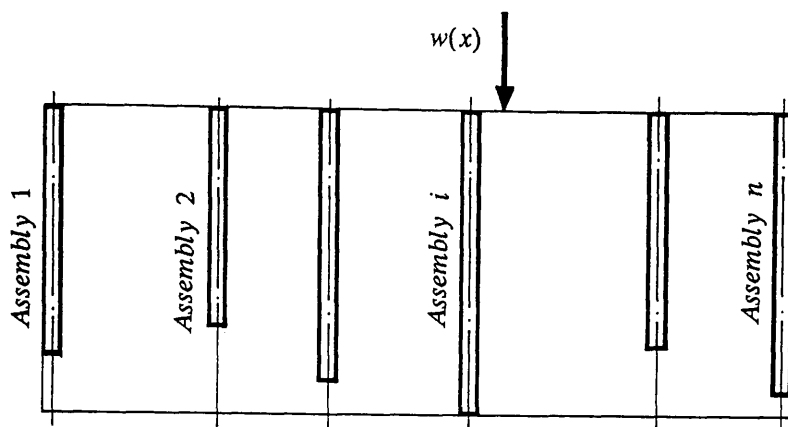
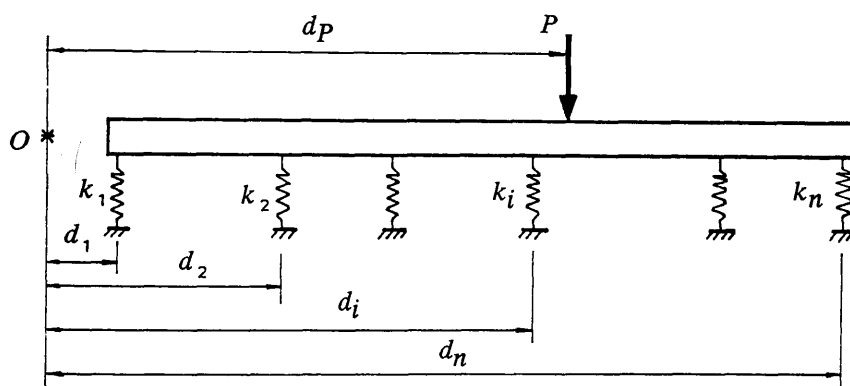
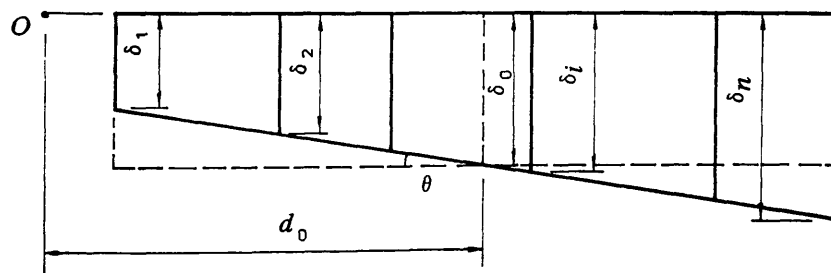


Fig. 5.5 Parallel Plane Shear Wall Structure



(a) Spring Supported Rigid Beam



(b) Displacement Diagram of Beam

Fig. 5.6 Representative Spring-Supported Rigid Beam Model

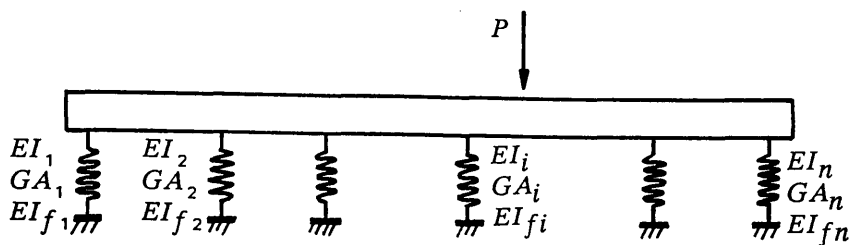


Fig. 5.7 Rigid Beam Model Supported by Springs of Multiple Rigidities

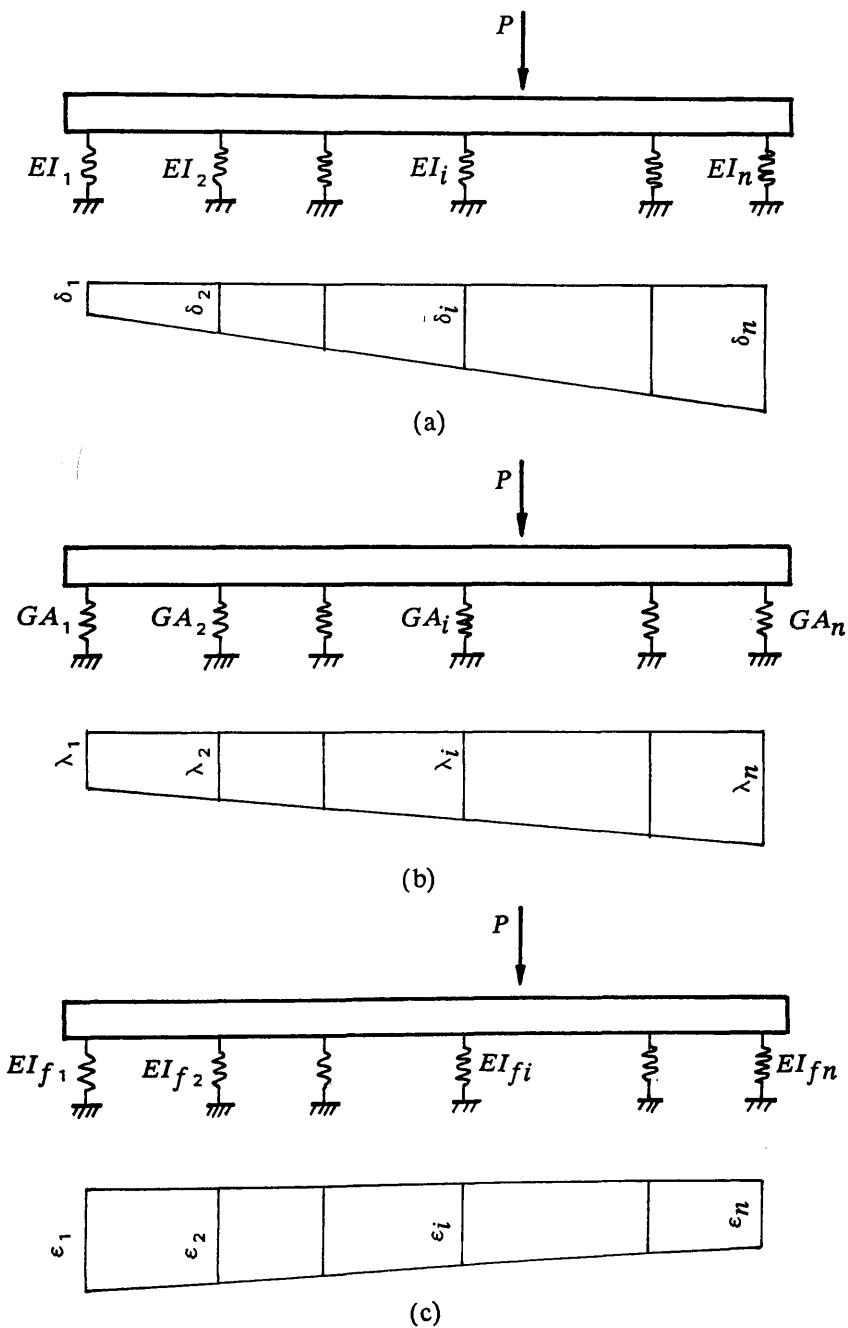


Fig. 5.8 Uncoupled Rigid Beams and Displacements

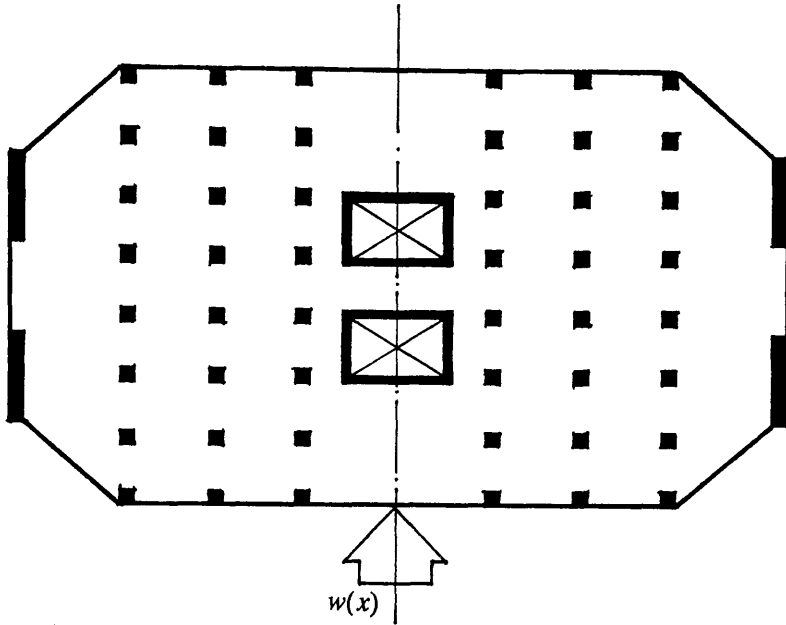


Fig. 5.9 30- Storey Symmetric Example Structure 1

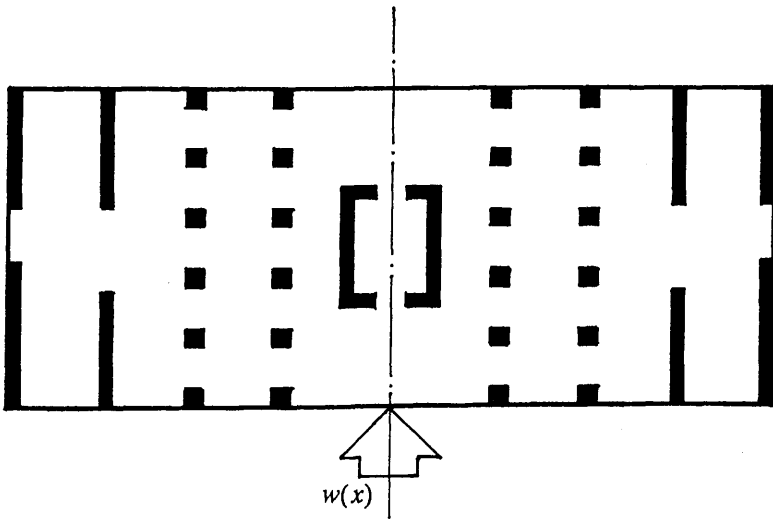
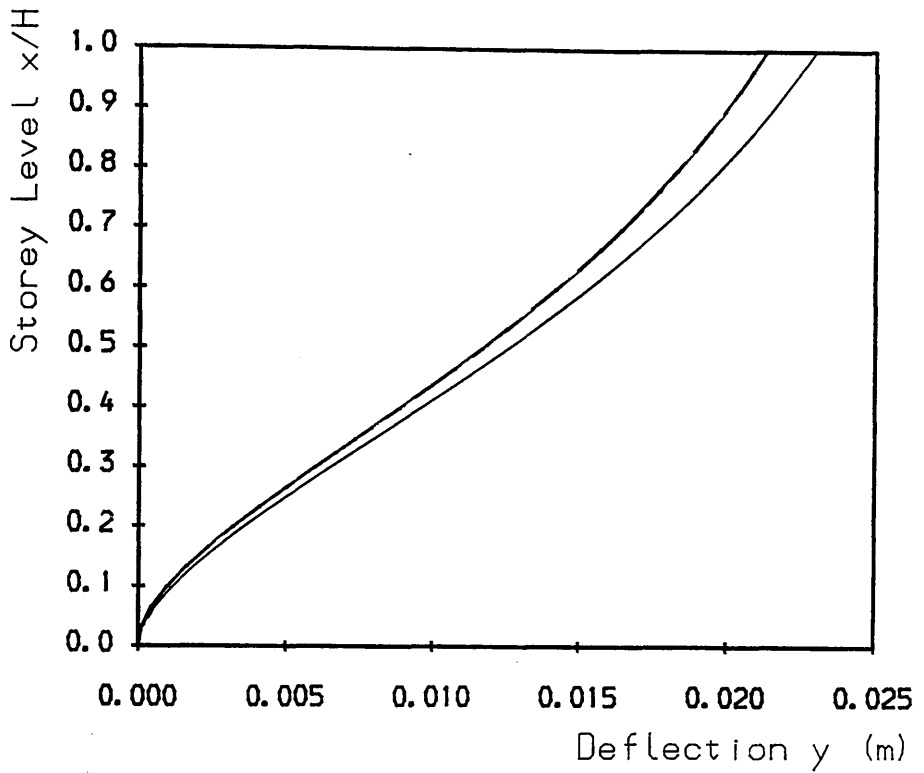
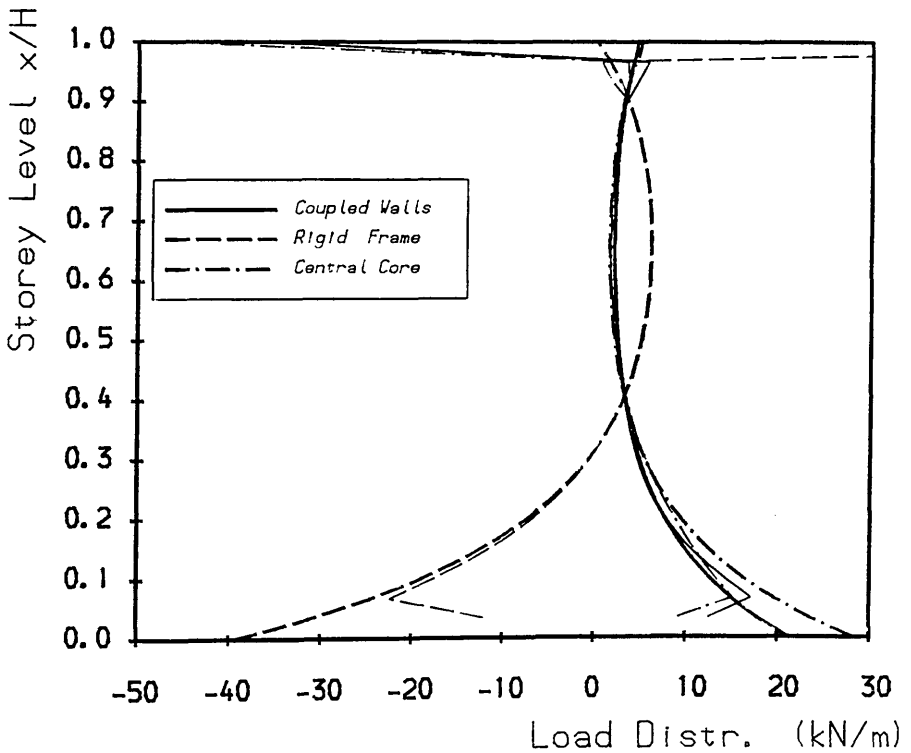


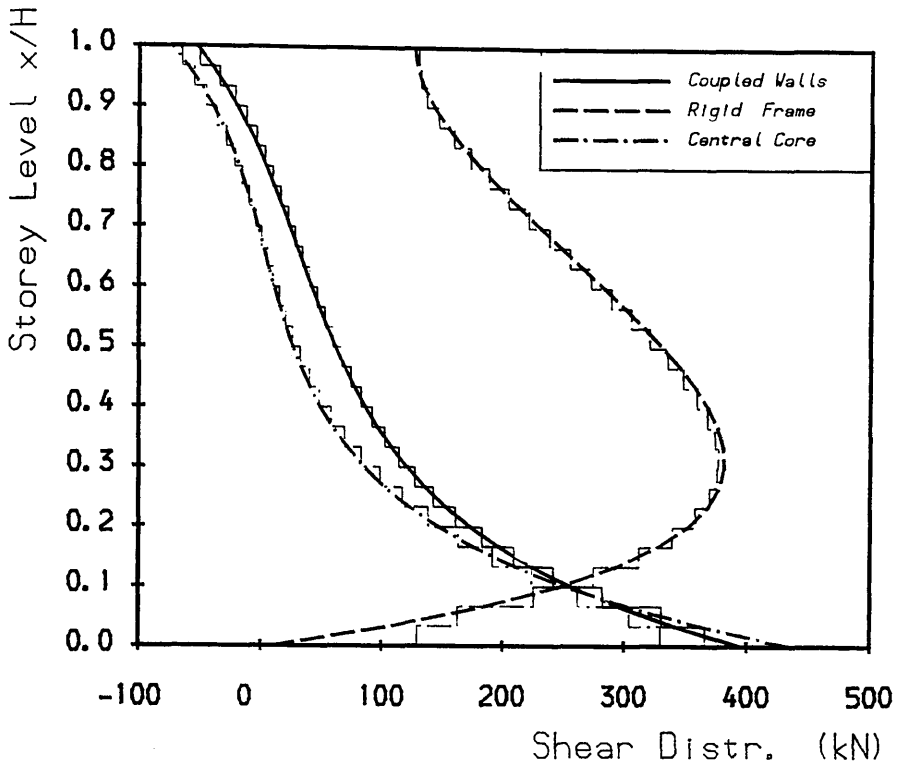
Fig. 5.11 40- Storey Symmetric Example Structure 2



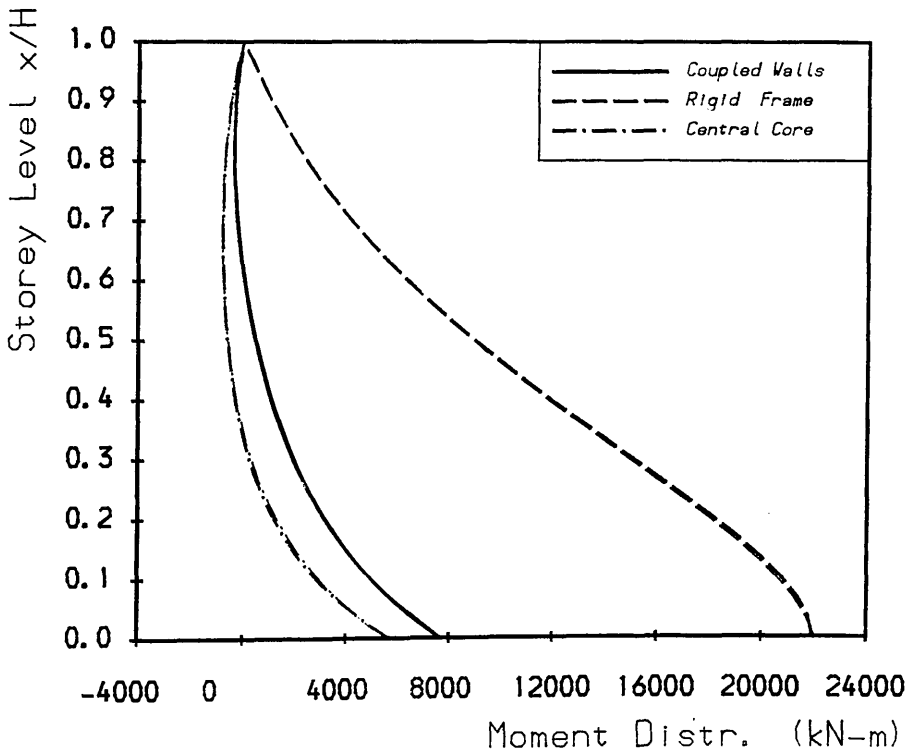
Symmetric Structure Example 1
Fig. 5.10a Deflection



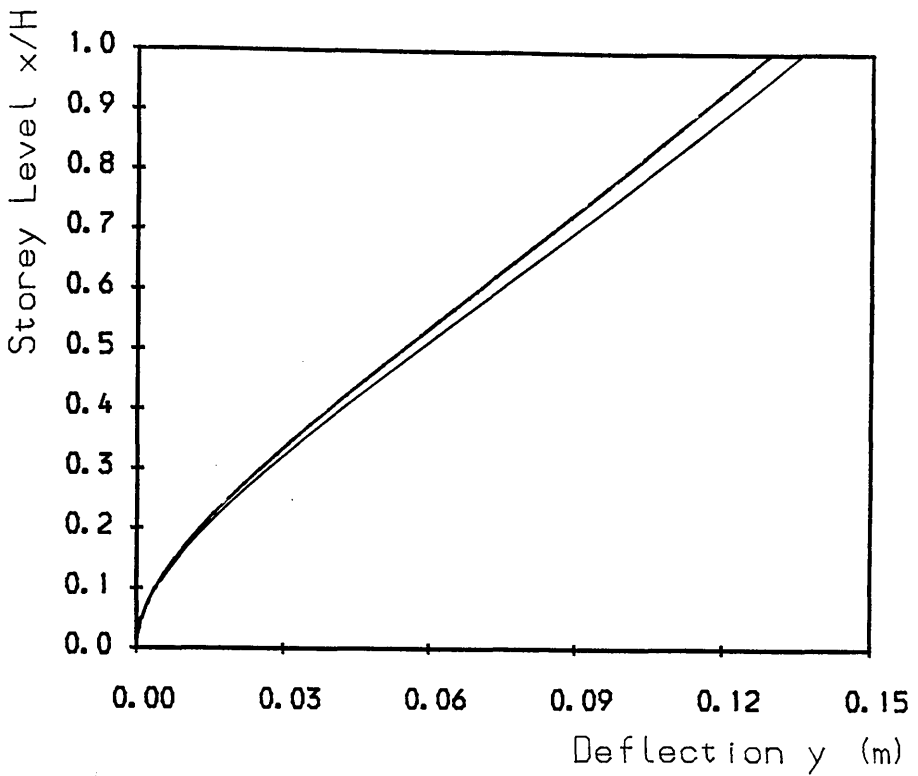
Symmetric Structure Example 1
Fig. 5.10b Load Distribution



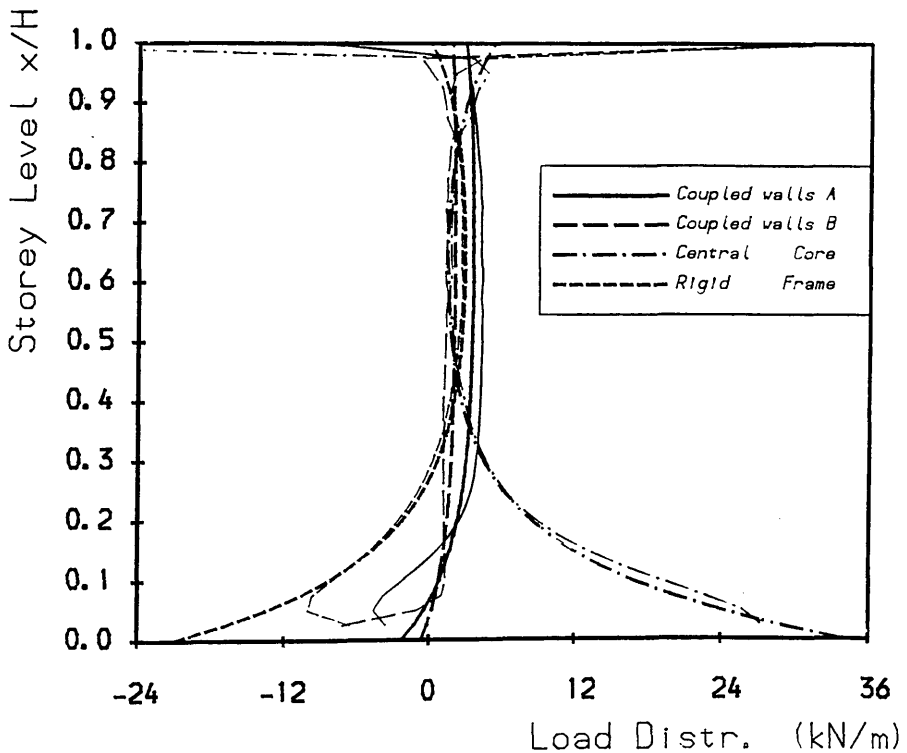
Symmetric Structure Example 1
Fig. 5.10c Shear Distribution



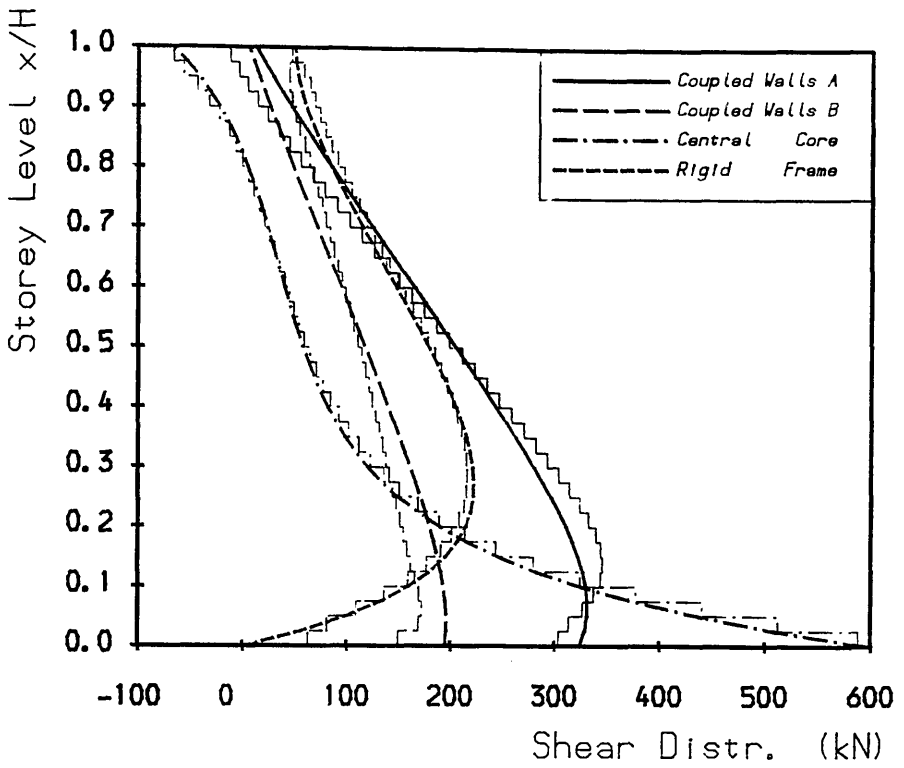
Symmetric Structure Example 1
Fig. 5.10d Moment Distribution



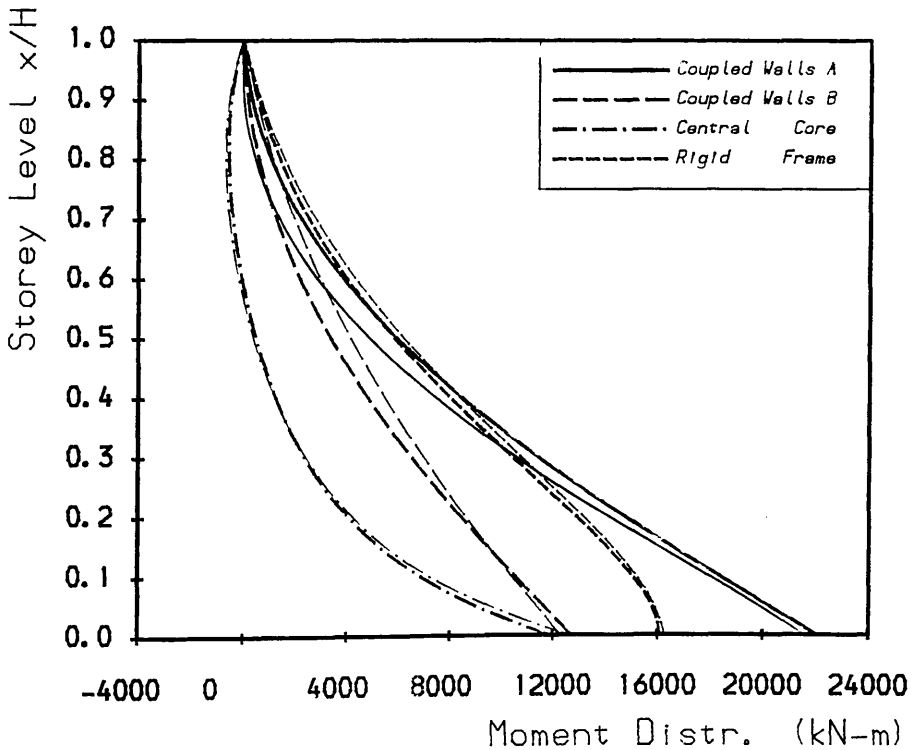
Symmetric Structure Example 2
Fig. 5.12a Deflection



Symmetric Structure Example 2
Fig. 5.12b Load Distribution



Symmetric Structure Example 2
Fig. 5.12c Shear Distribution



Symmetric Structure Example 2
Fig. 5.12d Moment Distribution

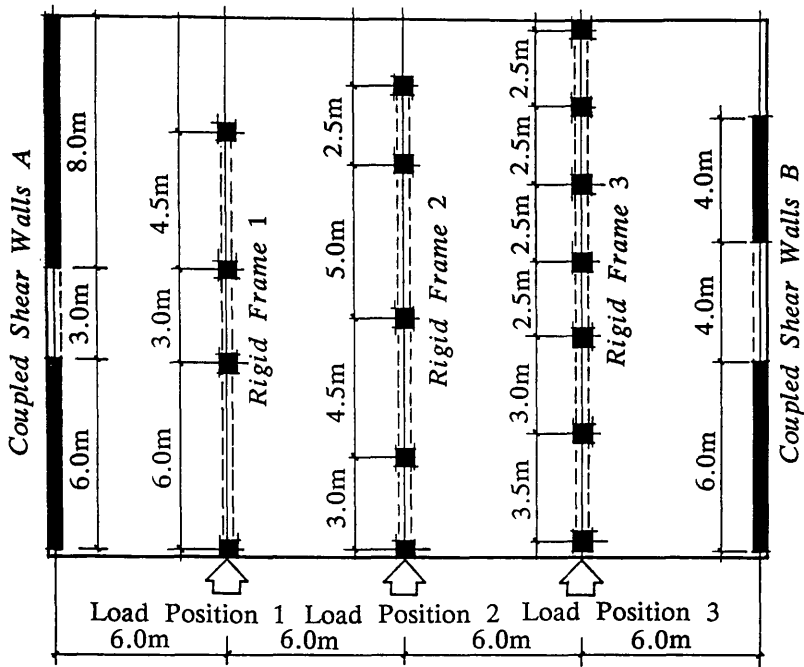


Fig. 5.13 Planform of Asymmetric Example Structure 1

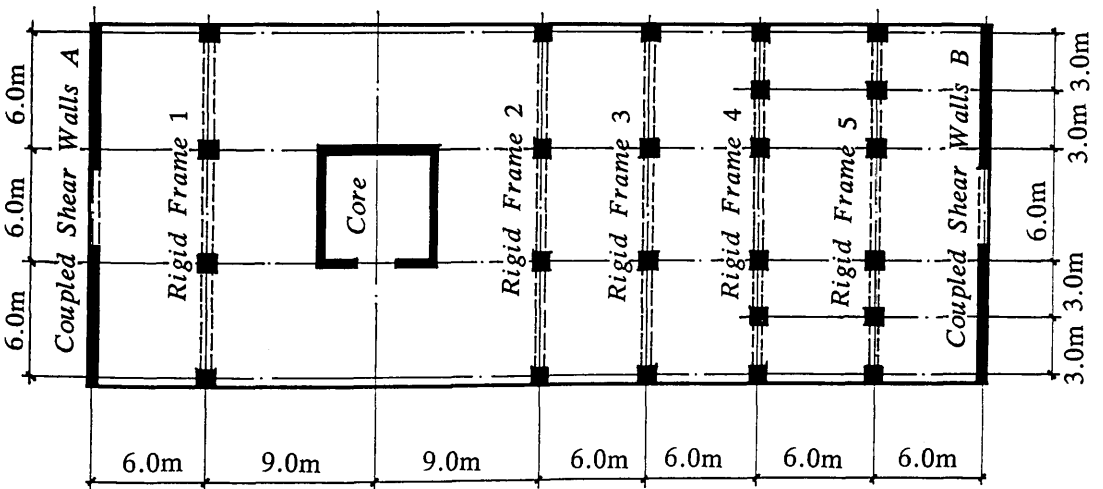
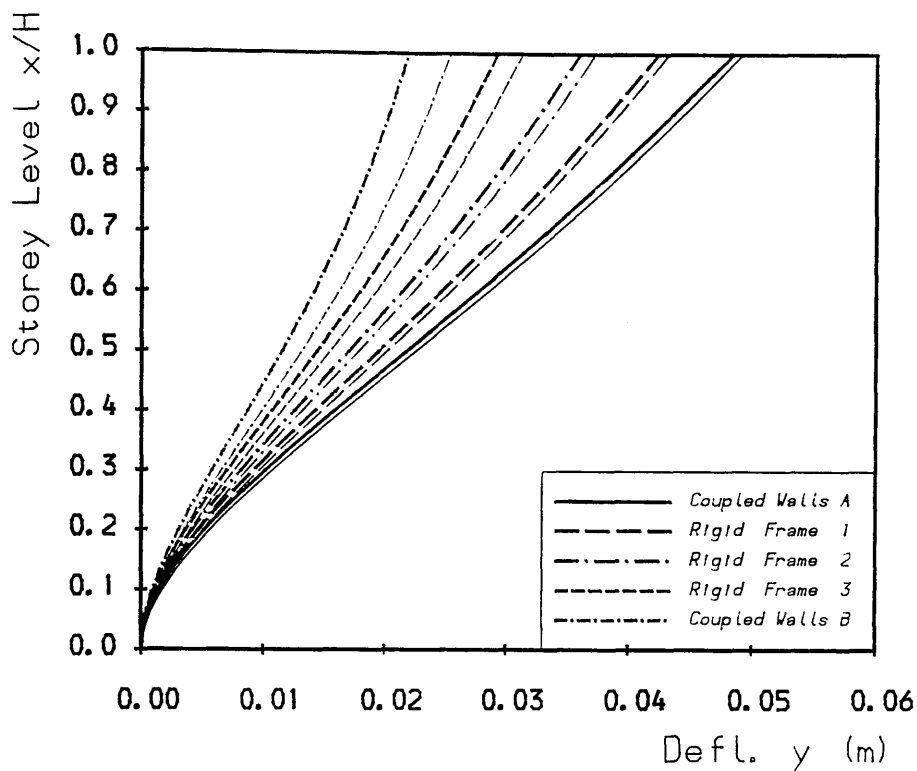
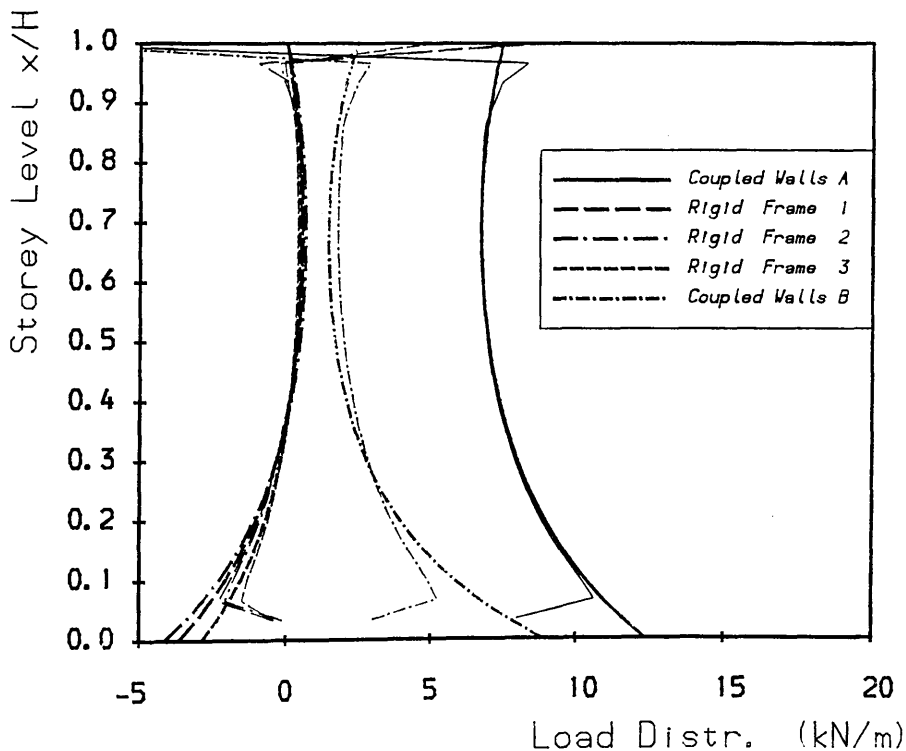


Fig. 5.17 Planform of Asymmetric Example Structure 2



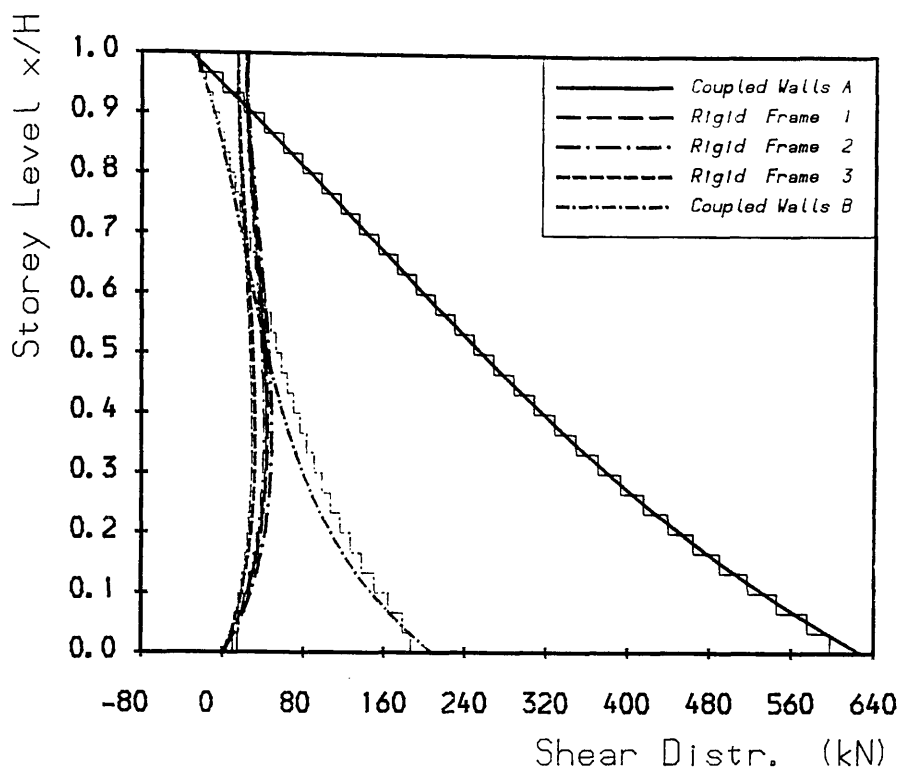
Asymmetric Structure Example 1

Fig. 5.14a Load Position 1, Deflections



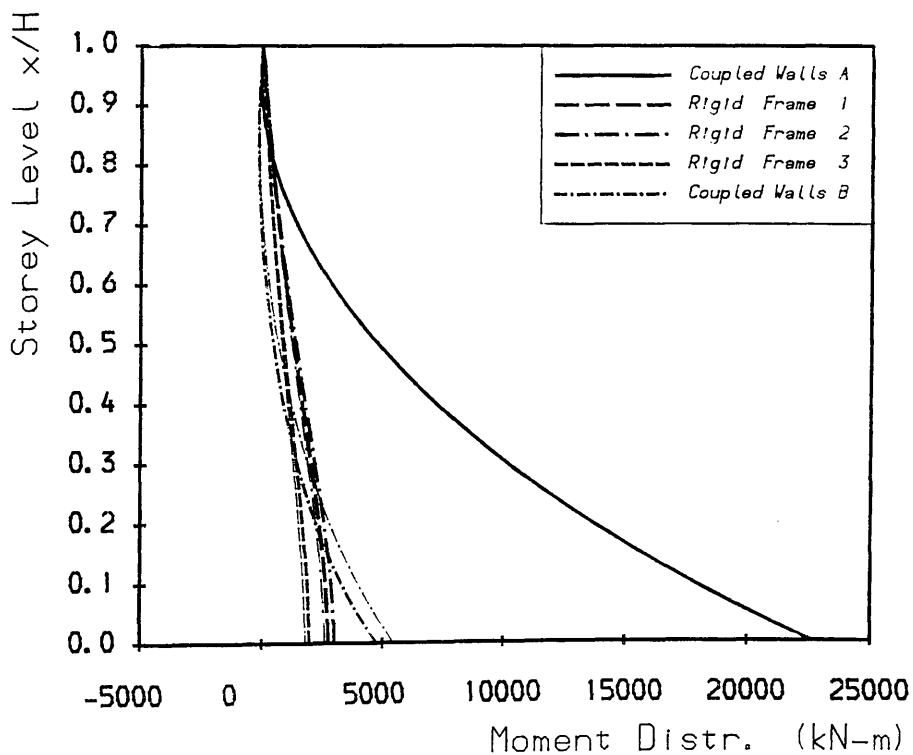
Asymmetric Structure Example 1

Fig. 5.14b Load Position 1, Load Distributions



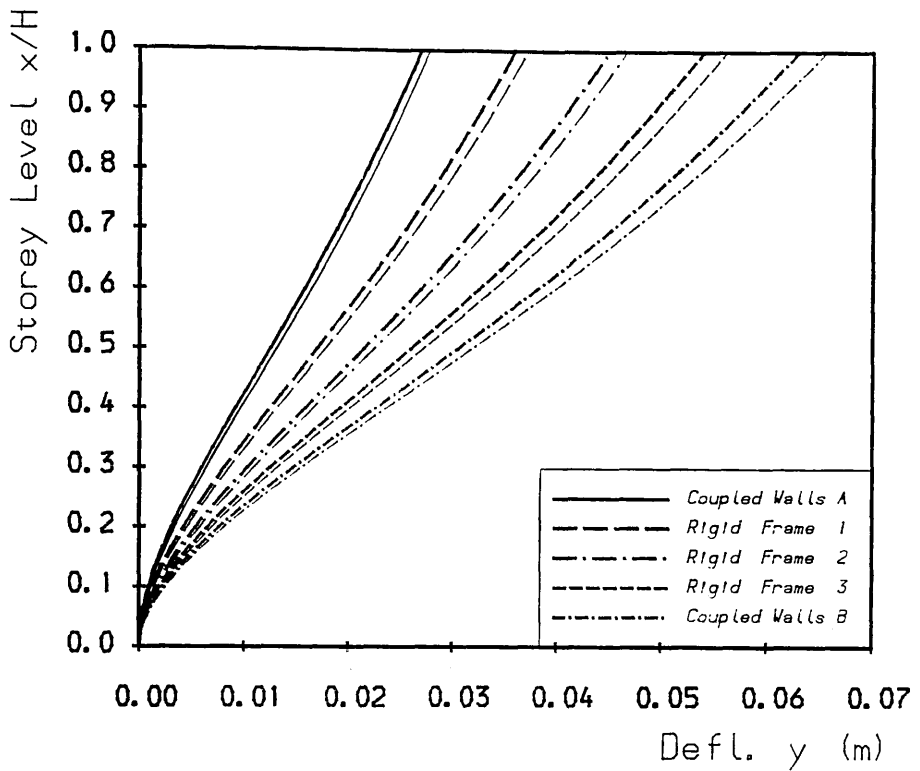
Asymmetric Structure Example 1

Fig. 5.14c Load Position 1, Shear Distributions



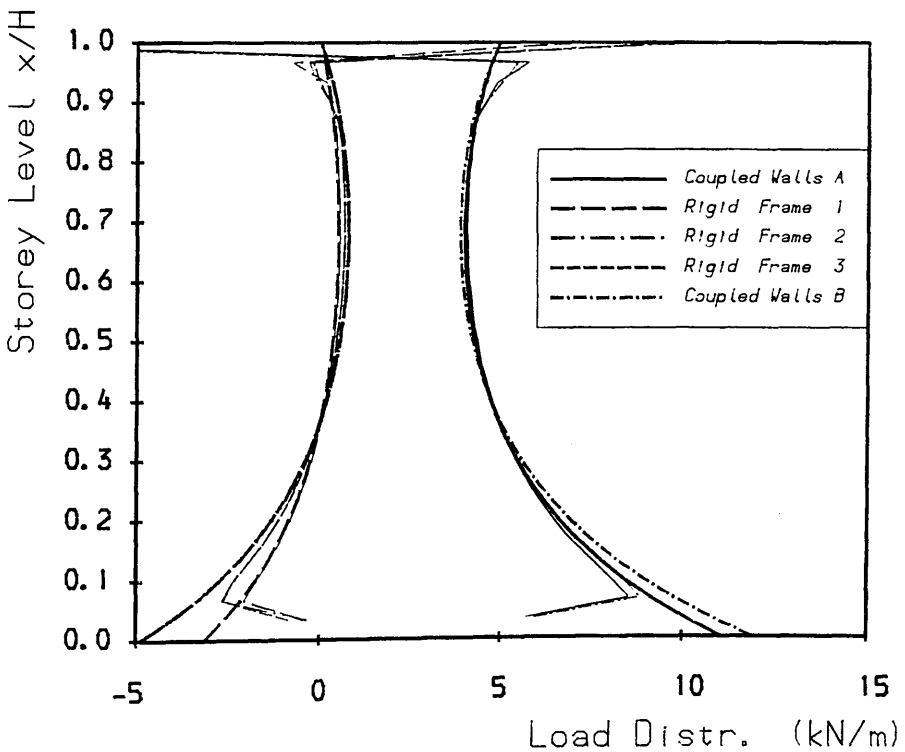
Asymmetric Structure Example 1

Fig. 5.14d Load Position 1, Moment Distributions



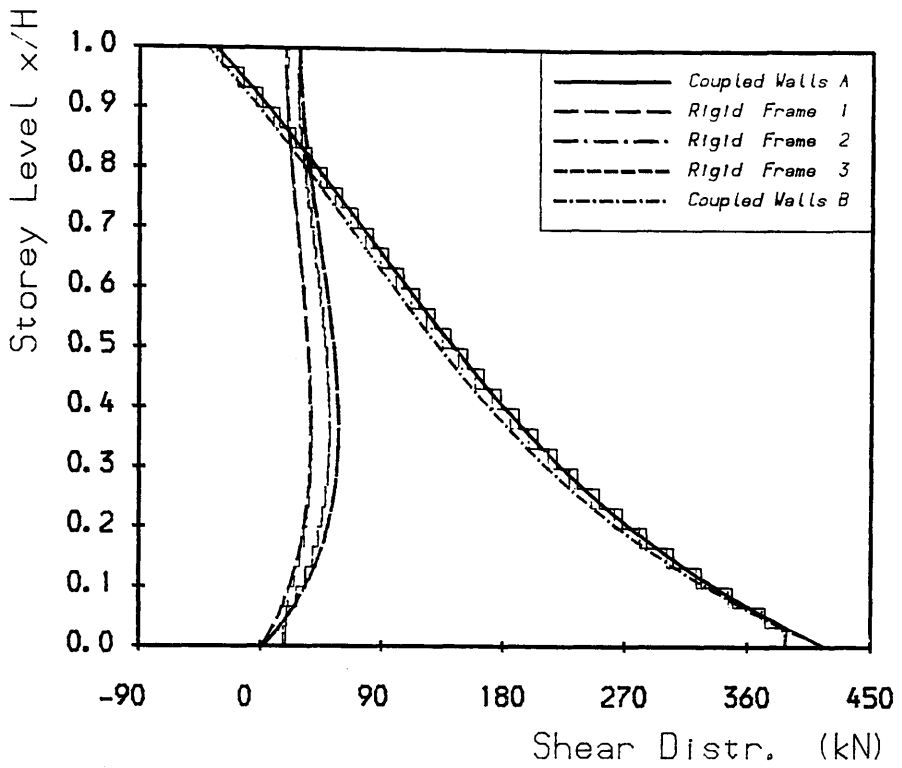
Asymmetric Structure Example 1

Fig. 5.15a Load Position 2, Deflections



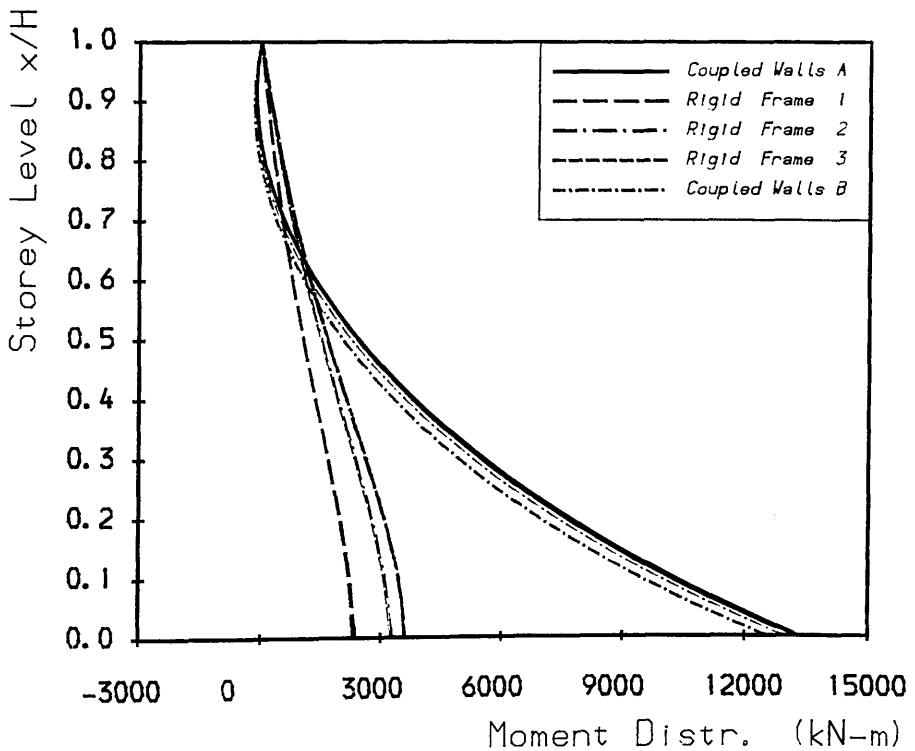
Asymmetric Structure Example 1

Fig. 5.15b Load Position 2, Load Distributions



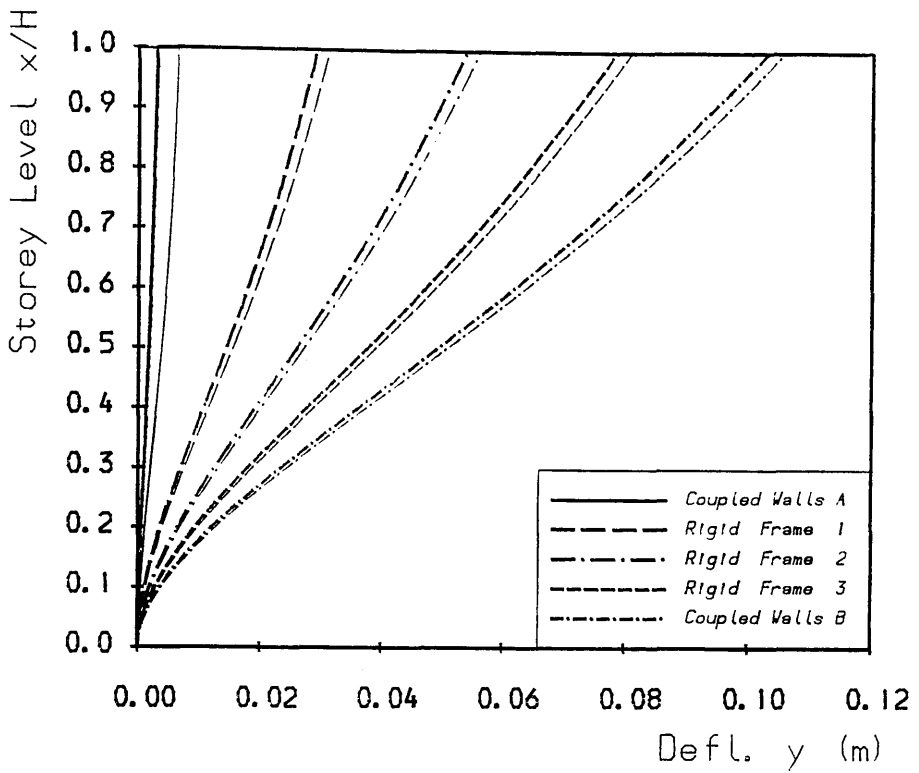
Asymmetric Structure Example 1

Fig. 5.15c Load Position 2, Shear Distributions



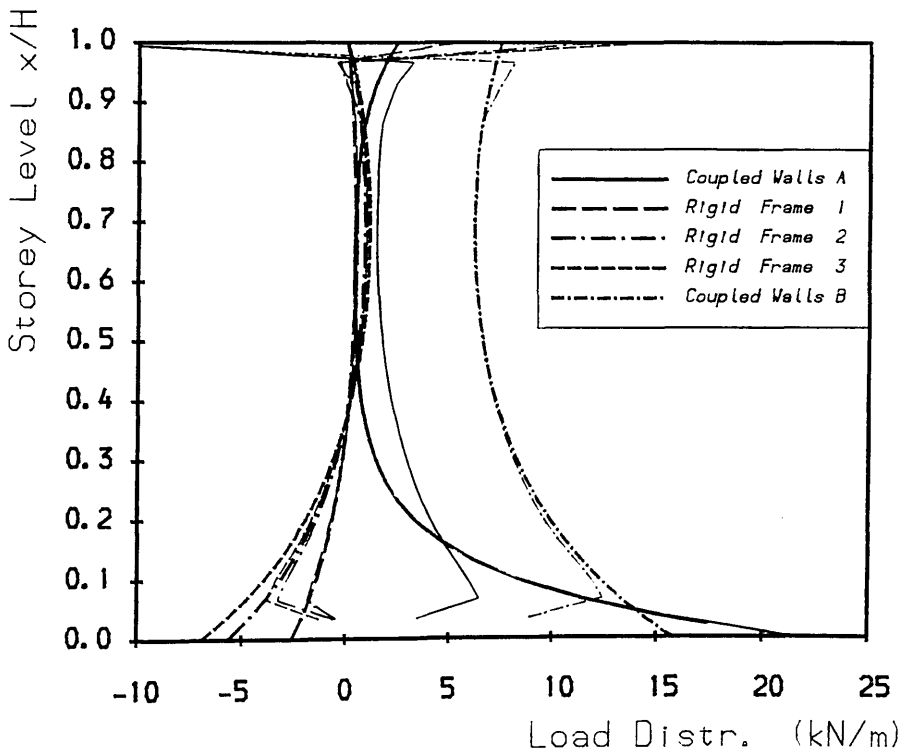
Asymmetric Structure Example 1

Fig. 5.15d Load Position 2, Moment Distributions



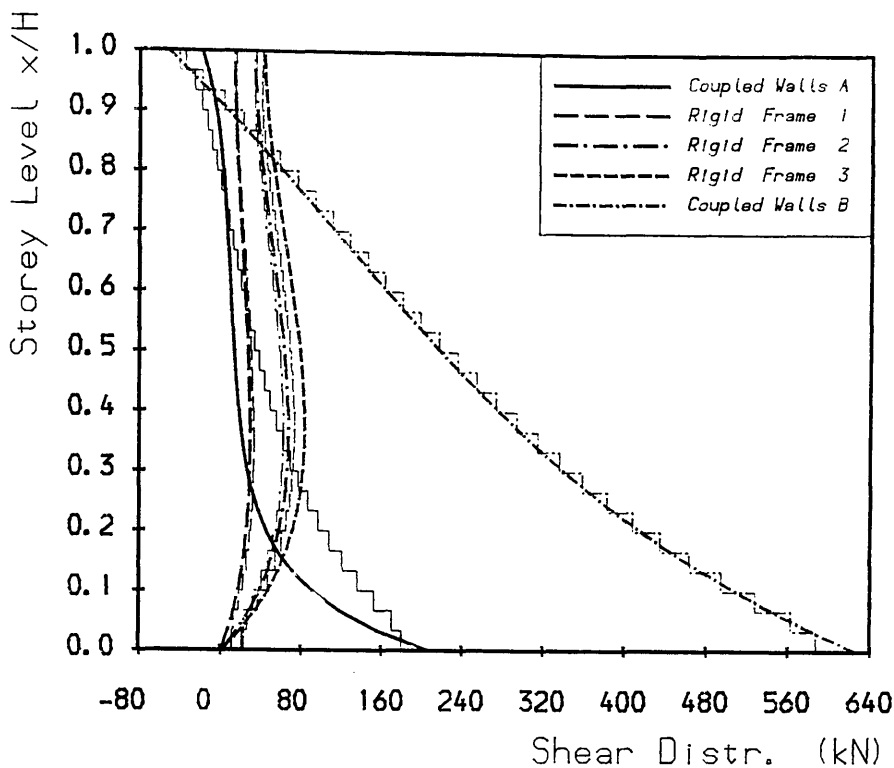
Asymmetric Structure Example 1

Fig. 5.16a Load Position 3, Deflections



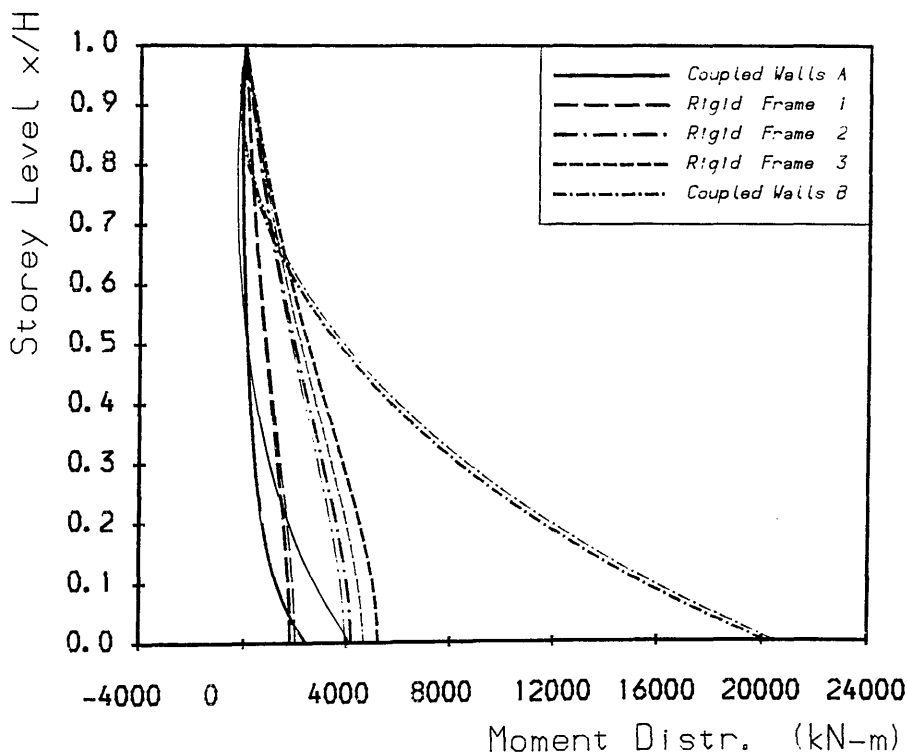
Asymmetric Structure Example 1

Fig. 5.16b Load Position 3, Load Distributions



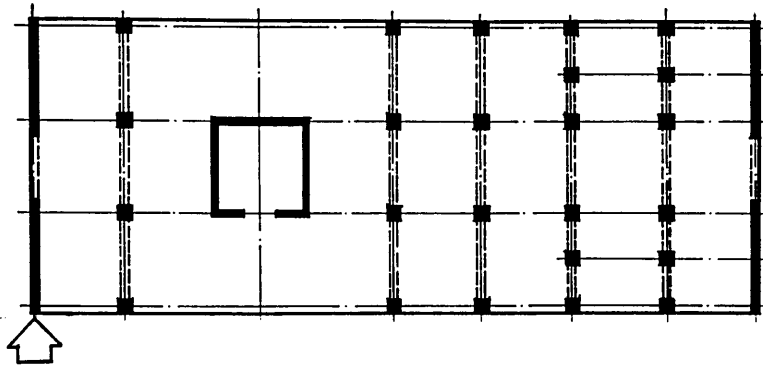
Asymmetric Structure Example 1

Fig. 5.16c Load Position 3, Shear Distributions

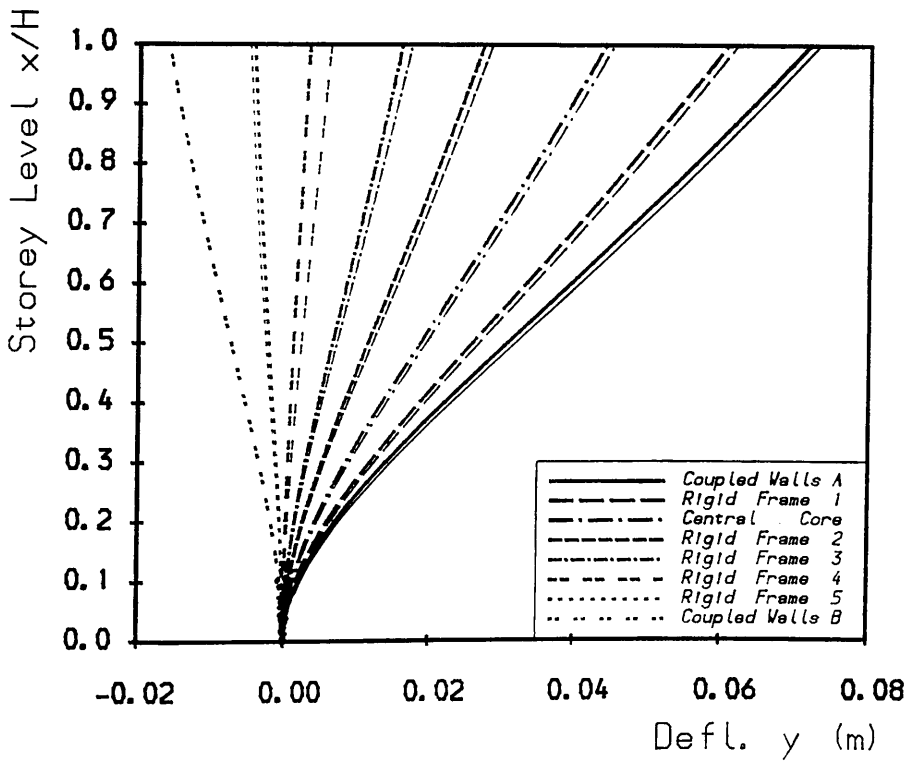


Asymmetric Structure Example 1

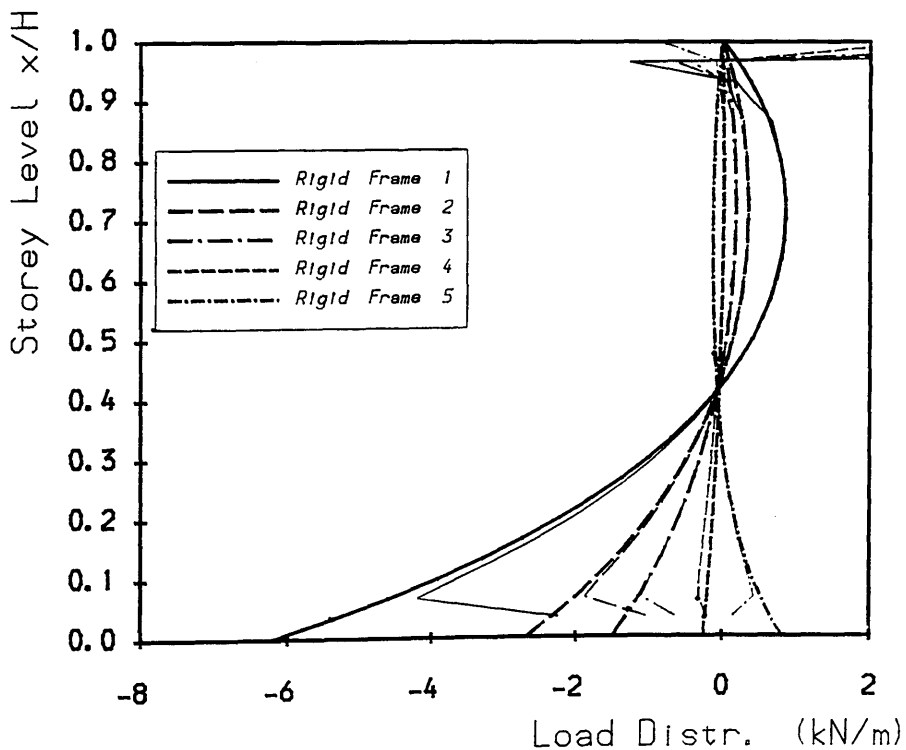
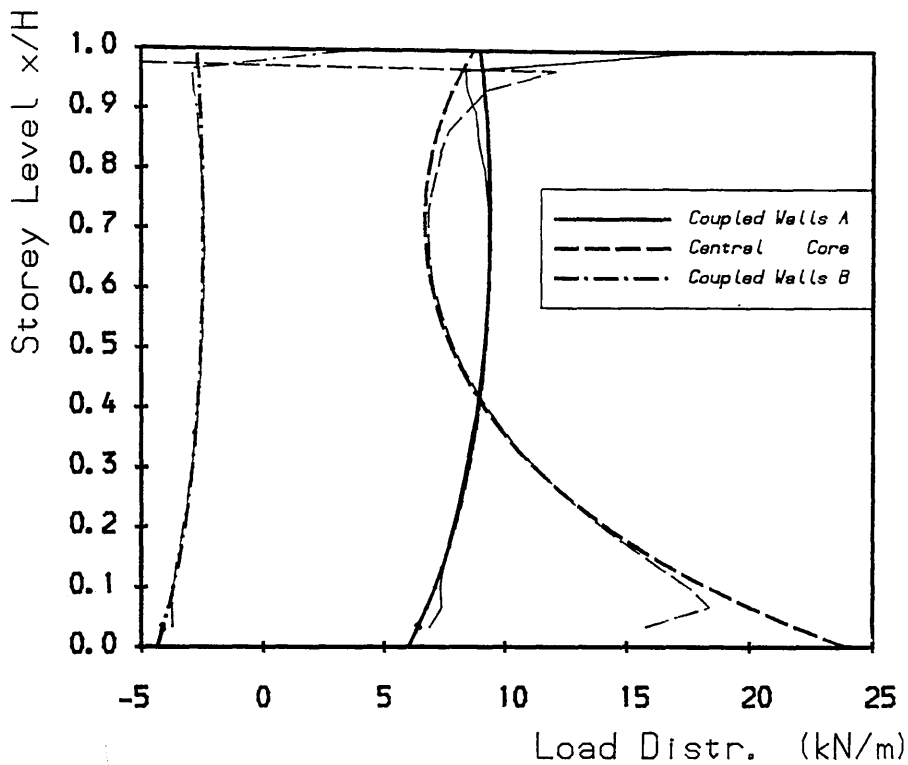
Fig. 5.16d Load Position 3, Moment Distributions



Load Position 1

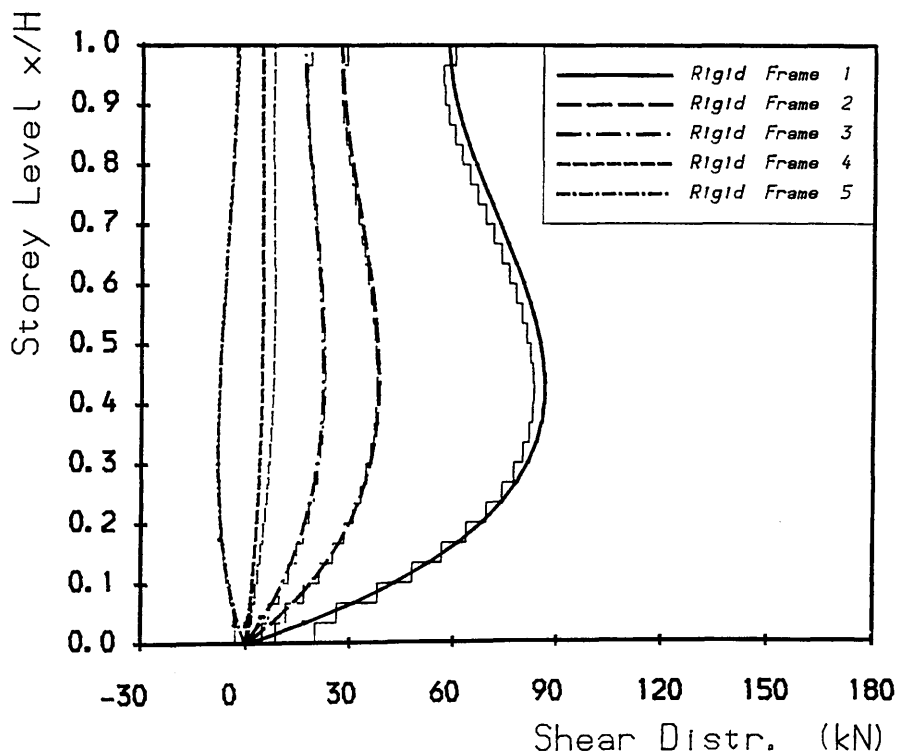
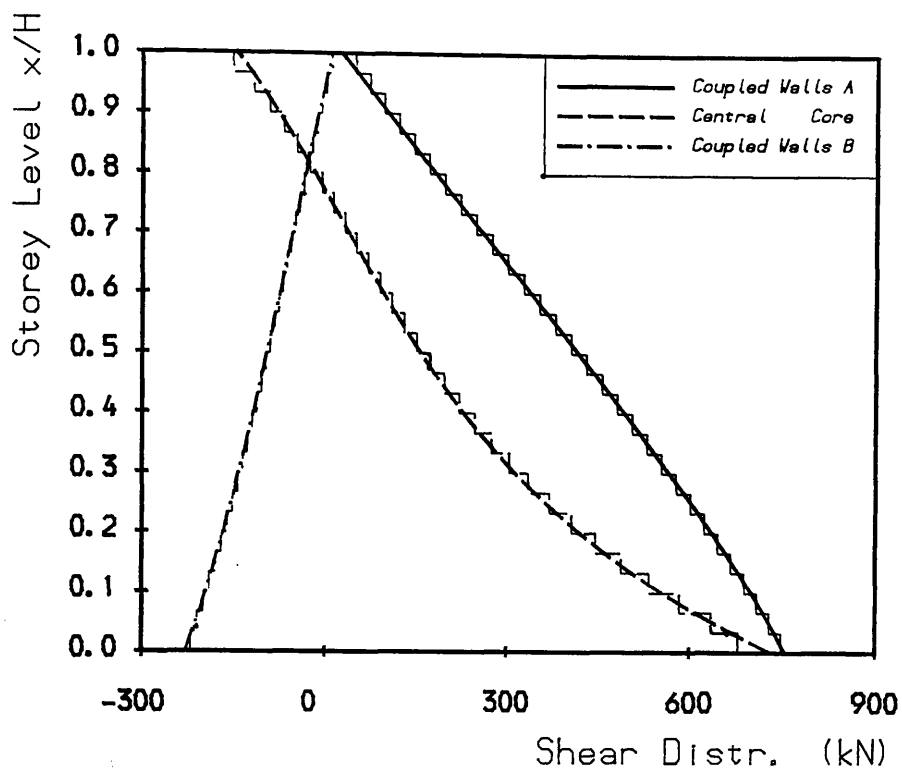


Asymmetric Structure Example 2
Fig. 5.18a Load Position 1. Deflections



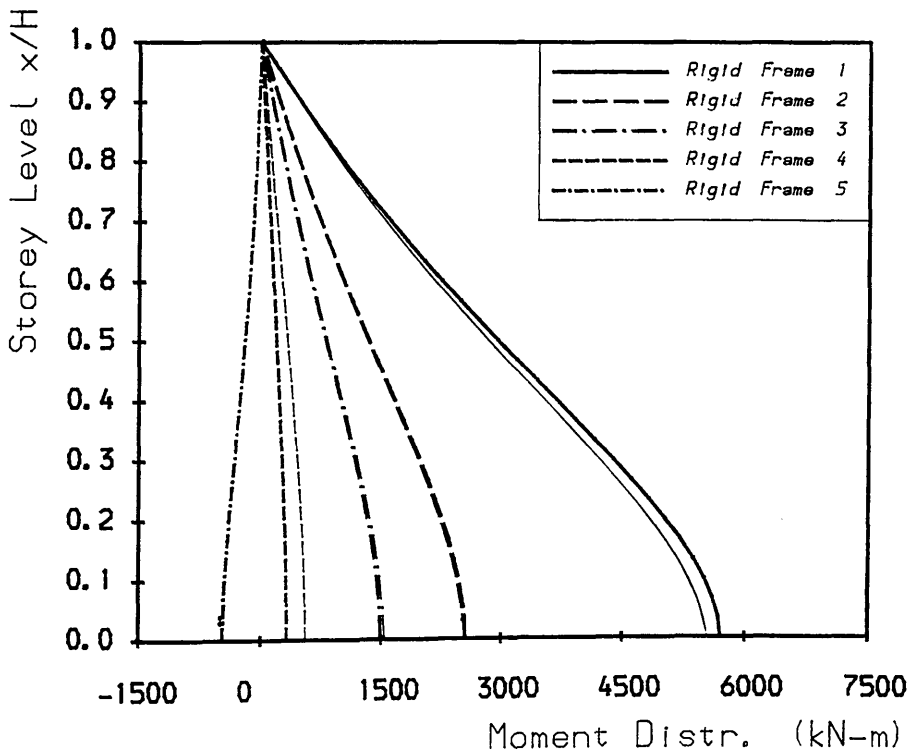
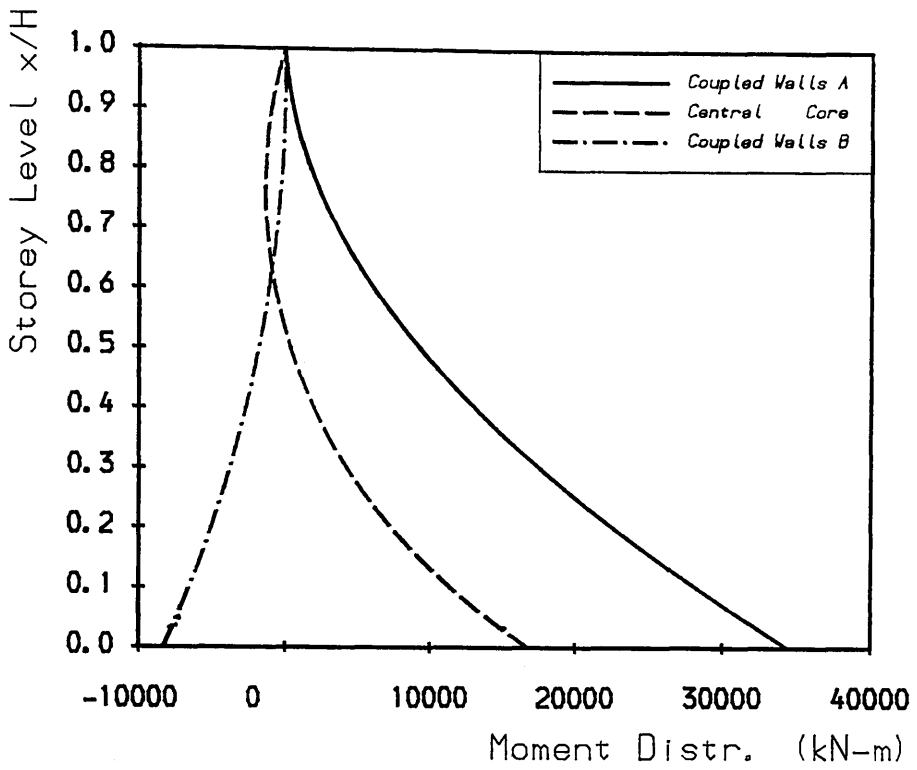
Asymmetric Structure Example 2

Fig. 5.18b Load Position 1. Load Distributions



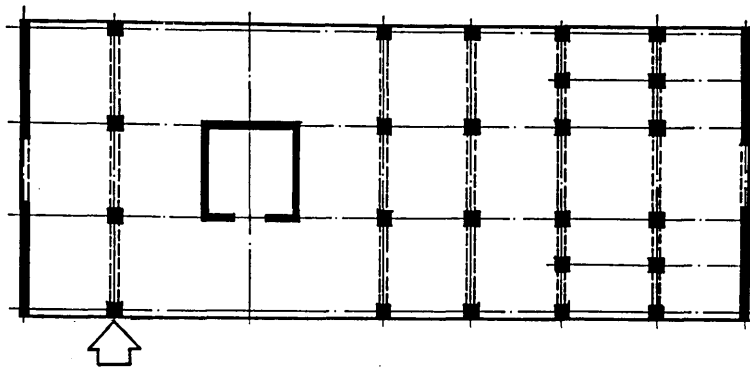
Asymmetric Structure Example 2

Fig. 5.18c Load Position 1, Shear Distributions

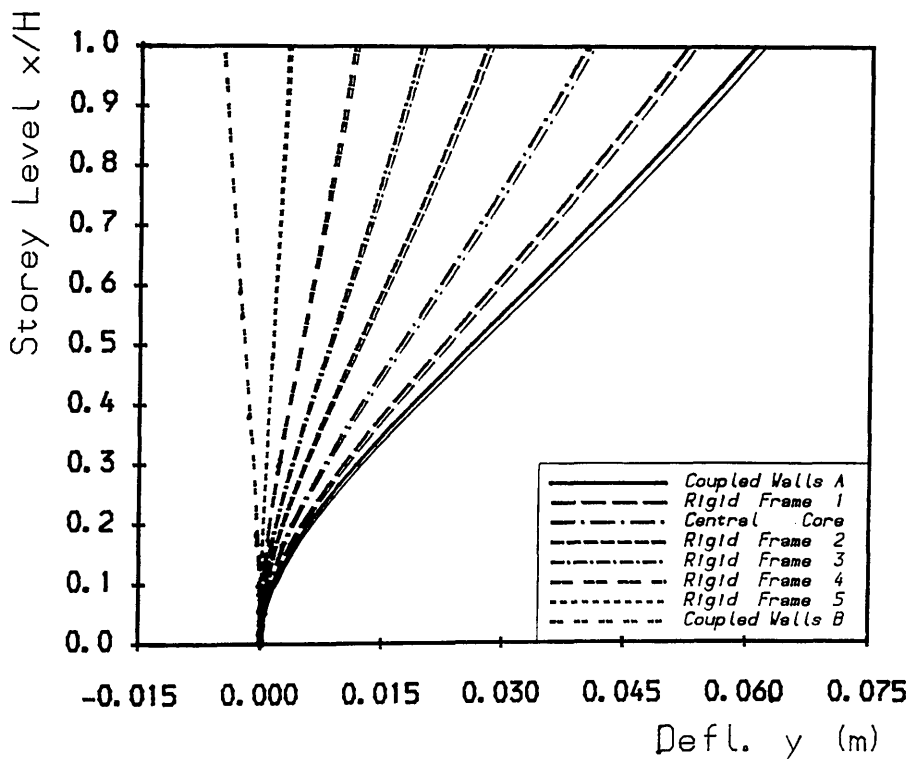


Asymmetric Structure Example 2

Fig. 5.18d Load Position 1, Moment Distributions

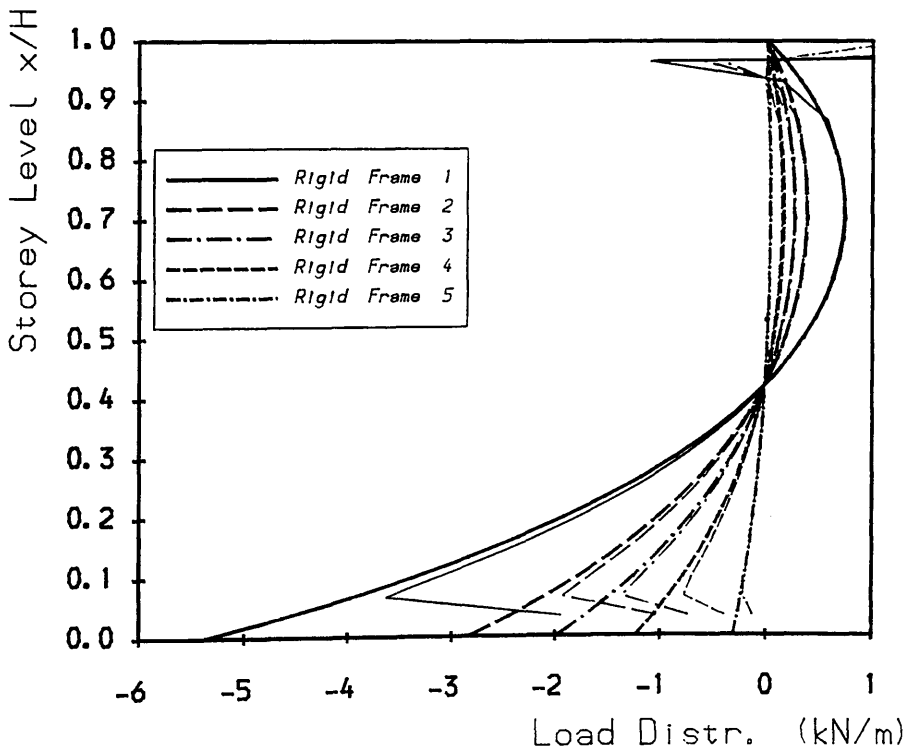
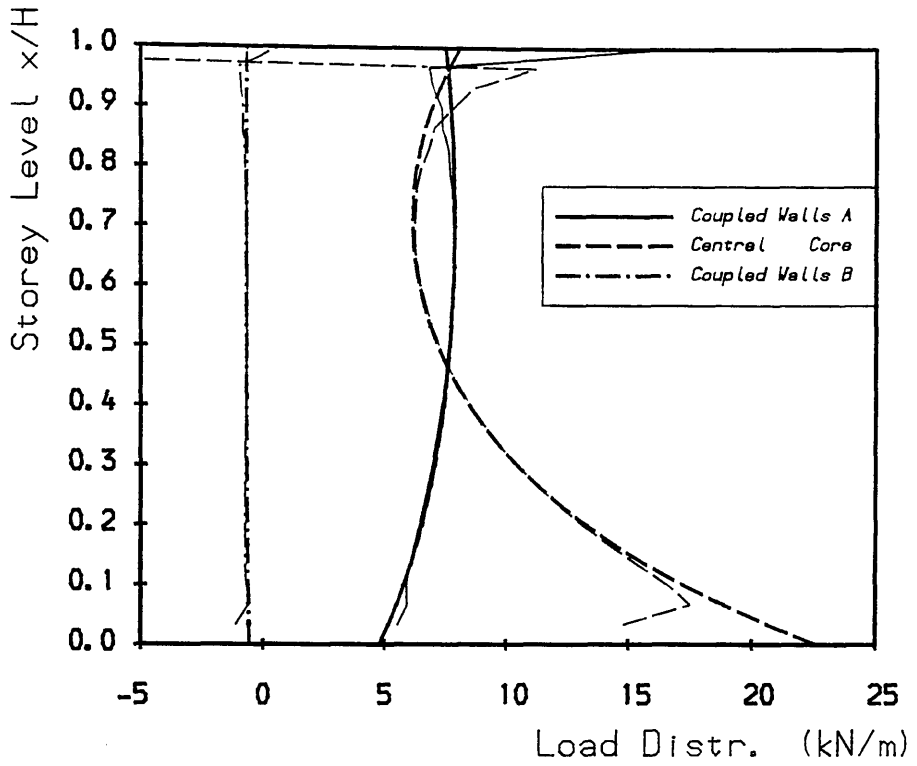


Load Position 2



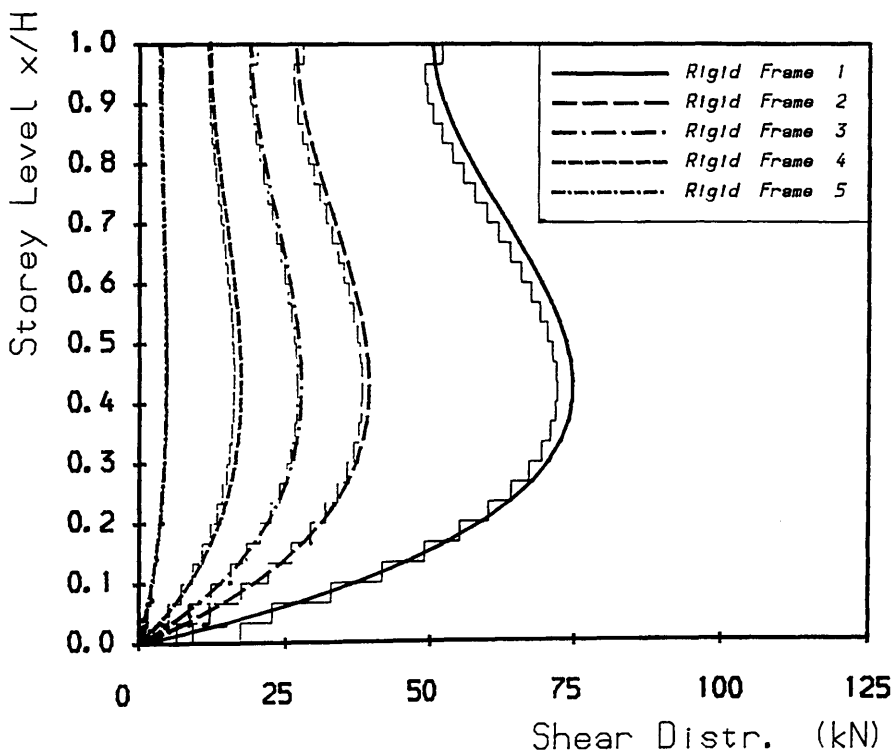
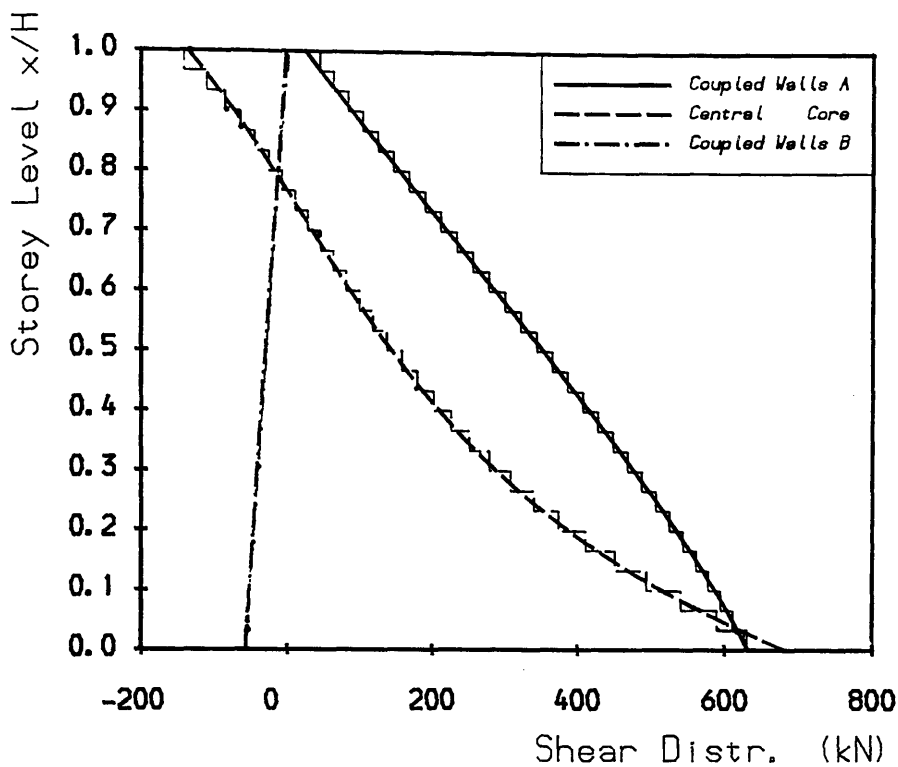
Asymmetric Structure Example 2

Fig. 5.19a Load Position 2. Deflections



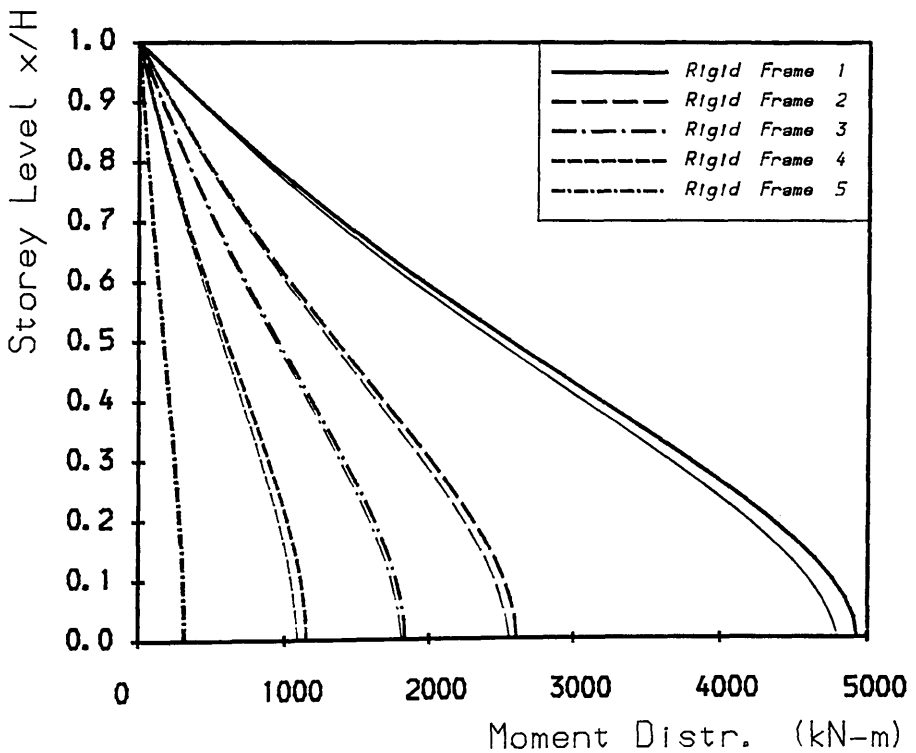
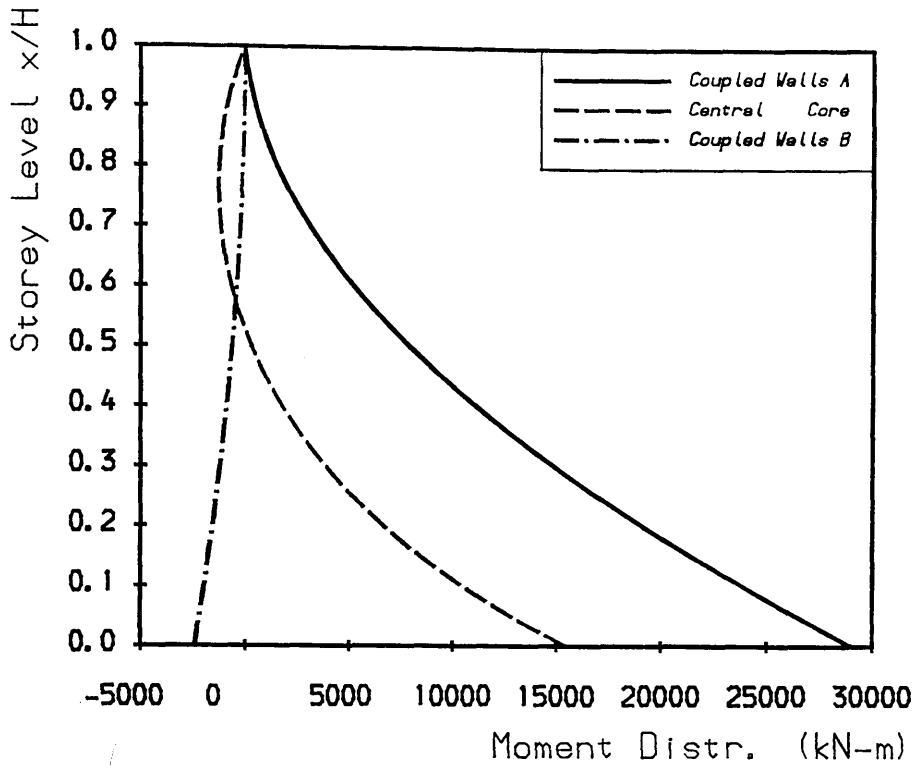
Asymmetric Structure Example 2

Fig. 5.19b Load Position 2. Load Distributions



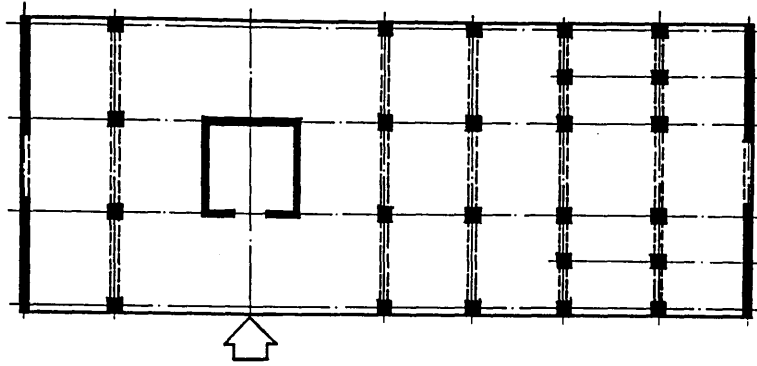
Asymmetric Structure Example 2

Fig. 5.19c Load Position 2, Shear Distributions

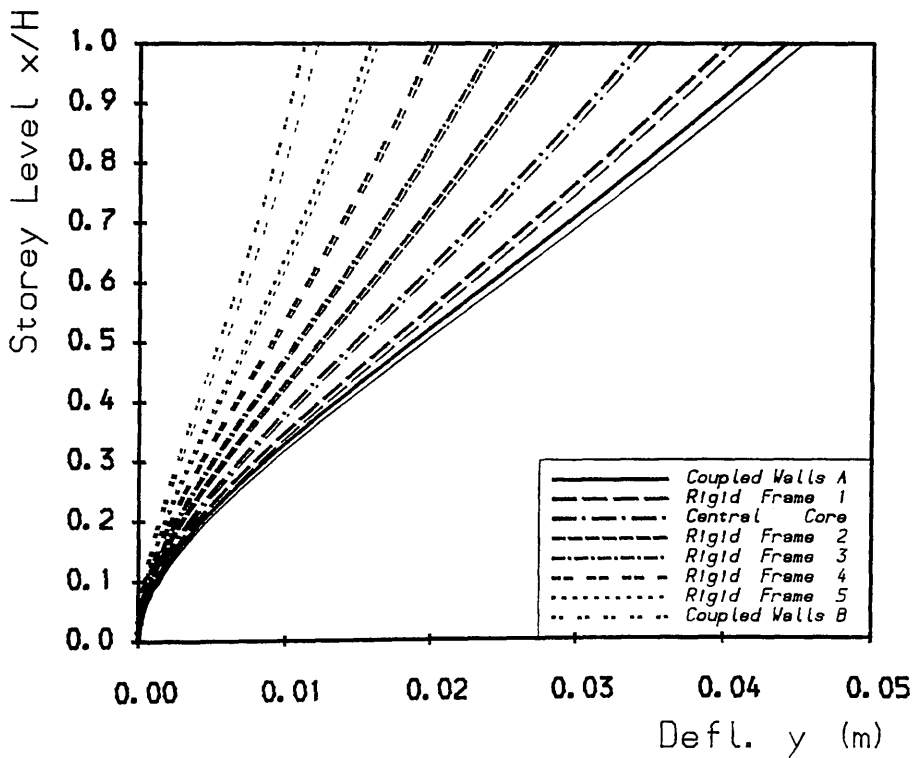


Asymmetric Structure Example 2

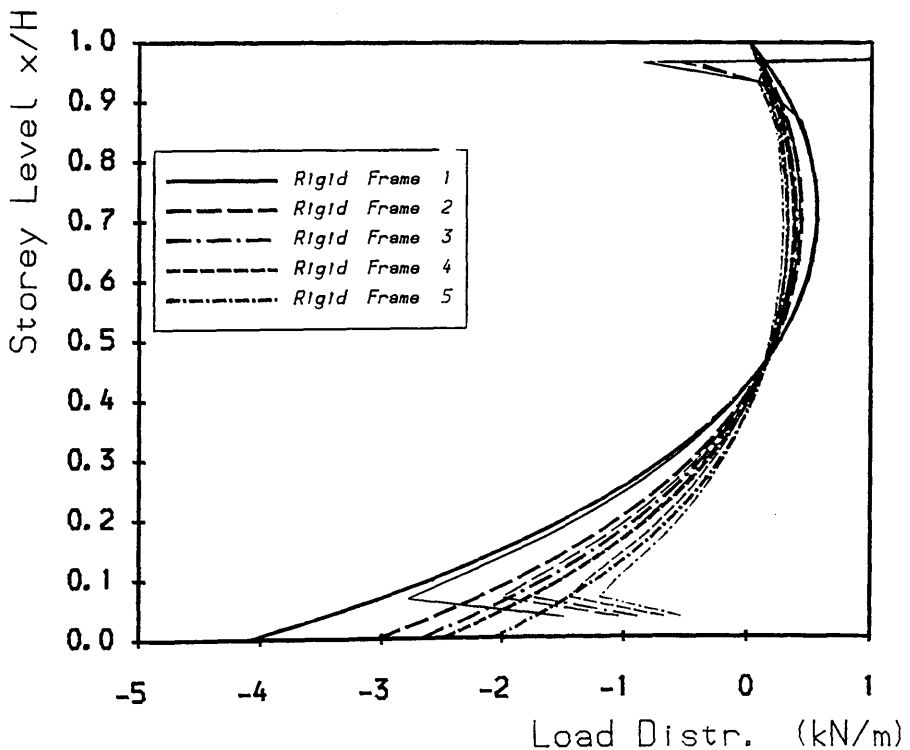
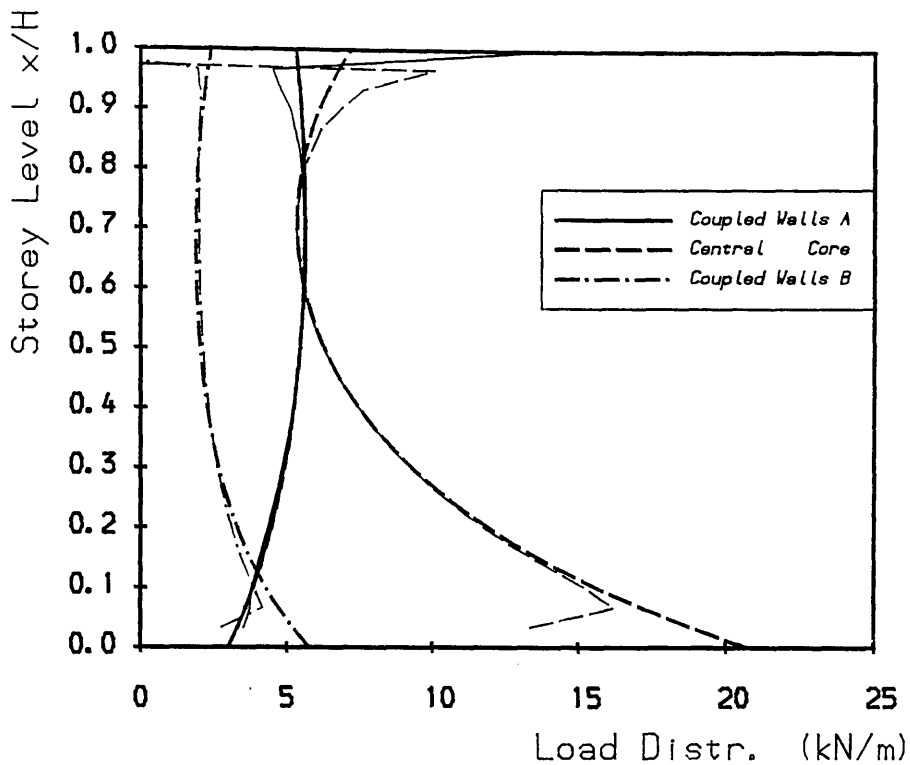
Fig. 5.19d Load Position 2, Moment Distributions



Load Position 3

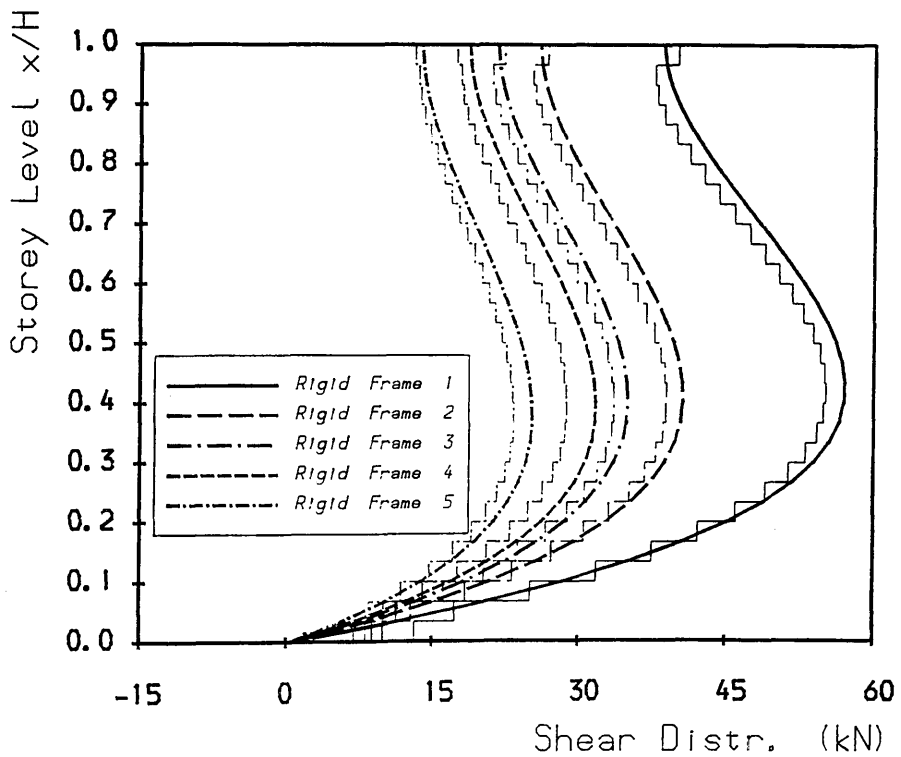
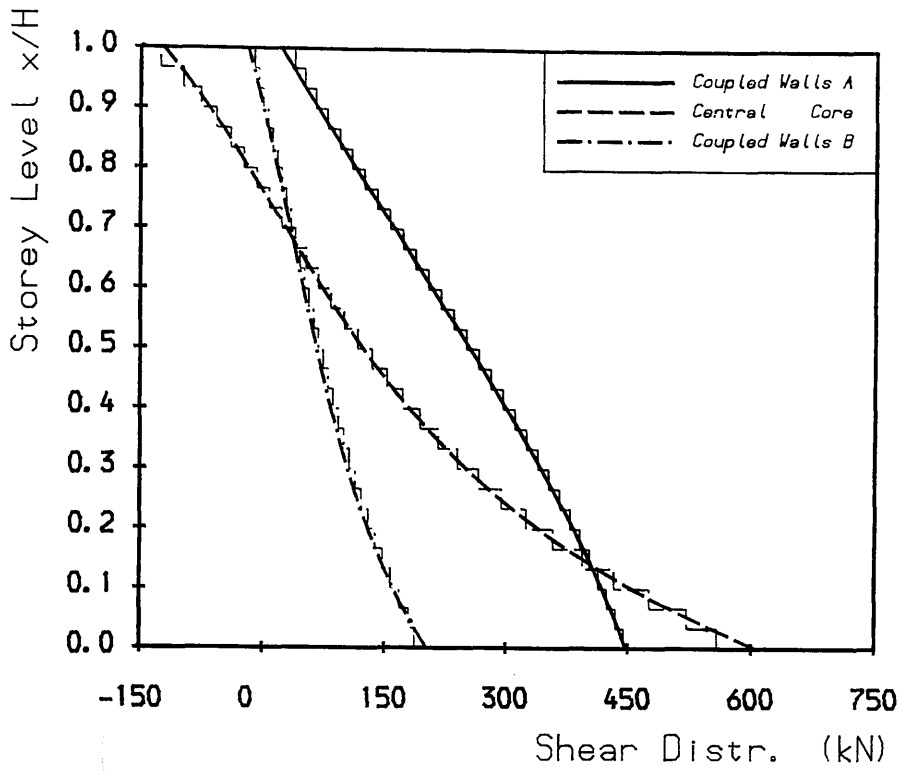


Asymmetric Structure Example 2
Fig. 5.20a Load Position 3. Deflections



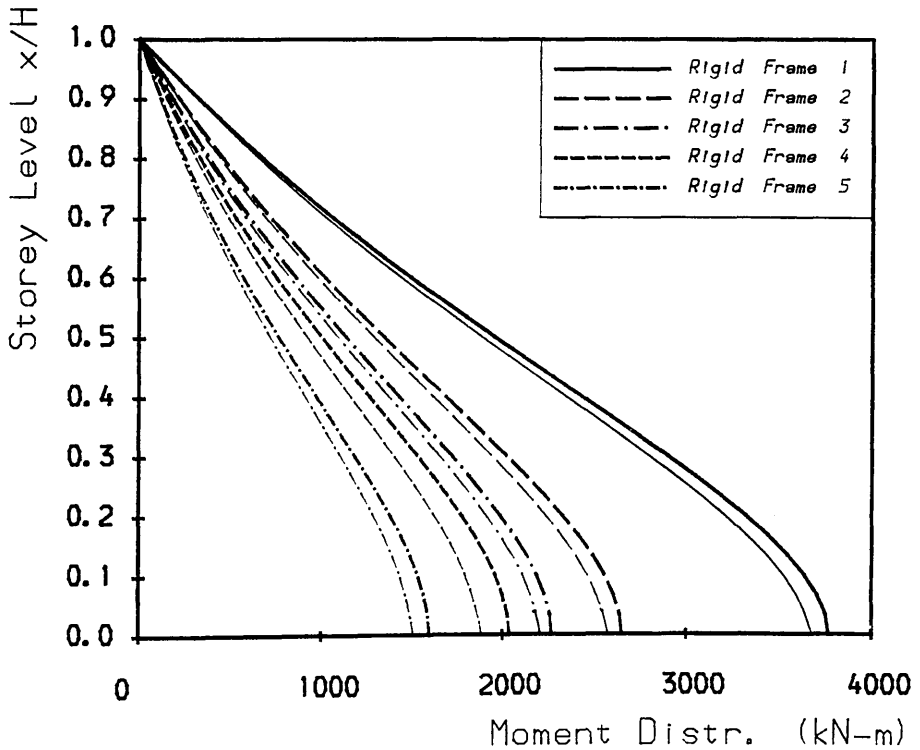
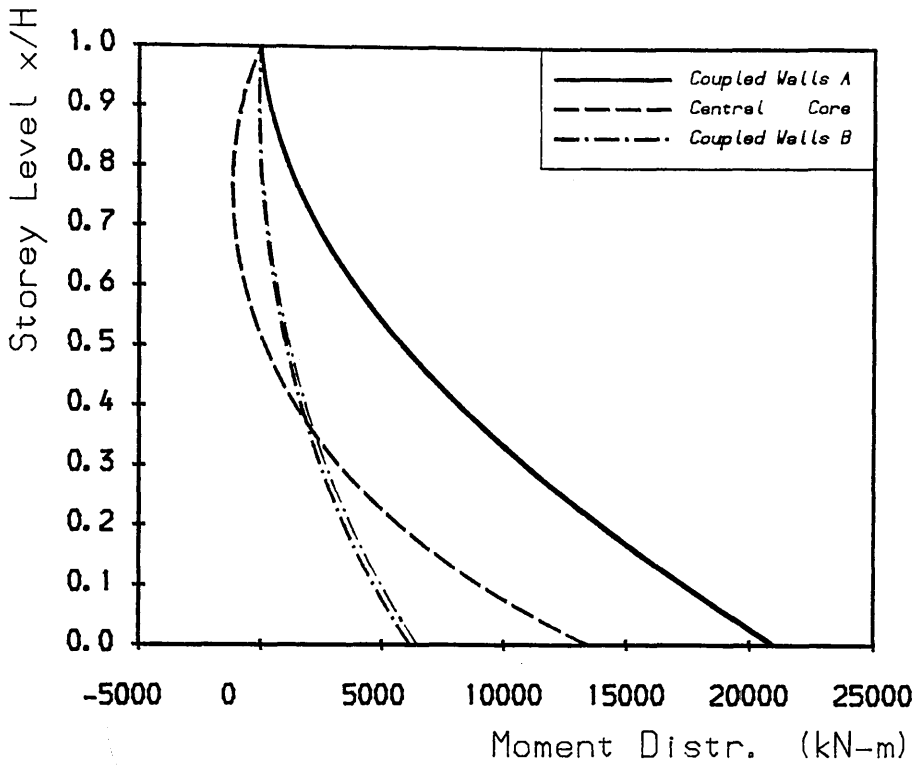
Asymmetric Structure Example 2

Fig. 5.20b Load Position 3. Load Distributions



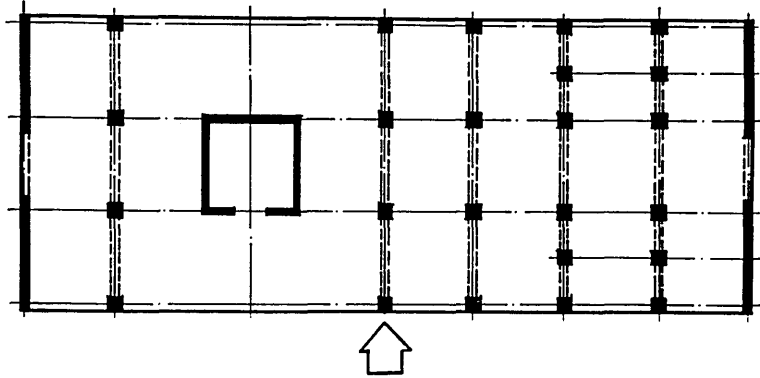
Asymmetric Structure Example 2

Fig. 5.20c Load Position 3, Shear Distributions

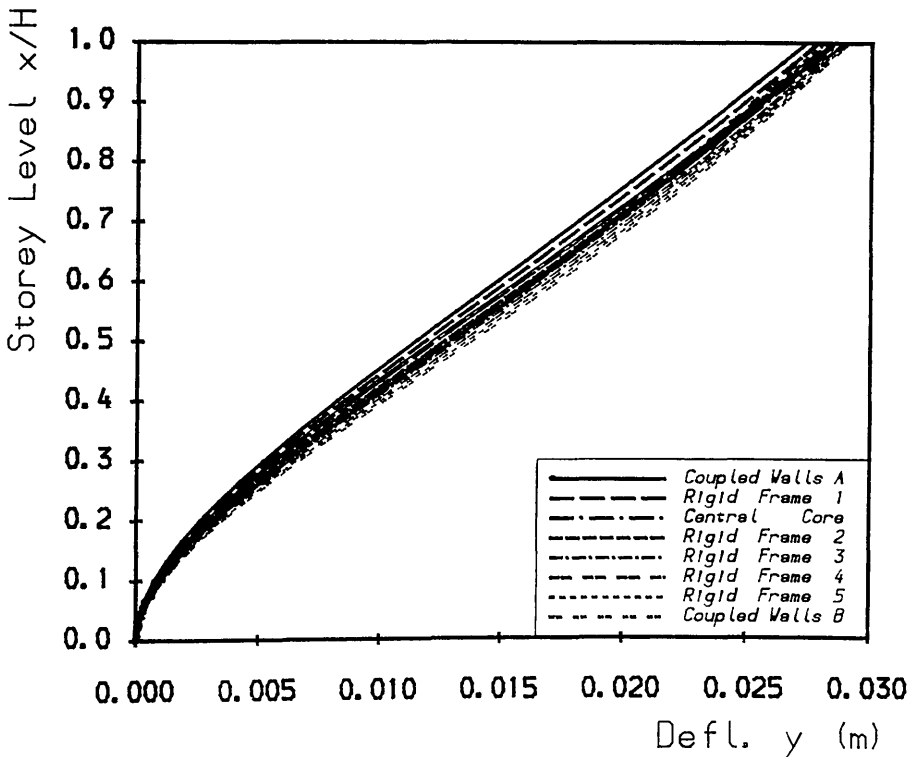


Asymmetric Structure Example 2

Fig. 5.20d Load Position 3, Moment Distributions

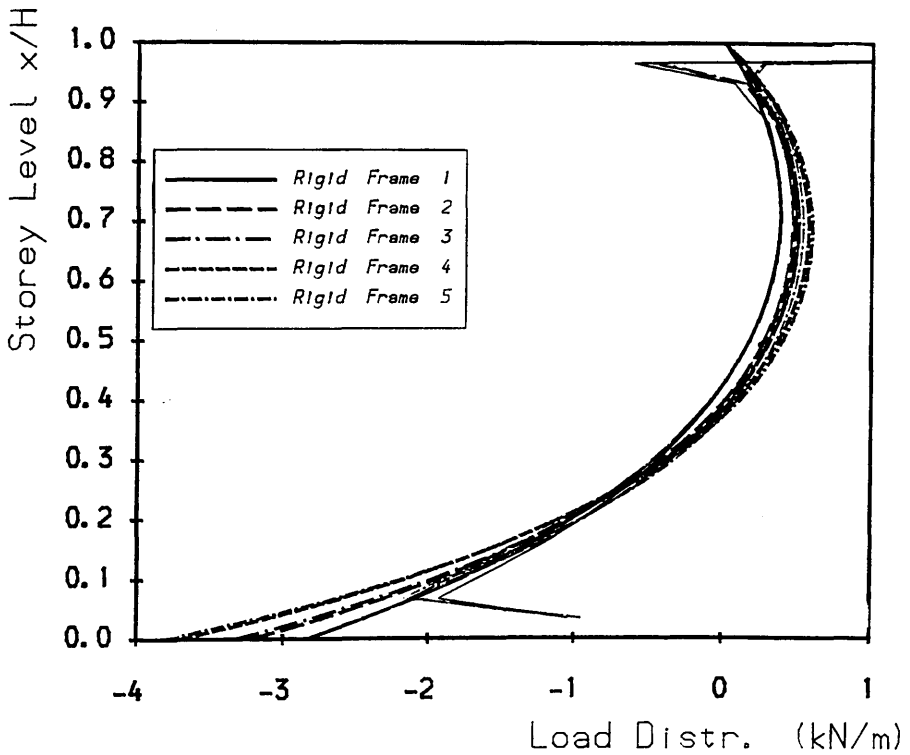
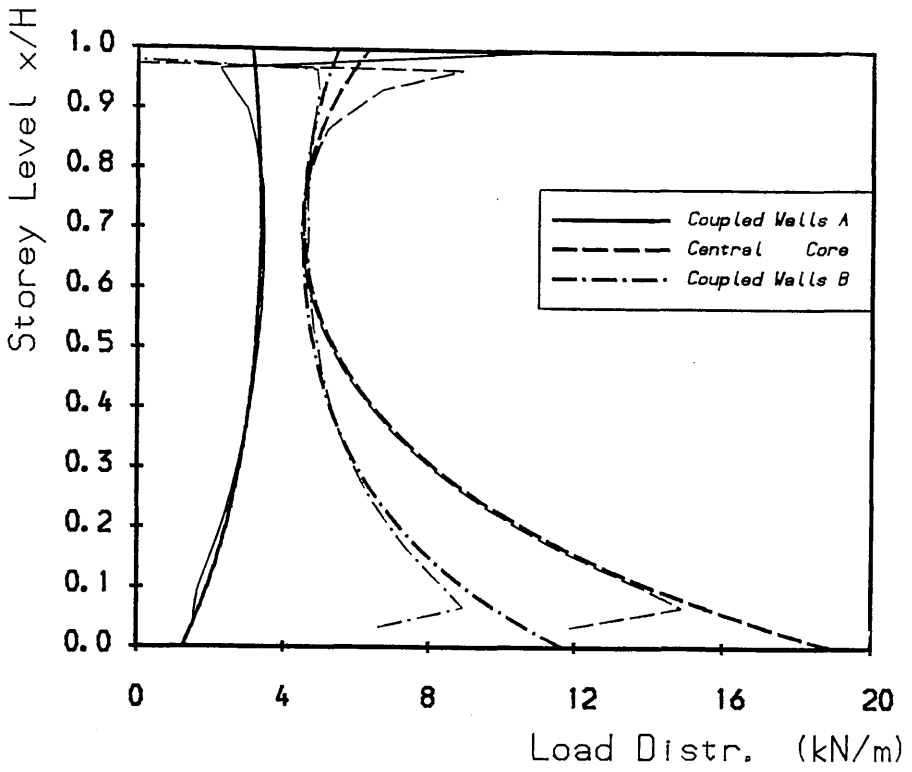


Load Position 4



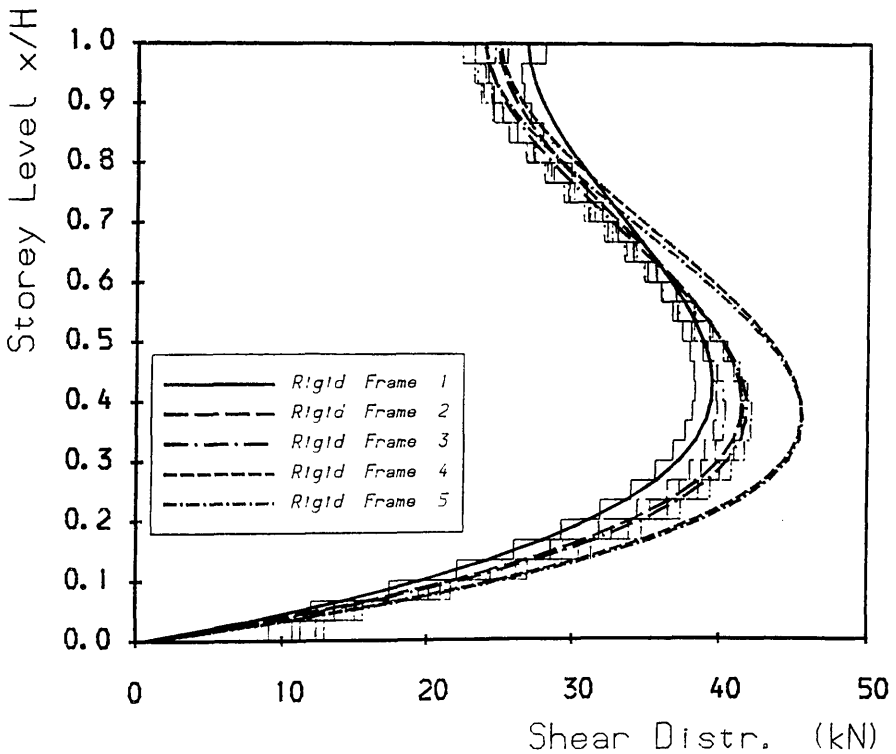
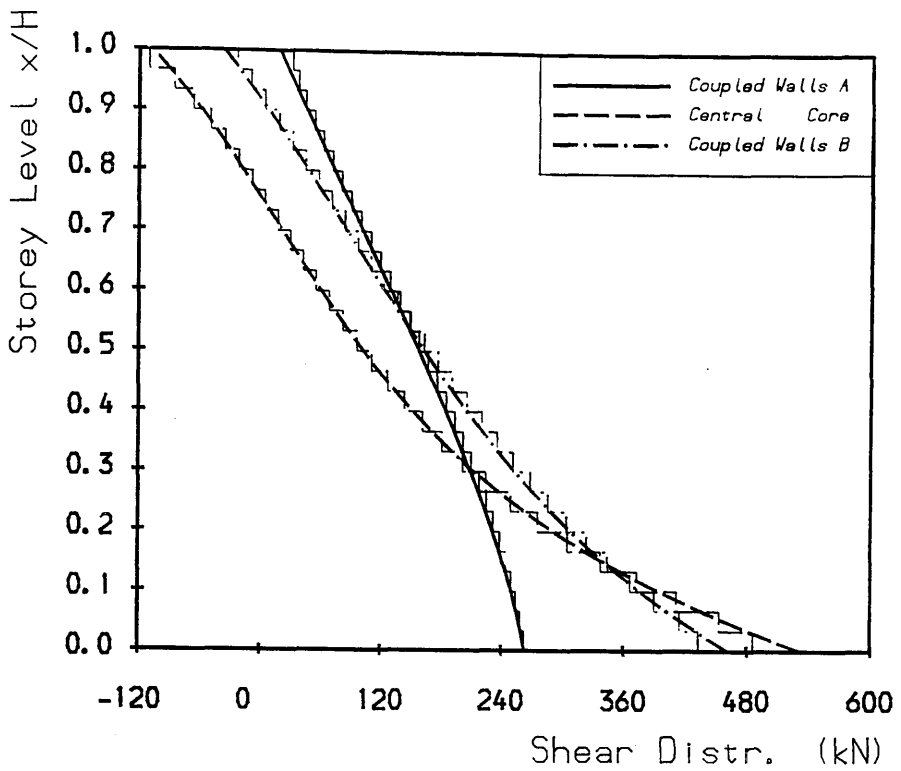
Asymmetric Structure Example 2

Fig. 5.21a Load Position 4. Deflections



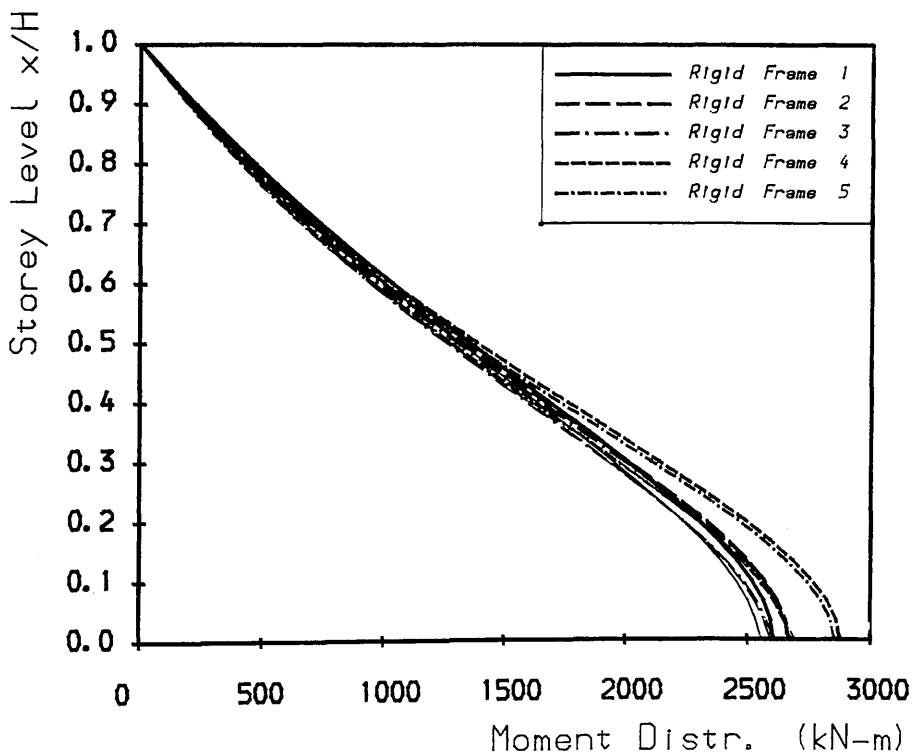
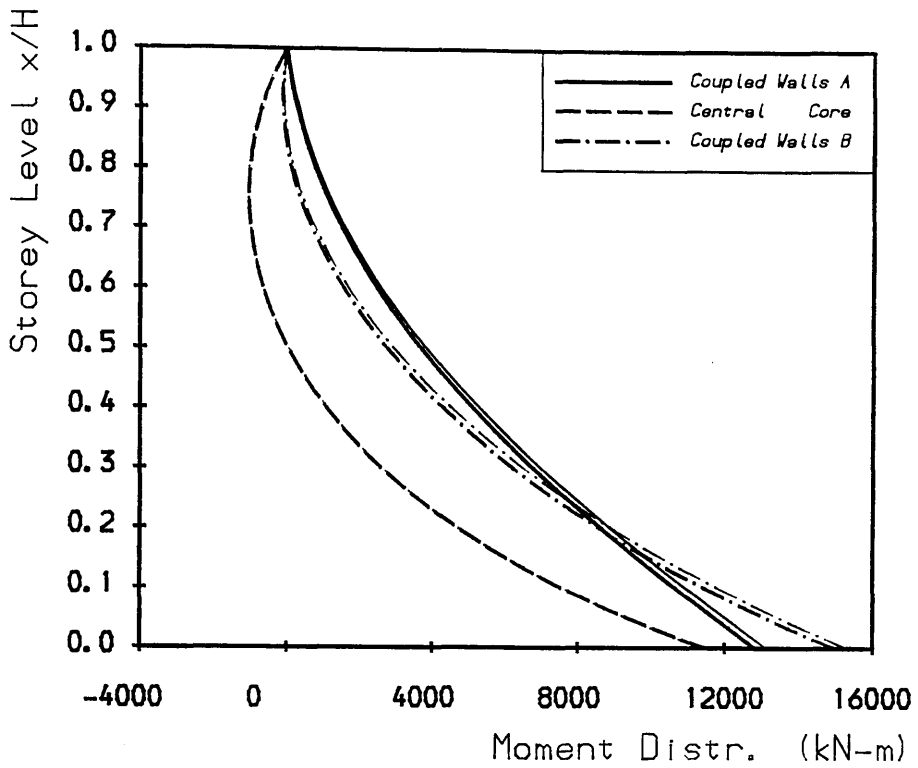
Asymmetric Structure Example 2

Fig. 5.21b Load Position 4. Load Distributions



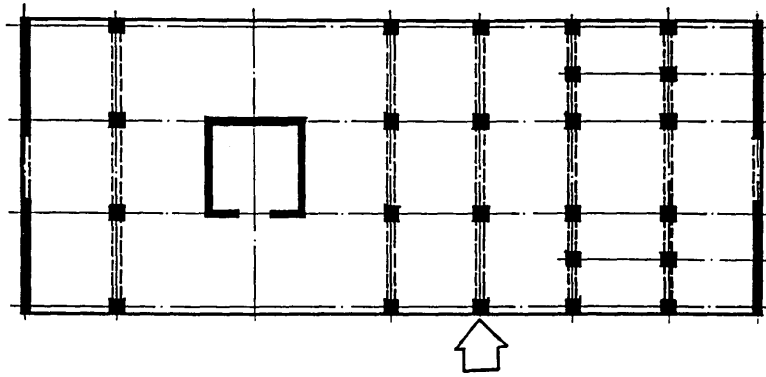
Asymmetric Structure Example 2

Fig. 5.21c Load Position 4, Shear Distributions

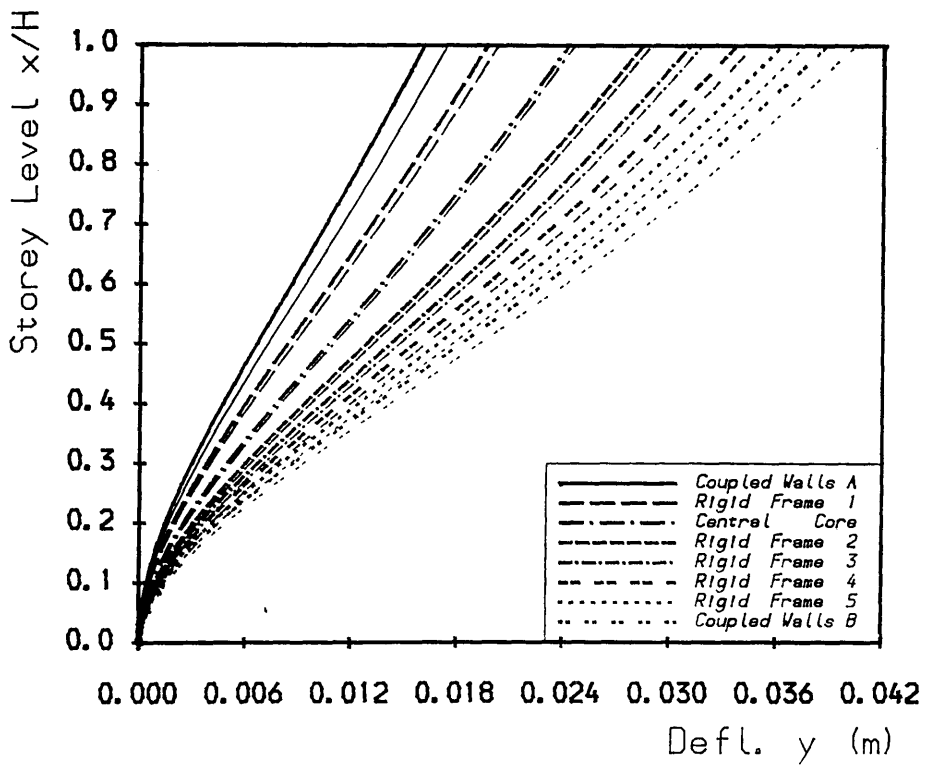


Asymmetric Structure Example 2

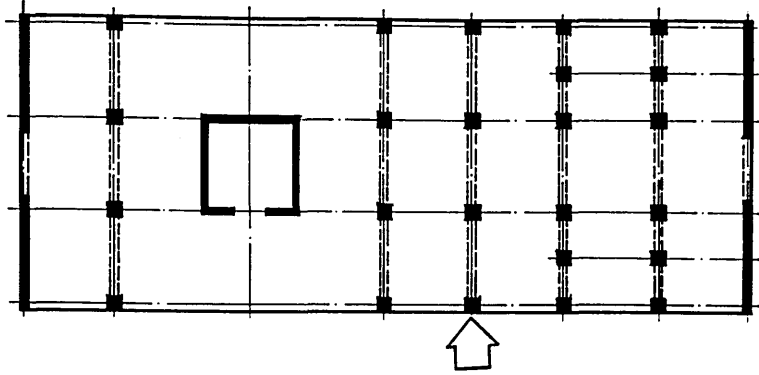
Fig. 5.21d Load Position 4, Moment Distributions



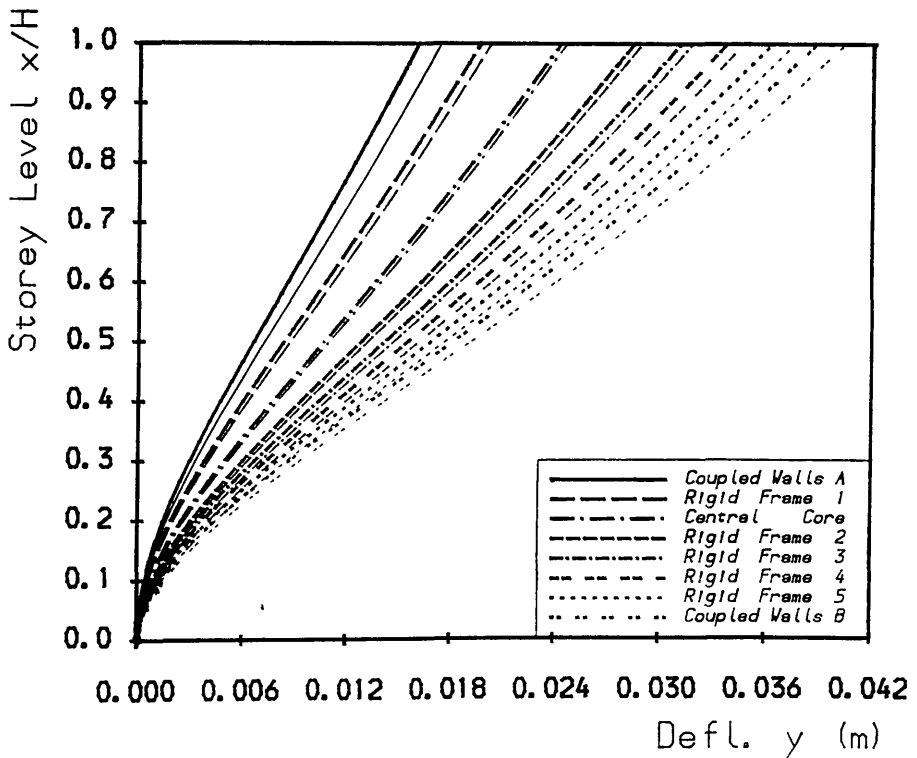
Load Position 5



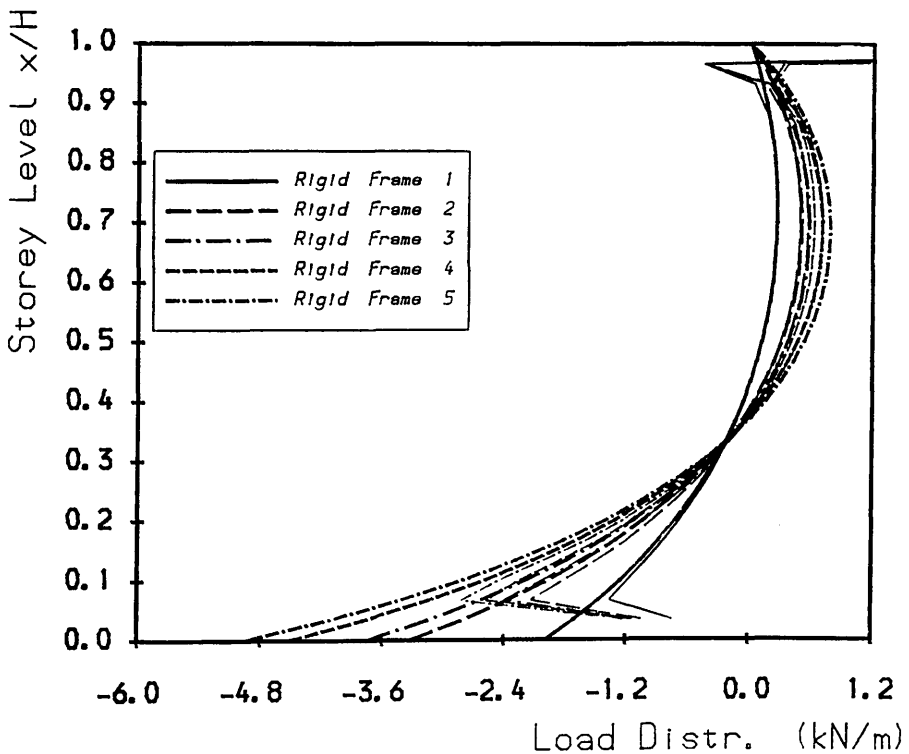
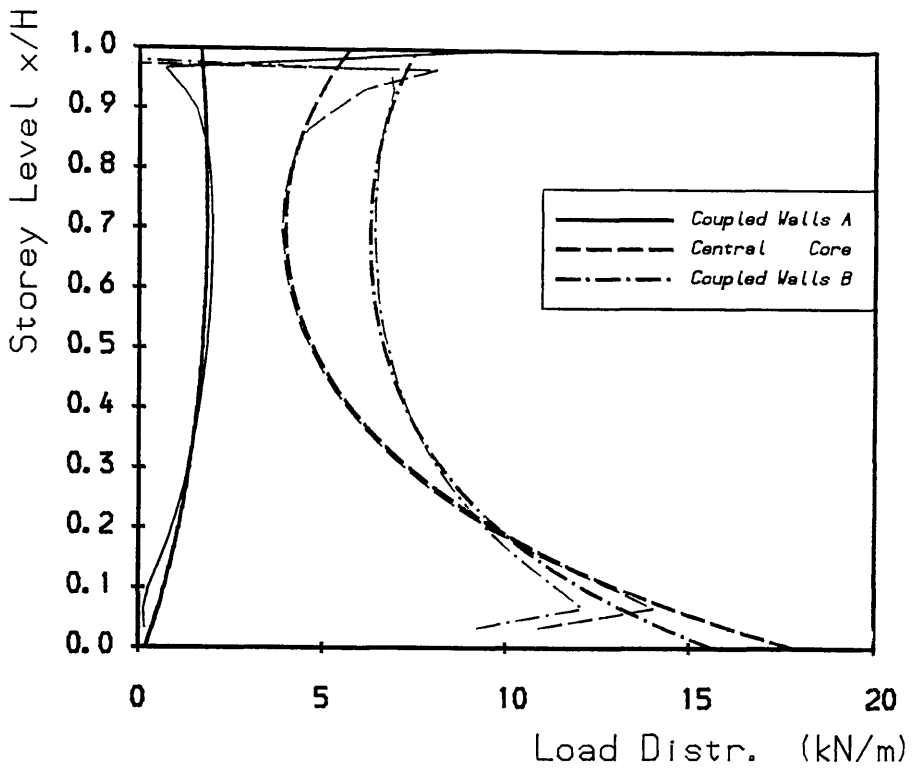
Asymmetric Structure Example 2
Fig. 5.22a Load Position 5. Deflections



Load Position 5

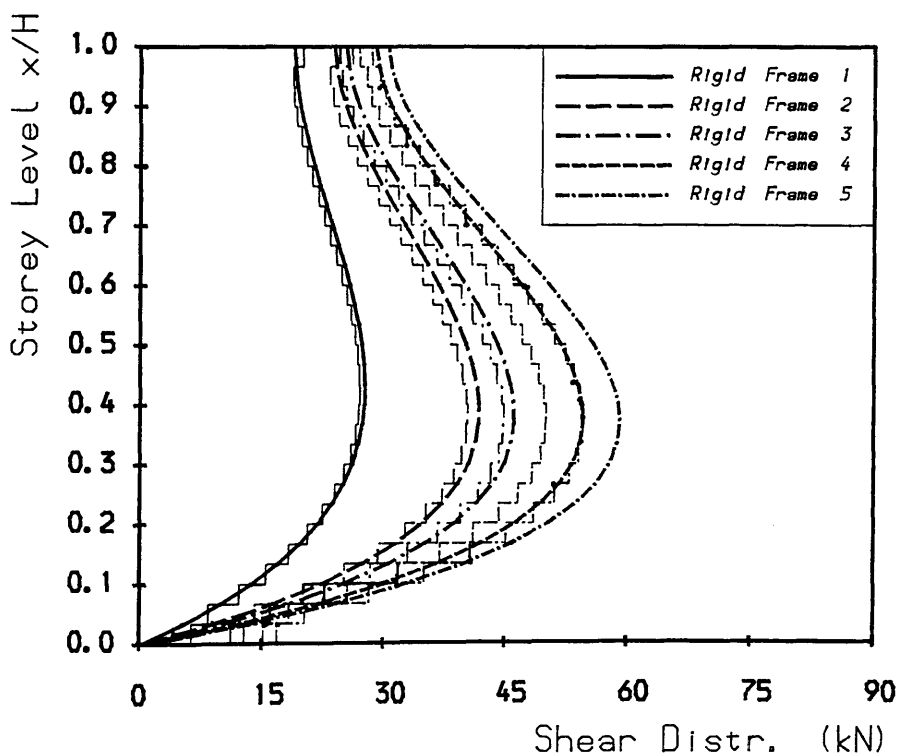
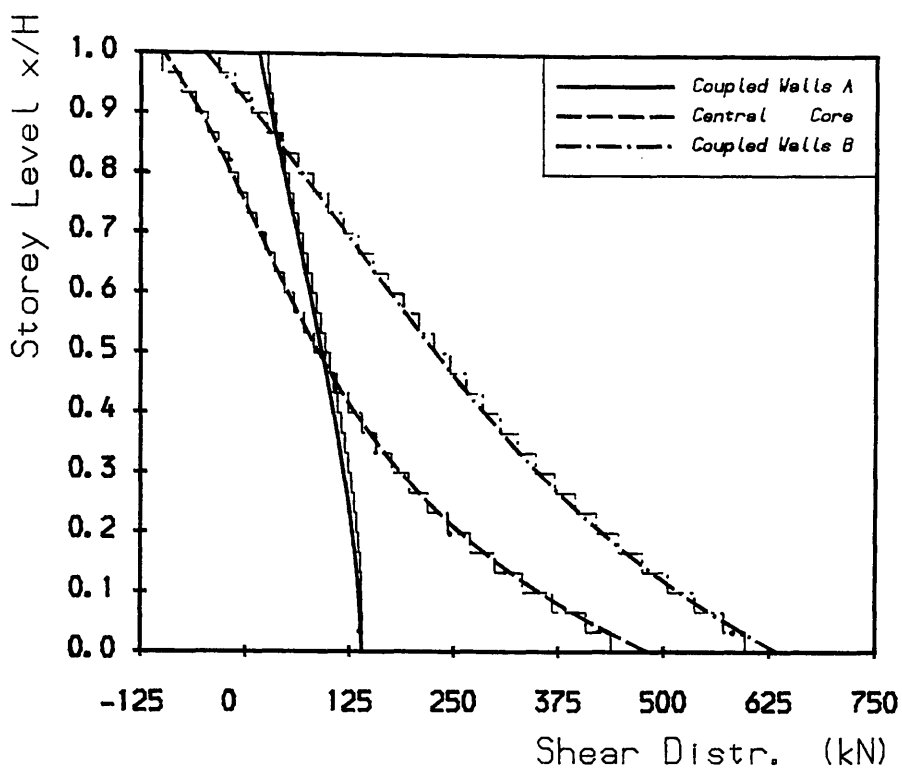


Asymmetric Structure Example 2
Fig. 5.22a Load Position 5. Deflections



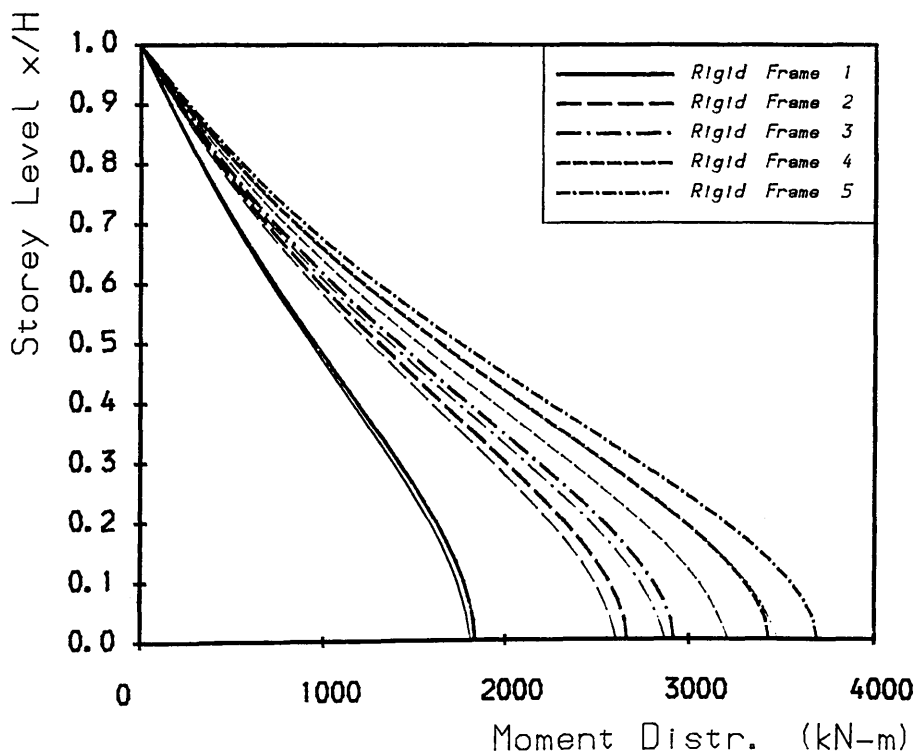
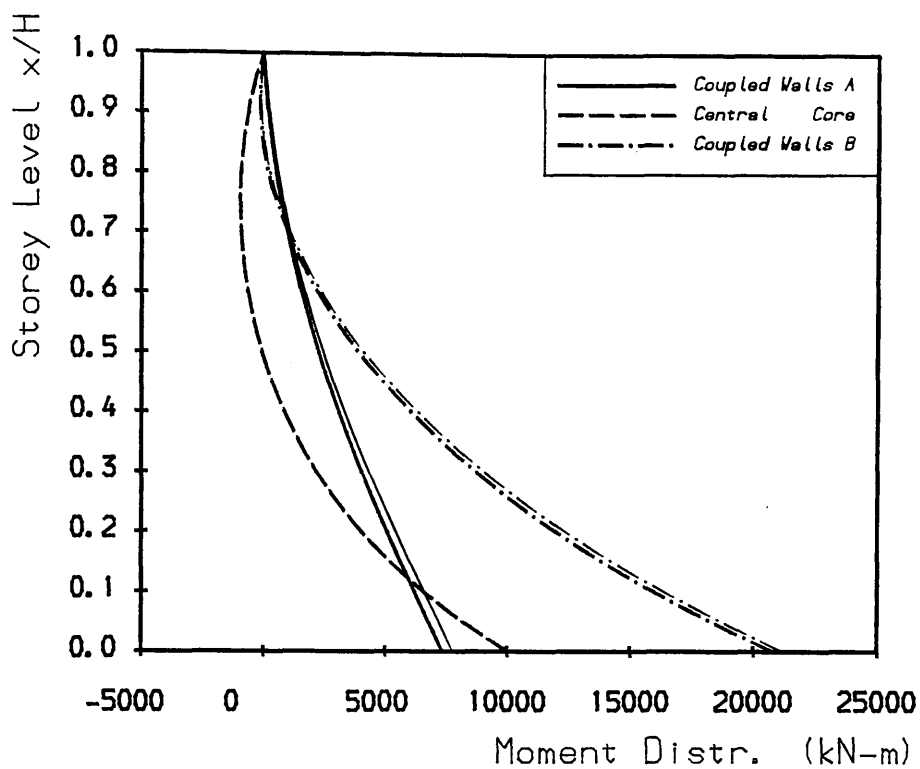
Asymmetric Structure Example 2

Fig. 5.22b Load Position 5. Load Distributions



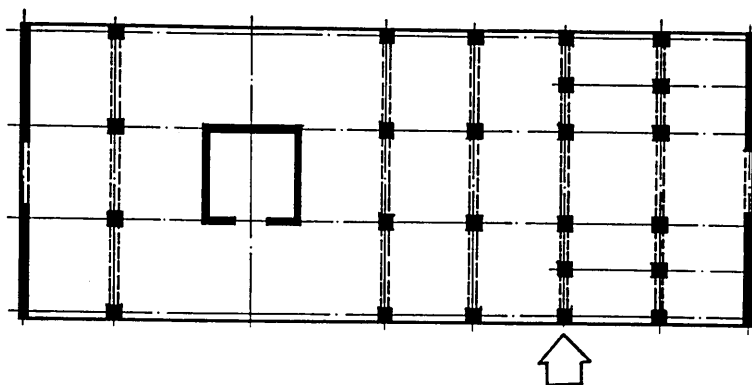
Asymmetric Structure Example 2

Fig. 5.22c Load Position 5, Shear Distributions

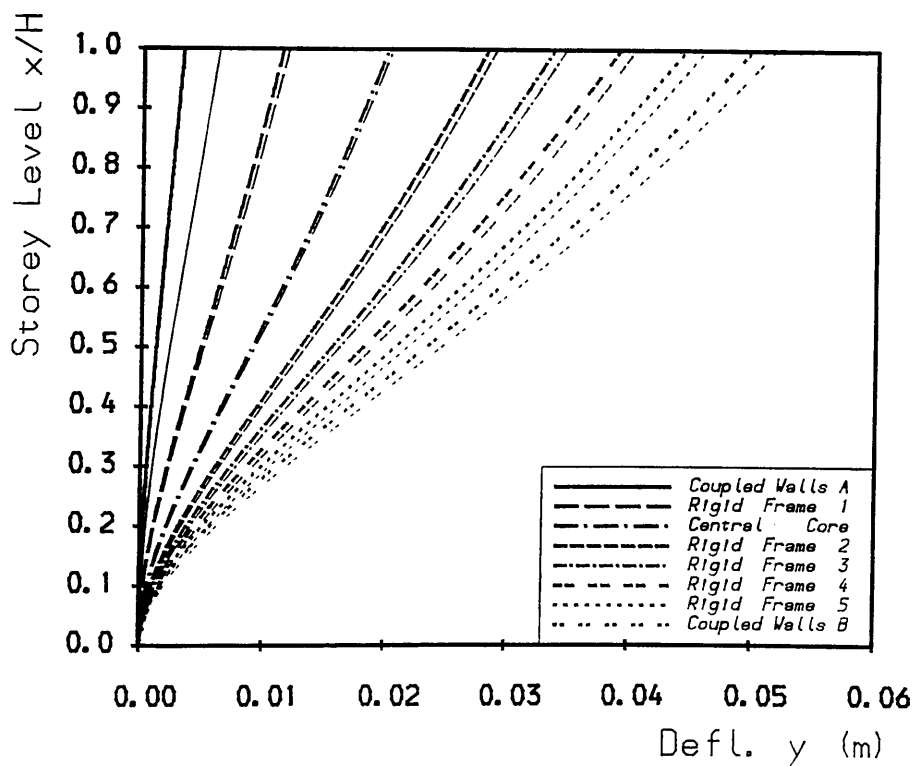


Asymmetric Structure Example 2

Fig. 5.22d Load Position 5, Moment Distributions

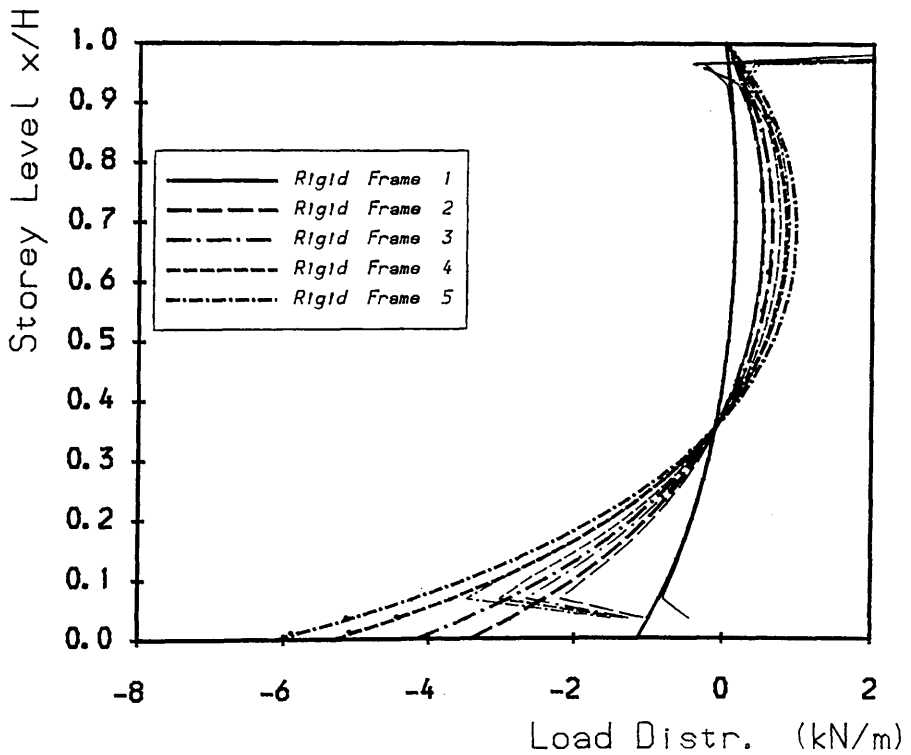
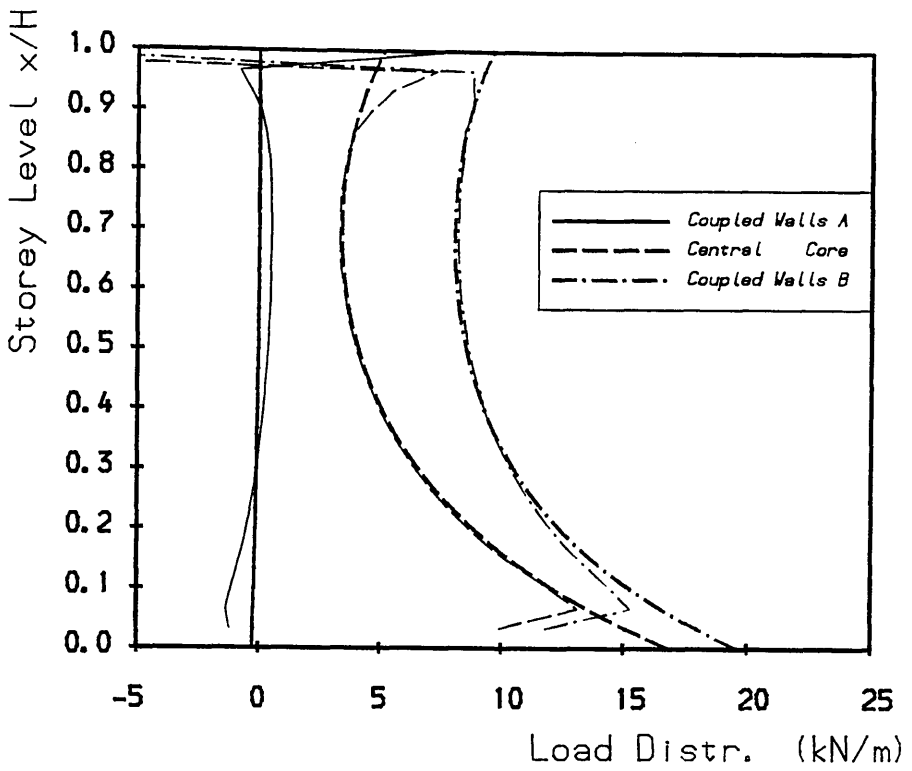


Load Position 6



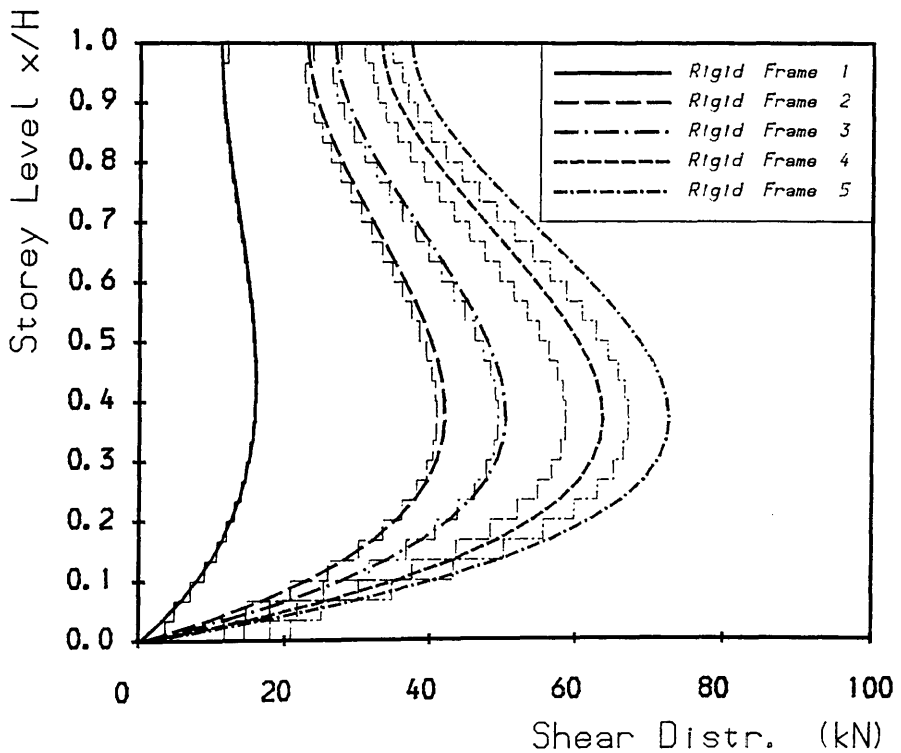
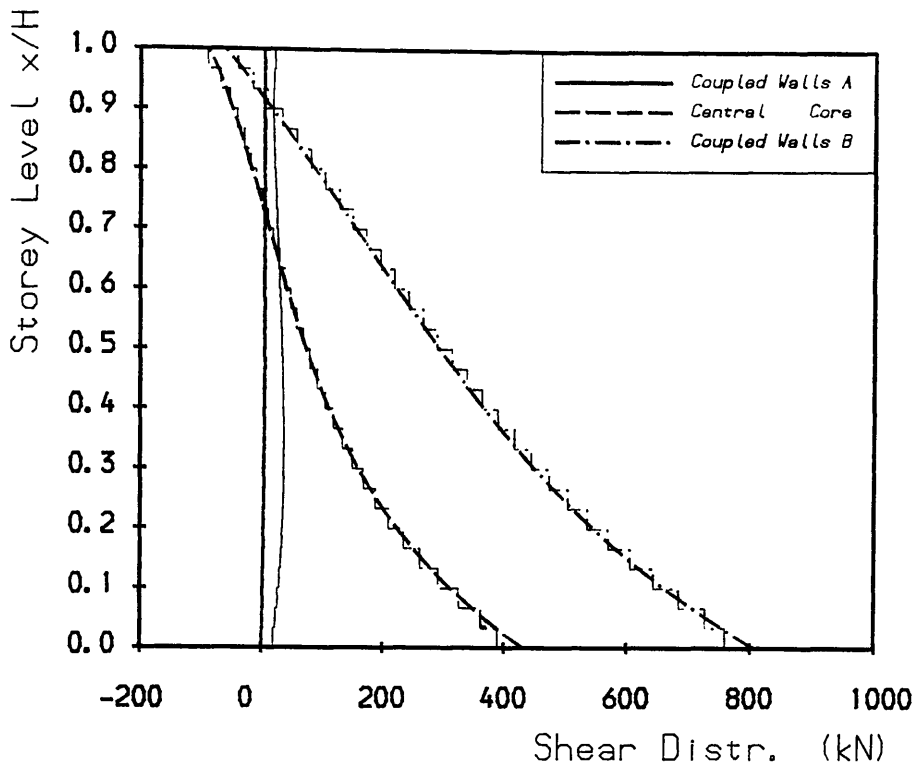
Asymmetric Structure Example 2

Fig. 5.23a Load Position 6. Deflections



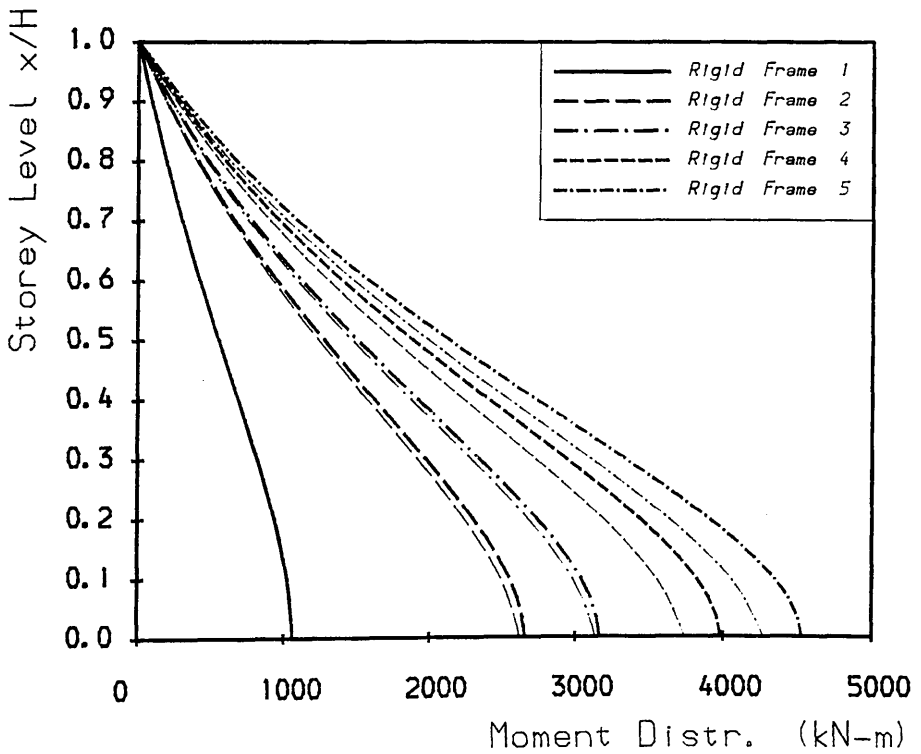
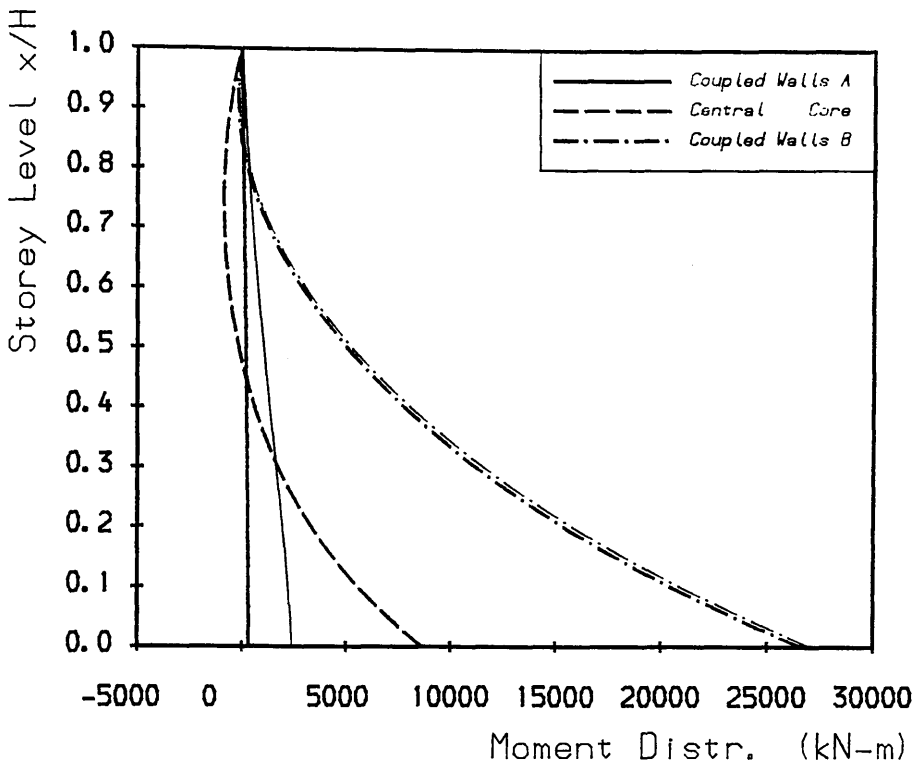
Asymmetric Structure Example 2

Fig. 5.23b Load Position 6. Load Distributions



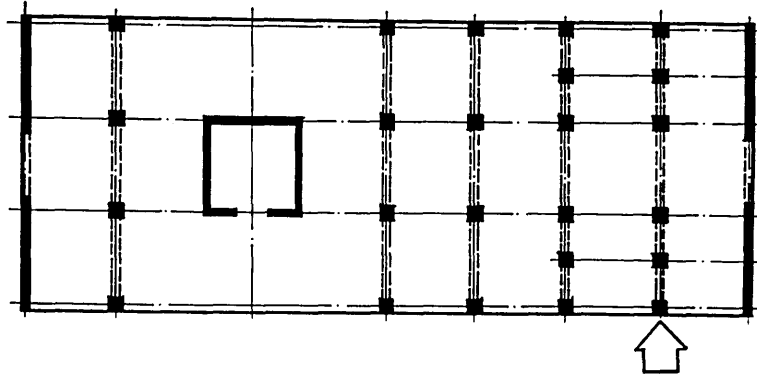
Asymmetric Structure Example 2

Fig. 5.23c Load Position 6, Shear Distributions

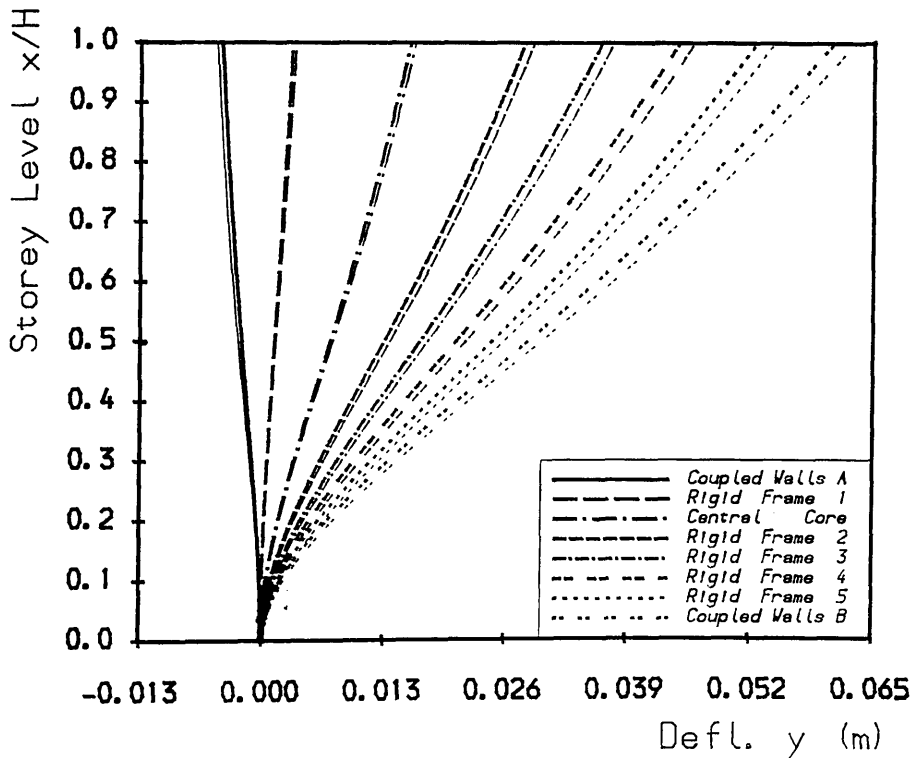


Asymmetric Structure Example 2

Fig. 5.23d Load Position 6, Moment Distributions

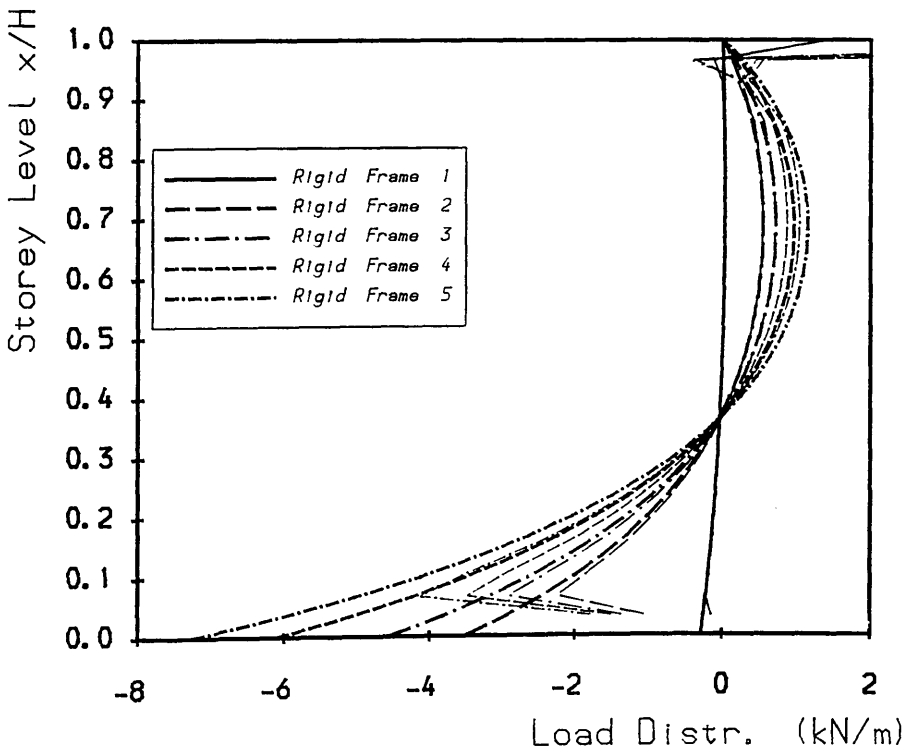
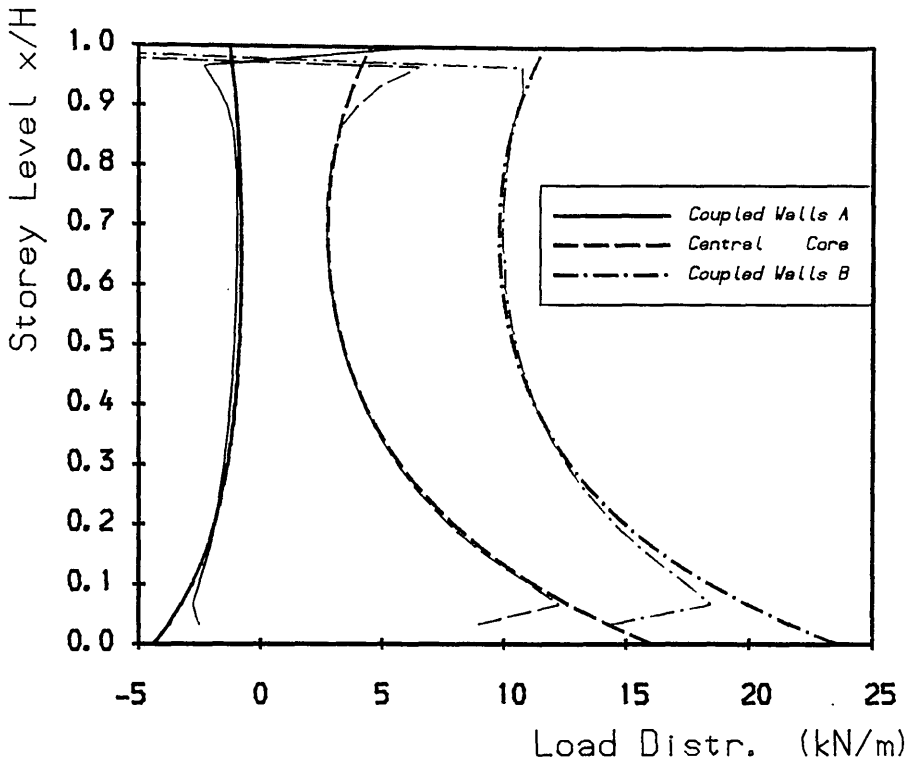


Load Position 7



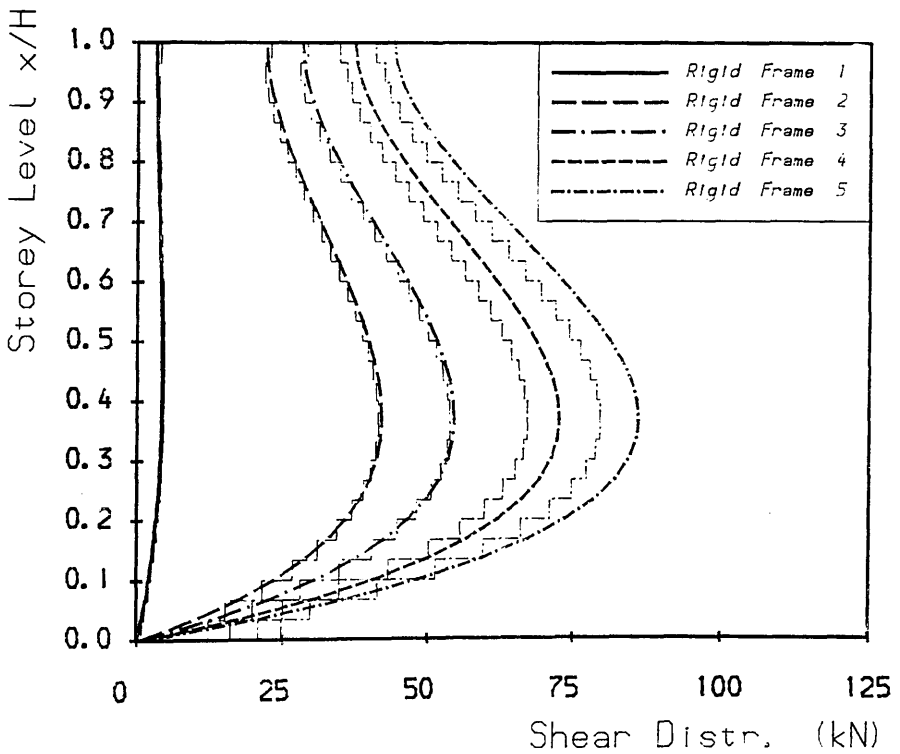
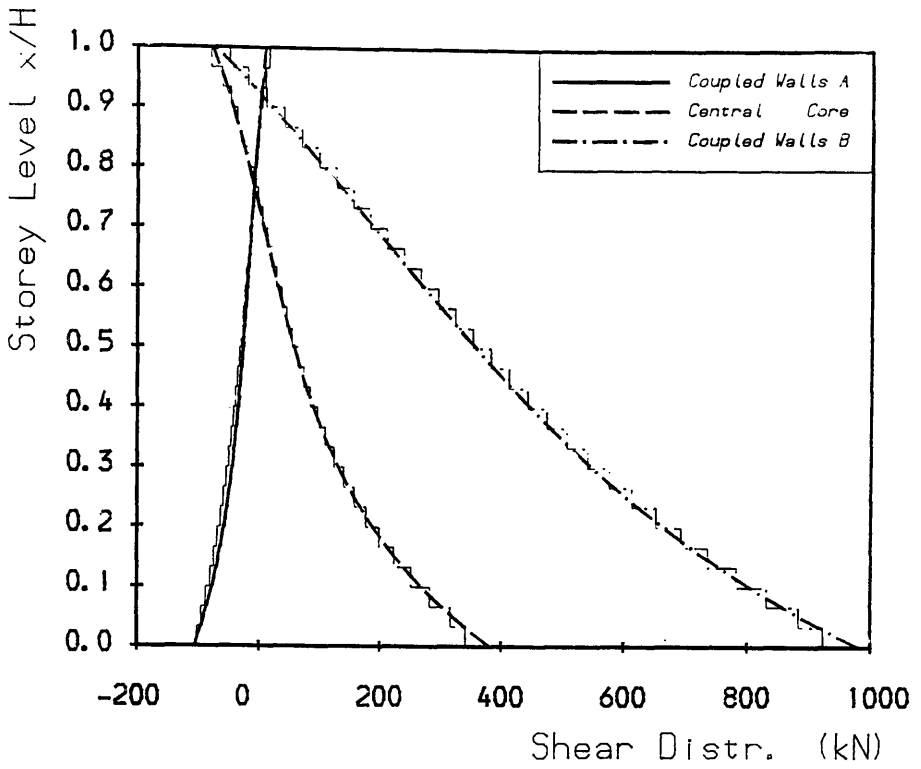
Asymmetric Structure Example 2

Fig. 5.24a Load Position 7. Deflections



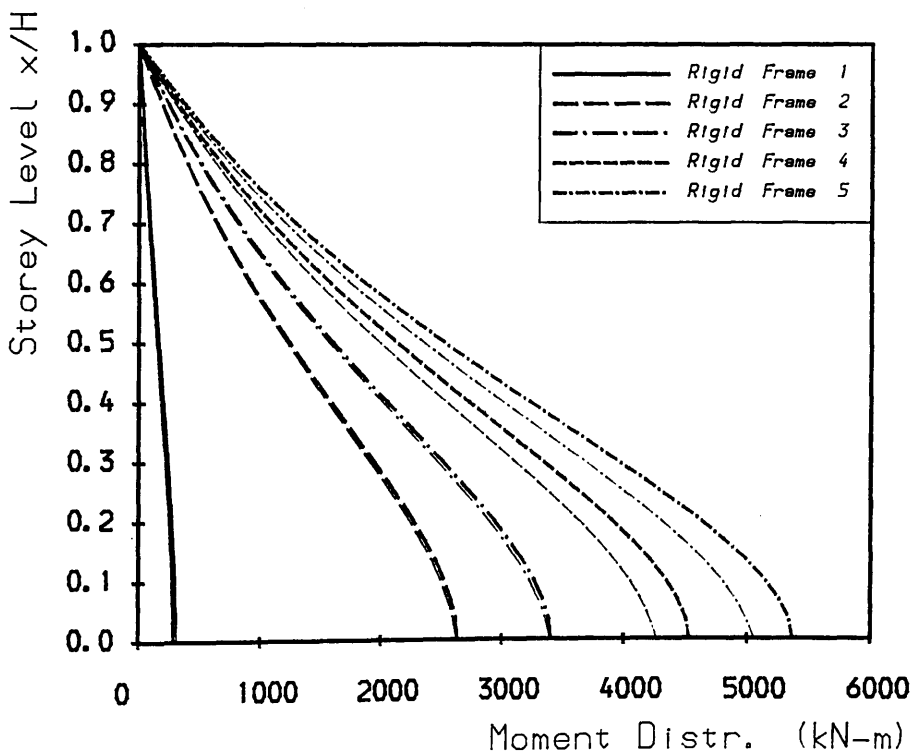
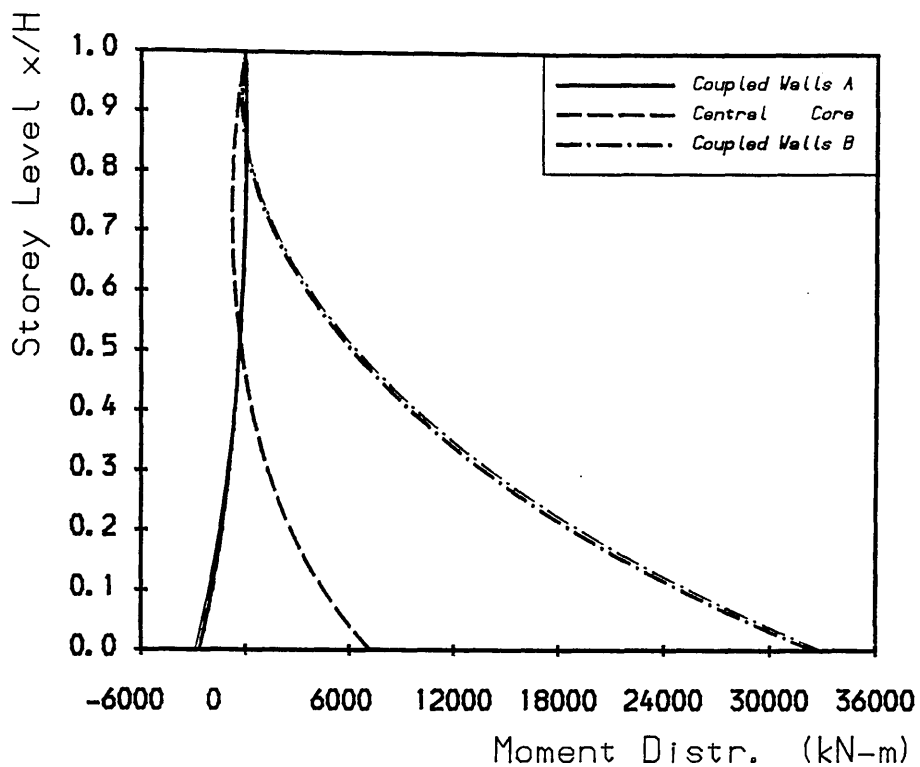
Asymmetric Structure Example 2

Fig. 5.24b Load Position 7. Load Distributions



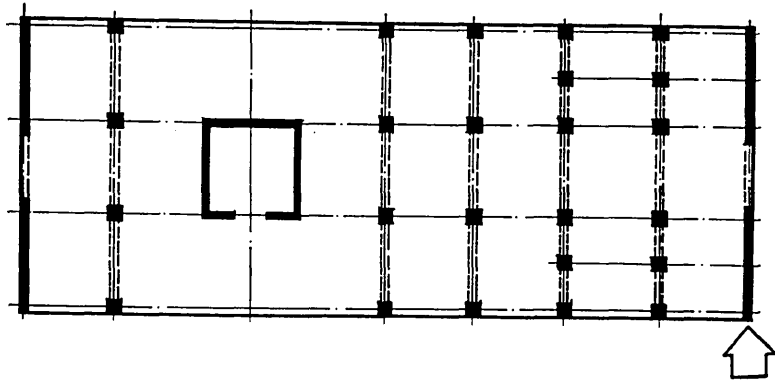
Asymmetric Structure Example 2

Fig. 5.24c Load Position 7, Shear Distributions

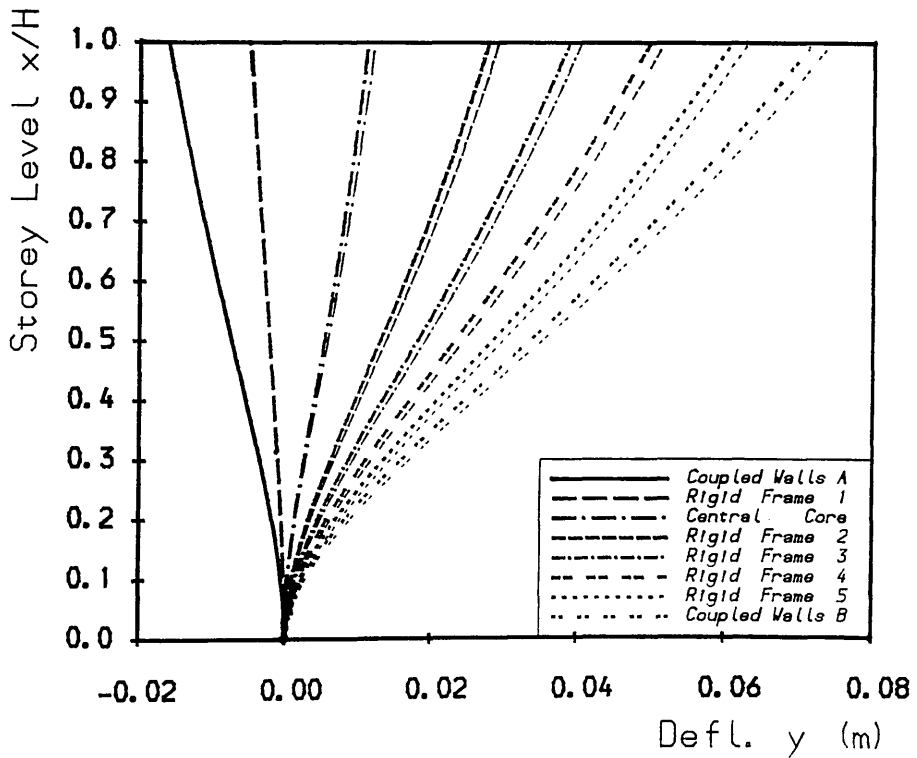


Asymmetric Structure Example 2

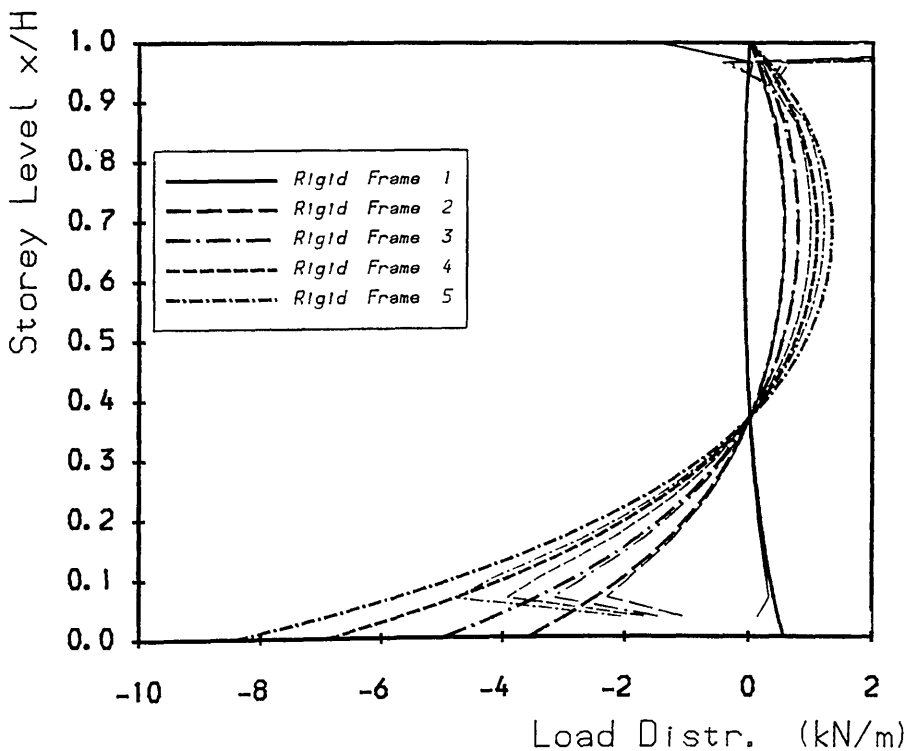
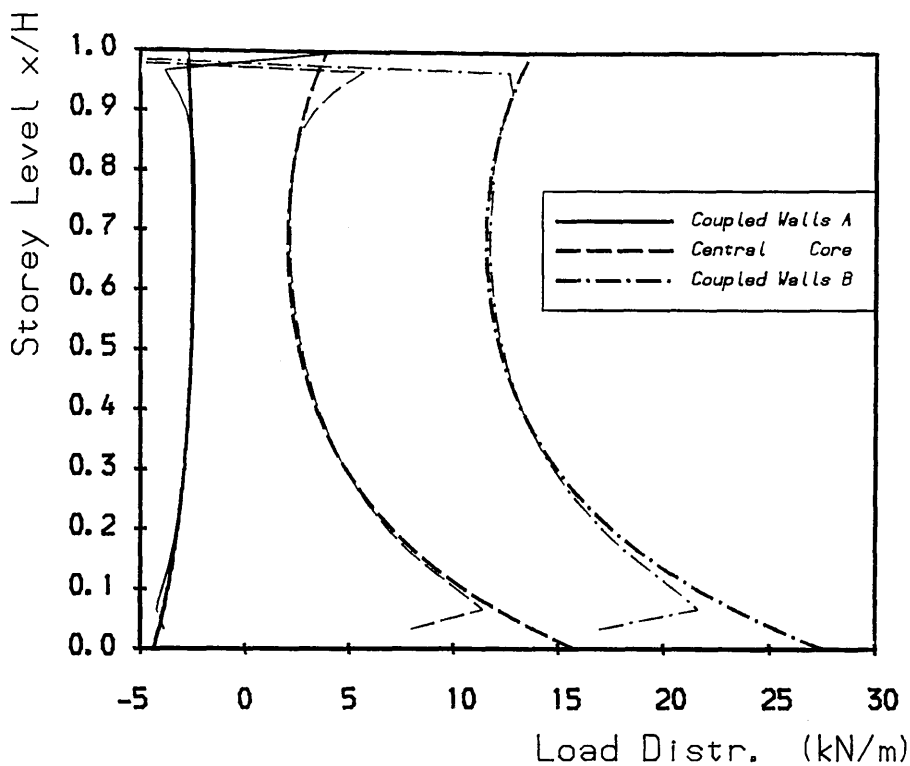
Fig. 5.24d Load Position 7, Moment Distributions



Load Position 8

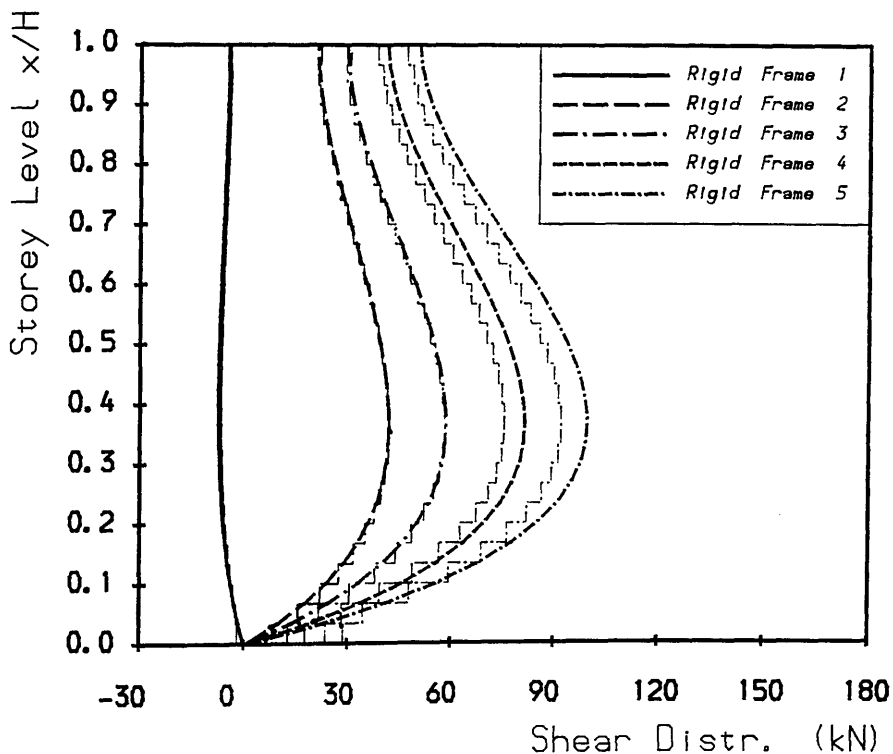
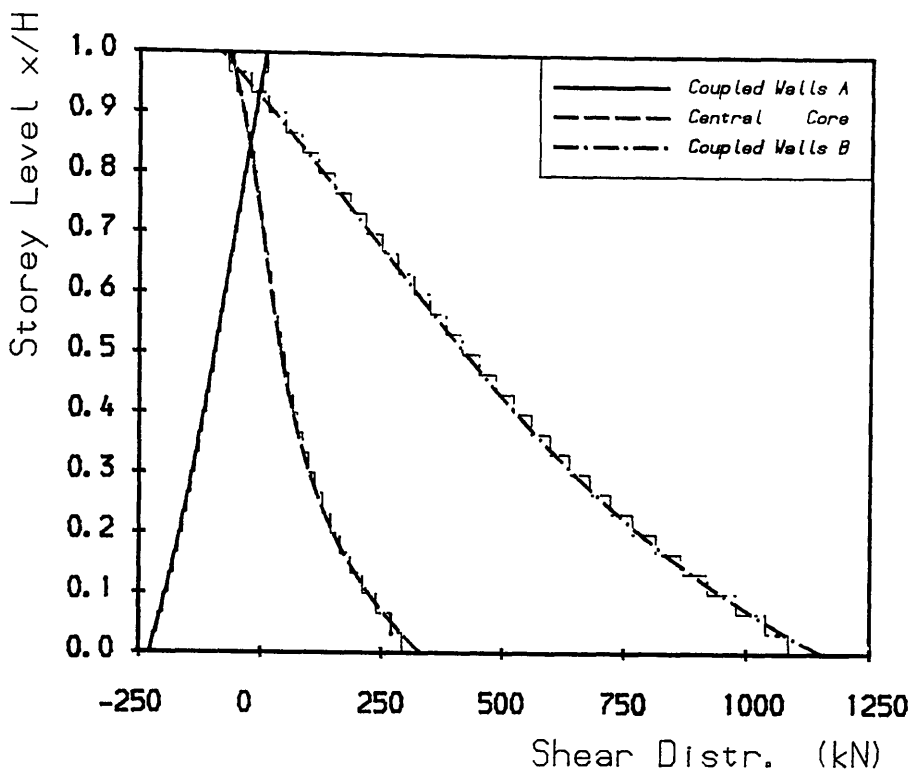


Asymmetric Structure Example 2
Fig. 5.25a Load Position 8. Deflections



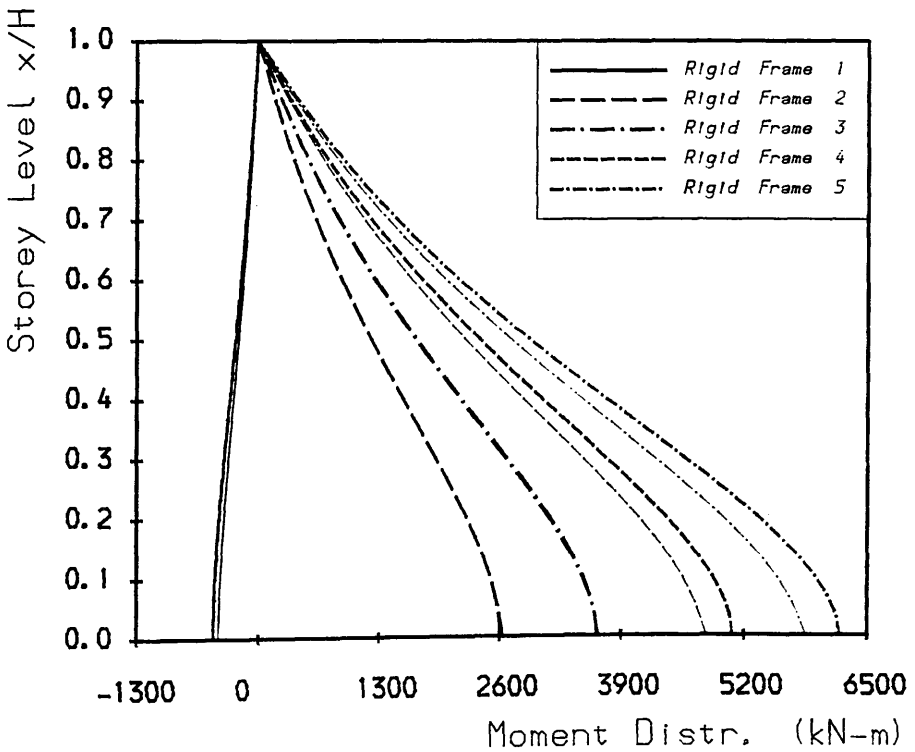
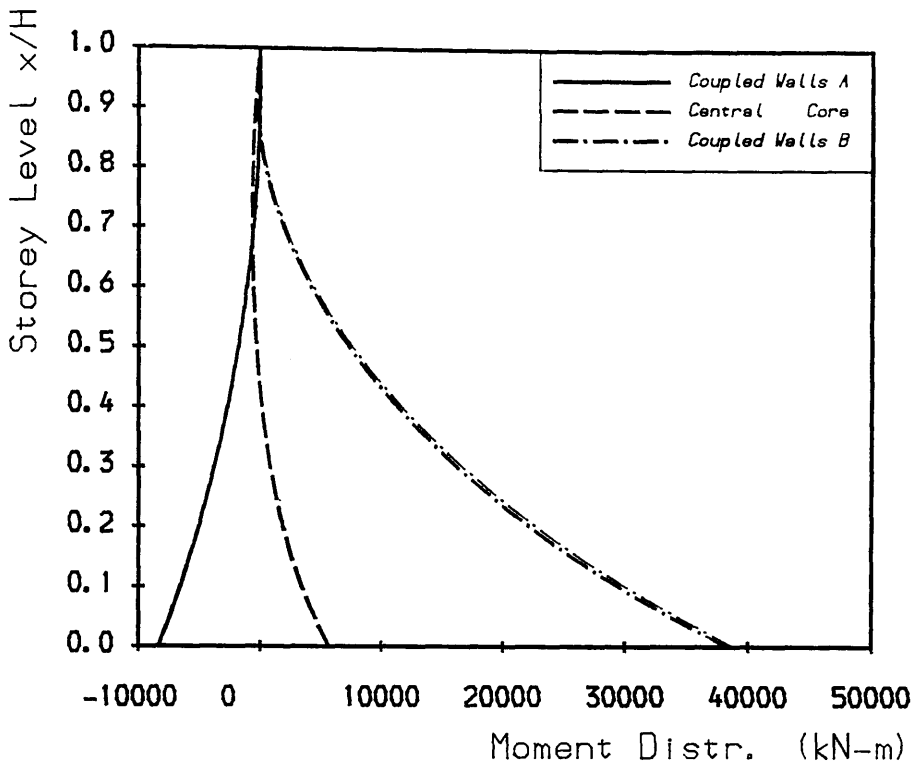
Asymmetric Structure Example 2

Fig. 5.25b Load Position 8. Load Distributions



Asymmetric Structure Example 2

Fig. 5.25c Load Position 8, Shear Distributions



Asymmetric Structure Example 2

Fig. 5.25d Load Position 8, Moment Distributions

CHAPTER 6
AREA INFLUENCE COEFFICIENT ANALYSIS
OF THREE-DIMENSIONAL WALL-FRAME STRUCTURES

6.1 Introduction

This chapter presents a simplified method, based on an 'area influence coefficient' approach, for the analysis of the distribution of lateral loads between the members of a three-dimensional tall building structure consisting of parallel assemblies of cores, shear walls, coupled shear walls and rigid frames.

The load distribution on each assembly is assumed to be represented sufficiently accurately by a combination of a uniformly and a triangularly distributed loading together with a horizontal top concentrated force. The latter is essential for representing the heavy concentrated interactions which occur at the tops of such structures, and is crucial to achieving accurate solutions with simple load distributions. The deflections of each assembly due to unit values of the three separate load components are then derived using the continuum technique presented in the previous chapters, and the horizontal compatibility conditions achieved by means of equating the top deflection, the area under the deflection diagram, and the first moment of area about the base of the deflection diagram for each assembly. Used in conjunction with the overall equations of horizontal force equilibrium, sufficient equations are obtained to solve for the amplitudes of the three load components acting on each assembly. The maximum size of matrix which has to be inverted in the solution is of the third order, so that hand calculations are possible even on a simple calculator, or by using simple programming on small PC computers. The forces in the members of the individual assemblies then follow.

6.2 Basic Assumptions

1. The structure considered consists of parallel assemblies which include almost all types of high-rise bents, such as:

(a) Flexural cantilever, characterized by its flexural rigidity EI , including plane shear walls and cores which do not involve coupling actions when laterally loaded. Such cantilevers and their modes of load-deformation behaviour were described in Section 2.2.1.

(b) Wall-frame assemblies, characterized by three distinct structural rigidity parameters EI , GA and EI_f , representing three primary modes of load-deformation behaviour, including coupled shear walls, interacting wall-frame assemblies, rigid and braced frames. Such cantilevers and their modes of deflection were described in Chapter 4.

Other types of assemblies may also be considered, provided their modes of lateral load-resisting deflection are known.

2. The structure is considered to be uniform with all the members having constant properties throughout their height.

3. The floor slabs connecting the assemblies at every storey level are considered to have such large in-plane stiffnesses that they are assumed to be rigid in their own plane. It follows that all the assemblies undergo a rigid body movement at every floor level, and hence the deflections of all the assemblies are related to each other by a linear relationship (Figs 6.1a and 6.1b). In particular, if the structure is symmetric in plan, subjected to a resultant lateral load at the centre, all the assemblies will then have identical deflections.

6.3 General Method of Analysis

As discussed in previous chapters, for a structure consisting of different types of assemblies, subjected to lateral loads, considerable load redistribution takes place among these assemblies when they are constrained to act together by the in-plane rigid floor slabs. In a previous method presented by Coull and Mohammed (Ref. 21), the load distribution on each assembly was assumed to be represented by a polynomial in the height coordinate, together with a concentrated force at the top. The continuous connection technique was used to derive the deflected form of an individual assembly, enabling a set of flexibility influence coefficients to be obtained, relating any given load term to the deflection at any level. By making use of the equilibrium and compatibility equations at any desired number of reference levels, the load distribution on each assembly could then be determined.

The proposed method assumes that the load distribution on each assembly (i) may be represented sufficiently accurately by a combination of the first two terms of the polynomial series, that is, a uniformly distributed load of intensity w_i and a triangularly distributed load of maximum intensity q_i at the top, together with a concentrated horizontal load P_i at the top (Fig. 6.2a). Instead of choosing any arbitrary reference levels as the previous method did, the present method uses the top deflection Y_i , the area A_i and the first moment of area \bar{A}_i , of the deflected diagram (Fig. 6.2b) to maintain the conditions of horizontal displacement compatibility. By using conditions of horizontal equilibrium, sufficient equations may be derived to determine the unknown coefficients of the three load components for each assembly. The use of the deflected curve area and the first moment of the curve area as the flexibility influence coefficients represents an effort to take into account the average deflection and shape of each

individual deflection diagram for the different assemblies, and thus to achieve reasonable results from the simple load distributions assumed. Since the deflection profiles for the individual assemblies are smooth curves, it is intuitively expected that the use of these three compatibility conditions will force the deflections of the assemblies in the complete structure to have very similar configurations.

On applying the method, in order to achieve the required force equilibrium conditions, only three lateral applied load cases according to the presumed components of load distributions on each assembly i can be considered, which are, a uniformly distributed lateral load of intensity w_0 , a triangularly distributed load with maximum intensity q_0 at the top, and a concentrated horizontal load P_0 at the top. For the complete three-dimensional structural analysis which involves both bending and twisting actions, the torsional-resisting actions of individual assemblies may be considered by assuming that the torsional load distributions on each assembly i can also be represented by three components of torsional load, which are, a uniformly distributed torque of intensity t_i , a triangularly distributed torque of maximum intensity r_i at the top, and a concentrated torque T_i at the top. The three standard applied torque cases which may be considered in the analysis thus are those of a uniformly distributed torque of intensity t_0 , a triangularly distributed torque of maximum intensity r_0 at the top, and a concentrated torque of T_0 at the top. These three applied lateral loads and three torsional loads, with their combinations, cover most of the applied lateral load cases in practical structural design, such as wind loading and earthquakes. In a structure which consists of parallel assemblies, however, the torsional stiffnesses of individual assemblies such as shear walls and planar rigid frames are of minor significance when compared with the overall torsional stiffness of the structure which derives primarily from the shearing stiffnesses of the different assemblies. Only cores contribute to substantial torsional stiffnesses in

the structure and have to be taken into consideration. Since the torsion–twisting relationships for individual cores are not included in this thesis, the torsional stiffnesses of individual assemblies and their torsional reactions are not considered in numerical studies and in the associated 'FLASH' analyses.

The detailed method of analysis is presented in the following three sections. First, as an introduction to the method, the analysis of the interactions between two linked components subjected to lateral loads is presented, and the area influence coefficients for individual assemblies are introduced, followed by an example to show the validity and accuracy of the method. Secondly, the method is presented for the analysis of symmetric structures involving various flexural and wall–frame assemblies, subjected to pure bending actions. Finally, the method is extended to a complete three–dimensional structural analysis involving both bending and torsional actions.

6.4 Analysis of Interaction Between Two Linked Components

6.4.1 Method of Analysis

In order to interpret the method and introduce the idea of area influence coefficients for different types of assemblies, consider first the simple case in which the structure consists of two linked assemblies, subjected to a uniformly distributed lateral load of intensity w_0 , as shown in Fig. 6.3a. It is assumed that the interactive axial forces in the links are represented by three components: a uniformly distributed force flow of intensity n_1 , a triangularly distributed force flow of maximum intensity n_2 at the top, and a concentrated horizontal force Q at the top, as shown in Fig. 6.3b. On using the conditions of horizontal force equilibrium, the distributions of load, which consist of three load components on

each of the assemblies, become, referring to Fig. 6.3c,

For the first assembly,

$$w_1 = w_0 - n_1, \quad q_1 = -n_2 \quad \text{and} \quad P_1 = -Q \quad (6.1)$$

And for the second assembly,

$$w_2 = n_1, \quad q_2 = n_2 \quad \text{and} \quad P_2 = Q \quad (6.2)$$

Under the action of the three load components from Eqs. 6.1 and 6.2, the resulting deflections of the two assemblies will be given as,

$$y_1 = w_1 y_{w1} + q_1 y_{q1} + P_1 y_{P1} \quad (6.3)$$

$$y_2 = w_2 y_{w2} + q_2 y_{q2} + P_2 y_{P2} \quad (6.4)$$

or,

$$y_i = w_i y_{wi} + q_i y_{qi} + P_i y_{Pi} \quad (i = 1, 2) \quad (6.5)$$

in which y_{wi} , y_{qi} and y_{Pi} are the three deflection components of assembly i ($i = 1, 2$), resulting respectively from the three unit load components (Fig. 6.4). The subscripts w , q and P refer to the unit uniformly and triangularly distributed lateral loads, and a unit top horizontal point load, respectively.

Having given the expressions for the deflections for each assembly i from Eqs. 6.5, the top deflections, the areas under the deflection curves and the first moments of curve areas are consequently given by,

$$Y_i = w_i Y_{wi} + q_i Y_{qi} + P_i Y_{Pi} \quad (i = 1, 2) \quad (6.6)$$

$$A_i = w_i A_{wi} + q_i A_{qi} + P_i A_{Pi} \quad (6.7)$$

$$\bar{A}_i = w_i \bar{A}_{wi} + q_i \bar{A}_{qi} + P_i \bar{A}_{Pi} \quad (6.8)$$

in which Y_{wi} , Y_{qi} and Y_{Pi} are the top deflections of assembly i ($i = 1, 2$), A_{wi} , A_{qi} and A_{Pi} are the areas under the deflected curves, and \bar{A}_{wi} , \bar{A}_{qi} and \bar{A}_{Pi} are the first moments of the deflected curve areas about the base (Fig. 6.4), all due to three unit load cases, respectively.

It is now assumed that the top deflections, the areas under the deflected curves and the first moments of the area curves of the two assemblies (Fig. 6.3c) are all equal. That is,

$$Y_1 = Y_2, \quad A_1 = A_2, \quad \text{and,} \quad \bar{A}_1 = \bar{A}_2 \quad (6.9)$$

From Eqs. 6.6 to 6.8, using Eq. 6.9, three equations are then obtained as,

$$w_1 Y_{w1} + q_1 Y_{q1} + P_1 Y_{P1} = w_2 Y_{w2} + q_2 Y_{q2} + P_2 Y_{P2} \quad (6.10)$$

$$w_1 A_{w1} + q_1 A_{q1} + P_1 A_{P1} = w_2 A_{w2} + q_2 A_{q2} + P_2 A_{P2} \quad (6.11)$$

$$w_1 \bar{A}_{w1} + q_1 \bar{A}_{q1} + P_1 \bar{A}_{P1} = w_2 \bar{A}_{w2} + q_2 \bar{A}_{q2} + P_2 \bar{A}_{P2} \quad (6.12)$$

From the conditions of horizontal force equilibrium, three other equations can be obtained (Eqs. 6.1 and 6.2) as,

$$w_1 + w_2 = w_0, \quad q_1 + q_2 = 0, \quad \text{and,} \quad P_1 + P_2 = 0 \quad (6.13)$$

On solving the six equations (Eqs. 6.10 to 6.13), the distributions of load on the two assemblies can be determined. These give the load components for which the two assemblies will deflect in similar configurations, by having the same top deflections, the same areas under the deflected curves, and the same first moments of the curve areas.

Having determined the distributions of load on each assembly, the shears and moments in the assembly i can be obtained as,

$$S_i = w_i H(1 - \xi) + \frac{q_i H}{2}(1 - \xi^2) + P_i \quad (i = 1, 2) \quad (6.14)$$

$$M_i = \frac{w_i H^2}{2}(1 - \xi)^2 + \frac{q_i H^2}{6}(2 - 3\xi + \xi^3) + P_i H(1 - \xi) \quad (6.15)$$

in which S_i and M_i are the shear and the moment in assembly i , resulting from the three load components, $\xi = x/H$ is the non-dimensional height coordinate measured from the base, and H is the total height of the structure.

6.4.2 Area Influence Coefficients For Individual Assemblies

Equations 6.6 to 6.8 can be written in matrix form as,

$$\begin{Bmatrix} Y_i \\ A_i \\ \bar{A}_i \end{Bmatrix} = \begin{bmatrix} Y_{wi} & Y_{qi} & Y_{pi} \\ A_{wi} & A_{qi} & A_{pi} \\ \bar{A}_{wi} & \bar{A}_{qi} & \bar{A}_{pi} \end{bmatrix} \begin{Bmatrix} w_i \\ q_i \\ P_i \end{Bmatrix} \quad (6.16)$$

or,

$$V_i = A_i F_i \quad (6.17)$$

in which V_i is a column vector consisting of the top deflection Y_i , the area under the deflected curve A_i , and the first moment of the curve area \bar{A}_i , for assembly i , F_i is a column vector of the load distribution coefficients for the assembly, and A_i is defined as the area influence coefficients in a square matrix form consisting of the top deflections, the areas under the deflected curves, and the first moments of the curve areas, for assembly i due to three unit load components, respectively, given by,

$$A_i = \begin{bmatrix} Y_{wi} & Y_{qi} & Y_{pi} \\ A_{wi} & A_{qi} & A_{pi} \\ \bar{A}_{wi} & \bar{A}_{qi} & \bar{A}_{pi} \end{bmatrix} \quad (6.18)$$

By making use of the continuum technique presented in the previous chapters, the expressions for the deflection for different types of individual cantilever assemblies, subjected to the three standard lateral load cases, and thus their area influence coefficients are as follows:

1. Flexural cantilevers of flexural rigidity EI :

Expressions for the deflections,

$$y_w = \frac{w_0 H^4}{24EI} (\xi^4 - 4\xi^3 + 6\xi^2) \quad (6.19)$$

$$y_q = \frac{q_0 H^4}{120EI} (\xi^5 - 10\xi^3 + 20\xi^2) \quad (6.20)$$

$$y_P = \frac{P_0 H^3}{6EI} (3\xi^2 - \xi^3) \quad (6.21)$$

The expressions for the area influence coefficients for the flexural cantilevers are then, with the three loads, w_0 , q_0 and P_0 having unit values,

Top deflections,

$$Y_w = \frac{w_0 H^4}{8EI}, \quad Y_q = \frac{11q_0 H^4}{120EI} \quad \text{and} \quad Y_P = \frac{P_0 H^4}{3EI} \quad (6.22)$$

Areas under deflected curves,

$$A_w = \frac{w_0 H^5}{20EI}, \quad A_q = \frac{13q_0 H^5}{360EI} \quad \text{and} \quad A_P = \frac{P_0 H^4}{8EI} \quad (6.23)$$

First moments of deflected curve areas,

$$\bar{A}_w = \frac{13w_0 H^6}{360EI}, \quad \bar{A}_q = \frac{11q_0 H^5}{420EI} \quad \text{and} \quad \bar{A}_P = \frac{11P_0 H^5}{120EI} \quad (6.24)$$

2. Wall-frame assemblies:

Wall-frame assemblies are those cantilevers involving three structural rigidities, EI , GA and EI_f as discussed in Chapter 4. The deflection equations are expressed in terms of the two structural parameters k and $k\alpha H$ which have been defined by Eqs. 4.16 and 4.17. The following equations are the expressions

for the deflection for such wall-frame assemblies, due to the three standard load components w_0 , q_0 and P_0 :

$$y_w = \frac{w_0 H^4}{EI} \left\{ \frac{k^2-1}{24k^2} (\xi^4 - 4\xi^3 + 6\xi^2) + \frac{1}{k^2(k\alpha H)^2} \left(\xi - \frac{\xi^2}{2} \right) + \frac{\cosh k\alpha H \xi + k\alpha H \sinh k\alpha H (1-\xi) - k\alpha H \sinh k\alpha H - 1}{k^2 (k\alpha H)^4 \cosh k\alpha H} \right\} \quad (6.25)$$

$$y_q = \frac{q_0 H^4}{EI} \left\{ \frac{k^2-1}{120k^2} (\xi^5 - 10\xi^3 + 20\xi^2) + \frac{1}{2k^2(k\alpha H)^2} \left(\xi - \frac{\xi^3}{3} \right) + \frac{\cosh k\alpha H \xi + (k\alpha H/2 - 1/k\alpha H) [\sinh k\alpha H (1-\xi) - \sinh k\alpha H] - \xi \cosh k\alpha H - 1}{k^2 (k\alpha H)^4 \cosh k\alpha H} \right\} \quad (6.26)$$

$$y_P = \frac{P_0 H^3}{EI} \left\{ \frac{k^2-1}{6k^2} (3\xi^2 - \xi^3) + \frac{\xi}{k^2(k\alpha H)^2} - \frac{\sinh k\alpha H - \sinh k\alpha H (1-\xi)}{k^2 (k\alpha H)^3 \cosh k\alpha H} \right\} \quad (6.27)$$

The expressions for the area influence coefficients for wall-frame assemblies are then, with the three loads w_0 , q_0 and P_0 having unit values:

Top deflections,

$$Y_w = \frac{w_0 H^4}{EI} \left\{ \frac{k^2-1}{8k^2} + \frac{1}{2k^2(k\alpha H)^2} + \frac{\cosh k\alpha H - k\alpha H \sinh k\alpha H - 1}{k^2 (k\alpha H)^4 \cosh k\alpha H} \right\} \quad (6.28)$$

$$Y_q = \frac{q_0 H^4}{EI} \left\{ \frac{11(k^2-1)}{120k^2} + \frac{1}{3k^2(k\alpha H)^2} - \frac{(k\alpha H/2 - 1/k\alpha H) \sinh k\alpha H + 1}{k^2 (k\alpha H)^4 \cosh k\alpha H} \right\} \quad (6.29)$$

$$Y_P = \frac{P_0 H^3}{EI} \left\{ \frac{k^2-1}{3k^2} + \frac{1}{k^2(k\alpha H)^2} - \frac{\sinh k\alpha H}{k^2 (k\alpha H)^3 \cosh k\alpha H} \right\} \quad (6.30)$$

Areas under deflected curves,

$$A_w = \frac{w_0 H^5}{EI} \left\{ \frac{k^2-1}{20k^2} + \frac{1}{3k^2(k\alpha H)^2} + \frac{k\alpha H(\cosh k\alpha H - 2) - [(k\alpha H)^2 - 1] \sinh k\alpha H}{k^2 (k\alpha H)^5 \cosh k\alpha H} \right\} \quad (6.31)$$

$$A_q = \frac{q_0 H^5}{EI} \left\{ \frac{13(k^2-1)}{360k^2} + \frac{5}{24k^2(k\alpha H)^2} - \frac{1}{k^2(k\alpha H)^6} + \frac{\sinh k\alpha H - (k\alpha H/2-1/k\alpha H)(k\alpha H \sinh k\alpha H + 1) - k\alpha H}{k^2(k\alpha H)^5 \cosh k\alpha H} \right\} \quad (6.32)$$

$$A_P = \frac{P_0 H^4}{EI} \left\{ \frac{k^2-1}{8k^2} + \frac{1}{2k^2(k\alpha H)^2} + \frac{\cosh k\alpha H - k\alpha H \sinh k\alpha H - 1}{k^2(k\alpha H)^4 \cosh k\alpha H} \right\} \quad (6.33)$$

First moments of deflected curve areas,

$$\bar{A}_w = \frac{w_0 H^6}{EI} \left\{ \frac{13(k^2-1)}{360k^2} + \frac{5}{24k^2(k\alpha H)^2} - \frac{1}{k^2(k\alpha H)^6} - \frac{[(k\alpha H)^2 - 4]k\alpha H \sinh k\alpha H + 3(k\alpha H)^2 - 2}{2k^2 (k\alpha H)^6 \cosh k\alpha H} \right\} \quad (6.34)$$

$$\bar{A}_q = \frac{q_0 H^6}{EI} \left\{ \frac{11(k^2-1)}{420k^2} + \frac{2}{15k^2(k\alpha H)^2} - \frac{(k\alpha H)^2 + 3}{3k^2(k\alpha H)^6} + \frac{4(k\alpha H/2-1/k\alpha H) \sinh k\alpha H - [(k\alpha H)^2-6]k\alpha H \sinh k\alpha H - 4(k\alpha H)^2 + 8}{4k^2(k\alpha H)^6 \cosh k\alpha H} \right\} \quad (6.35)$$

$$\bar{A}_P = \frac{P_0 H^5}{EI} \left\{ \frac{11(k^2-1)}{120k^2} + \frac{1}{3k^2(k\alpha H)^2} - \frac{[(k\alpha H)^2 - 2] \sinh k\alpha H + 2k\alpha H}{2k^2(k\alpha H)^5 \cosh k\alpha H} \right\} \quad (6.36)$$

6.4.3 Compatibility and Equilibrium Equations in Matrix Form

Using matrix notation, the compatibility conditions for the top deflections, the deflected curve areas, and the first moments of the curve areas (Eq. 6.9) can be written as,

$$V_1 - V_2 = 0 \quad (6.37)$$

or,

$$A_1 F_1 - A_2 F_2 = 0 \quad (6.38)$$

The horizontal force equilibrium equations from Eq. 6.13 can be written as,

$$\begin{bmatrix} 1 & 0 & 0 \\ 0 & 1 & 0 \\ 0 & 0 & 1 \end{bmatrix} \begin{Bmatrix} w_1 \\ q_1 \\ P_1 \end{Bmatrix} + \begin{bmatrix} 1 & 0 & 0 \\ 0 & 1 & 0 \\ 0 & 0 & 1 \end{bmatrix} \begin{Bmatrix} w_2 \\ q_2 \\ P_2 \end{Bmatrix} = \begin{Bmatrix} w_0 \\ q_0 \\ P_0 \end{Bmatrix} \quad (6.39)$$

or,

$$IF_1 + IF_2 = F_0 \quad (6.40)$$

in which I is the unit square matrix of the third order, and F_0 is the column vector representing the external lateral load case, given by,

$$F_0 = \{w_0 \ q_0 \ P_0\}^T \quad (6.41)$$

6.4.4 Numerical Example for the Interaction Between Two Linked Assemblies

An example of a 30-storey structure is shown in Fig. 6.5a, in which a pair of coupled shear walls interact, through the pin-ended links, with a lumped rigid frame consisting of 5 identical 5-span frames, subjected to a uniformly distributed lateral load of intensity, $w_0 = 10.0$ kN/m. This may be taken to represent half of a symmetric tall building structure whose planform consists of two coupled shear walls and ten rigid frames as shown in Fig. 6.5b. The following data are used:

Storey height h	2.8 m
Total height H	$30 \times 2.8 \text{ m} = 84.0 \text{ m}$
Uniformly distributed load w_0	10 kN/m
Modulus of elasticity E	$1.40 \times 10^7 \text{ kN/m}^2$

Coupled shear walls:

Depths of walls	$D_1 = D_2 = 8.0 \text{ m}$
Clear span of beams b	4.0 m
Depths of connecting beams D_b	0.5 m
Thickness of walls and beams t	0.3 m

Lumped rigid frame (total stiffnesses):

Beam spans b_i ($i = 1$ to 5)	4.0m
Inertias of beams I_{b_i}	$1.733 \times 10^{-2} \text{ m}^4$
Column storey heights h_c	2.8 m
Column section areas A_{c_1} and A_{c_6}	1.5125 m
A_{c_2} to A_{c_5}	1.0125 m
Inertias of columns I_{c_1} and I_{c_6}	$3.813 \times 10^{-2} \text{ m}^4$
I_{c_2} to I_{c_5}	$1.719 \times 10^{-2} \text{ m}^4$

Calculated parameters:

Coupled walls	$EI_1 = 3.584 \times 10^8 \text{ N m}^2$
	$\alpha_1 = 0.03359 \text{ m}^{-1}$, $k_1 = 1.07152$, $k\alpha H_1 = 3.0243$
Rigid frames	$EI_2 = 2.031 \times 10^6 \text{ N m}^2$
	$\alpha_2 = 0.64083 \text{ m}^{-1}$, $k_2 = 1.00019$, $k\alpha H_2 = 53.8397$

From Eqs. 6.28 to 6.36, the area influence coefficients for the two assemblies are calculated as follows,

$$A_1 = \begin{bmatrix} 5.80860E-03 & 4.21245E-03 & 1.76821E-04 \\ 2.17943E-01 & 1.53353E-01 & 5.80860E-03 \\ 1.28817E+01 & 9.13926E+00 & 3.53846E-01 \end{bmatrix}$$

$$A_2 = \begin{bmatrix} 5.22842E-03 & 3.58699E-03 & 1.35465E-04 \\ 2.62576E-01 & 1.69389E-01 & 5.22842E-03 \\ 1.42287E+01 & 9.37835E+00 & 3.01307E-01 \end{bmatrix}$$

Then, on solving the equations provided from Eqs. 6.38 and 6.40, the load distributions on the two assemblies, which are the three load components on each, are obtained as,

Coupled walls:

$$w_1 = 16.364 \text{ kN/m}, \quad q_1 = -14.911 \text{ kN/m}, \quad P_1 = -38.543 \text{ kN}$$

Rigid frames:

$$w_2 = -6.364 \text{ kN/m}, \quad q_2 = 14.911 \text{ kN/m}, \quad P_2 = 38.543 \text{ kN}$$

Substituting the load components into Eqs. 6.3 and 6.4, and using Eqs. 6.25 to 6.27, the deflections of the coupled shear walls and the rigid frame are shown in Fig. 6.6a. It can be seen that, by having the same top deflections, the deflected curve areas and the first moments of curve areas, the two resultant deflected curves are almost identical. For comparison and for showing the different properties of the two assemblies, the two free modes of deflected configurations, each resulting from half of the total applied load $w_0/2$, are shown in Fig. 6.6b.

On using Eqs. 6.14 and 6.15, the shears and moments resulting from the calculated load distributions on the assemblies can be obtained. In order to check the accuracy of the method, the average of the two deflections (Fig. 6.6a), and the shears and moments are compared with those given by the FLASH results, shown in Figs. 6.6c to 6.6e. In the figures, unless specified, the thicker lines

refer to the proposed method, and the thinner lines refer to the FLASH results. It can be seen from the curves that simple approximate load distributions can produce reasonably accurate deflection and force results for such structures.

6.5 Analysis of Symmetric Three-Dimensional Wall-Frame Structures Subjected to Pure Bending

6.5.1 Method of Analysis

For a symmetric three-dimensional tall building structure consisting of various types of assemblies, subjected to a known resultant lateral load through the centre, only pure bending actions will occur due to symmetry. If the floor slabs are considered to be rigid in their own plane, these assemblies will be constrained to deform in identical horizontal configurations. On applying the method, consider now the representative structure and loading system shown in Fig. 6.7a, in which, due to symmetry, only half the structure and half the applied load need be taken into account. The half structure is thus replaced by an equivalent plane system in which the assemblies interact through a series of pin-ended continuous connecting media, as shown in Fig. 6.7b.

In the analysis, the applied lateral loading is assumed to be a combination of three standard load components, a uniformly distributed load of intensity w_0 , a triangularly distributed load of maximum intensity q_0 at the top, and a concentrated horizontal load P_0 at the top (Fig. 6.7b). It can be written in a column vector form as, $\{F_0\} = \{w_0 \ q_0 \ P_0\}^T$.

Assume now that the load distribution on each assembly (i) is represented by a combination of three load components, of the same form as discussed in the

previous section, w_i , q_i and P_i , as shown in Fig. 6.7c. The deflection for the assembly i is then determined by Eq. 6.5, in which $i = 1$ to n if there are n assemblies. In an attempt to force all assemblies to have equal deflections, the conditions of horizontal compatibility are achieved by equating the top deflections, the areas under the deflected curves, and the first moments of the curve areas, for all the assemblies. Referring to Eq. 6.37, the equations can be written as,

$$V_1 - V_2 = 0, \quad V_2 - V_3 = 0, \quad \dots, \quad V_{n-1} - V_n = 0 \quad (6.42)$$

in which V_i , defined in Section 6.4, is the column vector of the top deflection, the deflected curve area and the first moment of the curve area, for assembly i , given by,

$$V_i = \{Y_i \quad A_i \quad \bar{A}_i\}^T \quad (6.43)$$

On substituting V_i from Eq. 6.17 for all the assemblies, Eqs. 6.42 become,

$$A_1 F_1 - A_2 F_2 = 0, \quad A_2 F_2 - A_3 F_3 = 0, \quad \dots, \quad A_{n-1} F_{n-1} - A_n F_n = 0 \quad (6.44)$$

Eqs. 6.44 give $3(n-1)$ compatibility equations.

For horizontal force equilibrium, the total applied shear S_t must equal the sum of the shears on the individual assemblies at any level. That is,

$$S_t = S_1 + S_2 + \dots + S_n = \sum_i^n S_i \quad (6.45)$$

Referring to Eq. 6.14, the shear in assembly i can be expressed as,

$$S_i = w_i H(1 - \xi) + \frac{q_i H}{2}(1 - \xi^2) + P_i \quad (i = 1 \text{ to } n) \quad (6.46)$$

For the applied load, which is a combination of three load components, w_0 , q_0 and P_0 , the total applied shear at any level can be written as,

$$S_t = w_0 H(1 - \xi) + \frac{q_0 H}{2}(1 - \xi^2) + P_0 \quad (6.47)$$

On substituting in Eqs. 6.46 and 6.47, Eq. 6.45 then becomes,

$$\begin{aligned}
 w_0 H(1 - \xi) + \frac{q_0 H}{2}(1 - \xi^2) + P_0 \\
 = H(1 - \xi) \sum_1^n w_i + \frac{H(1 - \xi^2)}{2} \sum_1^n q_i + \sum_1^n P_i
 \end{aligned}
 \tag{6.48}$$

Eq. 6.48 will be true at any height if,

$$w_0 = \sum_1^n w_i, \quad q_0 = \sum_1^n q_i \quad \text{and,} \quad P_0 = \sum_1^n P_i
 \tag{6.49}$$

or,

$$F_0 = F_1 + F_2 + \dots + F_n
 \tag{6.50}$$

Eqs. 6.44 and 6.50, provide $3n$ equations which are sufficient for solving the $3n$ load distribution coefficients for all assemblies.

6.5.2 Compatibility and Equilibrium Equations in Matrix Form

Eqs 6.44 and 6.50, can be written in matrix form as,

$$\begin{bmatrix}
 A_1 & -A_2 & 0 & \dots & 0 & 0 & \dots & 0 & 0 \\
 0 & A_2 & -A_3 & \dots & 0 & 0 & \dots & 0 & 0 \\
 \vdots & \vdots & \vdots & \dots & \vdots & \vdots & \dots & \vdots & \vdots \\
 0 & 0 & 0 & \dots & A_i & -A_{i+1} & \dots & 0 & 0 \\
 \vdots & \vdots & \vdots & \dots & \vdots & \vdots & \dots & \vdots & \vdots \\
 0 & 0 & 0 & \dots & 0 & 0 & \dots & A_{n-1} & -A_n \\
 I & I & I & \dots & I & I & \dots & I & I
 \end{bmatrix}
 \begin{bmatrix}
 F_1 \\
 F_2 \\
 \vdots \\
 F_i \\
 \vdots \\
 F_{n-1} \\
 F_n
 \end{bmatrix}
 =
 \begin{bmatrix}
 0 \\
 0 \\
 \vdots \\
 0 \\
 \vdots \\
 0 \\
 F_0
 \end{bmatrix}$$

(6.51)

or,

$$K_A F = L \tag{6.52}$$

in which the vector of load distribution coefficients F , and the vector of applied load coefficients L , are given respectively by,

$$F = \{F_1 \quad F_2 \quad \dots \quad F_n\}^T \tag{6.53}$$

$$L = \{0 \quad 0 \quad 0 \quad \dots \quad F_0\}^T \tag{6.54}$$

and K_A is a square matrix of order $3n$, referred to as the "area influence stiffness matrix" for the symmetric structure subjected to pure bending, given by,

$$K_A = \begin{bmatrix} A_1 & -A_2 & 0 & \dots & 0 & 0 & \dots & 0 & 0 \\ 0 & A_2 & -A_3 & \dots & 0 & 0 & \dots & 0 & 0 \\ \vdots & \vdots & \vdots & \dots & \vdots & \vdots & \dots & \vdots & \vdots \\ 0 & 0 & 0 & \dots & A_i & -A_{i+1} & \dots & 0 & 0 \\ \vdots & \vdots & \vdots & \dots & \vdots & \vdots & \dots & \vdots & \vdots \\ 0 & 0 & 0 & \dots & 0 & 0 & \dots & A_{n-1} & -A_n \\ I & I & I & \dots & I & I & \dots & I & I \end{bmatrix} \tag{6.55}$$

where, referring to Eq. 6.18, A_i is a square matrix of order 3, consisting of the area influence coefficients for assembly i , I is a unit square matrix of order 3, and 0 is a zero square matrix of order 3. In Eq. 6.53, F_i is a column vector of the load distribution on assembly i , defined by Eqs. 6.16 and 6.17, and F_0 is the vector of the applied loads, given by Eq. 6.41.

The load distribution coefficients for all the assemblies can then be determined by solving the matrix equation, 6.52, or,

$$F = K_A^{-1} L \tag{6.56}$$

6.5.3 Numerical Examples

A number of example structures with different configurations have been analyzed during the research, and two representative examples are given below to show the accuracy of the results obtained.

Example 1.

The plan of a forty-storey structure is shown in Fig. 6.8a. It consists of four pairs of coupled shear walls, four identical rigid frames and a central core, subjected to a resultant uniformly distributed lateral load at the centre of the building. Due to symmetry, only half of the structure is considered, which is replaced by an equivalent plane structural system as shown in Fig. 6.8b, in which the two identical rigid frames are lumped together as a single element, subjected to half of the load, $w_0 = 10$ kN/m. The original data for the structure are:

Storey height h	2.8 m
Number of storeys	40
Total height H	112.0 m
Uniformly distributed load w_0	10 kN/m'
Modulus of elasticity E	1.40×10^7 kN/m ²
Coupled shear walls (a):	
Depths of the two walls	$D_1 = 5.5$ m, $D_2 = 4.5$ m
Clear span of the beams	$b = 2.0$ m
Depths of the connecting beams	$D_b = 0.4$ m
Thickness of the walls and beams	$t = 0.3$ m

Coupled shear walls (b):

Depths of the two walls	$D_1 = 4.0 \text{ m}, D_2 = 4.5 \text{ m}$
Clear span of the beams	$b = 3.5 \text{ m}$
Depths of the connecting beams	$D_b = 0.4 \text{ m}$
Thickness of the walls and beams	$t = 0.3 \text{ m}$

Lumped 5-span rigid frame (total stiffnesses):

Beam spans b_i ($i=1$ to 5)	2.5, 2.5, 2.0, 2.5, 2.5 (m)
Inertias of the beams I_{bi}	$5.2083 \times 10^{-3} \text{ m}^4$
Column storey heights h_c	2.8 m
Column section areas A_{c1} to A_{c6}	0.50 m
Inertias of the columns I_{ci} ($i=1$ to 6)	$1.0417 \times 10^{-2} \text{ m}^4$

Half of the central core:

Flexural rigidity EI	$1.660 \times 10^8 \text{ N m}^2$
------------------------	-----------------------------------

The calculated parameters are:

Coupled walls (a)	$EI_1 = 9.0125 \times 10^7 \text{ N m}^2$
	$\alpha_1 = 0.07665 \text{ m}^{-1}, k_1 = 1.08487, k\alpha H_1 = 9.3137$
Coupled walls (b)	$EI_2 = 5.4294 \times 10^7 \text{ N m}^2$
	$\alpha_2 = 0.04890 \text{ m}^{-1}, k_2 = 1.04959, k\alpha H_2 = 5.7479$
Rigid frame	$EI_3 = 8.7500 \times 10^5 \text{ N m}^2$
	$\alpha_3 = 0.70139 \text{ m}^{-1}, k_3 = 1.00063, k\alpha H_3 = 78.6058$
Flexural element	$EI_4 = 1.6600 \times 10^8 \text{ N m}^2$

The area influence coefficients for the four assemblies are obtained as follows,

$$A_1 = \begin{bmatrix} 3.97217E-02 & 2.88642E-02 & 9.17488E-04 \\ 1.92713E+00 & 1.36227E+00 & 3.97217E-02 \\ 1.52575E+02 & 1.08752E+02 & 3.23279E+00 \end{bmatrix}$$

$$A_2 = \begin{bmatrix} 6.17784E-02 & 4.45300E-02 & 1.38306E-03 \\ 3.23203E+00 & 2.24685E+00 & 6.17784E-02 \\ 2.51647E+02 & 1.76767E+02 & 4.98736E+00 \end{bmatrix}$$

$$A_3 = \begin{bmatrix} 4.26443E-02 & 3.03865E-02 & 9.34221E-04 \\ 2.32001E+00 & 1.57889E+00 & 4.26443E-02 \\ 1.76836E+02 & 1.22280E+02 & 3.40328E+00 \end{bmatrix}$$

$$A_4 = \begin{bmatrix} 1.18489E-01 & 8.68921E-02 & 2.82117E-03 \\ 5.30832E+00 & 3.83379E+00 & 1.18489E-01 \\ 4.29384E+02 & 3.11421E+02 & 9.73192E+00 \end{bmatrix}$$

Then, on solving the equations given by Eq. 6.51, the three components of load distribution on each assemblies are obtained as,

Assembly	i	w _i (kN/m)	q _i (kN/m)	P _i (kN)
Coupled Walls a	1	3.7495	0.3566	-28.0402
Coupled Walls b	2	1.3056	0.0680	36.0187
Rigid Frame	3	-3.2461	8.9447	0.1432
Central Core	4	8.1910	-9.3693	-8.1217

The resulting deflections for all the assemblies, which have the same top deflections, the same areas under the deflected curves and same first moments of the curve areas, are shown in Fig. 6.9a. The average of the deflections is then compared with the result obtained from the FLASH program in Fig. 6.9b.

The curves in Figs. 6.9c and 6.9d show respectively the resultant shears and moments on each assembly, compared with those obtained from the FLASH program.

Example 2.

A second example structure is shown in Fig. 6.10a. It is replaced by an equivalent plane system as shown in Fig. 6.10b which consists of three assemblies, a pair of coupled shear walls, a rigid frame (which is a lumped sum of three frames), and a flexural member. In addition to the uniformly distributed load case, the other two load cases are also considered in this example. The following data define the structure:

Storey height h	2.8 m
Number of storeys	30
Total height H	84.0 m
Uniformly distributed load w_0	10 kN/m
Triangularly distributed load q_0	20 kN/m
Top horizontal point load P_0	840 kN
Modulus of elasticity E	1.40×10^7 kN/m ²

Coupled shear walls:

Depths of the two walls	$D_1 = 8.0$ m, $D_2 = 6.0$ m
Clear span of the beams	$b = 4.0$ m
Depths of the connecting beams	$D_b = 0.5$ m
Thickness of the walls and beams	$t = 0.25$ m

Lumped 5-span rigid frame (total stiffnesses):

Beam spans b_i ($i=1$ to 5)	4.0, 4.0, 4.0, 3.0, 3.0 (m)
Inertias of the beams I_{b_i} :	7.8125×10^{-3} m ⁴
Column storey heights h_c	2.8 m
Column section areas A_{c_1} to A_{c_6}	1.08 m
Inertias of the columns I_{c_i} ($i=1$ to 6)	3.2400×10^{-2} m ⁴

Flexural assembly:

Inertia of the beam I 11.857 m⁴

The resulting parameters are:

Coupled walls $EI_1 = 2.1233 \times 10^8$ N m²
 $\alpha_1 = 0.03652$ m⁻¹, $k_1 = 1.07062$, $k\alpha H_1 = 3.2844$

Rigid frame $EI_2 = 2.7216 \times 10^8$ N m²
 $\alpha_2 = 0.45626$ m⁻¹, $k_2 = 1.00039$, $k\alpha H_2 = 38.3405$

Flexural element $EI_3 = 1.6600 \times 10^8$ N m²

The area influence coefficients for the assemblies are,

$$A_1 = \begin{bmatrix} 9.08981E-03 & 6.58669E-03 & 2.75919E-04 \\ 3.43381E-01 & 2.41211E-01 & 9.08981E-03 \\ 2.02617E+01 & 1.43550E+01 & 5.53282E-01 \end{bmatrix}$$

$$A_2 = \begin{bmatrix} 7.67531E-03 & 5.28376E-03 & 2.00483E-04 \\ 3.81260E-01 & 2.47068E-01 & 7.67531E-03 \\ 2.07537E+01 & 1.37321E+01 & 4.43836E-01 \end{bmatrix}$$

$$A_3 = \begin{bmatrix} 3.74908E-02 & 2.74932E-02 & 1.19018E-03 \\ 1.25969E+00 & 9.09775E-01 & 3.74908E-02 \\ 7.64212E+01 & 5.54263E+01 & 2.30943E+00 \end{bmatrix}$$

Solutions are obtained for three applied lateral load cases, which are, load case 1: a uniformly distributed lateral load, load case 2: a triangularly distributed lateral load, and load case 3: a top concentrated horizontal load. The three assemblies are defined as, assembly 1: coupled shear walls, assembly 2: rigid frame, and assembly 3: flexural central core. The load distributions on the

assemblies are obtained as:

Load Case	i	w_i (kN/m)	q_i (kN/m)	P_i (kN)
Load Case 1	1	7.9931	-4.8717	-22.8467
	2	-5.9427	12.7198	63.1800
	3	7.9496	-7.8481	-40.3333
Load Case 2	1	3.6930	4.2085	-43.2653
	2	-9.6171	18.7861	119.2350
	3	5.9241	-2.9946	-75.9697
Load Case 3	1	4.9800	-6.4486	299.6278
	2	-13.3382	17.2418	482.5259
	3	8.3582	-10.7932	57.8463

The resulting curves for the three load cases are shown respectively in Figs. 6.11a to 6.11d, 6.12a to 6.12d, and 6.13a to 6.13d. These include the deflections, the average deflections compared with the FLASH results, and the shears and moments compared with the FLASH results.

From the examples, it can be seen that the method gives reasonably good results for the interaction between more than two different forms of components.

6.6 Analysis of Three-Dimensional Structures Subjected to Bending and Torsion Actions

6.6.1 Method of Analysis

For an asymmetric three-dimensional structure subjected to a system of lateral loading $w(x)$, the structure will tend to bend as well as twist as shown in Fig. 6.1a. If the structure considered consists of n assemblies, the deflections are represented by y_1, y_2, \dots, y_n , and the spacings between the assemblies are denoted by d_1, d_2, \dots, d_{n-1} (Fig. 6.14), the deflection relationship between the assemblies at any height level are then,

$$y_2 - y_1 = d_1\theta, \quad y_3 - y_2 = d_2\theta, \quad \dots, \quad y_n - y_{n-1} = d_{n-1}\theta \quad (6.57)$$

in which θ is the rotation of the structure at the height level considered.

For the top deflections, the equations becomes,

$$Y_2 - Y_1 = d_1\Theta, \quad Y_3 - Y_2 = d_2\Theta, \quad \dots, \quad Y_n - Y_{n-1} = d_{n-1}\Theta \quad (6.58)$$

in which Y_1, Y_2, \dots, Y_n are the top deflections of the assemblies, and Θ is the top rotation of the structure.

The integration for both sides of the expressions in Eq. 6.57 for the height coordinate x from the base to the top will yield,

$$A_2 - A_1 = d_1\Omega, \quad A_3 - A_2 = d_2\Omega, \quad \dots, \quad A_n - A_{n-1} = d_{n-1}\Omega \quad (6.59)$$

in which, obviously, A_1, A_2, \dots, A_n are the deflected curve areas, and Ω is the area under the rotation curve.

On multiplying both sides of the expressions in Eq. 6.57 by x , and integrating the equations for the height coordinate from the base to the top, the equations become,

$$\bar{A}_2 - \bar{A}_1 = d_1\Pi, \bar{A}_3 - \bar{A}_2 = d_2\Pi, \dots, \bar{A}_n - \bar{A}_{n-1} = d_{n-1}\Pi \quad (6.60)$$

in which $\bar{A}_1, \bar{A}_2, \dots, \bar{A}_n$ are the first moments of the deflected curve areas, and Π is the first moment of the rotation curve areas.

In the analysis, the applied lateral and torsional loads considered are a combination of a uniformly distributed lateral load and torque of intensities w_0 and t_0 respectively, a triangularly distributed lateral load and torque of maximum intensities at the top of the structure q_0 and r_0 respectively, and a concentrated horizontal lateral load and torque of magnitudes P_0 and T_0 respectively. In matrix form, they can be written as,

$$\{F_0\} = \{w_0 \ q_0 \ P_0\}^T \text{ and } \{T_0\} = \{t_0 \ r_0 \ T_0\}^T \quad (6.61)$$

(1) Omission of Individual Torsional Stiffnesses

In the first instance, if the torsional stiffnesses of individual assemblies are neglected as being small, the load distribution on each assembly i ($i = 1$ to n) is then represented by a combination of three lateral load components w_i, q_i and P_i , as shown in Fig. 6.15. Under such a load combination, each assembly will have a deflection y_i , determined by Eq. 6.5, in which $i = 1$ to n . It is assumed that the conditions of horizontal deflection compatibility can be established by assuming that the approximate deflections satisfy the three conditions given by Eqs. 6.58, 6.59 and 6.60, that is,

$$V_i - V_{i+1} = -d_i R \quad (i = 1 \text{ to } n-1) \quad (6.62)$$

in which the column vector V_i has been defined in Eq. 6.43 for assembly i and can be expressed by Eq. 6.17, and R , referred to as the overall rotational coefficient column vector for the structure, is defined now as,

$$R = \{\Theta \ \Omega \ \Pi\}^T \quad (6.63)$$

On substituting V_i ($i = 1$ to n) from Eq. 6.17, Eq. 6.62 becomes,

$$A_i F_i - A_{i+1} F_{i+1} = -d_i R \quad (6.64)$$

1. For horizontal force equilibrium, the total applied shear at any height level must be equal to the sum of the shear forces in all individual assemblies (Fig. 6.16). That is,

$$S_t = S_1 + S_2 + \dots + S_n = \sum_1^n S_i \quad (6.65)$$

This, as discussed earlier, (Eqs. 6.45 to 6.48) will give three equilibrium equations as,

$$F_0 = F_1 + F_2 + \dots + F_n \quad (6.66)$$

2. For horizontal twisting moment equilibrium, the sum of the moments of all the shear forces about any chosen datum must equal the applied twisting moment M_{t_0} . Normally, any datum position may be adopted for the analysis, but some points may be more efficient than others. For example, it may be useful to choose a datum position to coincide with the position of the resultant lateral force on the building so that no applied torque occurs about the datum. This will be found as the case in the following analysis. So, on choosing as the datum the particular position at which the external resultant load is applied, and referring to Fig. 6.16,

$$S_1 z_1 + S_2 z_2 + \dots + S_n z_n = \sum_1^n S_i z_i = M_{t_0} \quad (6.67)$$

in which z_i ($i = 1$ to n) is the distance between assembly i and the datum, and the applied twisting moment M_{t_0} at any level is given by,

$$M_{t_0} = t_0 H(1-\xi) + r_0 H \frac{1-\xi^2}{2} + T_0 \quad (6.68)$$

On substituting in S_i ($i=1$ to n) and M_{t_0} from Eq. 6.46 and 6.68, Eq. 6.67 becomes,

$$\begin{aligned}
 & H(1-\xi)\sum_1^n w_i z_i + \frac{H(1-\xi^2)}{2}\sum_1^n q_i z_i + \sum_1^n P_i z_i \\
 & = H(1-\xi)t_0 + \frac{H(1-\xi^2)}{2}r_0 + T_0
 \end{aligned}
 \tag{6.69}$$

It is obvious that Eq. 6.69 is true for any height only when,

$$\sum_1^n w_i z_i = t_0, \quad \sum_1^n q_i z_i = r_0 \quad \text{and} \quad \sum_1^n P_i z_i = T_0
 \tag{6.70}$$

The twisting moment equilibrium then is given by three equations as,

$$T_0 = z_1 F_1 + z_2 F_2 + \dots + z_n F_n
 \tag{6.71}$$

Eqs. 6.64, 6.66 and 6.71 then provide sufficient equations to determine the unknown coefficients, which are $3n$ load components on n assemblies and the 3 additional rotational coefficients in Eq. 6.63.

These $3(n+1)$ equations together can be written in matrix form as,

$$\begin{bmatrix}
 A_1 & -A_2 & 0 & \dots & 0 & 0 & \dots & 0 & 0 & D_1 \\
 0 & A_2 & -A_3 & \dots & 0 & 0 & \dots & 0 & 0 & D_2 \\
 \cdot & \cdot & \cdot & \dots & \cdot & \cdot & \dots & \cdot & \cdot & \cdot \\
 \cdot & \cdot & \cdot & \dots & \cdot & \cdot & \dots & \cdot & \cdot & \cdot \\
 0 & 0 & 0 & \dots & A_i & -A_{i+1} & \dots & 0 & 0 & D_i \\
 \cdot & \cdot & \cdot & \dots & \cdot & \cdot & \dots & \cdot & \cdot & \cdot \\
 \cdot & \cdot & \cdot & \dots & \cdot & \cdot & \dots & \cdot & \cdot & \cdot \\
 0 & 0 & 0 & \dots & 0 & 0 & \dots & A_{n-1} & -A_n & D_{n-1} \\
 E & E & E & \dots & E & E & \dots & E & E & 0 \\
 Z_1 & Z_2 & Z_3 & & Z_i & Z_{i+1} & & Z_{n-1} & Z_n & 0
 \end{bmatrix}
 \begin{Bmatrix}
 F_1 \\
 F_2 \\
 \cdot \\
 \cdot \\
 F_i \\
 \cdot \\
 \cdot \\
 F_{n-1} \\
 F_n \\
 R
 \end{Bmatrix}
 =
 \begin{Bmatrix}
 0 \\
 0 \\
 \cdot \\
 \cdot \\
 0 \\
 \cdot \\
 \cdot \\
 0 \\
 F_0 \\
 T_0
 \end{Bmatrix}$$

(6.72)

or,

$$K_A F = L \tag{6.73}$$

where F is the vector consisting of load distribution coefficients F_i and rotational coefficients R , and L is the vector of applied load cases, given respectively by,

$$F = \{F_1 \ F_2 \ \dots \ F_n \ R\}^T \tag{6.74}$$

$$L = \{0 \ 0 \ \dots \ 0 \ F_0 \ T_0\}^T \tag{6.75}$$

and K_A is the area influence stiffness square matrix, of order $3(n+1)$, for an asymmetric structure, given by,

$$K_A = \begin{bmatrix} A_1 & -A_2 & 0 & \dots & 0 & 0 & \dots & 0 & 0 & D_1 \\ 0 & A_2 & -A_3 & \dots & 0 & 0 & \dots & 0 & 0 & D_2 \\ \vdots & \vdots & \vdots & \dots & \vdots & \vdots & \dots & \vdots & \vdots & \vdots \\ 0 & 0 & 0 & \dots & A_i & -A_{i+1} & \dots & 0 & 0 & D_i \\ \vdots & \vdots & \vdots & \dots & \vdots & \vdots & \dots & \vdots & \vdots & \vdots \\ 0 & 0 & 0 & \dots & 0 & 0 & \dots & A_{n-1} & -A_n & D_{n-1} \\ I & I & I & \dots & I & I & \dots & I & I & 0 \\ Z_1 & Z_2 & Z_3 & & Z_i & Z_{i+1} & & Z_{n-1} & Z_n & 0 \end{bmatrix} \tag{6.76}$$

in which, except for those terms already defined in Eq. 6.55, D_i and Z_i are defined as,

$$D_i = \begin{bmatrix} d_i & 0 & 0 \\ 0 & d_i & 0 \\ 0 & 0 & d_i \end{bmatrix} \quad (i = 1 \text{ to } n-1) \tag{6.77}$$

$$Z_i = \begin{bmatrix} z_i & 0 & 0 \\ 0 & z_i & 0 \\ 0 & 0 & z_i \end{bmatrix} \quad (i = 1 \text{ to } n) \tag{6.78}$$

The solution to Eq. 6.72 determines the unknown load distribution coefficients and the rotational coefficients. That is,

$$F = K_A^{-1}L \tag{6.79}$$

(2) Inclusion of Individual Torsional Stiffnesses

If the individual torsional stiffnesses of the assemblies are included, it is then assumed that, in addition to the three lateral load components, w_i , q_i and P_i , the torsional load distribution on assembly i ($i=1$ to n) can be represented by three torsional load components, a uniformly distributed torque of intensity t_i , a triangularly distributed torque of maximum intensity r_i at the top, and a concentrated torque T_i at the top (Fig. 6.17). It is also assumed that, for assembly i , the torque-rotation relationships under the three corresponding torque components are known, so that when subjected to the three torque components, the rotation of assembly i is given by,

$$\theta_i = t_i \theta_{t_i} + r_i \theta_{r_i} + T_i \theta_{T_i} \quad (6.80)$$

in which θ_{t_i} , θ_{r_i} and θ_{T_i} are the three torque-rotation relationships under the three unit torques (Fig. 6.17).

Having obtained the general expression for the rotation in Eq. 6.80, the top rotation, the area under the rotation curve and the first moment of the rotation curve area about the base can be derived. That is, in matrix form,

$$\begin{Bmatrix} \Theta_i \\ \Omega_i \\ \Pi_i \end{Bmatrix} = \begin{bmatrix} \Theta_{t_i} & \Theta_{r_i} & \Theta_{T_i} \\ \Omega_{t_i} & \Omega_{r_i} & \Omega_{T_i} \\ \Pi_{t_i} & \Pi_{r_i} & \Pi_{T_i} \end{bmatrix} \begin{Bmatrix} t_i \\ r_i \\ T_i \end{Bmatrix} \quad (i = 1 \text{ to } n) \quad (6.81)$$

or,

$$R_i = A r_i T_i \quad (6.82)$$

in which R_i is the rotational coefficient vector consisting of the top rotation Θ_i , the rotation curve area Ω_i and the first moment of the rotation curve area Π_i , for assembly i , T_i is the torsional load vector for assembly i , and the square matrix $A r_i$ is now defined as the rotational area coefficient matrix for assembly i , given by,

$$Ar_i = \begin{bmatrix} \Theta_{ti} & \Theta_{ri} & \Theta_{Ti} \\ \Omega_{ti} & \Omega_{ri} & \Omega_{Ti} \\ \Pi_{ti} & \Pi_{ri} & \Pi_{Ti} \end{bmatrix} \quad (6.83)$$

in which Θ_{ti} , Θ_{ri} and Θ_{Ti} are the top rotations, Ω_{ti} , Ω_{ri} and Ω_{Ti} are the rotation curve areas, and Π_{ti} , Π_{ri} and Π_{Ti} are the first moments of the rotation curve areas about the base, for assembly i , due to the three corresponding unit torque load components, respectively.

Since all the assemblies should have the same rotation at any level which equals the overall rotation of the structure, it is assumed that the rotational coefficient vector for each assembly i , which includes the top rotation, the rotation curve area and the first moment of the rotation curve area, must equal the overall rotational coefficient vector for the structure (Eq. 6.63). That is, referring to Fig. 6.18,

$$R_i = R \quad (i = 1 \text{ to } n) \quad (6.84)$$

On using Eq. 6.81, that is,

$$Ar_i T_i = R \quad (i = 1 \text{ to } n) \quad (6.85)$$

Eq. 6.85, regarding as the conditions of rotational compatibility, will give $3n$ equations.

On using the position of the external resultant load as the datum, for horizontal twisting moment equilibrium, the sum of the moments of all the shear forces and the twisting moments on individual assemblies must be zero. Referring to Fig. 6.19, that is,

$$\sum_1^n S_i z_i + \sum_1^n M_{ti} = M_{t0} \quad (i = 1 \text{ to } n) \quad (6.86)$$

in which M_{ti} is the twisting moment on assembly i , subjected to the three torque components, given by,

$$M_{ti} = t_i H(1-\xi) + r_i H \frac{1-\xi^2}{2} + T_i \quad (6.87)$$

On using Eqs. 6.46 and 6.87, Eq. 6.86 becomes,

$$\begin{aligned} & H(1-\xi) \sum_1^n (w_i z_i + t_i) + \frac{H(1-\xi^2)}{2} \sum_1^n (q_i z_i + r_i) + \sum_1^n (P_i z_i + T_i) \\ & = H(1-\xi) t_0 + \frac{H(1-\xi^2)}{2} r_0 + T_0 \end{aligned} \quad (6.88)$$

It is obvious that Eq. 6.88 is true for any height coordinate only when,

$$\sum_1^n (w_i z_i + t_i) = t_0 \quad (6.89)$$

$$\sum_1^n (q_i z_i + r_i) = r_0 \quad (6.90)$$

$$\sum_1^n (P_i z_i + T_i) = T_0 \quad (6.91)$$

The horizontal twisting moment equilibrium then can be give from Eqs. 6.89 to 6.91,

$$\begin{aligned} T_0 &= (T_1 + T_2 + \dots + T_n) \\ &+ (z_1 F_1 + z_2 F_2 + \dots + z_n F_n) \end{aligned} \quad (6.92)$$

Eqs. 6.64, 6.85, 6.66 and 6.92 altogether provide sufficient $(6n + 3)$ equations to determine the unknown coefficients, the lateral load distribution coefficients $\{w_i \ q_i \ P_i\}^T$ ($i = 1$ to n), the torsional load distribution coefficients $\{t_i \ r_i \ T_i\}^T$ ($i = 1$ to n) and the overall rotational coefficients $\{\theta \ \Omega \ \Pi\}^T$.

6.6.2 Numerical Example of Three-Dimensional Structure Subjected to Bending and Torsion Actions

The same example used in Chapter 5, the Asymmetric Structure Example 2, is again used as an example to examine the accuracy of the present method. The planform of the 30-storey structure is as shown in Fig. 5.17, and it is subjected to a uniformly distributed lateral load, $w_0 = 15$ kN/m, at the same eight different load positions. The original data for the structure and the parameters for the assemblies have been given in Section 5.5. Since the analysis of the torsional behaviour of individual assemblies is not included in the thesis, the torsional stiffnesses of individual assemblies are not considered in both the present method and the FLASH analysis.

The area influence coefficients for each assembly are,

$$[A_1] = \begin{bmatrix} 7.14955E-03 & 5.17952E-03 & 2.16827E-04 \\ 2.70677E-01 & 1.90047E-01 & 7.14955E-03 \\ 1.59639E+01 & 1.13053E+01 & 4.35080E-01 \end{bmatrix}$$

$$[A_2] = \begin{bmatrix} 3.34661E-02 & 2.30265E-02 & 8.74373E-04 \\ 1.66059E+00 & 1.07513E+00 & 3.34661E-02 \\ 9.03107E+01 & 5.97185E+01 & 1.93423E+00 \end{bmatrix}$$

$$[A_3] = \begin{bmatrix} 1.42604E-02 & 1.04576E-02 & 4.52712E-04 \\ 4.79150E-01 & 3.46053E-01 & 1.42604E-02 \\ 2.90684E+01 & 2.10826E+01 & 8.78442E-01 \end{bmatrix}$$

$$[A_4] = \begin{bmatrix} 3.34661E-02 & 2.30265E-02 & 8.74373E-04 \\ 1.66059E+00 & 1.07513E+00 & 3.34661E-02 \\ 9.03107E+01 & 5.97185E+01 & 1.93423E+00 \end{bmatrix}$$

$$[A_5] = \begin{bmatrix} 3.34661E-02 & 2.30265E-02 & 8.74373E-04 \\ 1.66059E+00 & 1.07513E+00 & 3.34661E-02 \\ 9.03107E+01 & 5.97185E+01 & 1.93423E+00 \end{bmatrix}$$

$$[A_6] = \begin{bmatrix} 3.34661E-02 & 2.30265E-02 & 8.74373E-04 \\ 1.66059E+00 & 1.07513E+00 & 3.34661E-02 \\ 9.03107E+01 & 5.97185E+01 & 1.93423E+00 \end{bmatrix}$$

$$[A_7] = \begin{bmatrix} 3.34661E-02 & 2.30265E-02 & 8.74373E-04 \\ 1.66059E+00 & 1.07513E+00 & 3.34661E-02 \\ 9.03107E+01 & 5.97185E+01 & 1.93423E+00 \end{bmatrix}$$

$$[A_8] = \begin{bmatrix} 7.14955E-03 & 5.17952E-03 & 2.16827E-04 \\ 2.70677E-01 & 1.90047E-01 & 7.14955E-03 \\ 1.59639E+01 & 1.13053E+01 & 4.35080E-01 \end{bmatrix}$$

Using the area influence coefficients provided above, and considering the the load positions described in Section 5.5, the area influence stiffness matrixes for different load cases can be established. On solving the resulting equations, the solutions for the load distributions on each assembly, for the 8 different load positions are obtained and listed as follows,

Load Case	<i>i</i>	<i>w_i</i> (kN/m)	<i>q_i</i> (kN/m)	<i>P_i</i> (kN)
Load Position 1	1	8.211399	1.591677	21.912014
	2	-2.599562	4.806156	42.412139
	3	14.510322	-10.774519	-110.252207
	4	-1.197468	2.167790	20.668489
	5	-0.730104	1.288335	13.420606
	6	-0.262739	0.408880	6.172723
	7	0.204626	-0.470576	-1.075161
	8	-3.136475	0.982257	6.741398
Load Position 2	1	6.791887	1.517628	19.997992
	2	-2.248409	4.156329	36.712123
	3	13.607252	-10.327397	-101.118834
	4	-1.194811	2.206484	19.616890
	5	-0.843612	1.556536	13.918479
	6	-0.492413	0.906588	8.220068
	7	-0.141214	0.256640	2.521657
	8	-0.478679	-0.272807	0.131624

Load Position 3	1	4.662619	1.406554	17.126960
	2	-1.721679	3.181588	28.162099
	3	12.252647	-9.656714	-87.418775
	4	-1.190827	2.264525	18.039492
	5	-1.013876	1.958838	14.665289
	6	-0.836925	1.653150	11.291087
	7	-0.659974	1.347463	7.916885
	8	3.508014	-2.155404	-9.783036
Load Position 4	1	2.533351	1.295481	14.255927
	2	-1.194950	2.206847	19.612075
	3	10.898042	-8.986031	-73.718716
	4	-1.186842	2.322566	16.462093
	5	-1.184139	2.361140	15.412099
	6	-1.181436	2.399713	14.362106
	7	-1.178734	2.438286	13.312112
	8	7.494708	-4.038001	-19.697696
Load Position 5	1	1.113839	1.221432	12.341906
	2	-0.843797	1.557020	13.912059
	3	9.994972	-8.538909	-64.585343
	4	-1.184185	2.361260	15.410494
	5	-1.297648	2.629341	15.909973
	6	-1.411111	2.897421	16.409451
	7	-1.524574	3.165501	16.908930
	8	10.152503	-5.293066	-26.307470
Load Position 6	1	-0.305673	1.147383	10.427884
	2	-0.492644	0.907192	8.212043
	3	9.091902	-8.091787	-55.451970
	4	-1.181529	2.399955	14.358895
	5	-1.411157	2.897542	16.407846
	6	-1.640785	3.395129	18.456797
	7	-1.870413	3.892717	20.505748
	8	12.810299	-6.548131	-32.917244
Load Position 7	1	-1.725185	1.073333	8.513863
	2	-0.141491	0.257365	2.512027
	3	8.188831	-7.644665	-46.318597
	4	-1.178872	2.438649	13.307296
	5	-1.524666	3.165743	16.905720
	6	-1.870459	3.892838	20.504143
	7	-2.216253	4.619932	24.102566
	8	15.468095	-7.803196	-39.527017
Load Position 8	1	-3.144697	0.999284	6.599841
	2	0.209662	-0.392462	-3.187989
	3	7.285761	-7.197543	-37.185224
	4	-1.176215	2.477343	12.255697
	5	-1.638175	3.433944	17.403593
	6	-2.100134	4.390546	22.551489
	7	-2.562093	5.347148	27.699384
	8	18.125890	-9.058260	-46.136791

From these resulting load distributions, the approximate deflection of each assembly, and the shear and moment on each assembly can be obtained by using Eqs. 6.5, 6.14 and 6.15, in which $i = 1$ to 8. These results, compared with the results obtained from the FLASH analysis, are shown in Figs. 6.20 to 6.27, for the 8 load cases, respectively.

6.7 Hand Calculation For Load Distributions

So far, the analysis has presented three matrix equations, Eqs. 6.51, 6.72 and 6.93, due to the particular problems concerned. Using a digital computer, the analysis can be easily carried out through simple programming to solve the equations involved. At first sight, therefore, it appears that the analysis could require the inversion of a matrix of high order, although the aim is to achieve a simplified hand analysis method.

However, an inspection of the component equations involved reveals that the solution involves only the inversions of a series of matrices of order three for structures subjected to pure bending. If bending and torsion occur, the analysis again requires the inversion of a series of third order matrices, but the final equation is of the sixth order, necessitating a single inversion of a sixth order matrix. The calculations could thus be done using a pocket calculator.

For a complete three-dimensional structure involving bending and torsion actions, on using Eq. 6.64, the conditions of displacement compatibility can be written as,

$$\begin{array}{lcl}
 A_1 F_1 - A_2 F_2 = -d_1 R & (1) & \\
 A_2 F_2 - A_3 F_3 = -d_2 R & (2) & \\
 \dots & & \\
 A_{n-1} F_{n-1} - A_n F_n = -d_{n-1} R & (n-1) &
 \end{array} \quad \left. \vphantom{\begin{array}{l} \\ \\ \\ \end{array}} \right\} \quad (6.100)$$

By adding the above equations (1) to (n-1), (2) to (n-1), etc., until (n-2) to (n-1), Eqs. 6.100 become,

$$\left. \begin{aligned} A_1 F_1 - A_n F_n &= -(d_1 + d_2 + \dots + d_{n-1})R & (1) \\ A_2 F_2 - A_n F_n &= -(d_2 + d_3 + \dots + d_{n-1})R & (2) \\ \dots & \dots & \dots \\ A_{n-1} F_{n-1} - A_n F_n &= -(d_{n-1})R & (n-1) \end{aligned} \right\} \quad (6.101)$$

From Eqs. 6.101, the force distributions on assemblies 1 to (n-1) can be all expressed by F_n and R ,

$$\left. \begin{aligned} F_1 &= A_1^{-1} A_n F_n - l_1 A_1^{-1} R & (1) \\ F_2 &= A_2^{-1} A_n F_n - l_2 A_2^{-1} R & (2) \\ \dots & \dots & \dots \\ F_{n-1} &= A_{n-1}^{-1} A_n F_n - l_{n-1} A_{n-1}^{-1} R & (n-1) \end{aligned} \right\} \quad (6.102)$$

in which $l_1 = d_1 + d_2 + \dots + d_{n-1}$, $l_2 = d_2 + d_3 + \dots + d_{n-1}$,, and $l_{n-1} = d_{n-1}$.

From the conditions of twisting compatibility, Eqs. 6.85, the torsional force distribution on each assembly can be expressed by,

$$T_i = A r_i^{-1} R \quad (i = 1 \text{ to } n) \quad (6.103)$$

On using the horizontal force equilibrium, Eq. 6.66, substituting F_1, F_2, \dots, F_{n-1} from Eqs. 6.102, the equation becomes,

$$\begin{aligned} F_0 &= [(A_1^{-1} + A_2^{-1} + \dots + A_{n-1}^{-1})A_n + I]F_n \\ &\quad - (l_1 A_1^{-1} + l_2 A_2^{-1} + \dots + l_{n-1} A_{n-1}^{-1})R \end{aligned} \quad (6.104)$$

or,

$$F_0 = K_{f_1} F_n - K_{t_1} R \quad (6.105)$$

in which K_{f_1} and K_{t_1} are both square matrices of order three, to be given by,

$$K_{f_1} = (A_1^{-1} + A_2^{-1} + \dots + A_{n-1}^{-1})A_n + I \quad (6.106)$$

$$K_{t_1} = l_1 A_1^{-1} + l_2 A_2^{-1} + \dots + l_{n-1} A_{n-1}^{-1} \quad (6.107)$$

On using the horizontal twisting moment equilibrium, Eqs. 6.92, substituting T_1, T_2, \dots, T_n , and F_1, F_2, \dots, F_{n-1} from Eqs. 6.102 and 6.103, the equation becomes,

$$T_0 = [(z_1 A_1^{-1} + z_2 A_2^{-1} + \dots + z_{n-1} A_{n-1}^{-1}) A_n + z_n] F_n - [(z_1 l_1 A_1^{-1} + z_2 l_2 A_2^{-1} + \dots + z_{n-1} l_{n-1} A_{n-1}^{-1}) - (Ar_1^{-1} + Ar_2^{-1} + \dots + Ar_n^{-1})] R \tag{6.108}$$

or,

$$T_0 = K_{f_2} F_n - K_{t_2} R \tag{6.109}$$

in which,

$$K_{f_2} = (z_1 A_1^{-1} + z_2 A_2^{-1} + \dots + z_{n-1} A_{n-1}^{-1}) A_n + z_n \tag{6.110}$$

$$K_{t_2} = (Ar_1^{-1} + Ar_2^{-1} + \dots + Ar_n^{-1}) - (z_1 l_1 A_1^{-1} + z_2 l_2 A_2^{-1} + \dots + z_{n-1} l_{n-1} A_{n-1}^{-1}) \tag{6.111}$$

Eqs. 6.105, together with Eqs. 6.109, are six equations with six unknown coefficients, $F_n = \{w_n \ q_n \ P_n\}^T$ and $R = \{\Theta \ \Omega \ \Pi\}^T$. On solving the equations, the force and torque distributions on each assembly can be obtained by substituting F and R into Eqs. 6.102 and 6.103.

If the torsion-resisting assemblies considered are only a few in number, it can be seen that the numbers of equations involved could be reduced from Eqs. 6.103 and 6.108. In particular, the calculation in the analysis becomes much easier when twisting action is not involved in the structure. In such a case, as it is known that, $R = \{0 \ 0 \ 0\}^T$, Eqs. 6.102 then becomes,

$$\left. \begin{aligned} F_1 &= A_1^{-1} A_n F_n && (1) \\ F_2 &= A_2^{-1} A_n F_n && (2) \\ \dots & && \dots \\ F_{n-1} &= A_{n-1}^{-1} A_n F_n && (n-1) \end{aligned} \right\} \tag{6.112}$$

Eqs. 6.104 then become,

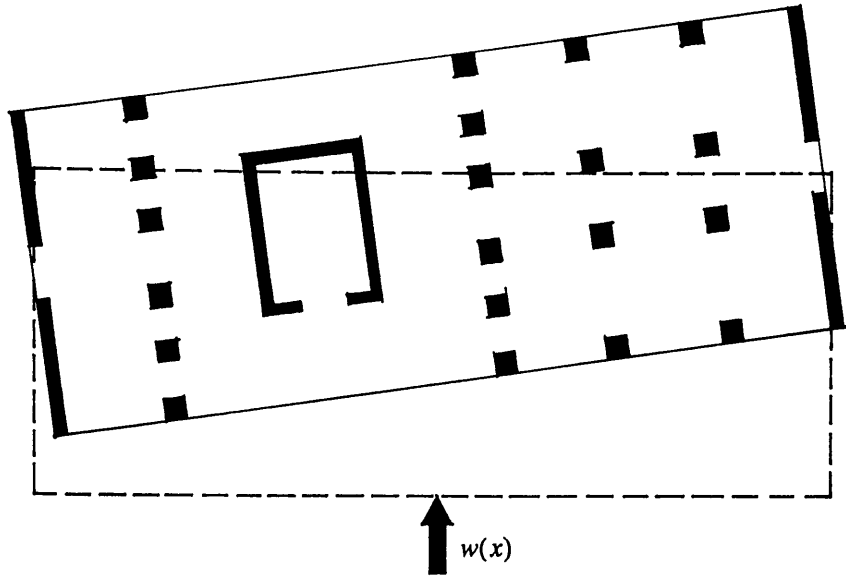
$$F_0 = [(A_1^{-1} + A_2^{-1} + \dots + A_{n-1}^{-1}) A_n + I] F_n \tag{6.113}$$

which are three equations with three unknown coefficients, F_n . On solving F_n from the three equations, the force distribution on each assembly, F_i , then follows from Eqs. 6.112.

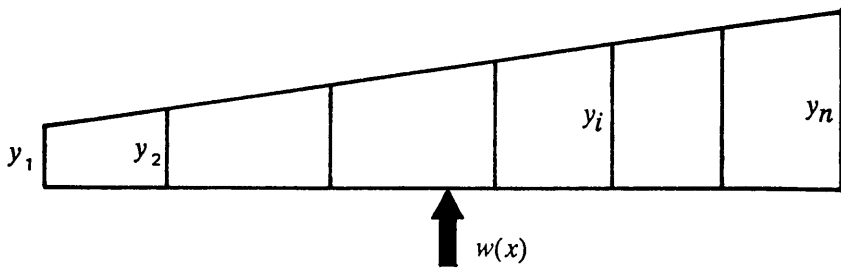
6.8 Convergence of Solution

As has been noted, the assumed distributed load components involve only the first two terms of a general load polynomial, and it may be expected that the inclusion of more terms would give rise to more accurate solutions. However, the use of more than two terms, in association with the top concentrated interactive force, would require more extensive calculations, and would make it laborious to achieve a solution by hand calculation. Consequently, no attempt has been made to use more than three terms in the analysis, particularly in view of the earlier work by Coull and Mohammed (Ref. 21), who found that good convergence was generally achieved by using no more than about four load terms.

A number of representative example structures were used to investigate the difference between using two load interactive components (a top point load and a uniformly distributed load), and all three components. It was found that if all structural assemblies belonged to one family with similar load-deformation characteristics, for example coupled shear walls, the influence of the triangularly distributed load term was generally not of great practical significance. However, if dissimilar structural assemblies existed, it was advisable to include all three load components to achieve reasonably accurate results. In general, therefore, the use of all three components is to be recommended.



(a) Rigid Body Movement of Floor Slab



(b) Linearly Related Deflections of Assemblies

Fig. 6.1 Three-Dimensional Tall Building Structure Subjected to Bending and Torsion Actions

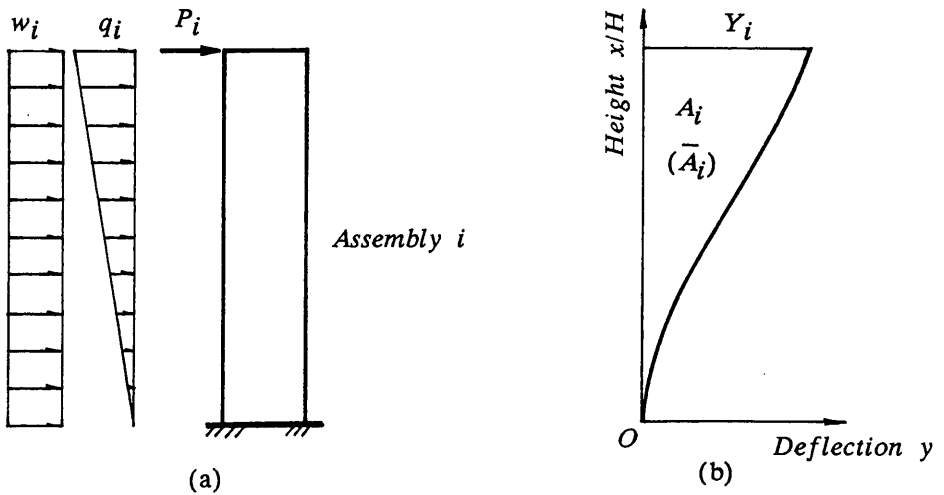
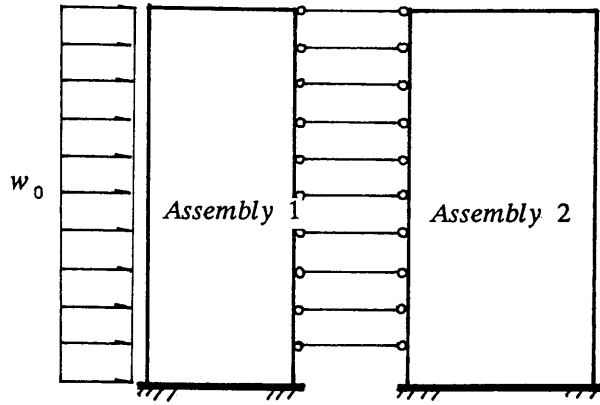
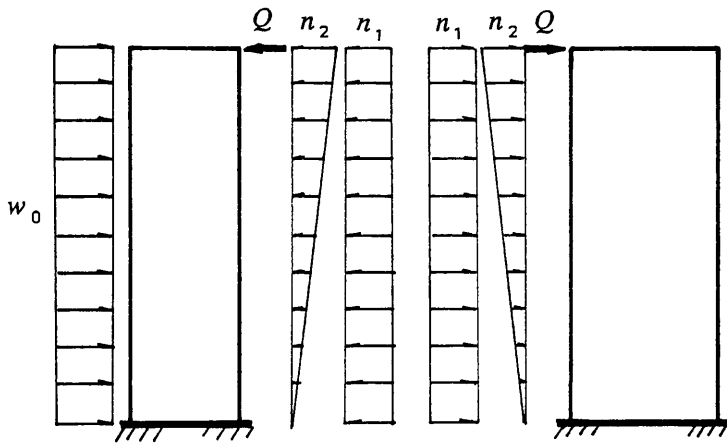


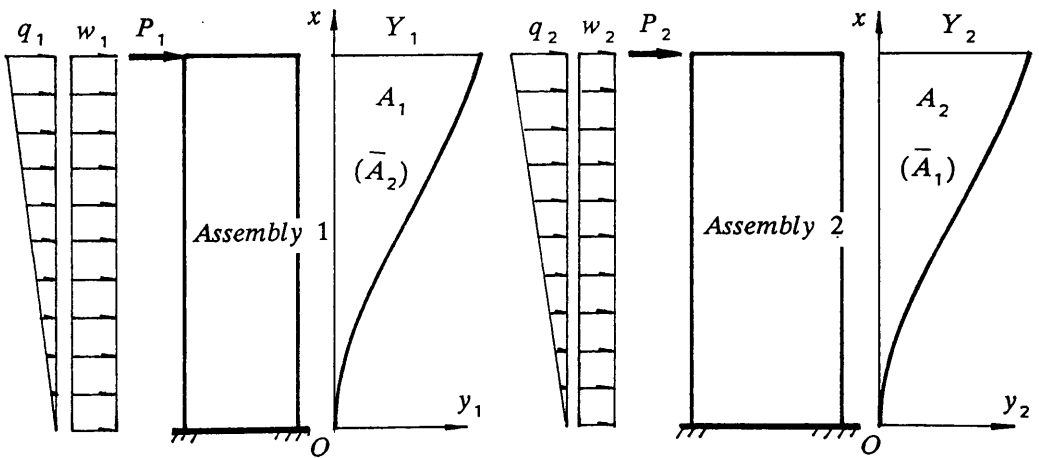
Fig. 6.2 Assumed Load Distribution (a) and Deflected Diagram (b)



(a) Representation of Structure



(b) Assumed Interactive Forces Within Links



(c) Illustration of Horizontal Force Equilibrium and Displacement Compatibility

Fig. 6.3 Two Linked Assemblies Subjected to Lateral Load

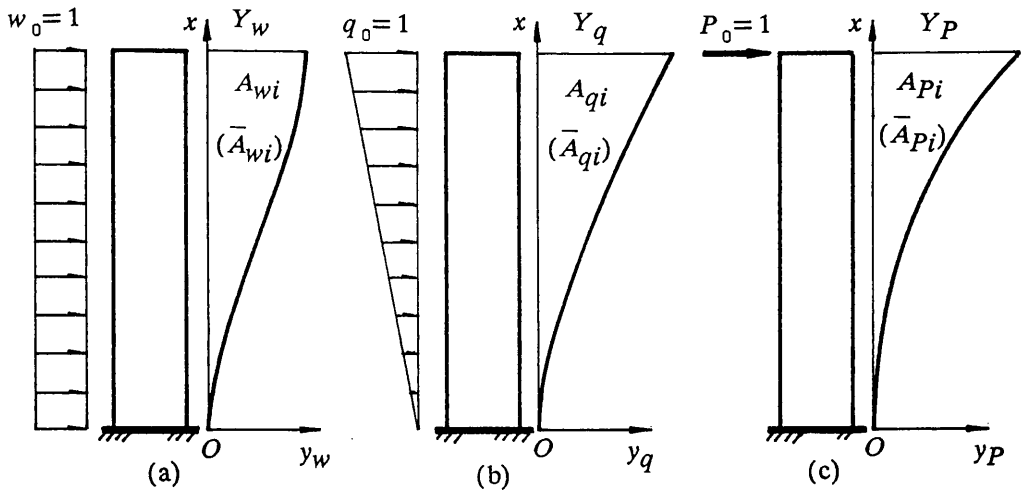
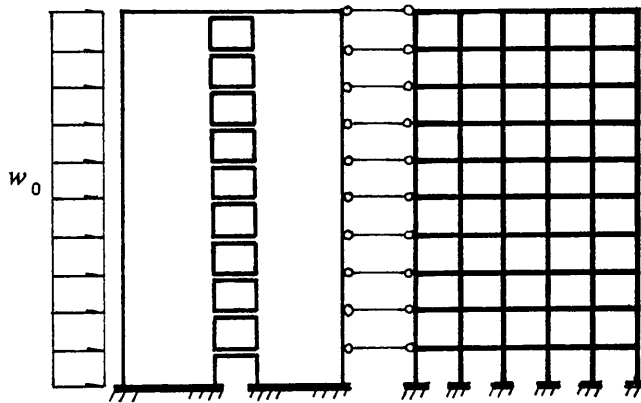
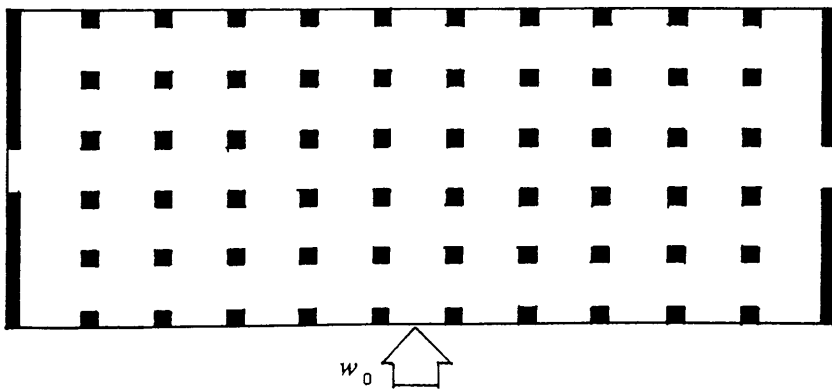


Fig. 6.4 Illustration of Area Influence Coefficients For an Assembly

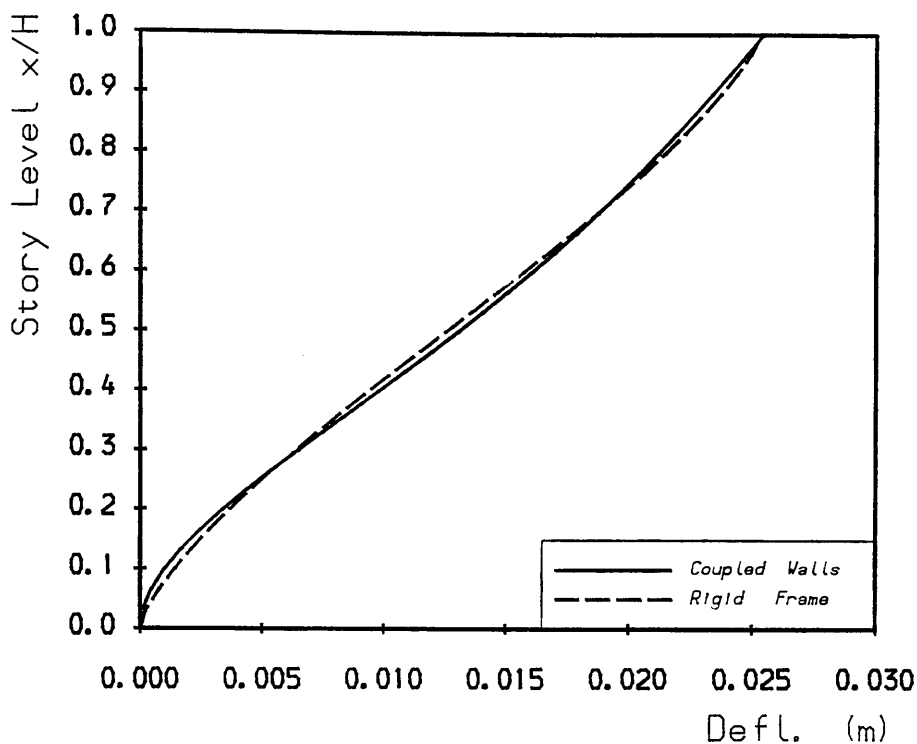


(a) Equivalent Plane System



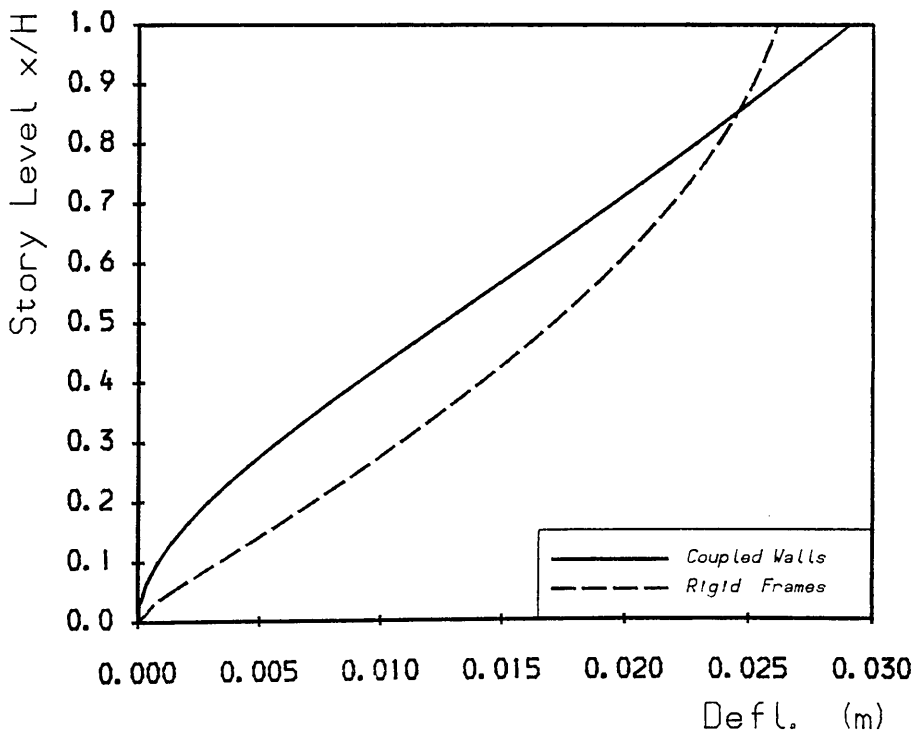
(b) Planform of the Structure

Fig. 6.5 Example of Interactive Coupled Shear Walls and Rigid Frame



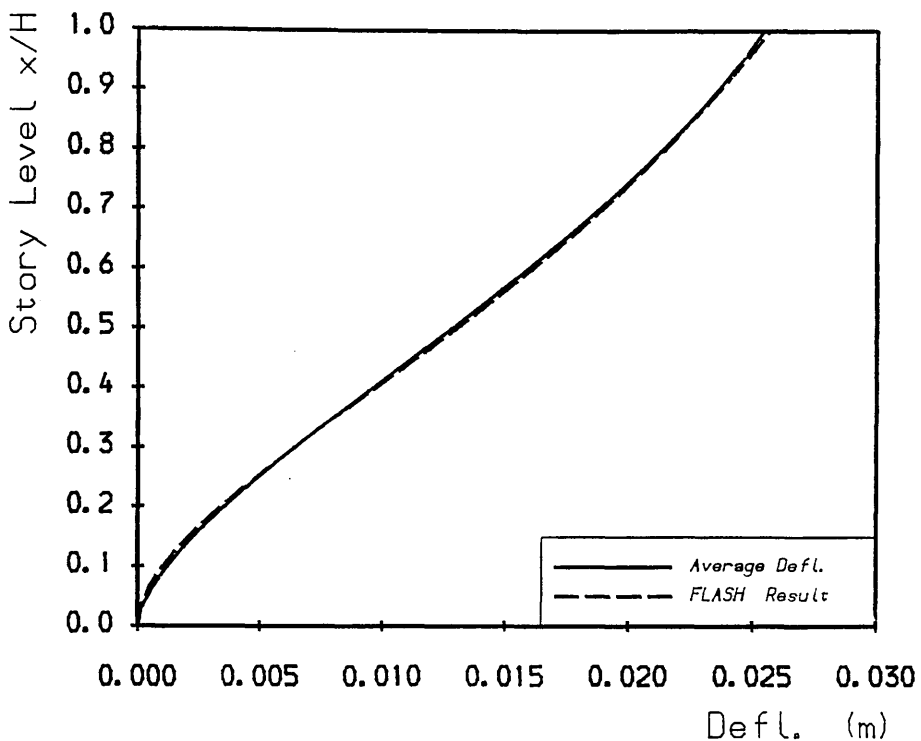
Linked Coupled Walls and Rigid Frame

Fig. 6.6a Resultant Deflections

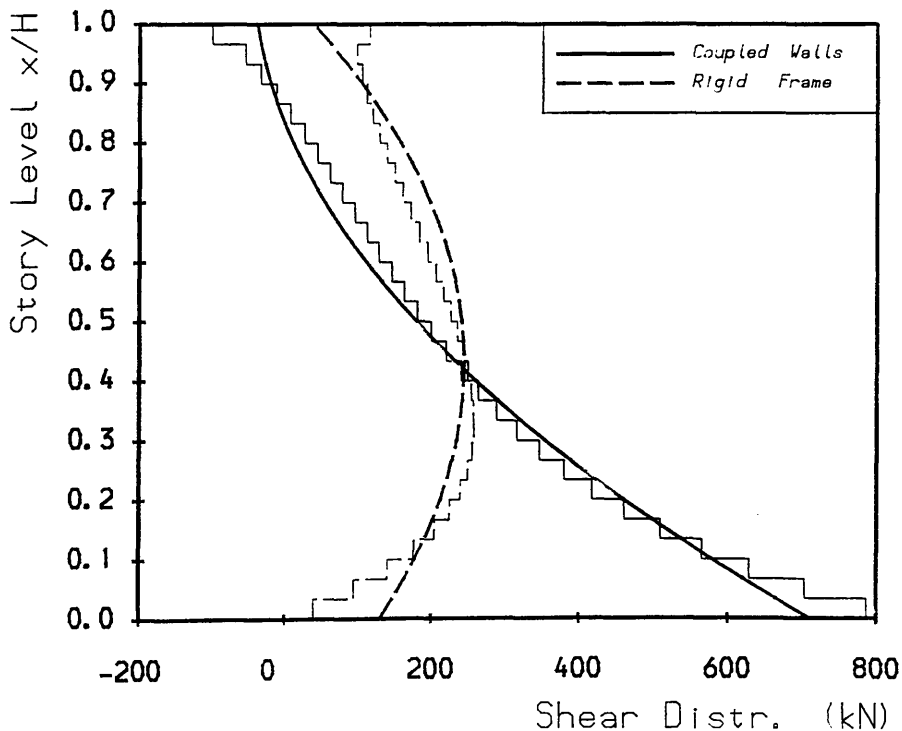


Example Coupled Walls and Rigid Frame

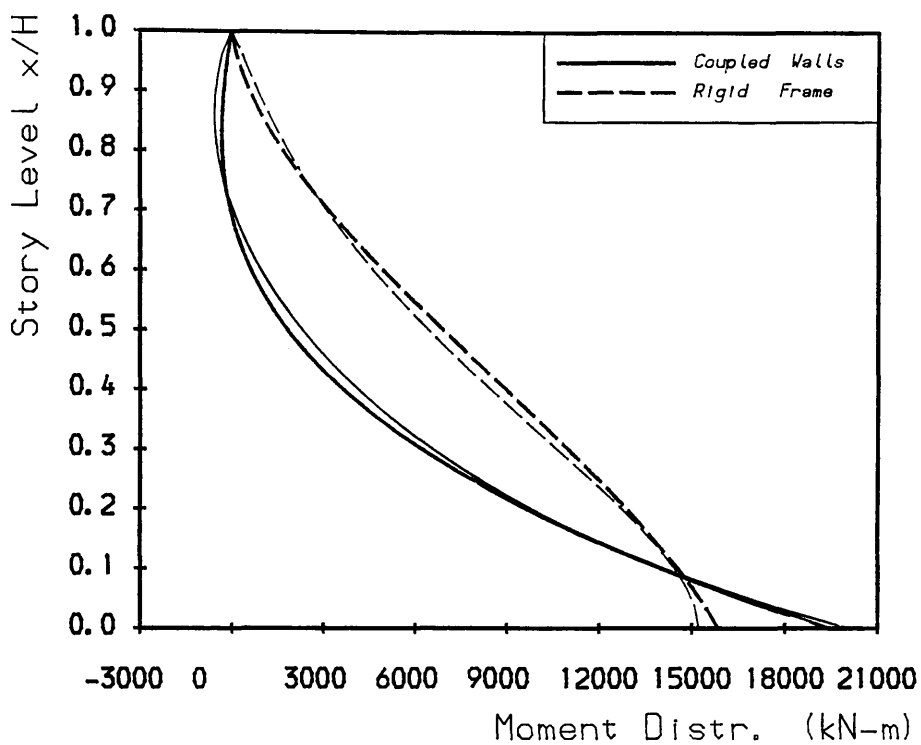
Fig. 6.6b Free Mode of Deflections



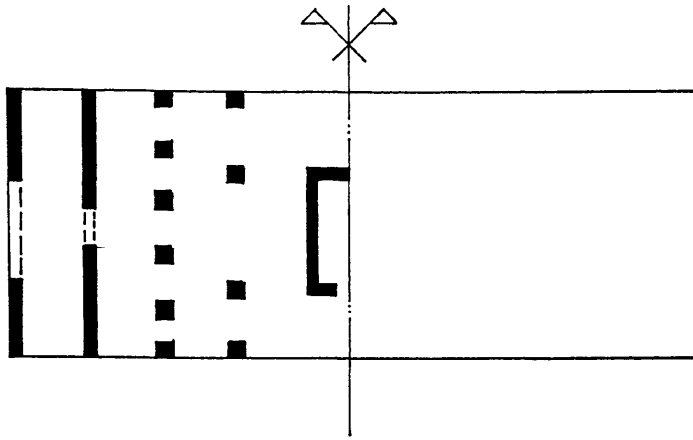
Linked Coupled Walls and Rigid Frame
Fig. 6.6c Deflection



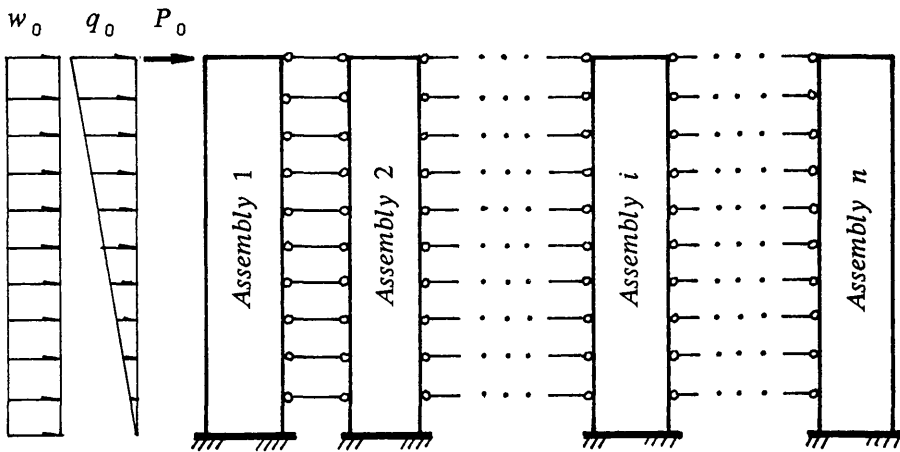
Linked Coupled Walls and Rigid Frame
Fig. 6.6d Shear Distribution



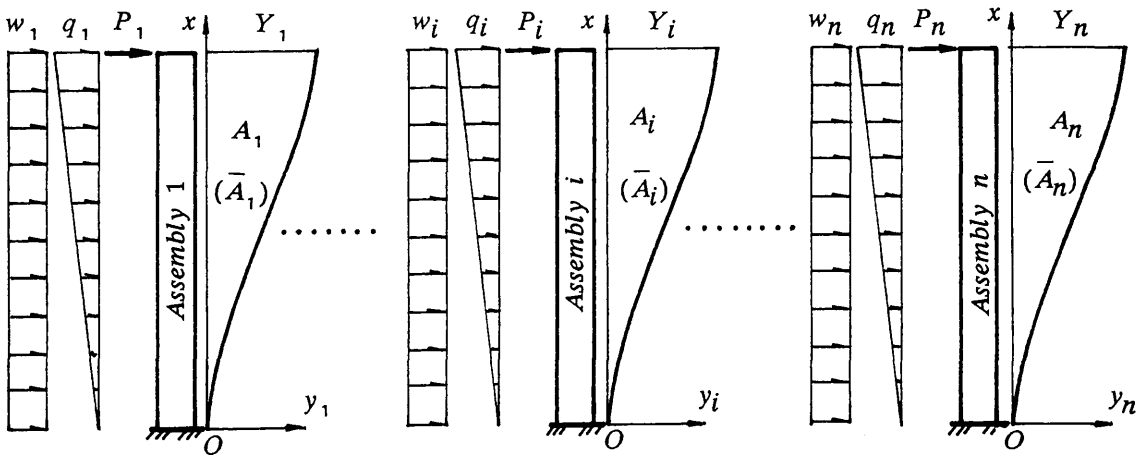
Linked Coupled Walls and Rigid Frame
Fig. 6.6e Moment Distribution



(a) Planform of Representative Structure

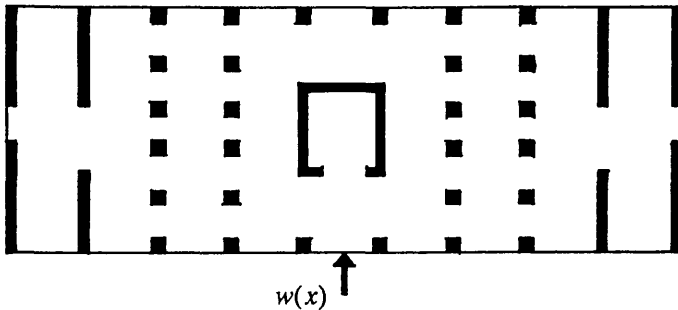


(b) Equivalent Plane System

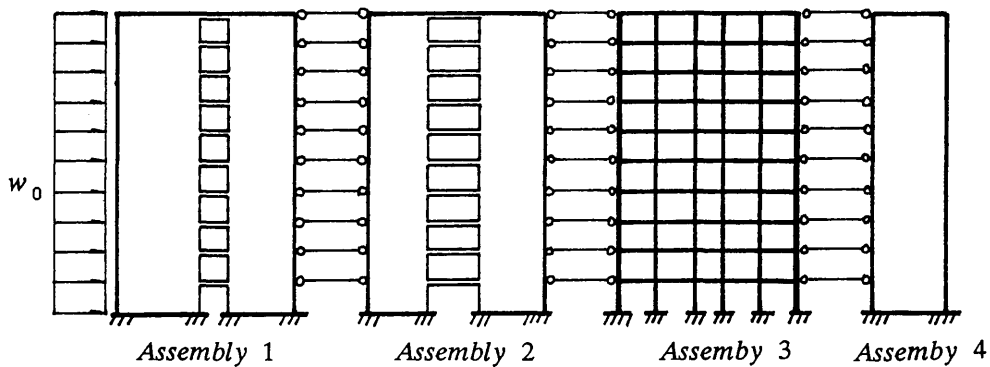


(c) Assumed Load Distributions and Deflections

Fig. 6.7 Symmetric Structure Subjected to Pure Bending

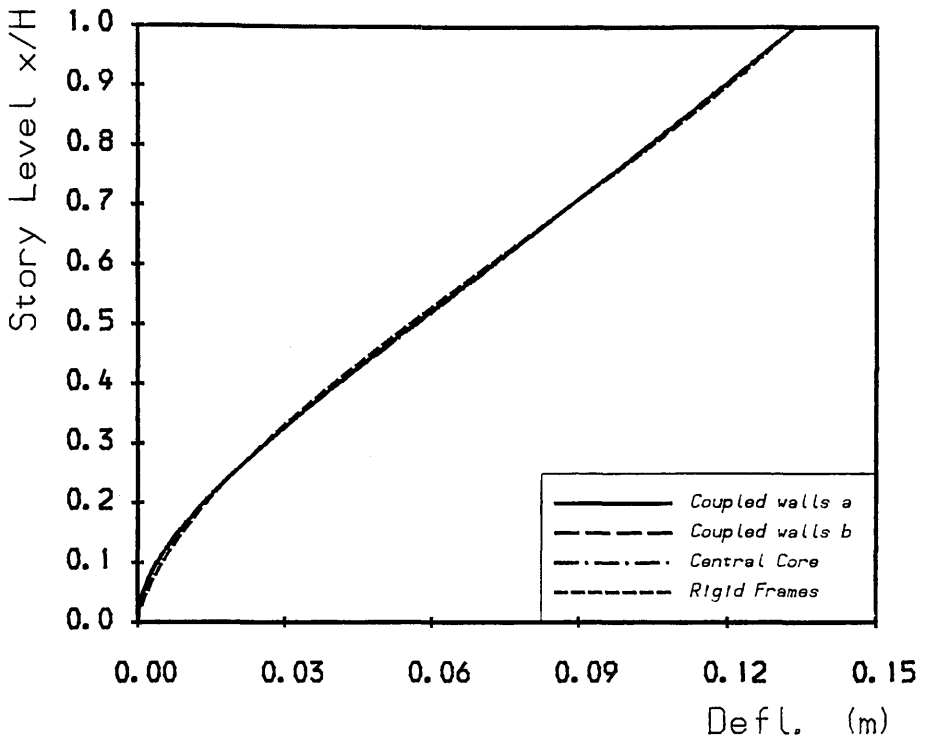


(a) Planform of Structure

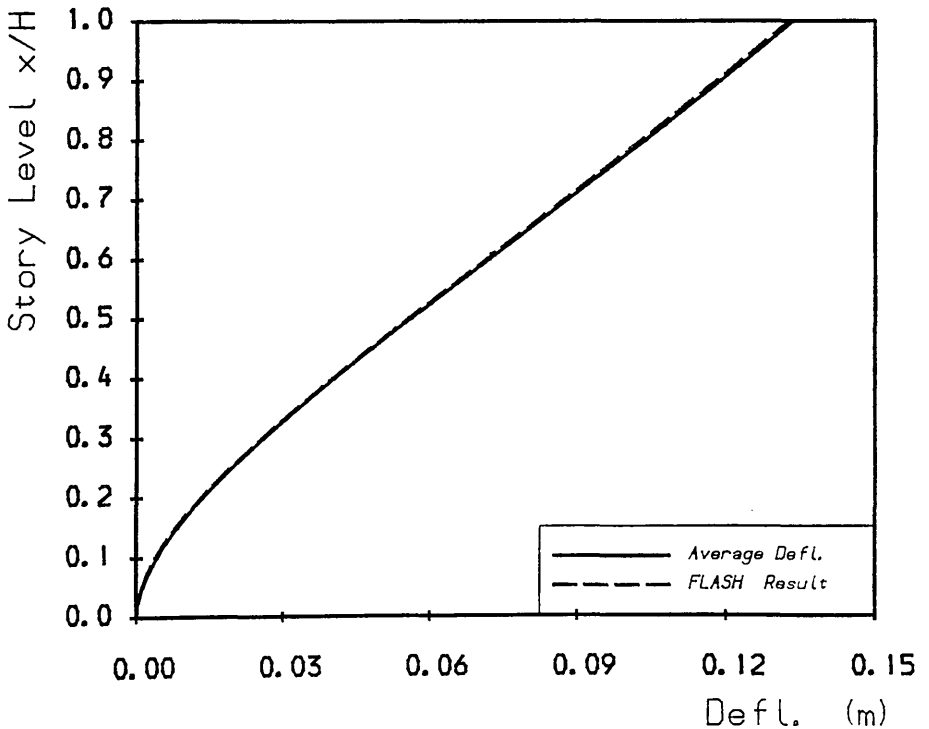


(b) Equivalent Plane System

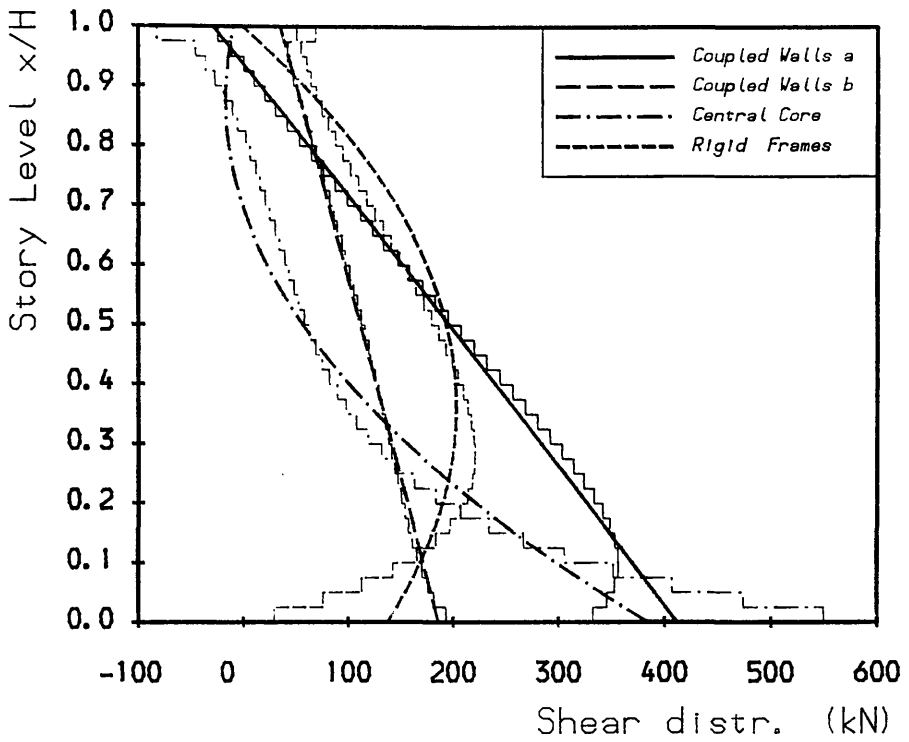
Fig. 6.8 Symmetric Example Structure 1



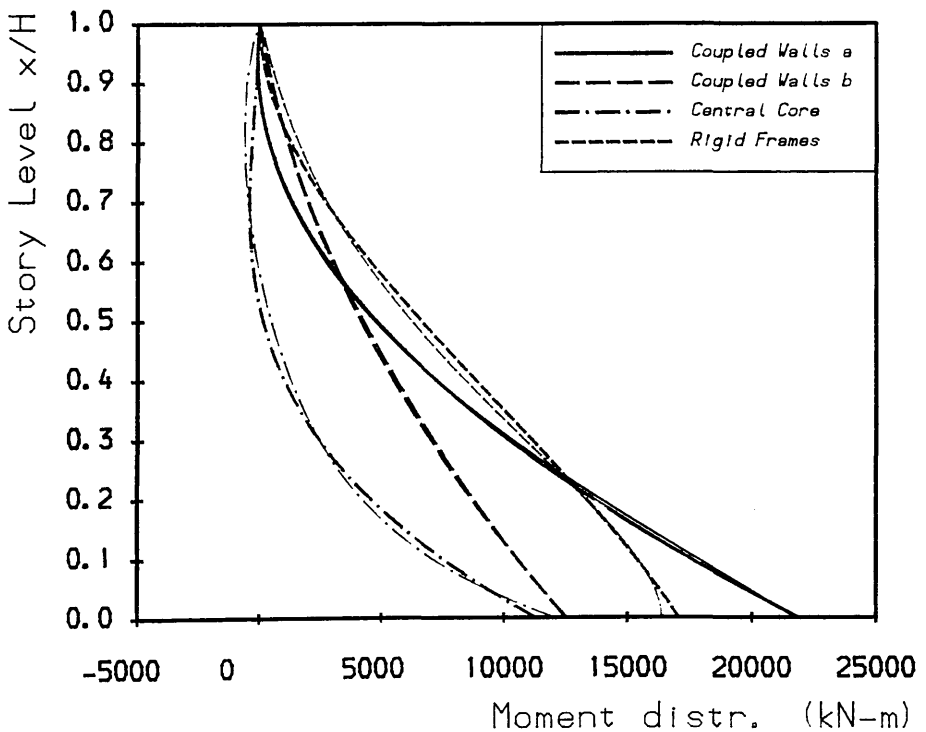
Symmetric Structure Example 1
Fig. 6.9a Resultant Deflections



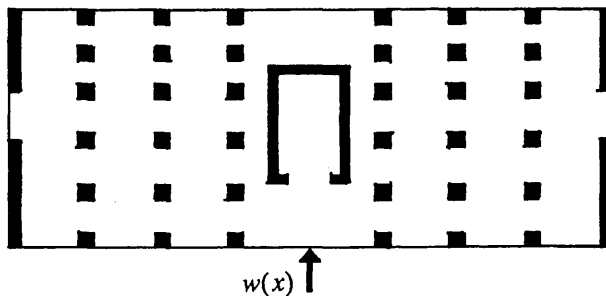
Symmetric Structure Example 1
Fig. 6.9b Deflection



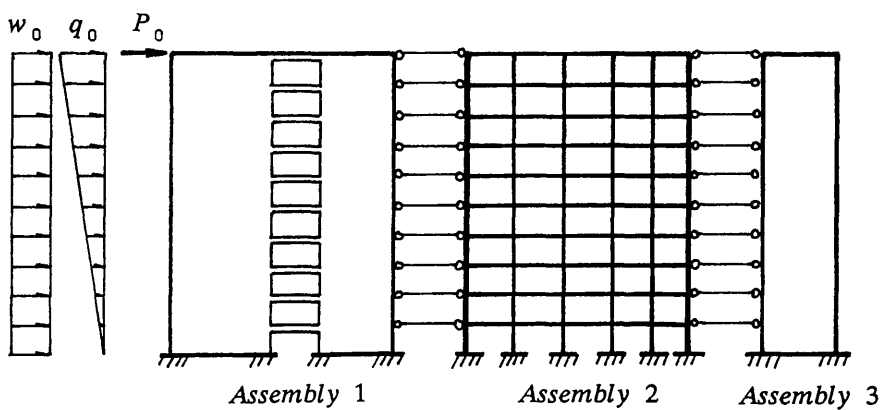
Symmetric Structure Example 1
Fig. 6.9c Shear Distribution



Symmetric Structure Example 1
Fig. 6.9d Moment Distribution

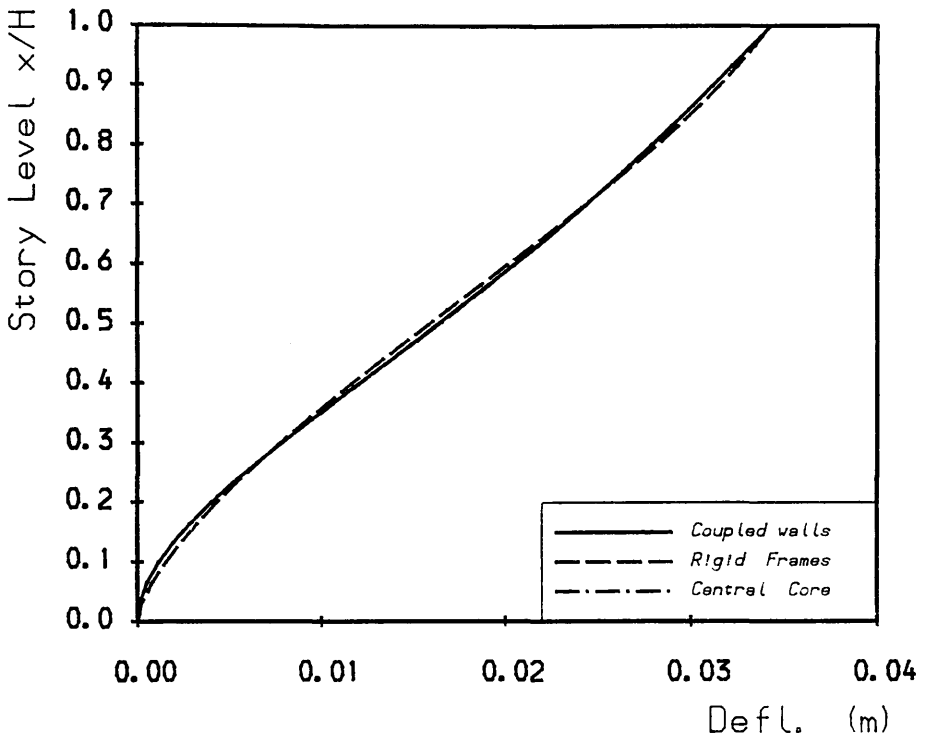


(a) Planform of Structure



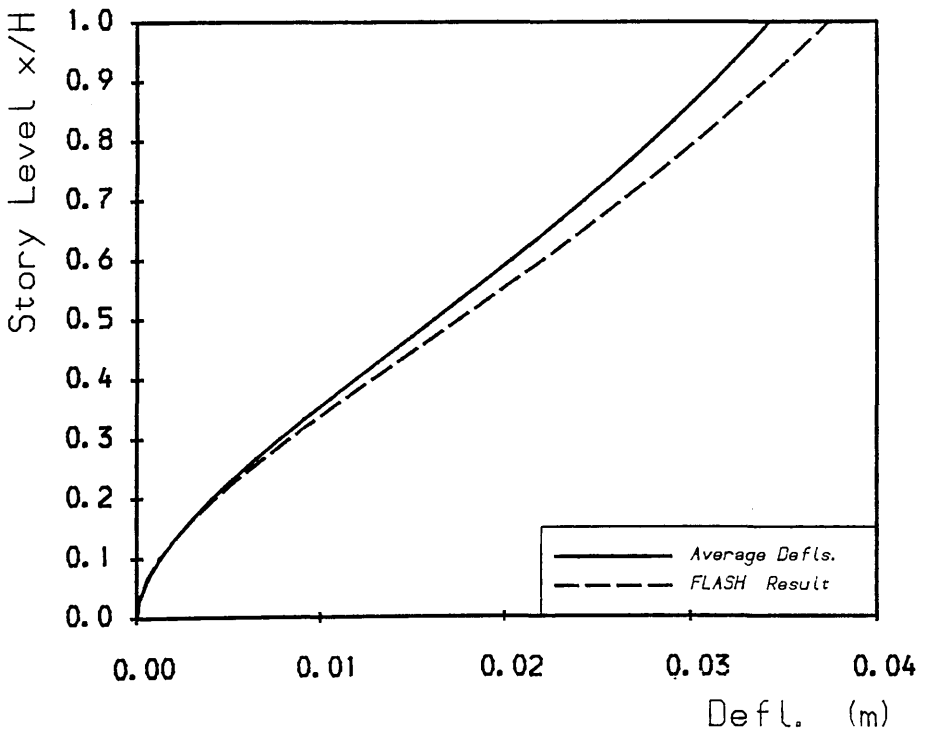
(b) Equivalent Plane System

Fig. 6.10 Symmetric Example Structure 2



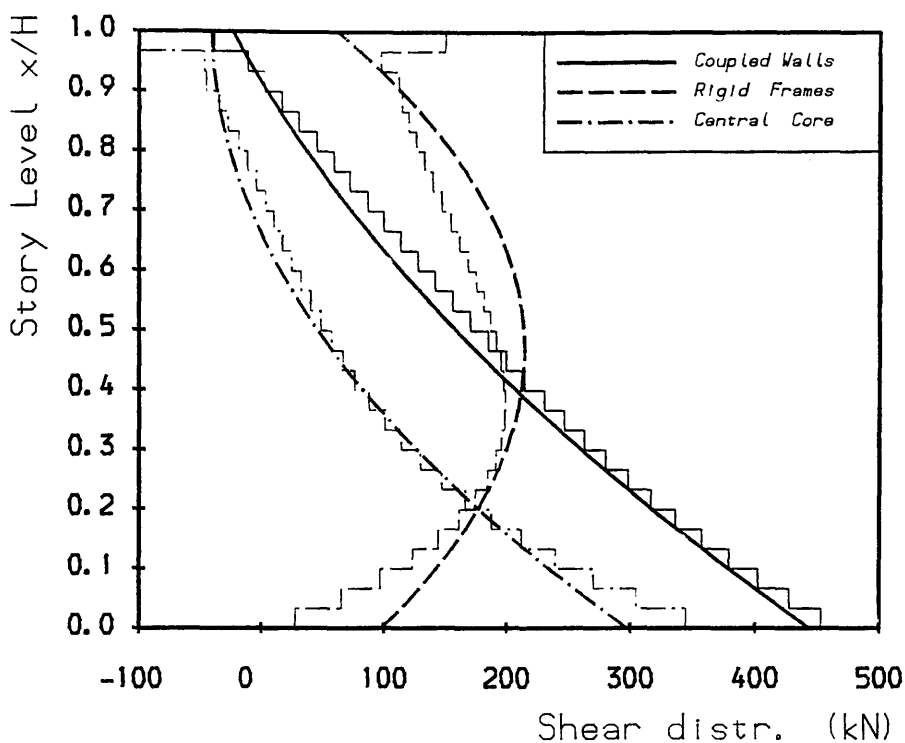
Symmetric Structure Example 2

Fig. 6.11a Load Case 1, Resultant Deflections



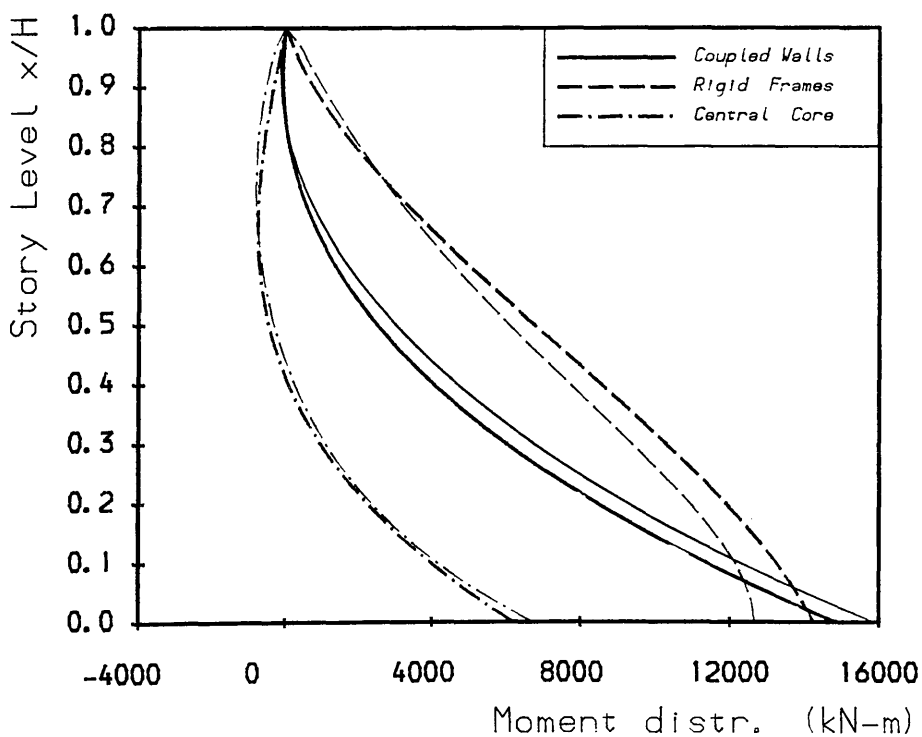
Symmetric Structure Example 2

Fig. 6.11b Load Case 1, Deflection



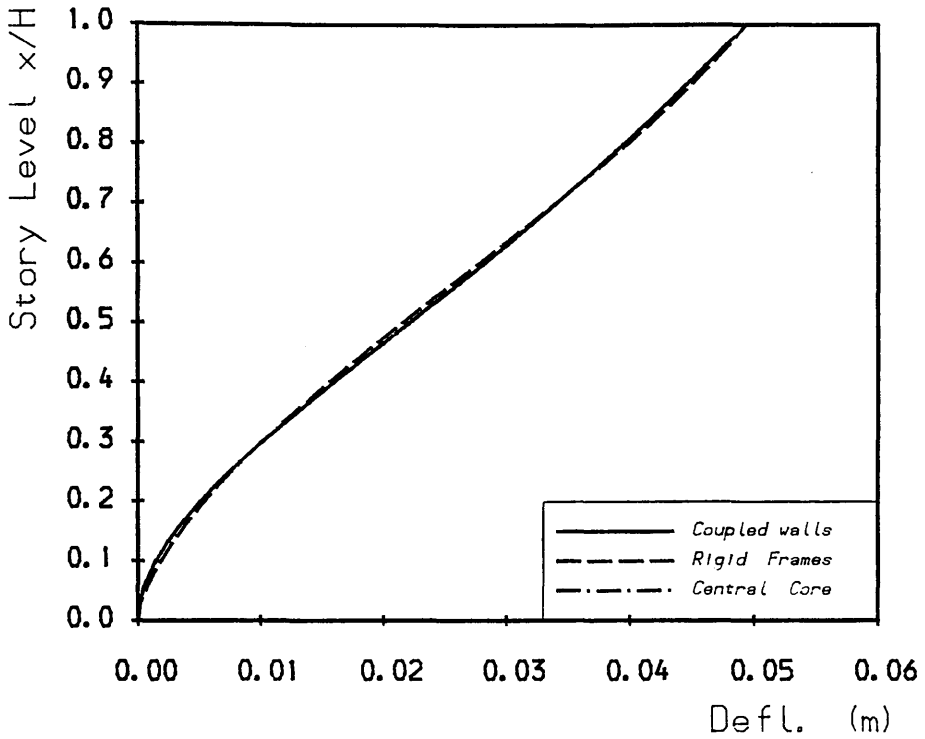
Symmetric Structure Example 2

Fig. 6.11c Load Case 1, Shear Distribution



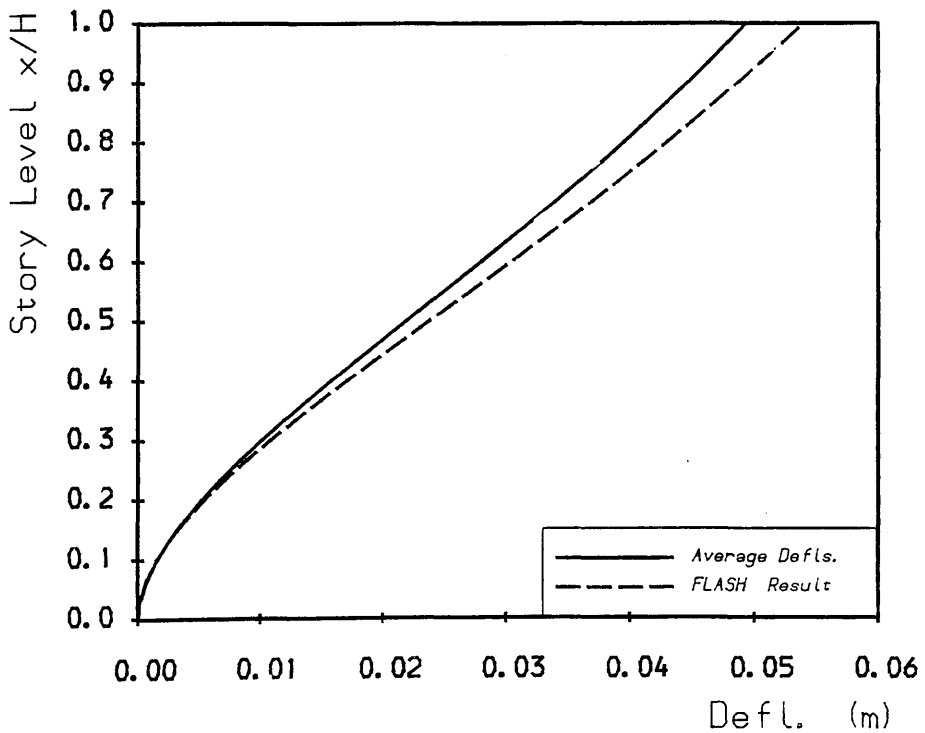
Symmetric Structure Example 2

Fig. 6.11d Load Case 1, Moment Distribution



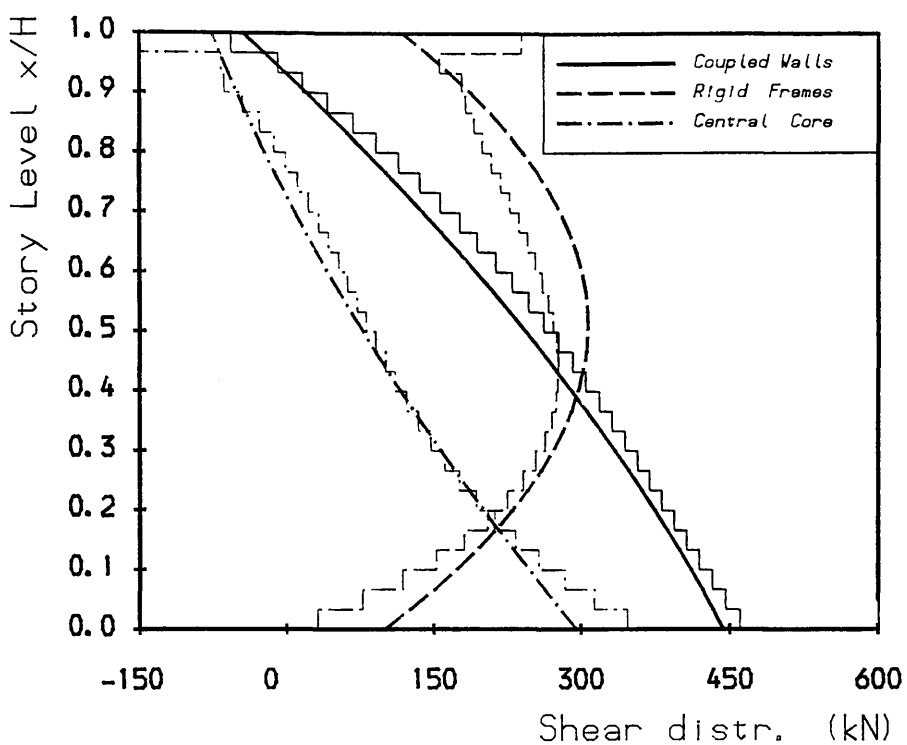
Symmetric Structure Example 2

Fig. 6.12a Load Case 2, Resultant Deflections



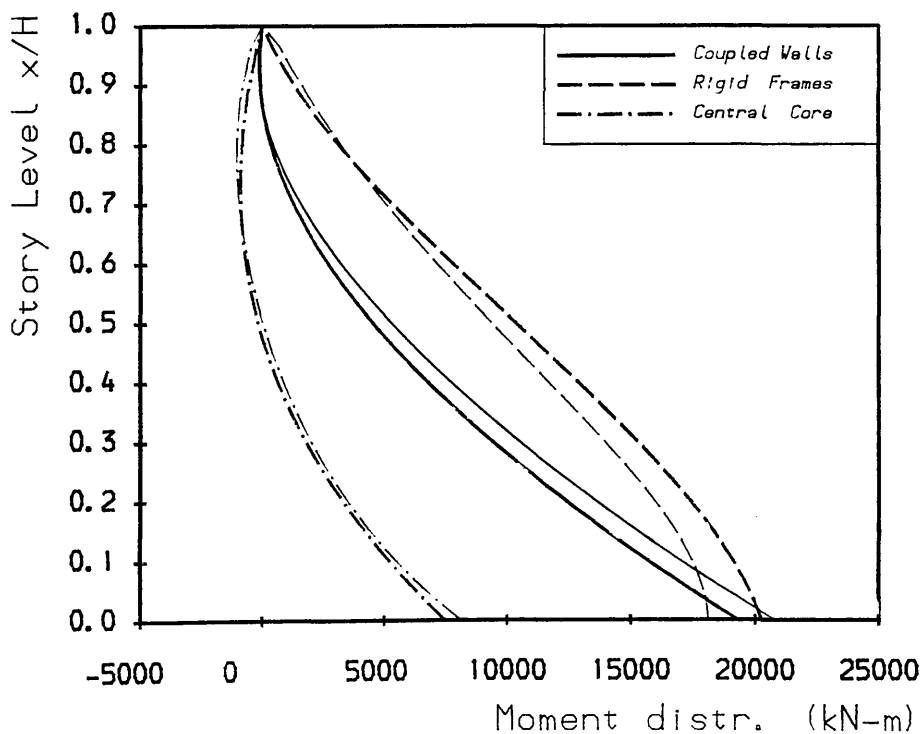
Symmetric Structure Example 2

Fig. 6.12b Load Case 2, Deflection



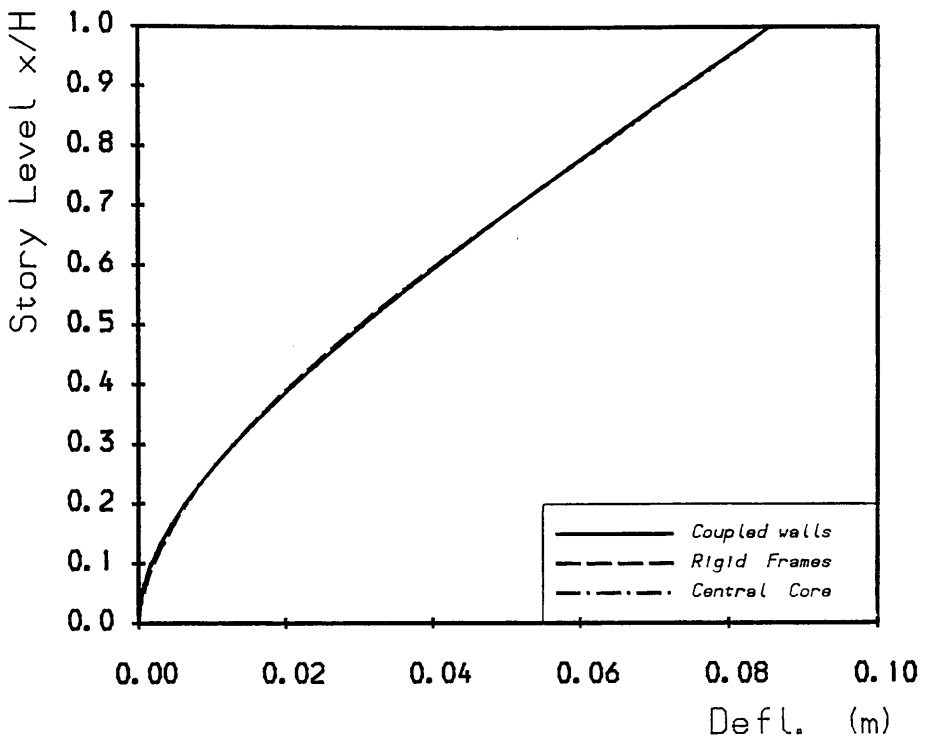
Symmetric Structure Example 2

Fig. 6.12c Load Case 2, Shear Distribution



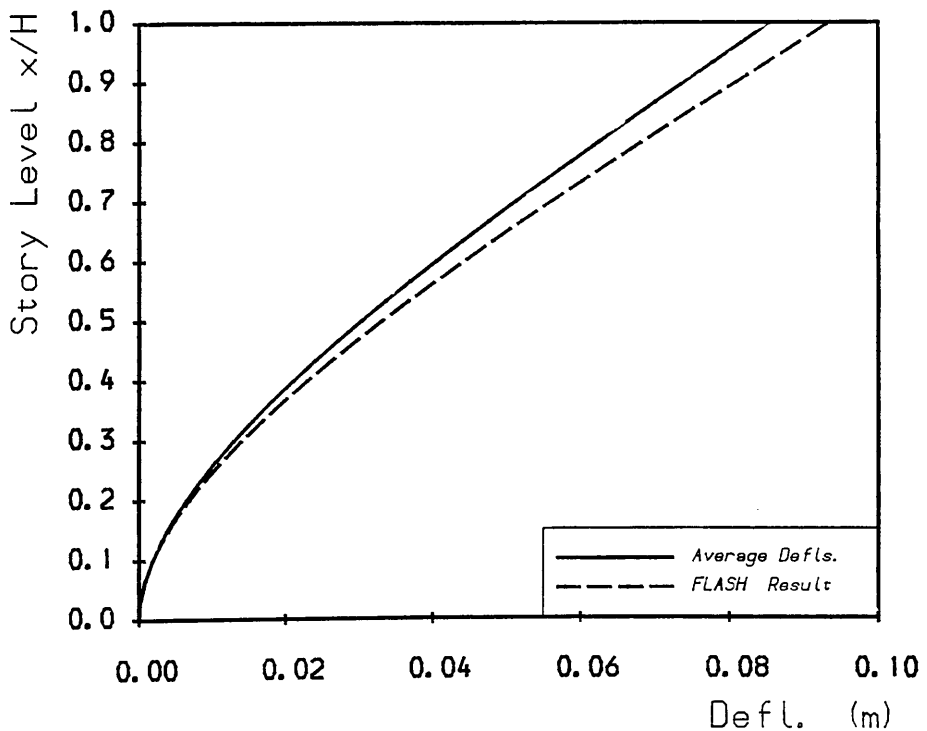
Symmetric Structure Example 2

Fig. 6.12d Load Case 2, Moment Distribution



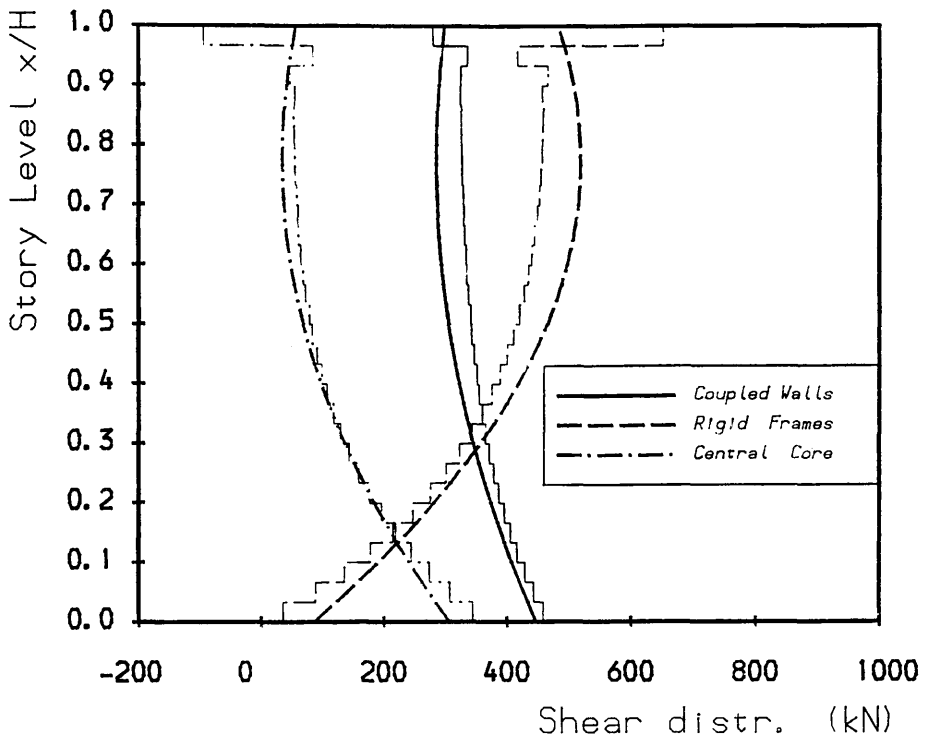
Symmetric Structure Example 2

Fig. 6.13a Load Case 3, Resultant Deflections



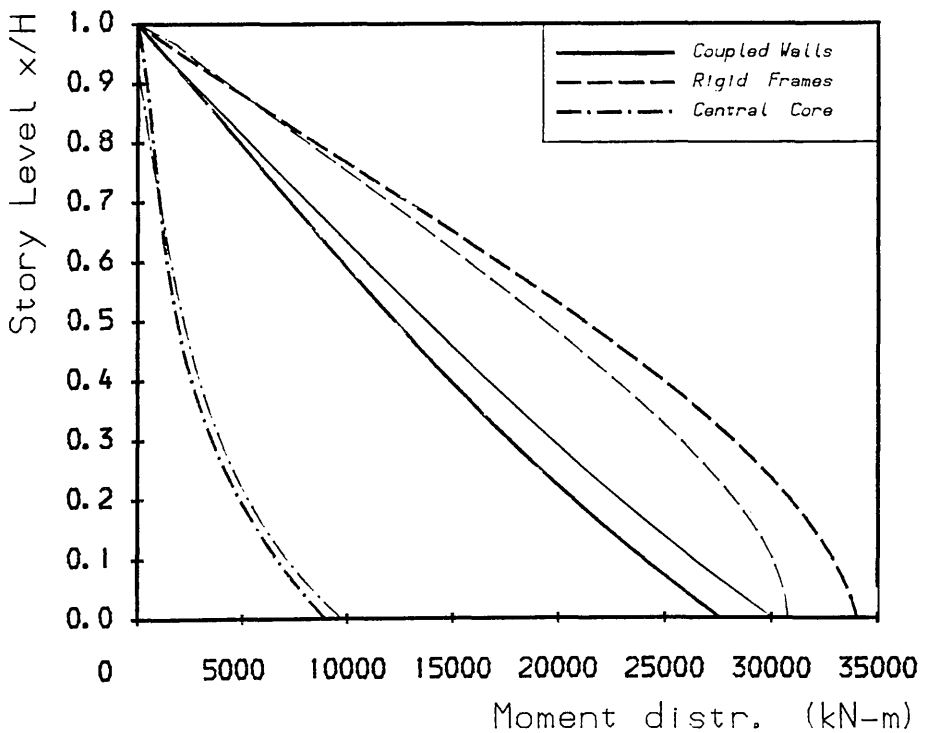
Symmetric Structure Example 2

Fig. 6.13b Load Case 3, Deflection



Symmetric Structure Example 2

Fig. 6.13c Load Case 3, Shear Distribution



Symmetric Structure Example 2

Fig. 6.13d Load Case 3, Moment Distribution

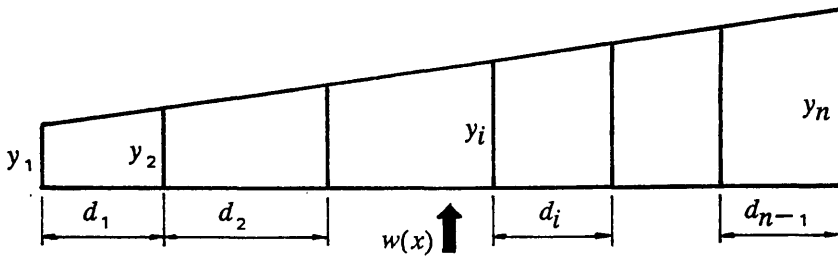


Fig. 6.14 Displacement Diagram of Assembly

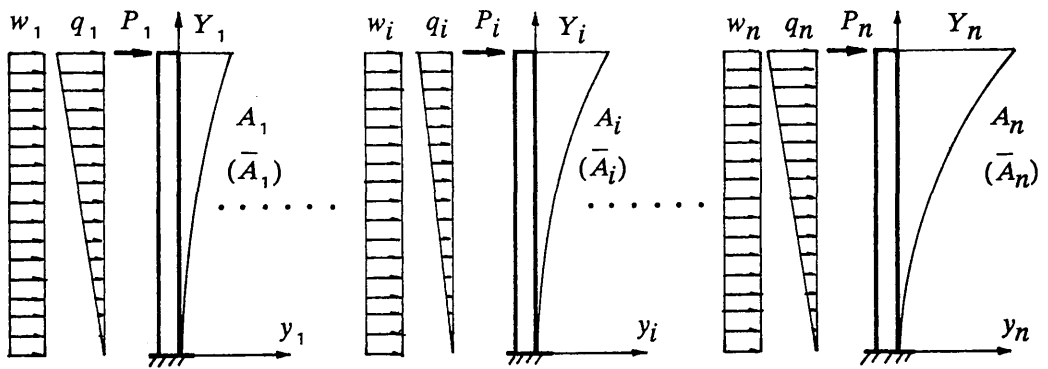


Fig. 6.15 Assumed Load Distribution and Deflection

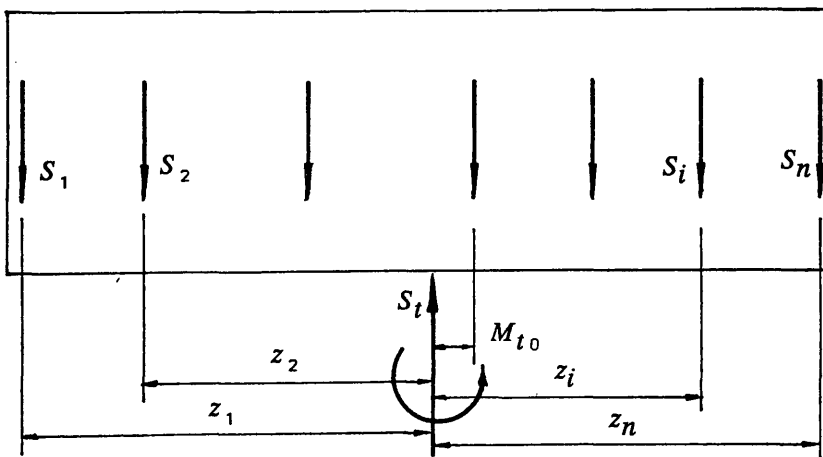


Fig. 6.16 Illustration of Horizontal Force and Twisting Moment Equilibrium

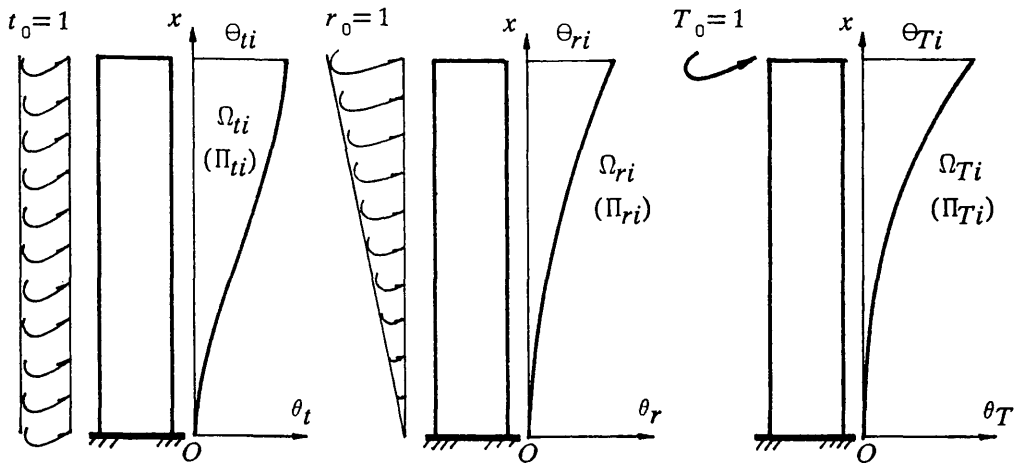


Fig. 6.17 Torsional Area Influence Coefficients For an Assembly

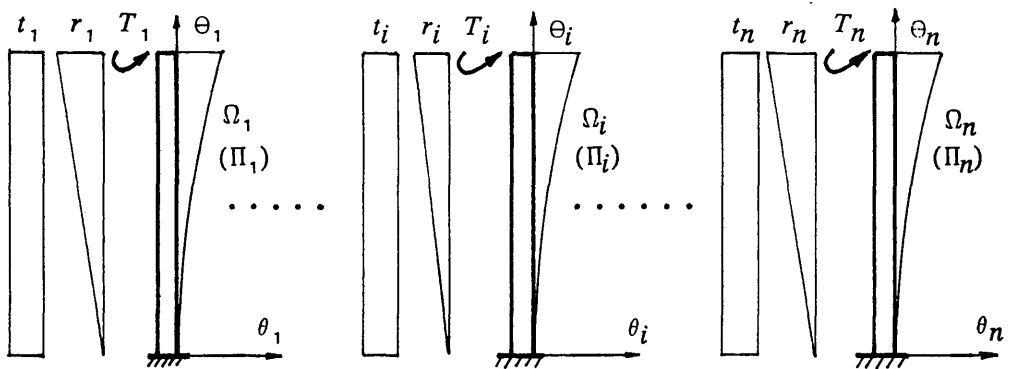


Fig. 6.18 Assumed Torsion Distribution and Rotation

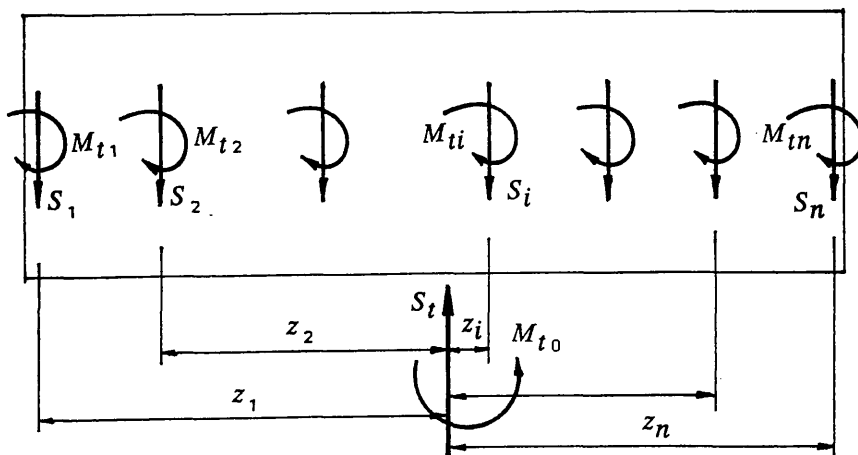
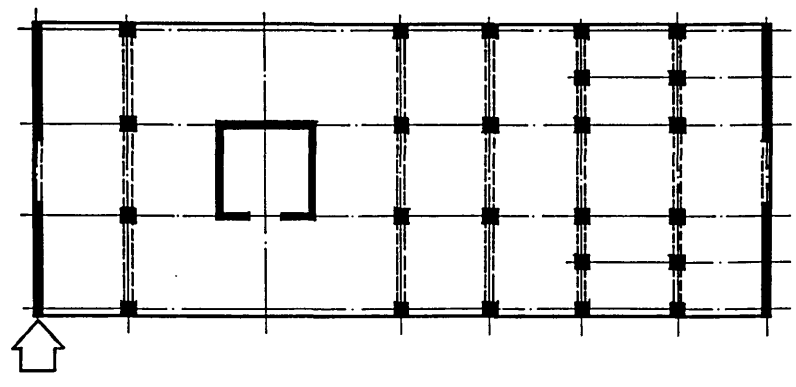
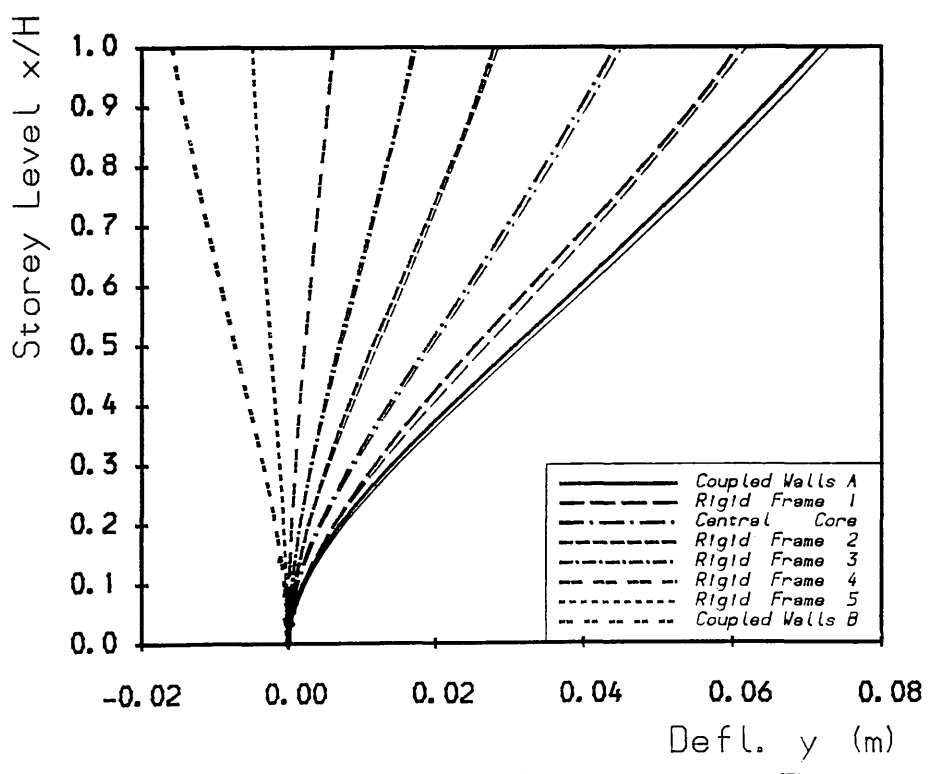


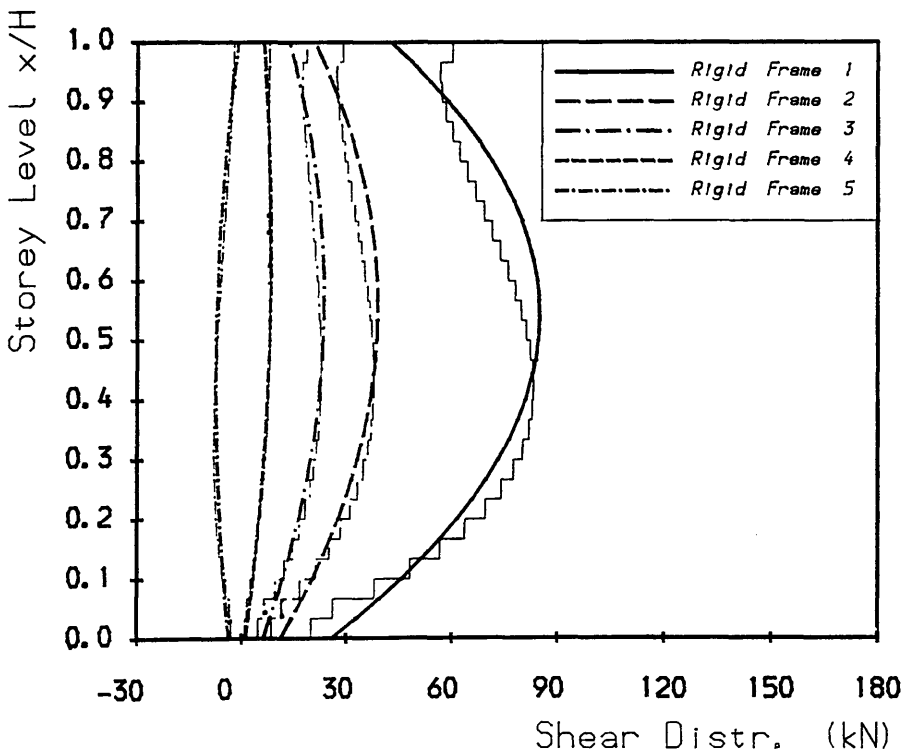
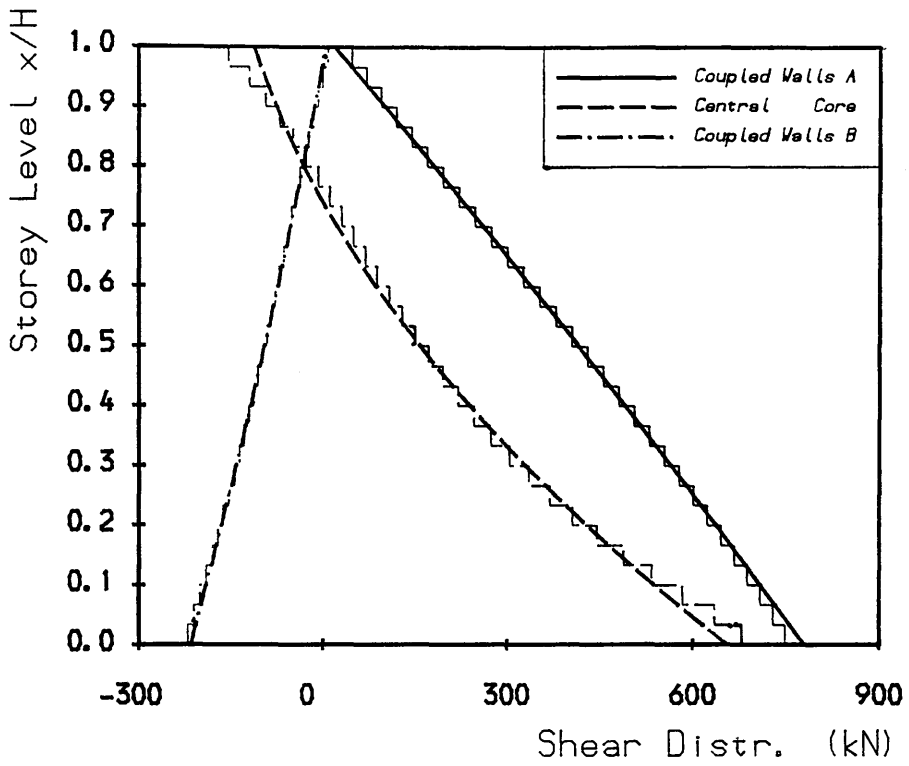
Fig. 6.19 Illustration of Horizontal Force and Twisting Moment Equilibrium



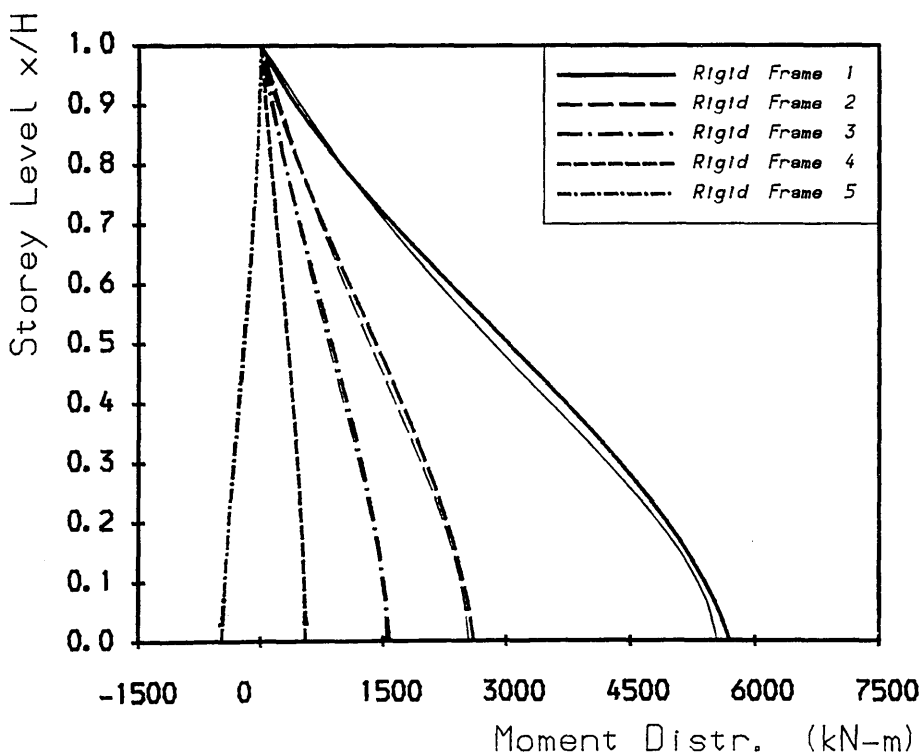
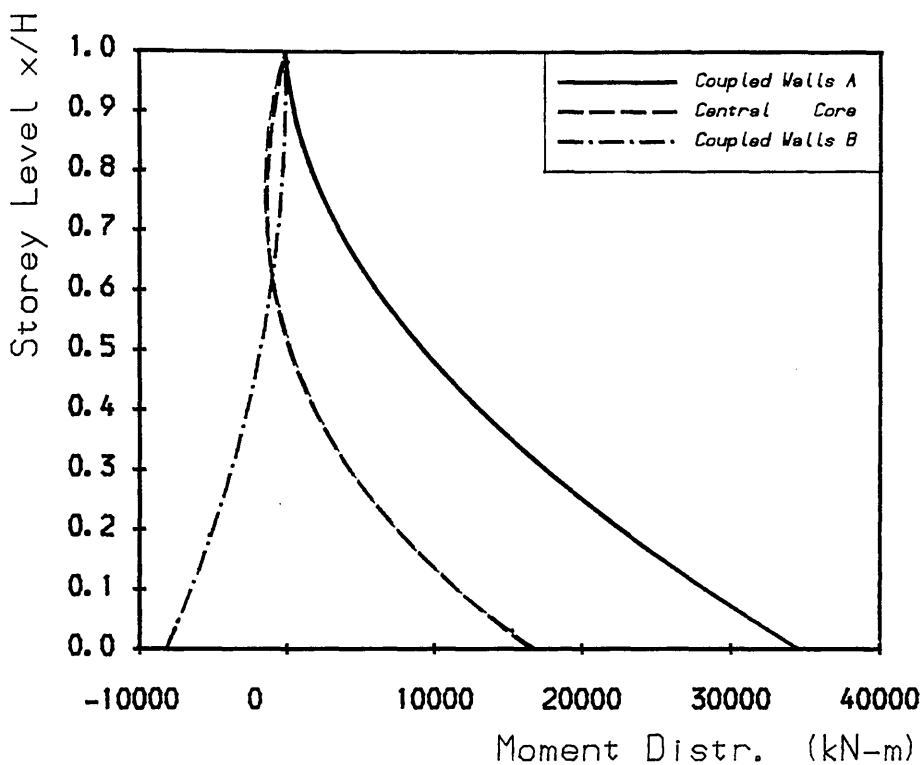
Load Position 1



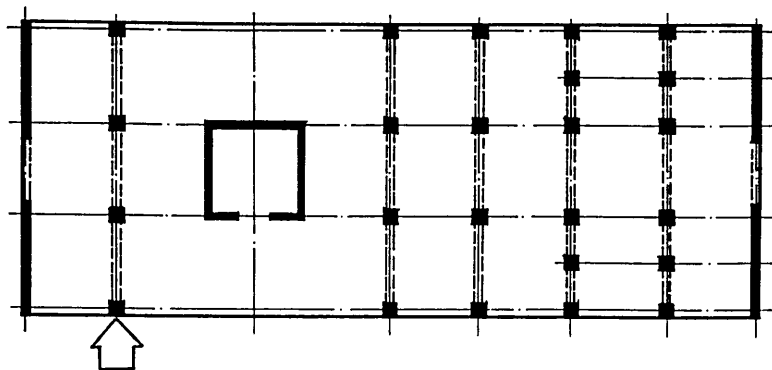
Three-Dimensional Structure Example
Fig. 6.20a Load Position 1. Deflections



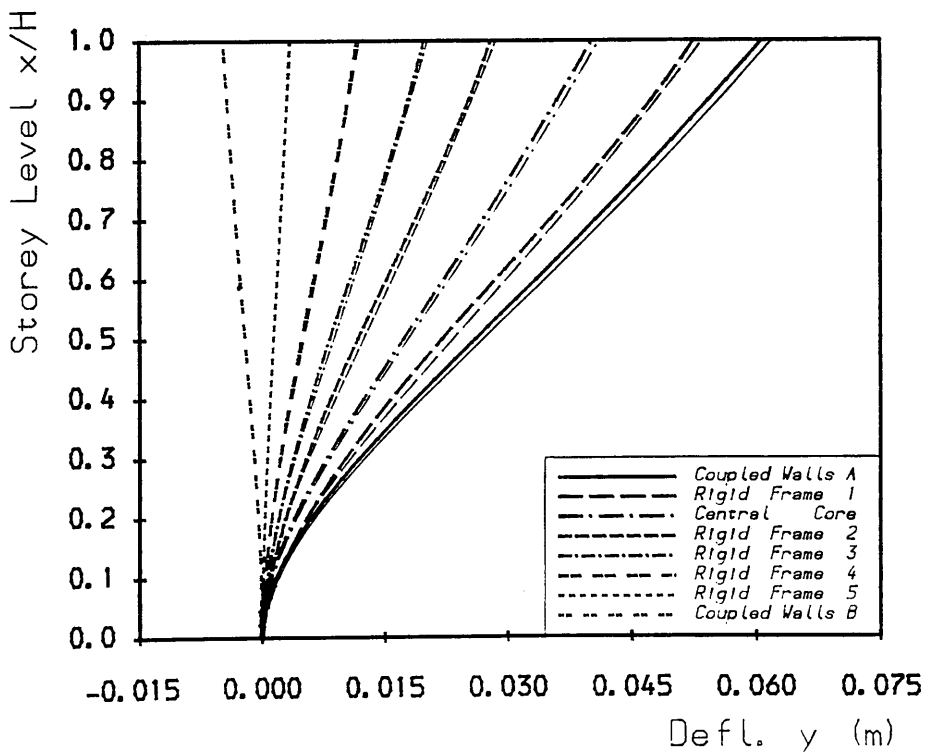
Three-Dimensional Structure Example
Fig. 6.20b Load Position 1, Shear Distributions



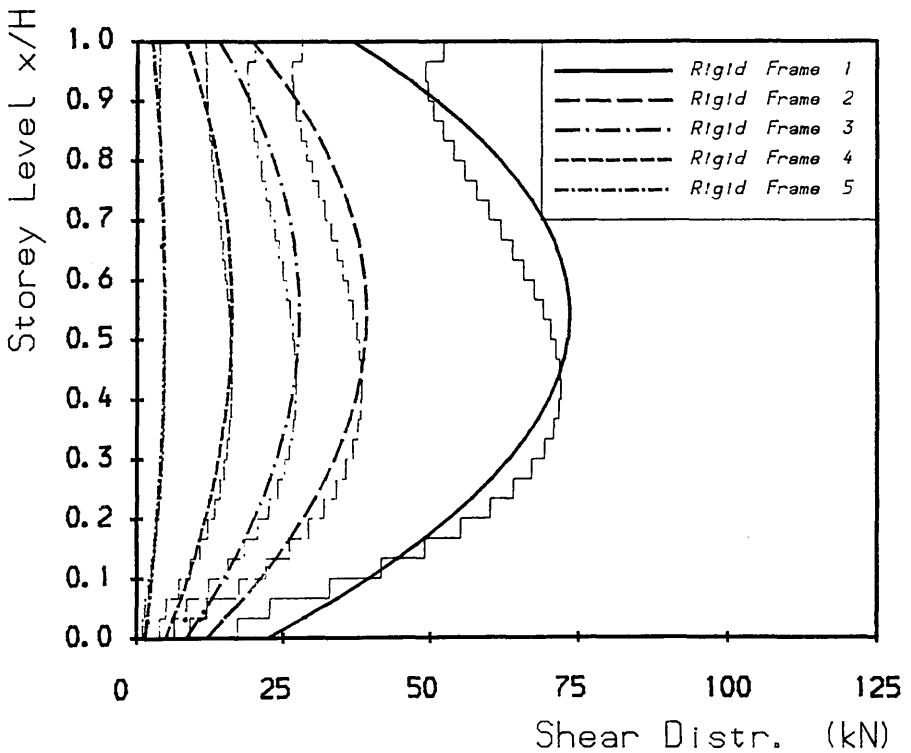
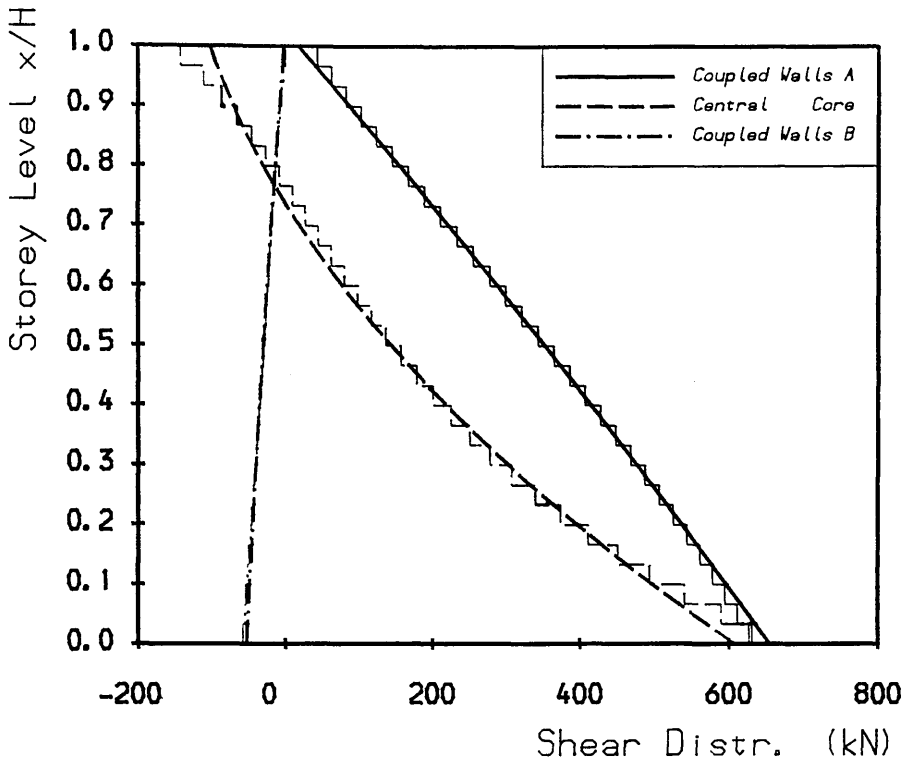
Three-Dimensional Structure Example
Fig. 6.20c Load Position 1, Moment Distributions



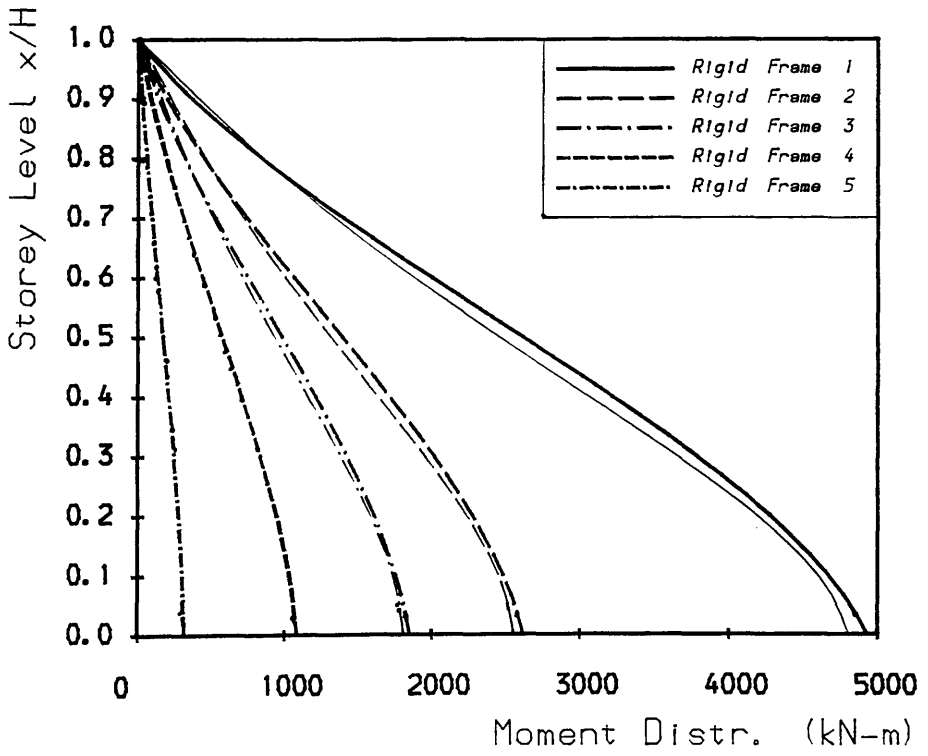
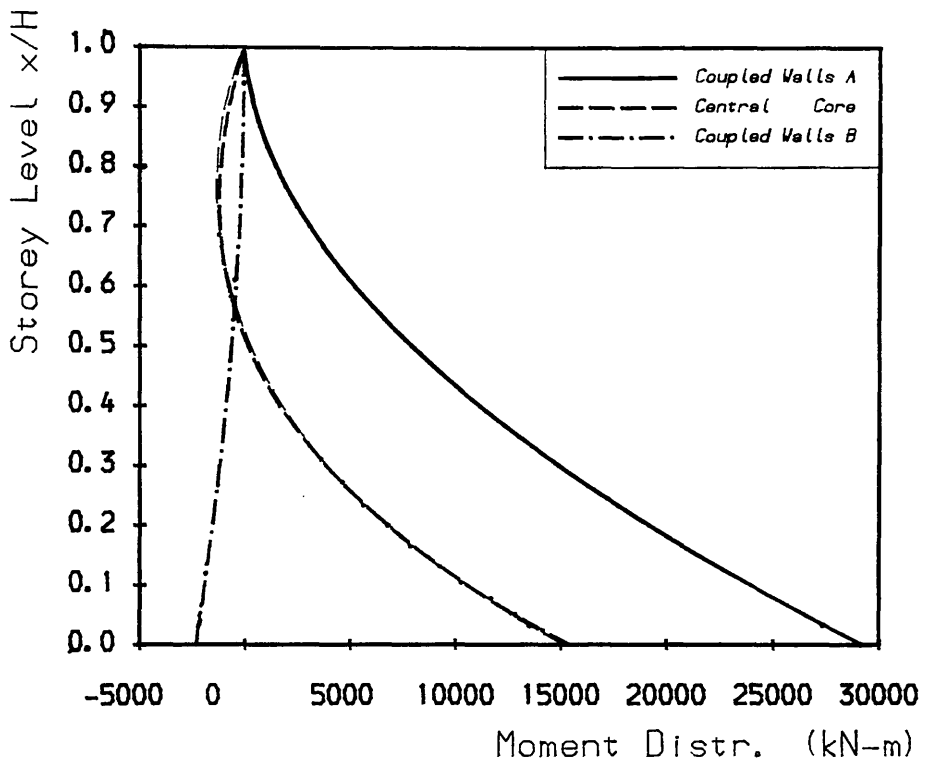
Load Position 2



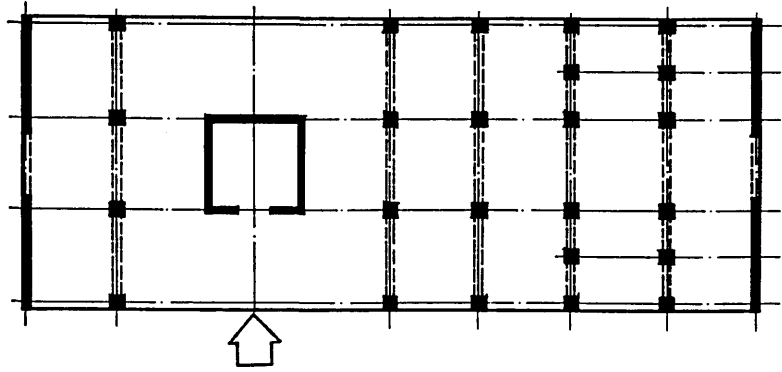
Three-Dimensional Structure Example
Fig. 6.21a Load Position 2. Deflections



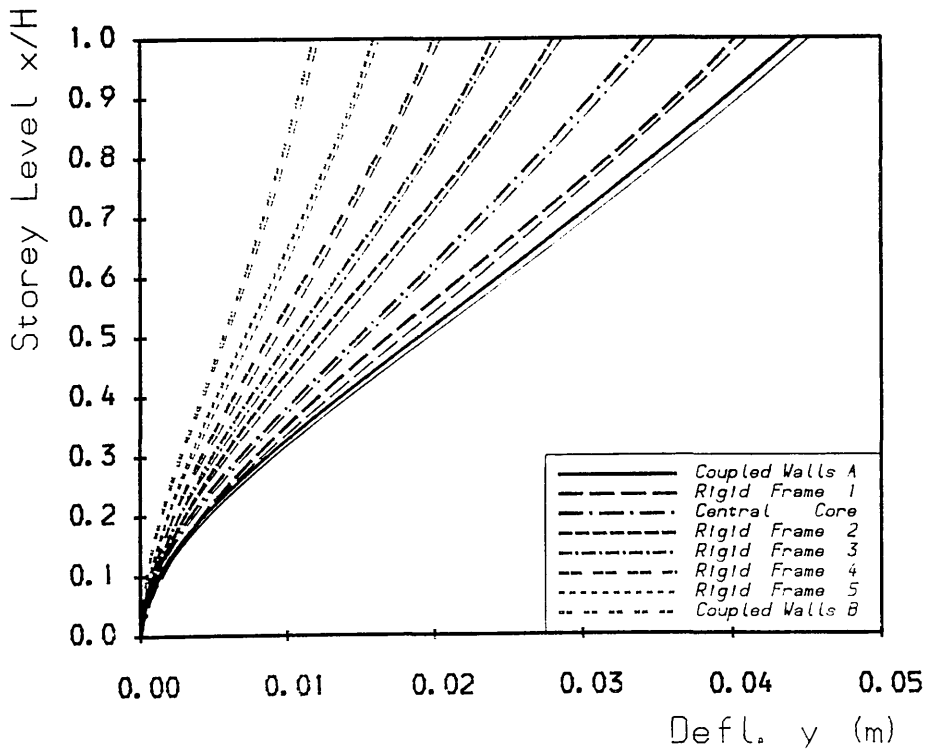
Three-Dimensional Structure Example
Fig. 6.21b Load Position 2, Shear Distributions



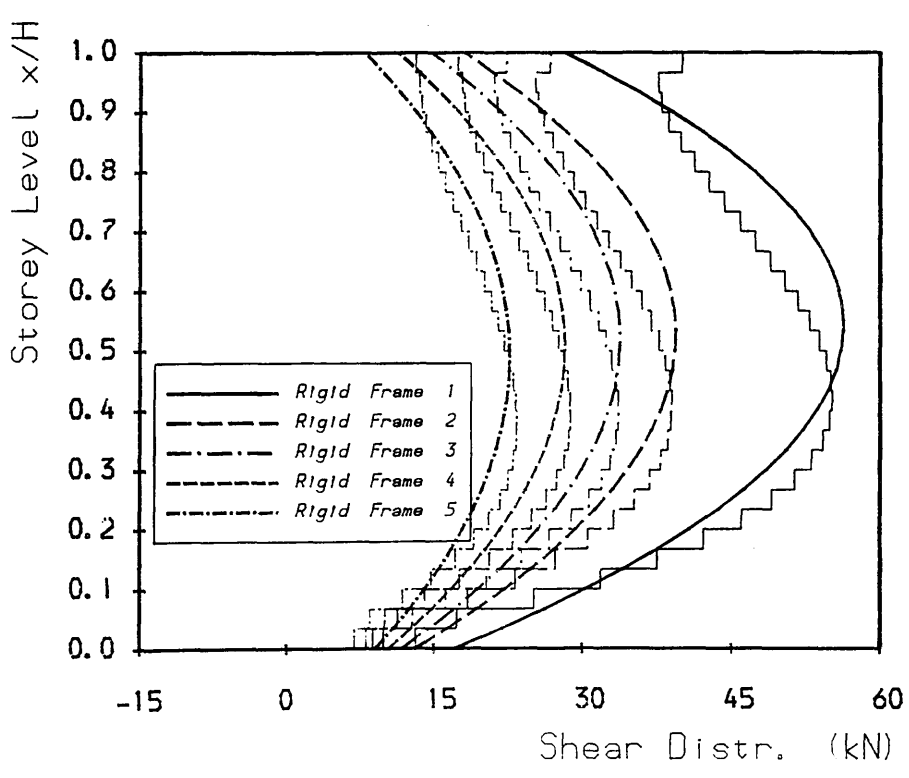
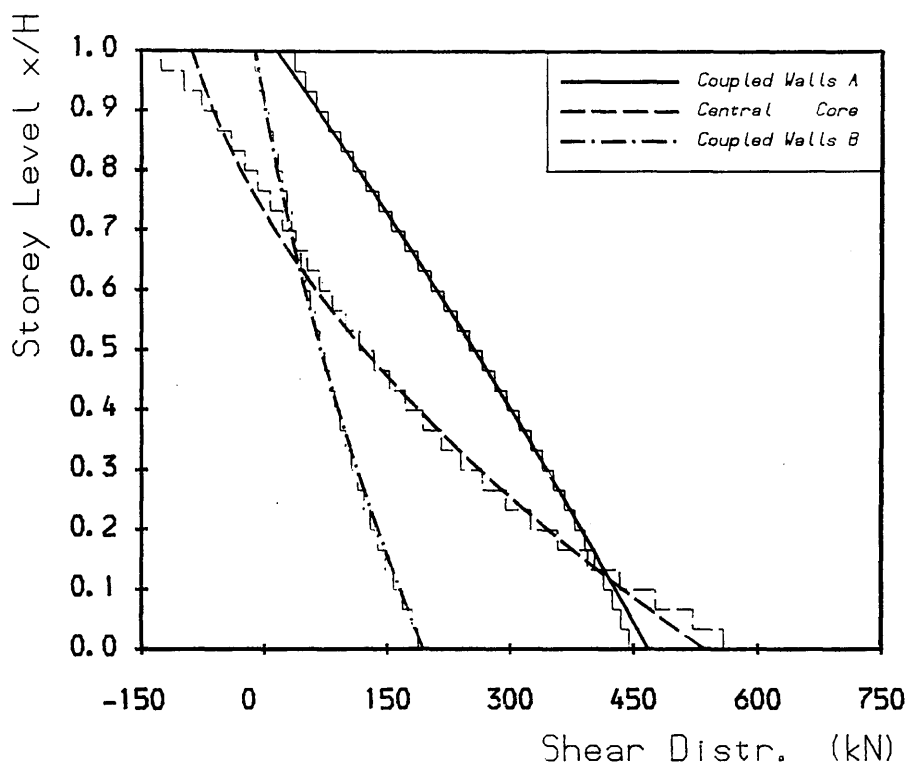
Three-Dimensional Structure Example
Fig. 6.21c Load Position 2, Moment Distributions



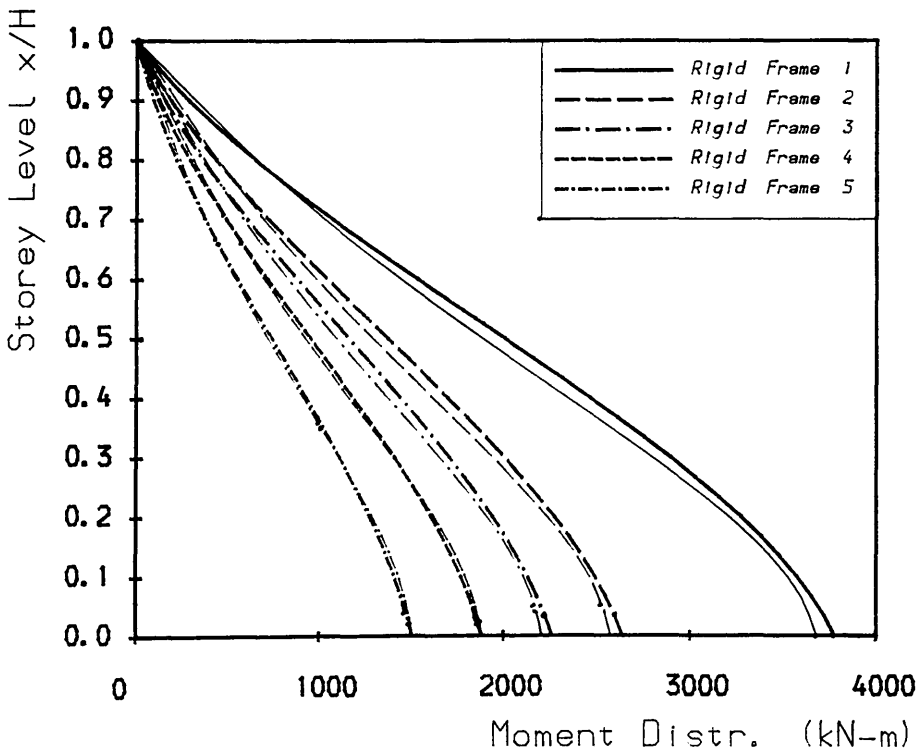
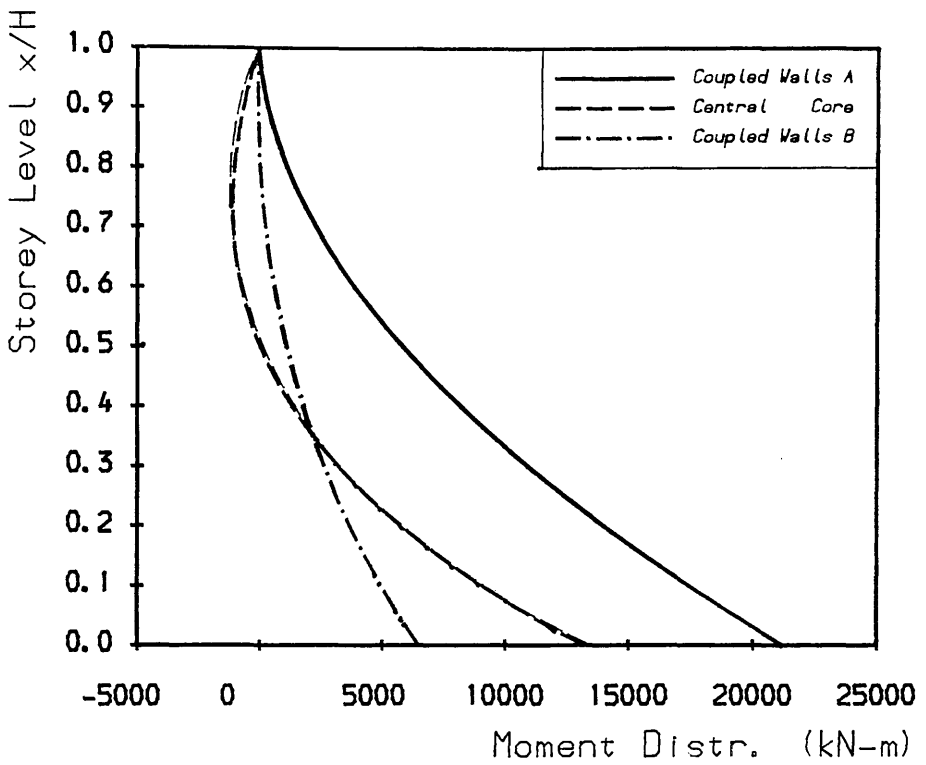
Load Position 3



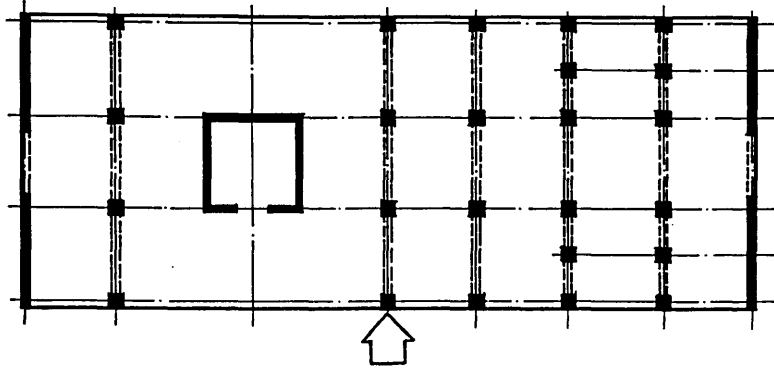
Three-Dimensional Structure Example
Fig. 6.22a Load Position 3. Deflections



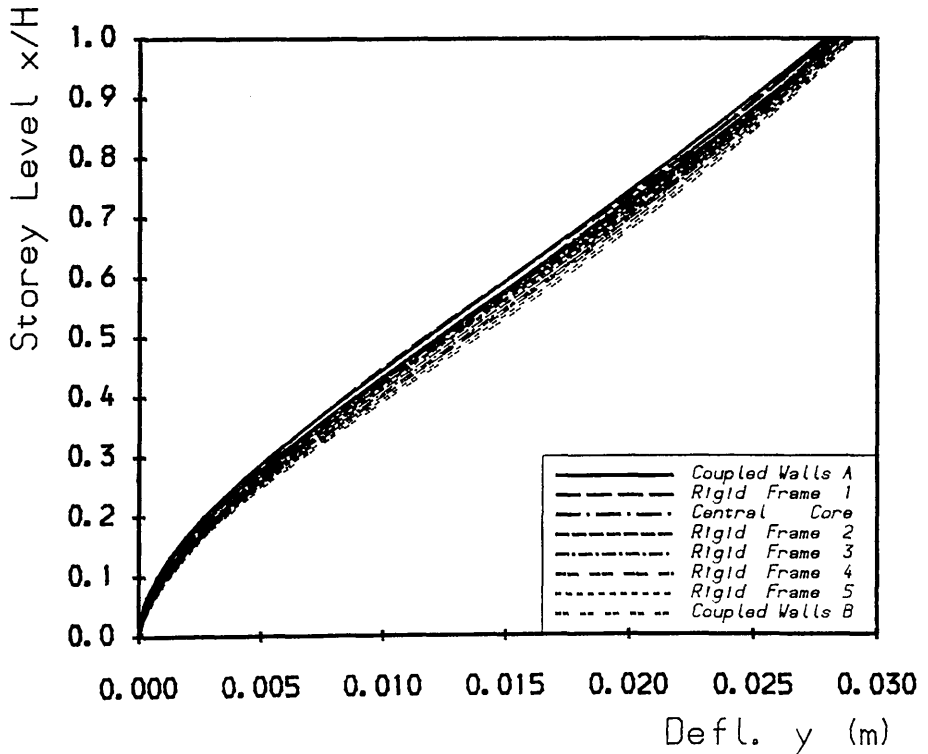
Three-Dimensional Structure Example
Fig. 6.22b Load Position 3, Shear Distributions



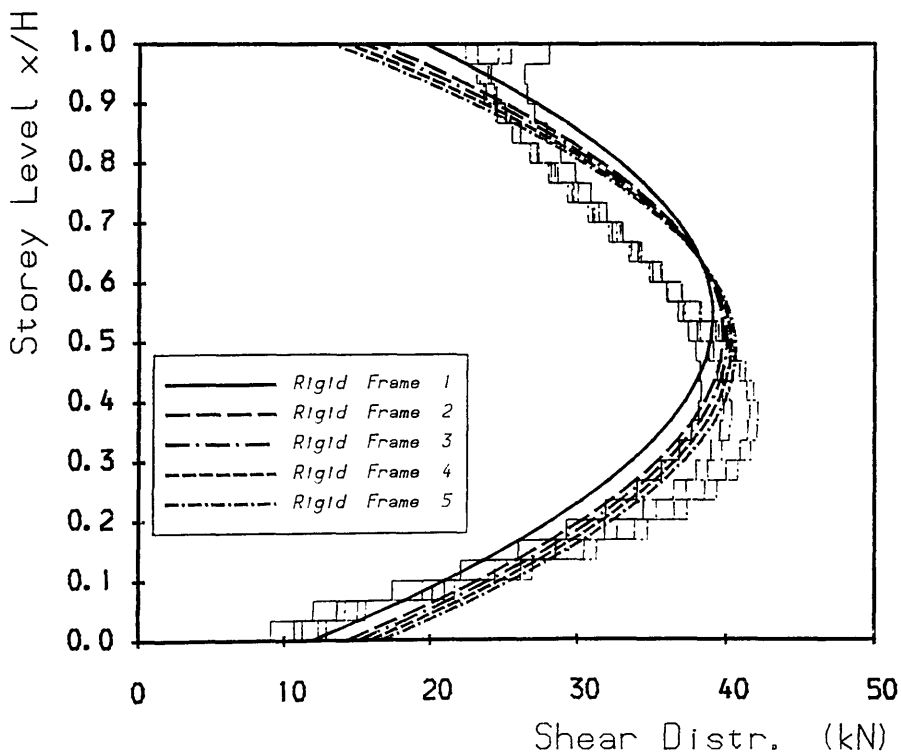
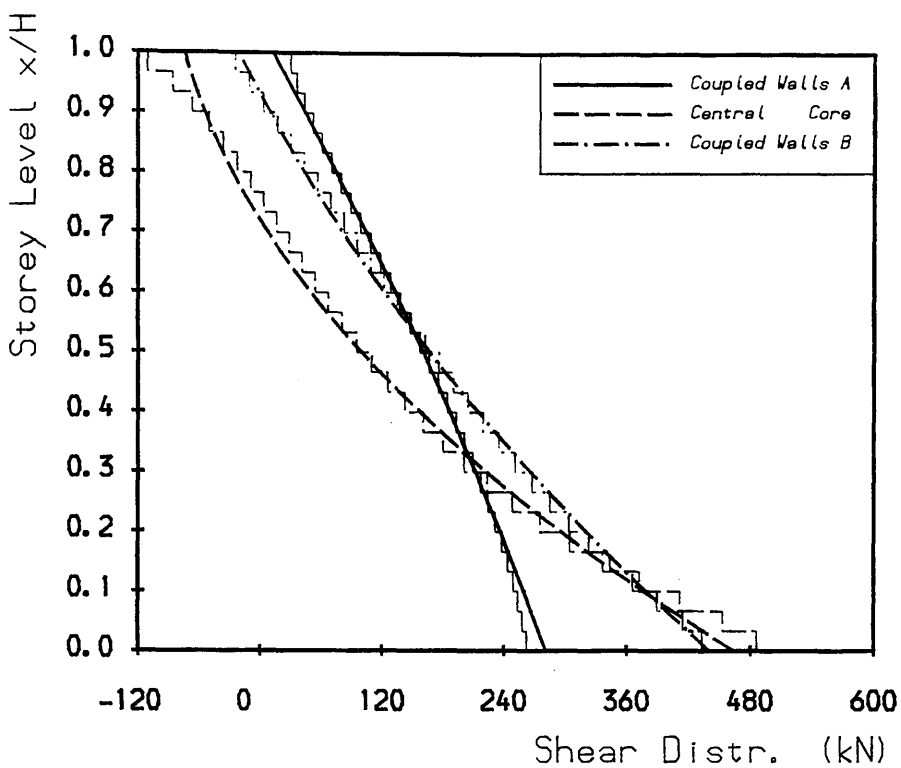
Three-Dimensional Structure Example
Fig. 6.22c Load Position 3, Moment Distributions



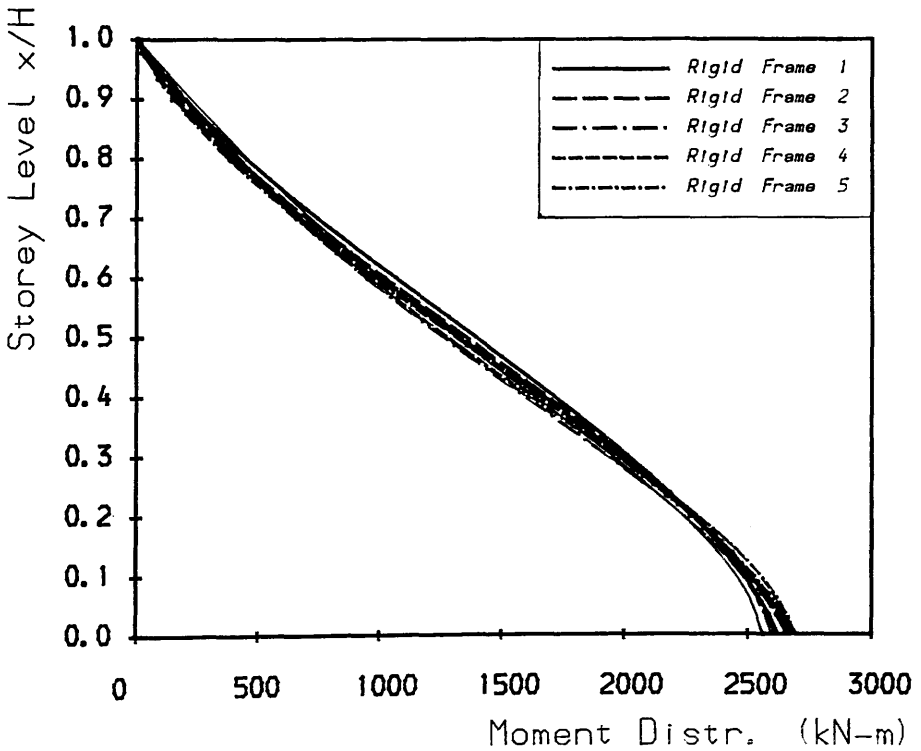
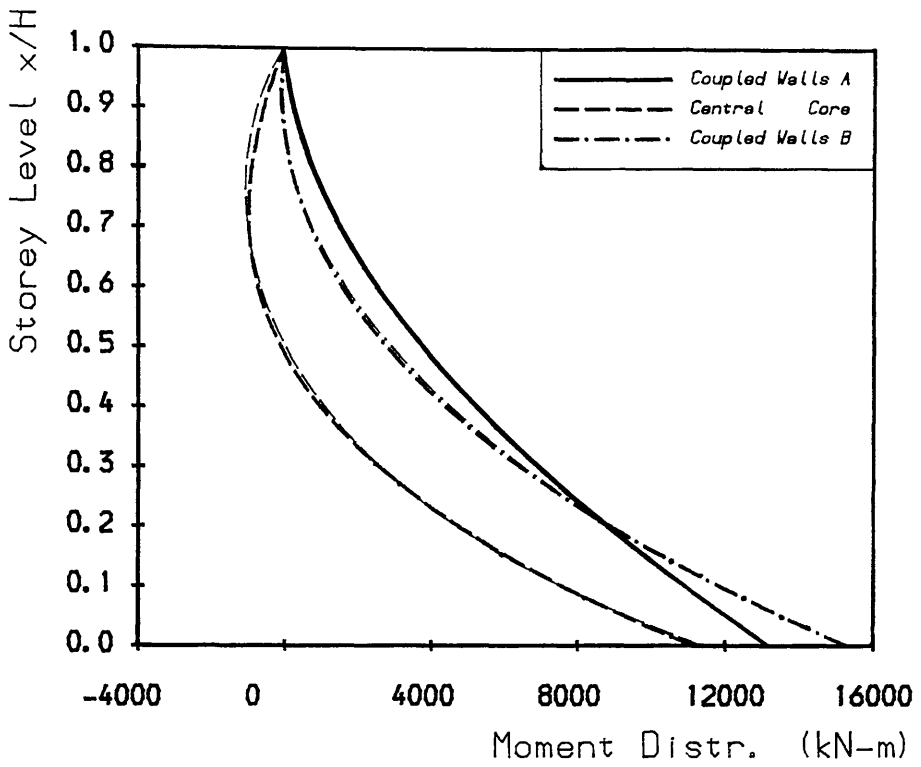
Load Position 4



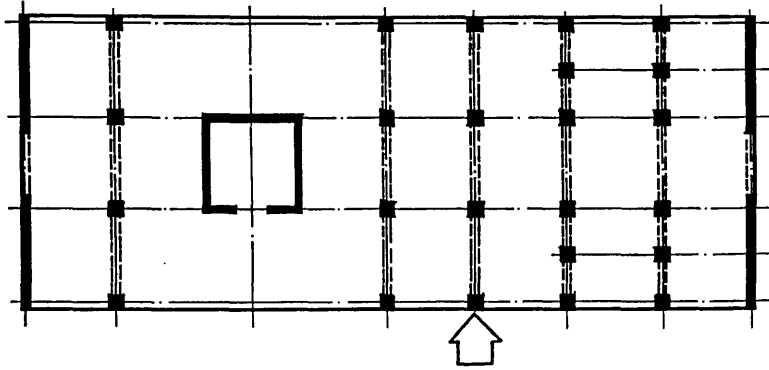
Three-Dimensional Structure Example
Fig. 6.23a Load Position 4. Deflections



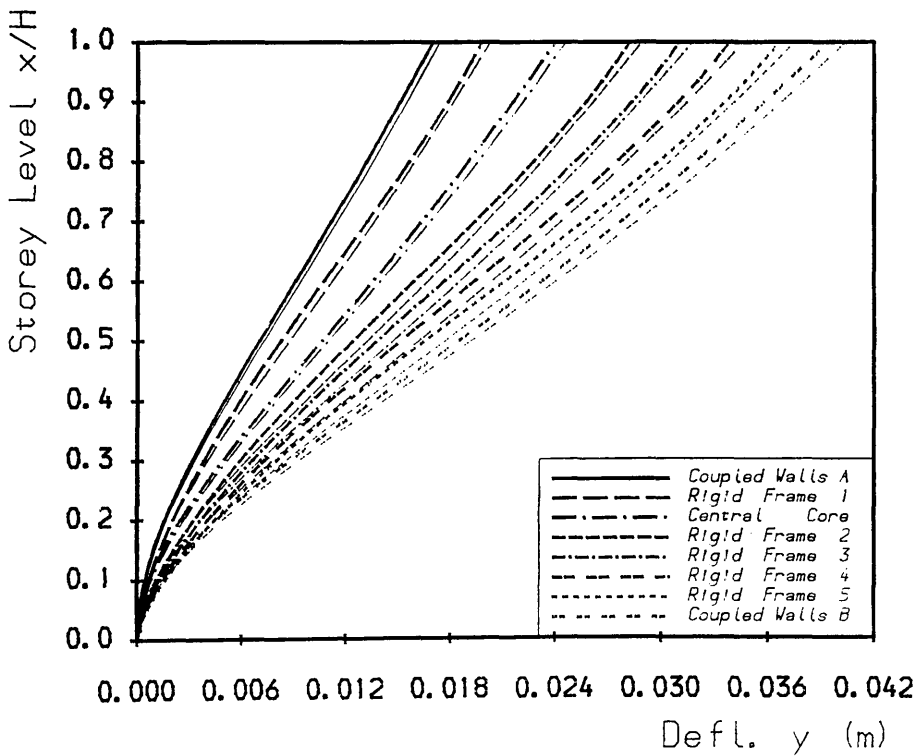
Three-Dimensional Structure Example
Fig. 6.23b Load Position 4, Shear Distributions



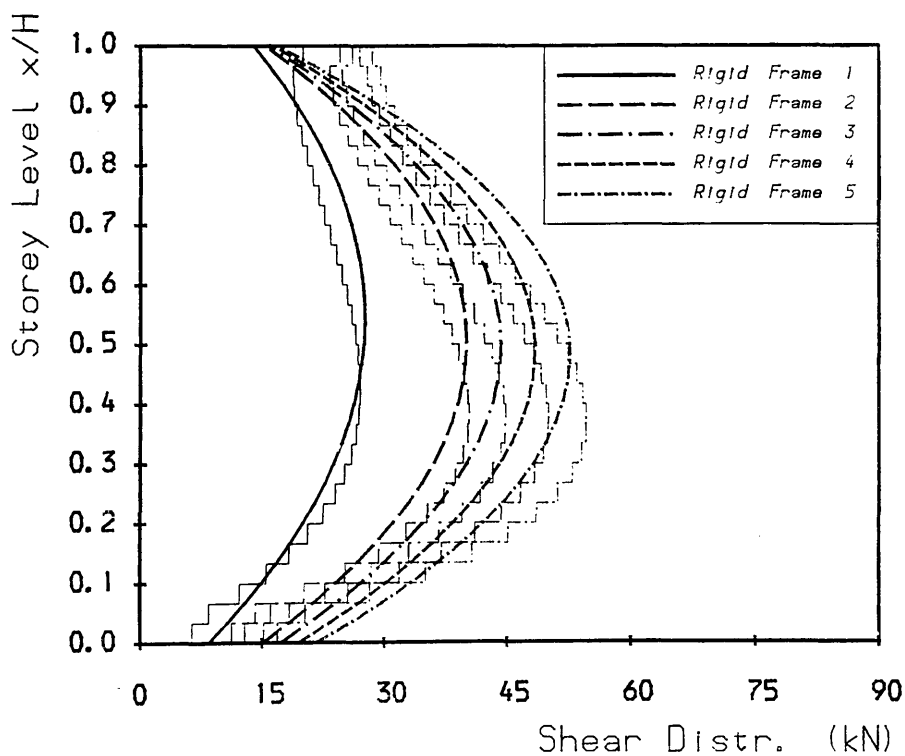
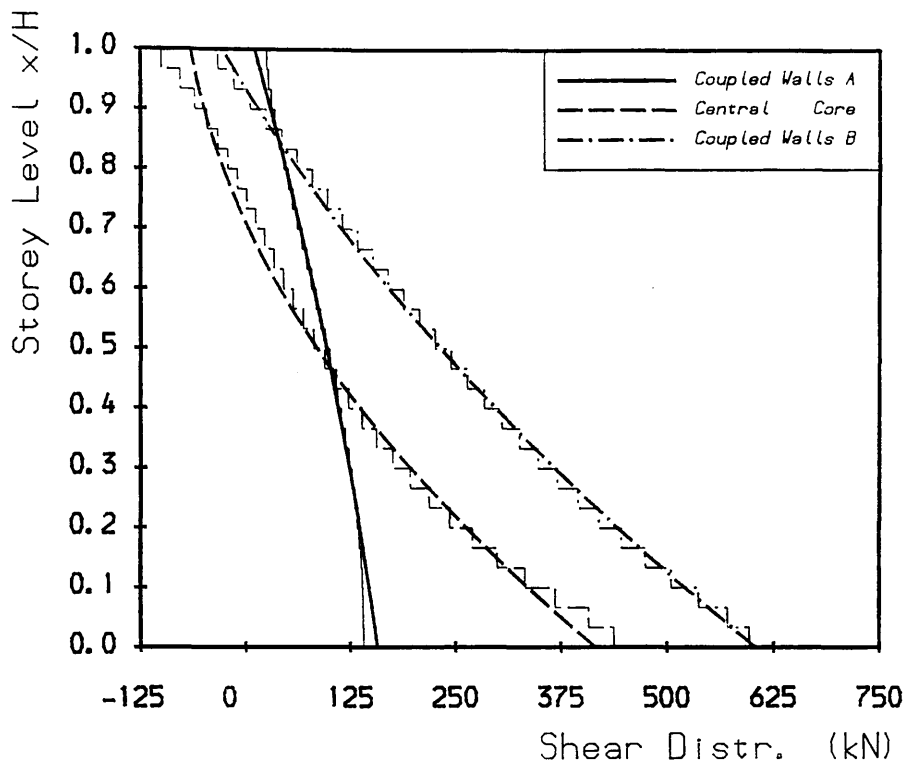
Three-Dimensional Structure Example
Fig. 6.23c Load Position 4, Moment Distributions



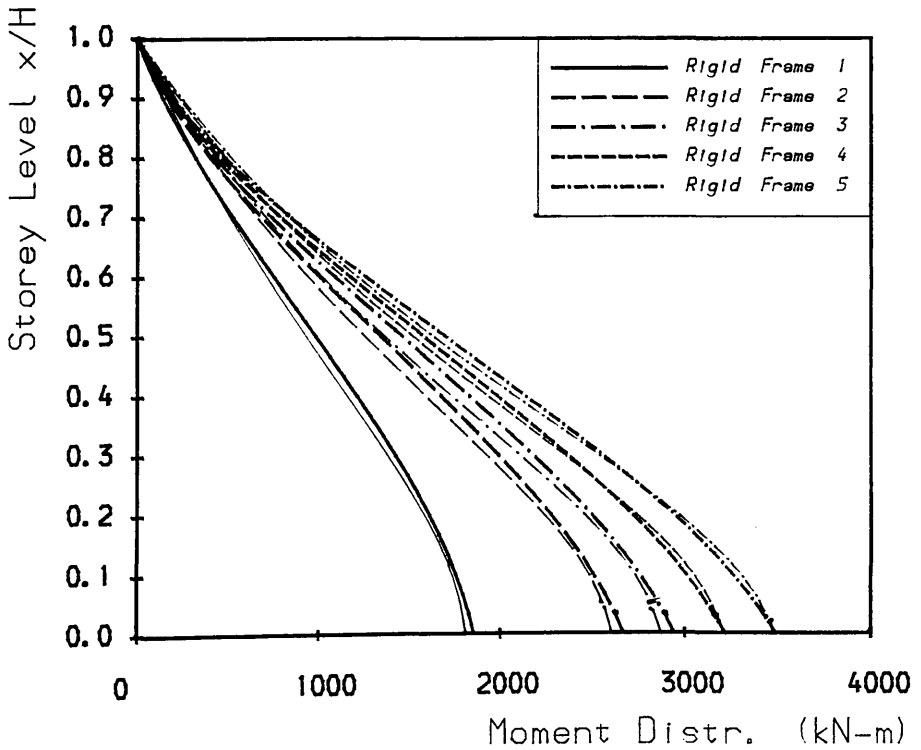
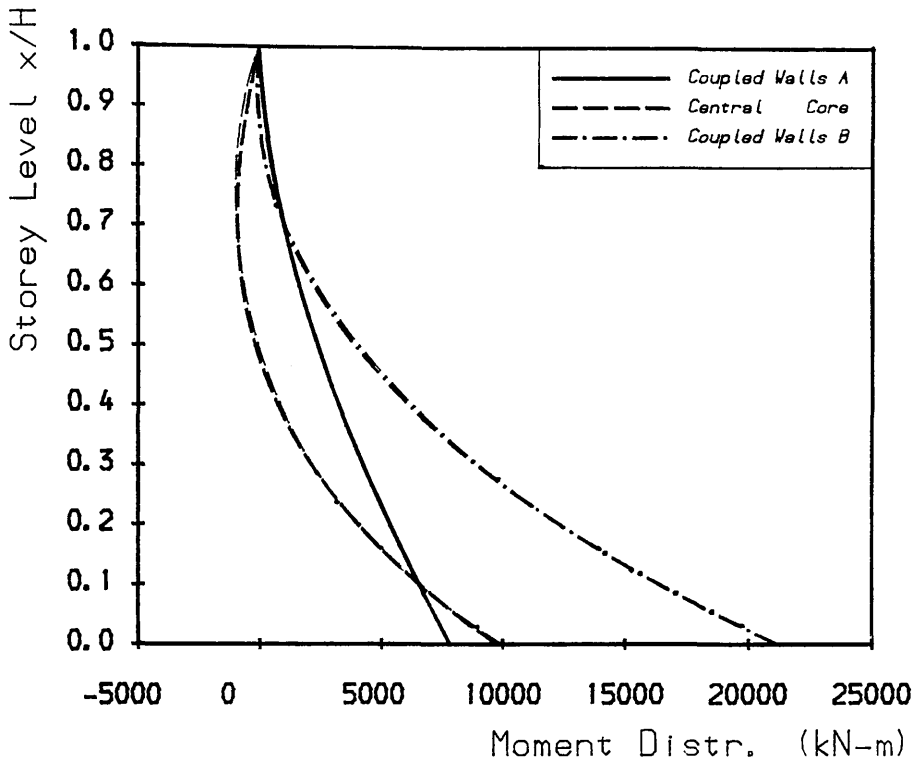
Load Position 5



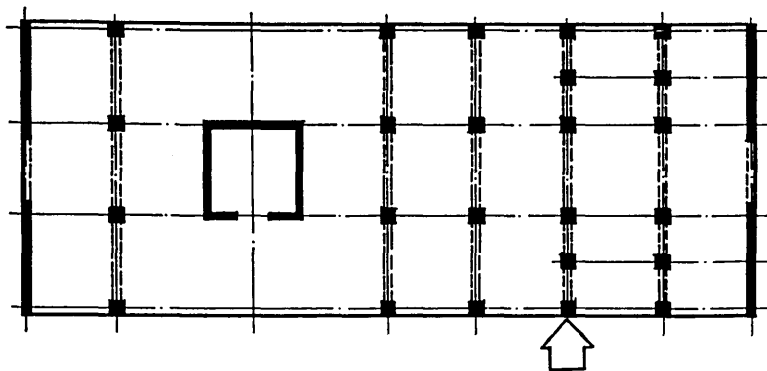
Three-Dimensional Structure Example
Fig. 6.24a Load Position 5. Deflections



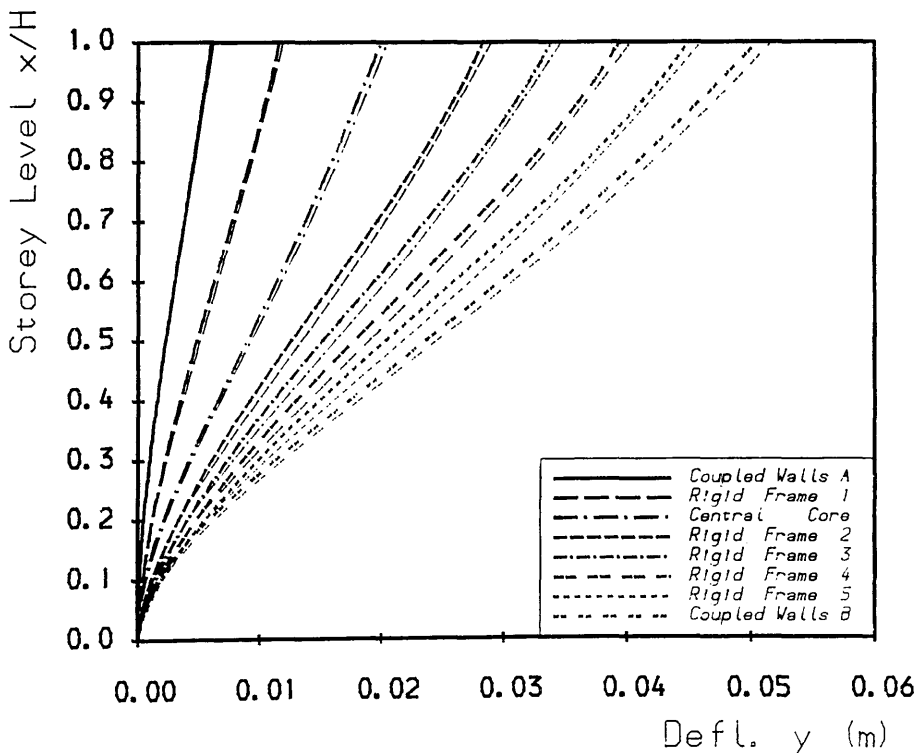
Three-Dimensional Structure Example
Fig. 6.24b Load Position 5, Shear Distributions



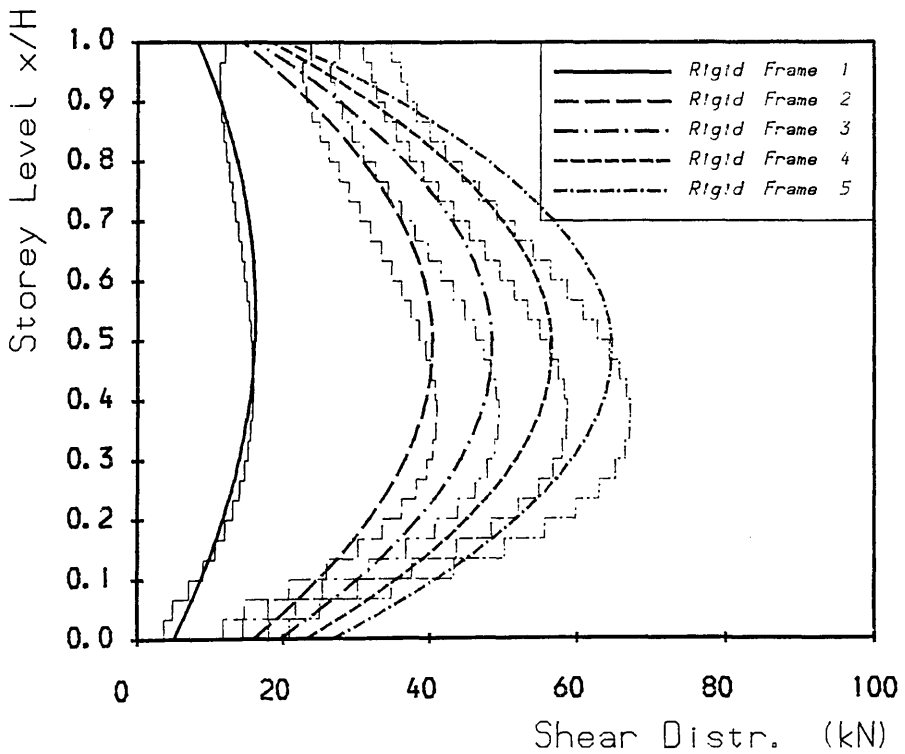
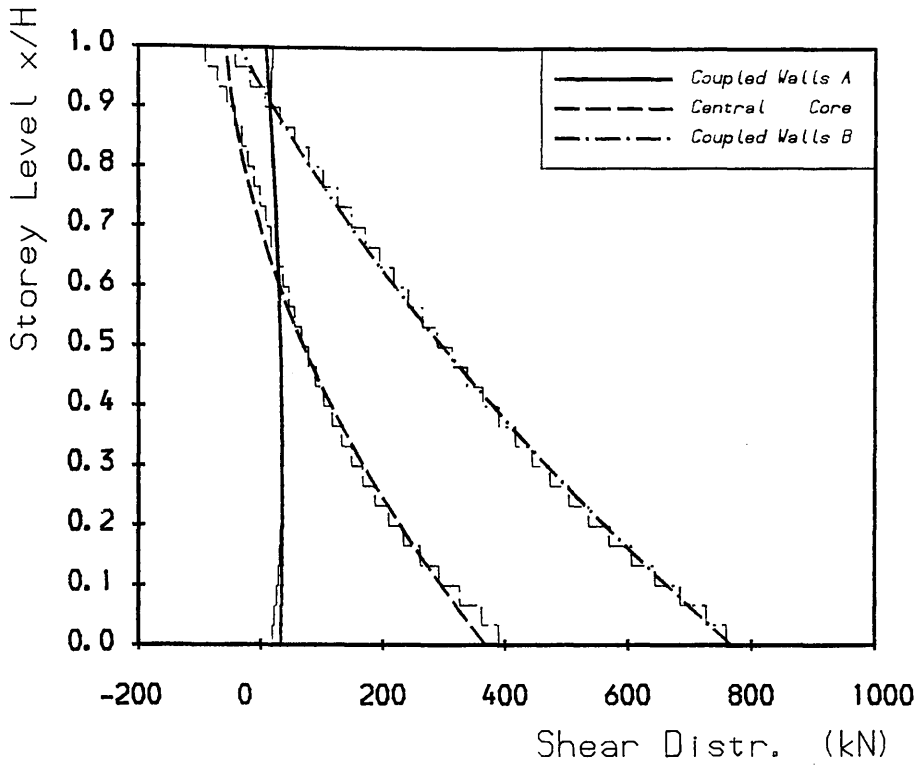
Three-Dimensional Structure Example
Fig. 6.24c Load Position 5, Moment Distributions



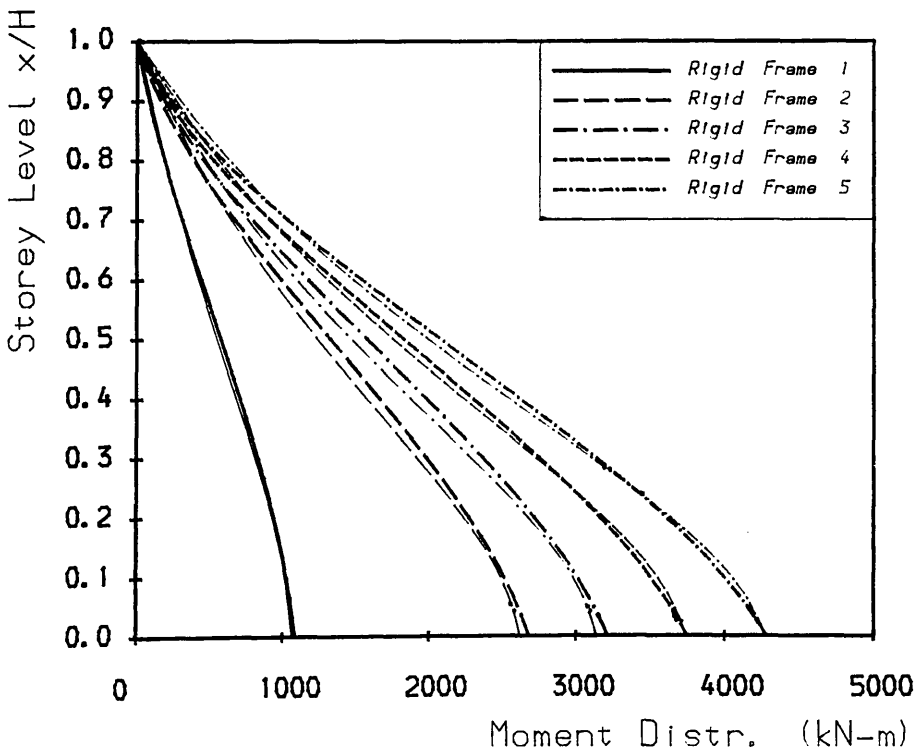
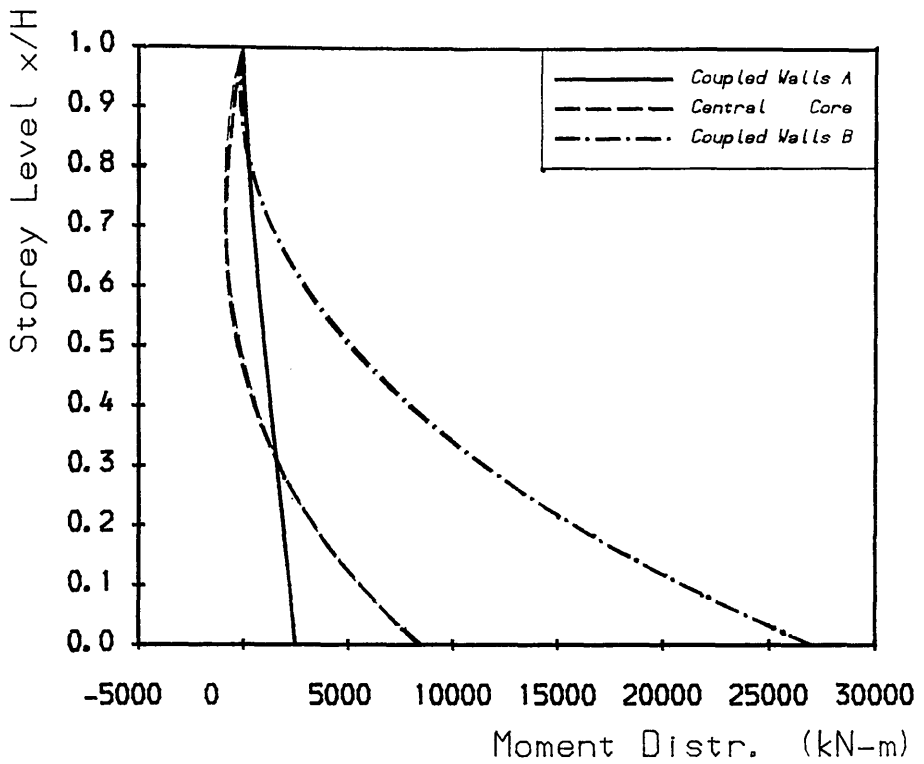
Load Position 6



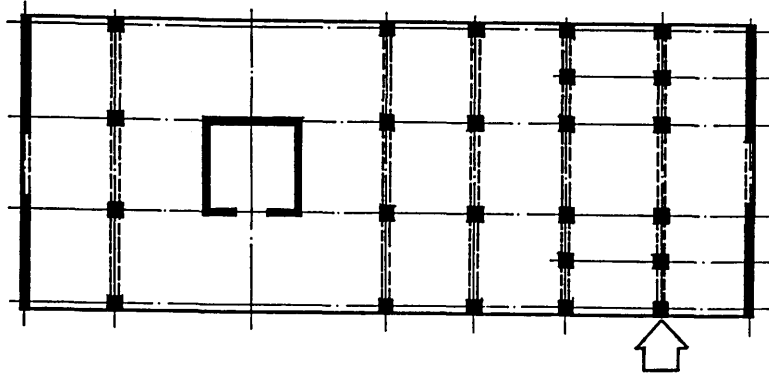
Three-Dimensional Structure Example
Fig. 6.25a Load Position 6. Deflections



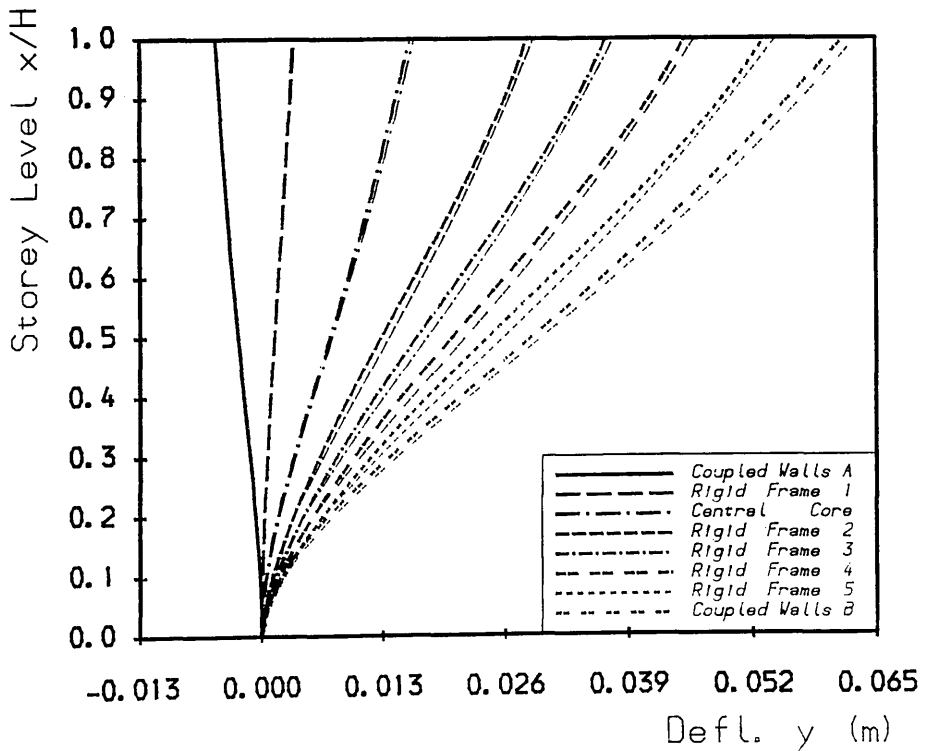
Three-Dimensional Structure Example
Fig. 6.25b Load Position ϕ , Shear Distributions



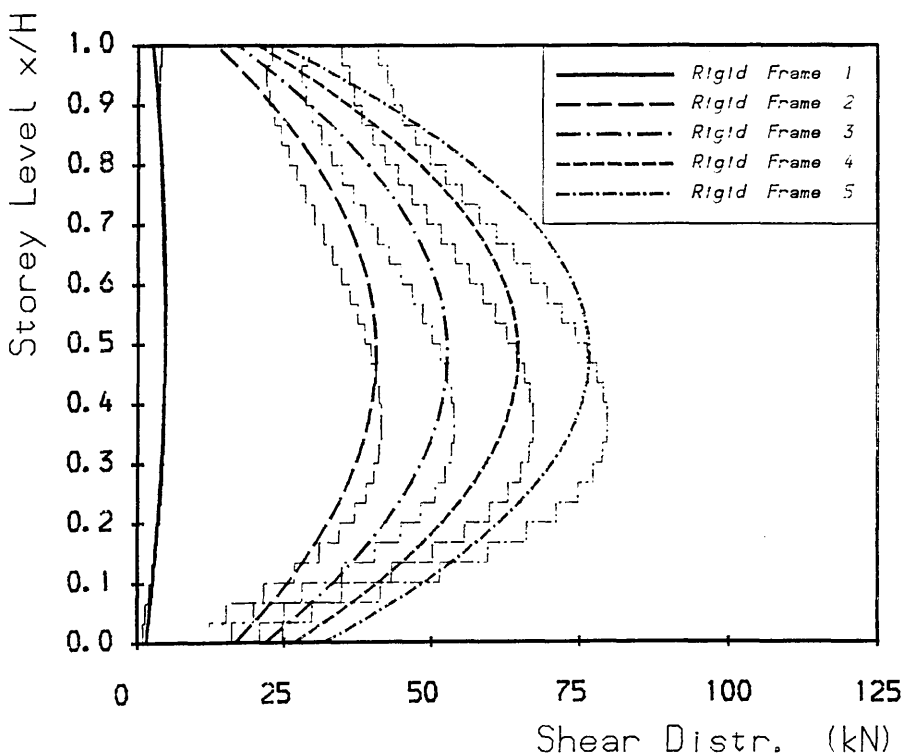
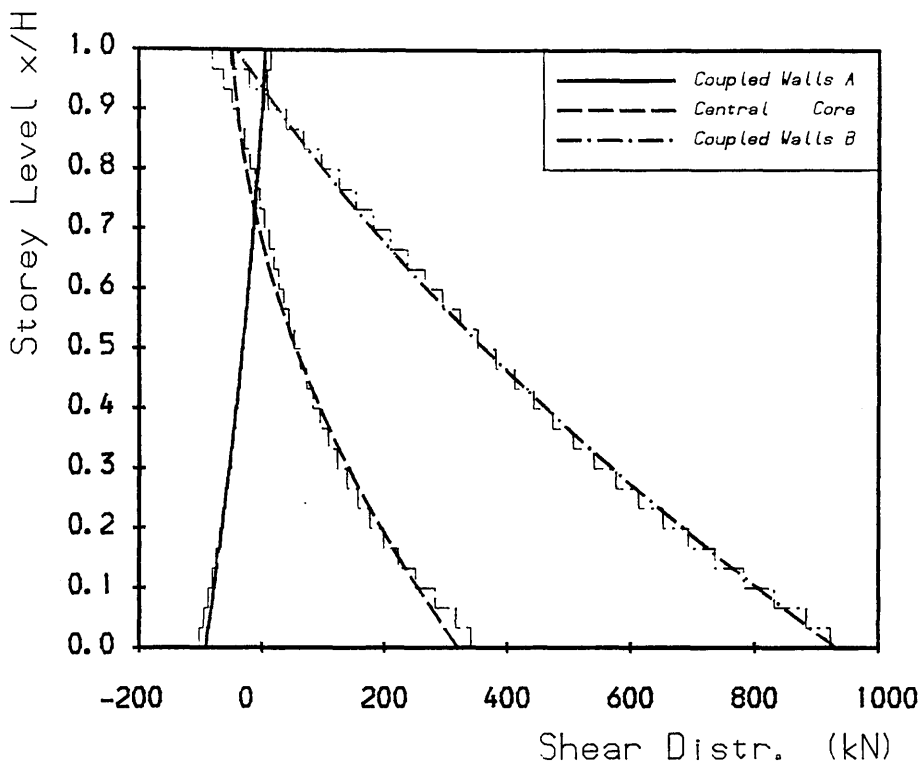
Three-Dimensional Structure Example
Fig. 6.25c Load Position 6, Moment Distributions



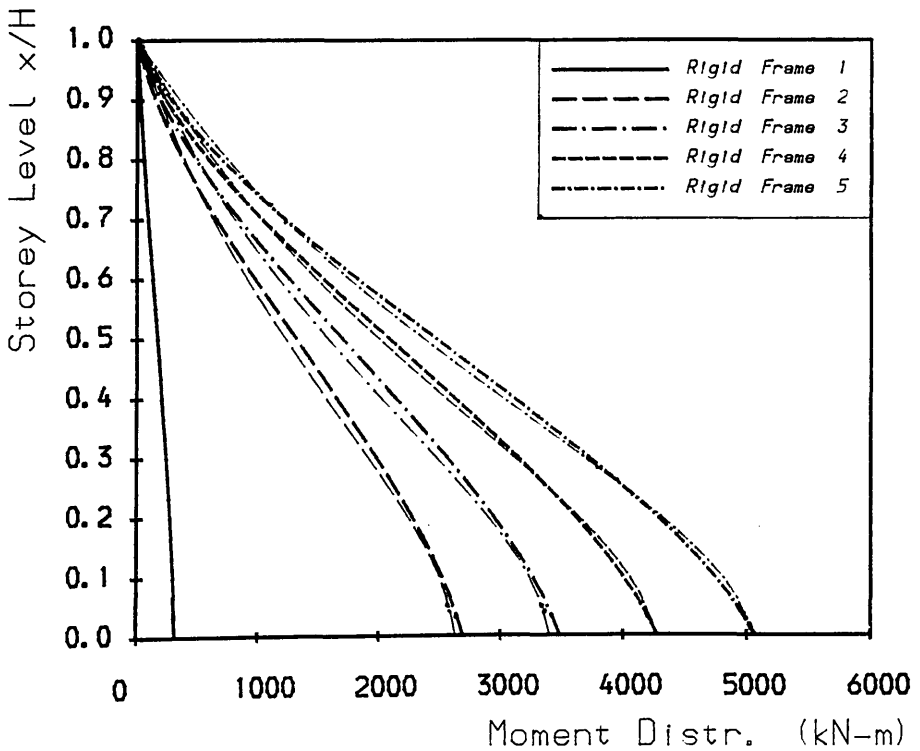
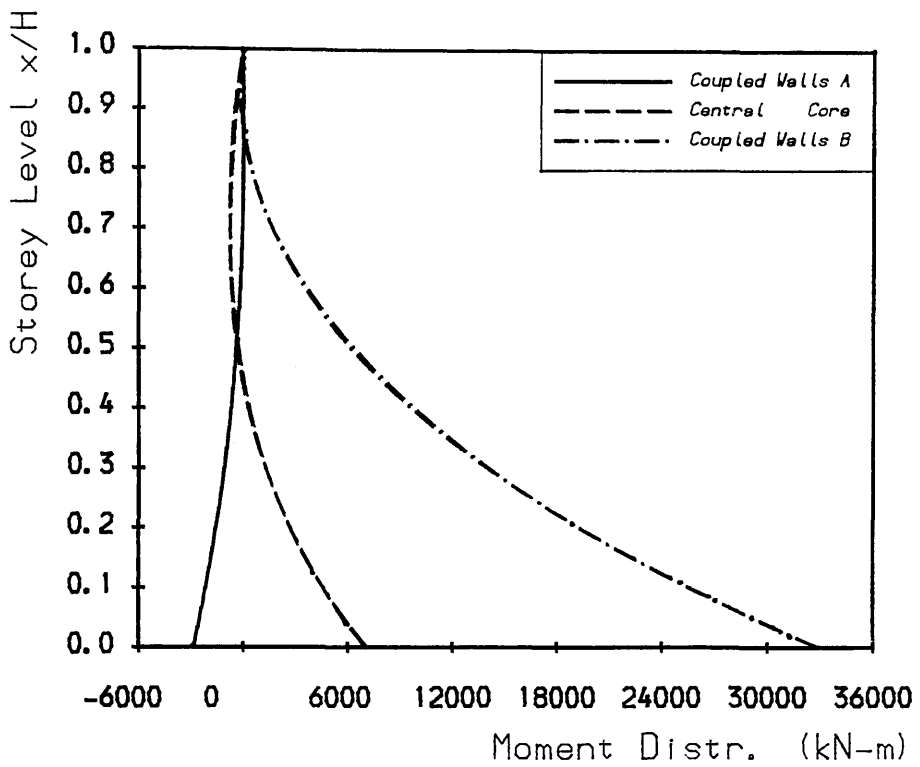
Load Position 7



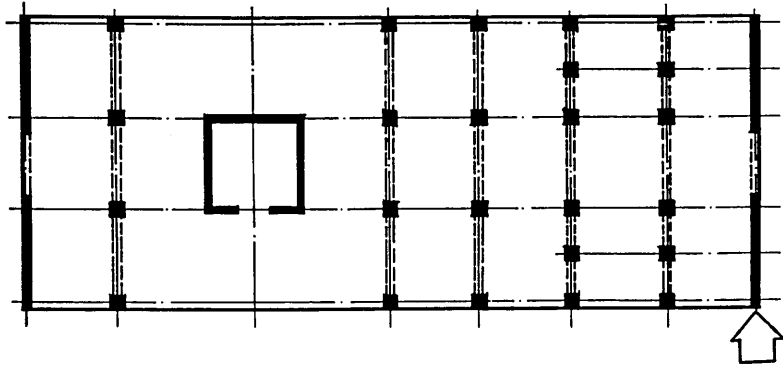
Three-Dimensional Structure Example
Fig. 6.26a Load Position 7. Deflections



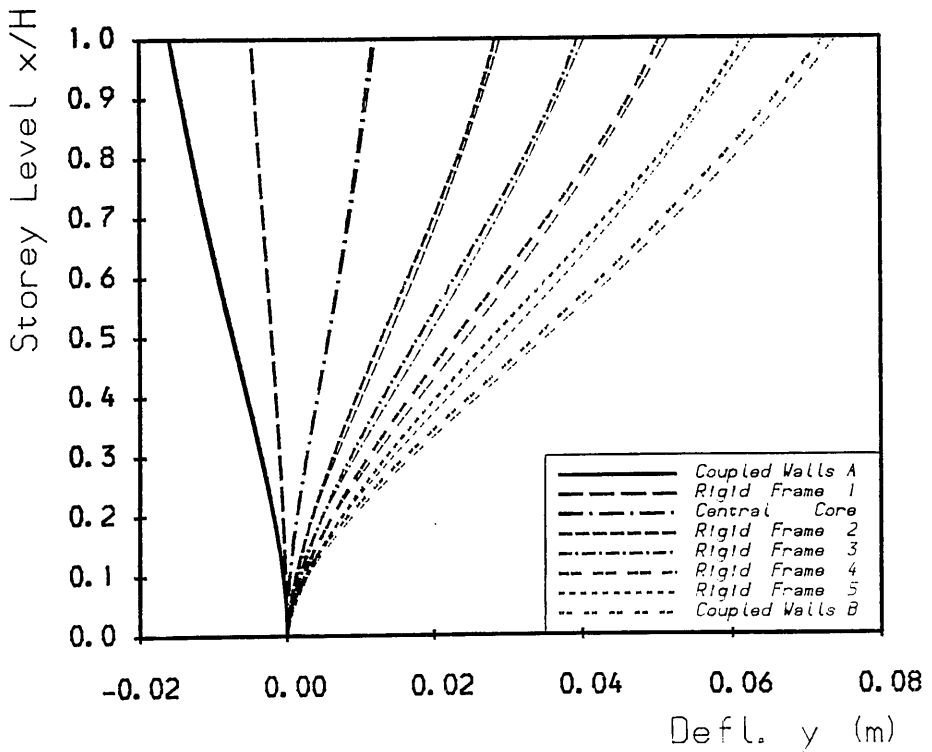
Three-Dimensional Structure Example
Fig. 6.26b Load Position 7, Shear Distributions



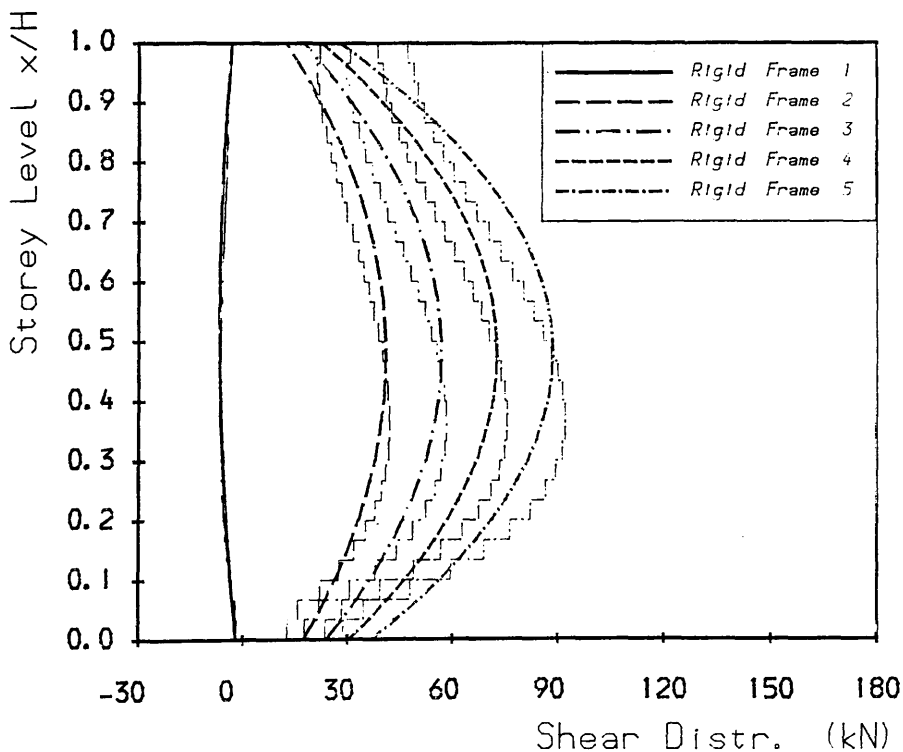
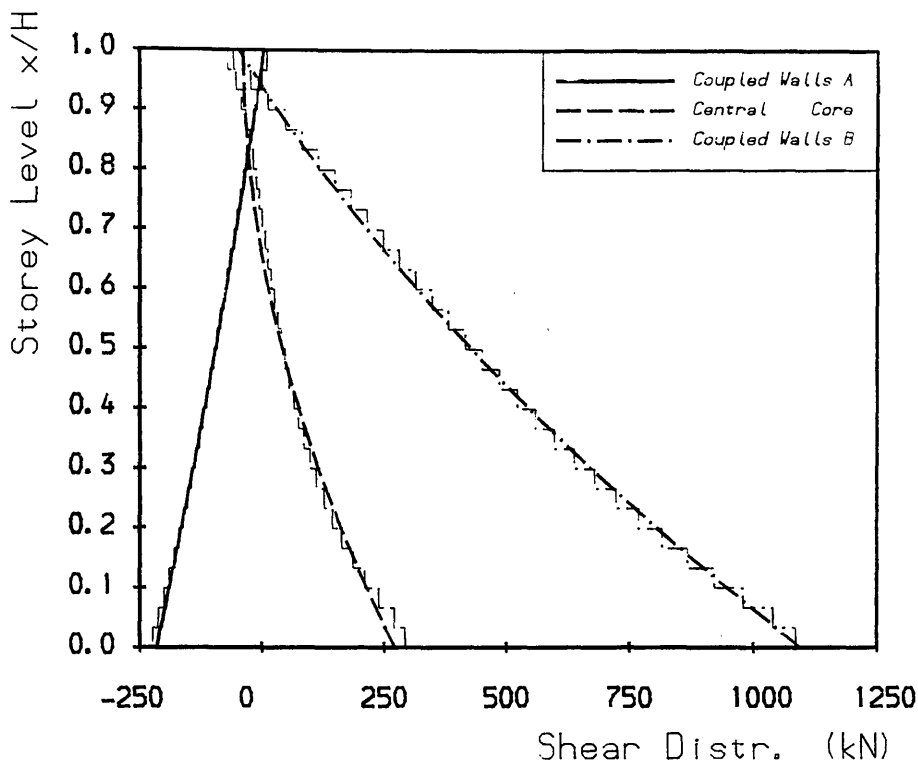
Three-Dimensional Structure Example
Fig. 6.26c Load Position 7, Moment Distributions



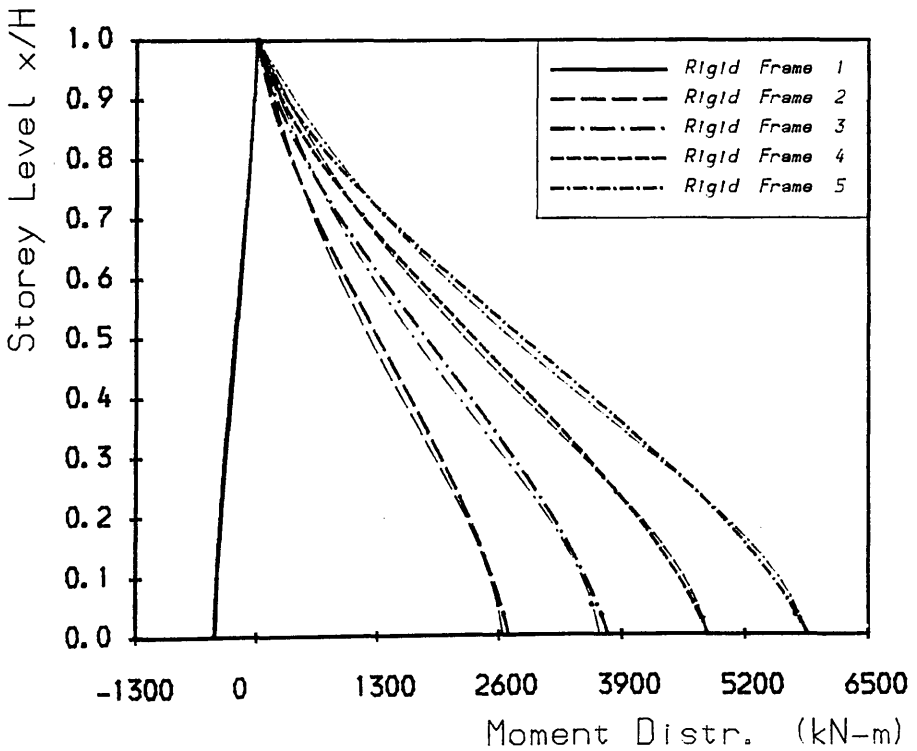
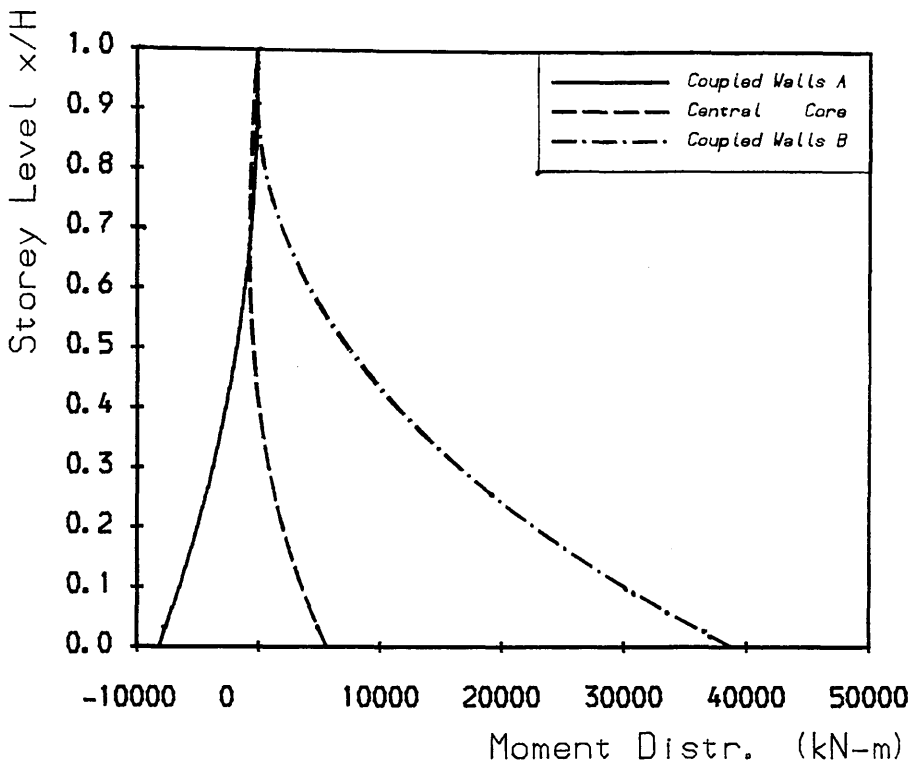
Load Position 8



Three-Dimensional Structure Example
Fig. 6.27a Load Position 8. Deflections



Three-Dimensional Structure Example
Fig. 6.27b Load Position 8, Shear Distributions



Three-Dimensional Structure Example
Fig. 6.27c Load Position 8, Moment Distributions

CHAPTER 7

CONCLUSIONS AND RECOMMENDATIONS FOR FUTURE WORK

7.1 Conclusions

This thesis has re-examined the coupled shear wall continuum theory, and methods for coupled wall structures have been presented, using a series of systematic parameters for such structures. These analyses include the interactions between two pairs of linked coupled shear walls and the interactions between coupled shear walls and flexural and shear cantilevers. The reasonably accurate results shown from the numerical studies indicate that these methods can be used directly in the analysis of symmetric coupled shear wall structures subjected to lateral loads which cause pure bending actions, and produce relatively precise solutions for the deflections and internal forces in the structure.

Studies of the structural parameters of a group of wall-frame assemblies have shown that these assemblies, including coupled shear walls, plane shear walls, cores and rigid frames, belong to a general family of structural cantilevers whose modes of load-deformation behaviour can be characterized by three primary distinct structural rigidities, namely, the flexural rigidity EI , the racking shear rigidity GA , and the overall axial bending rigidity EI_f . By making use of the revised wall-frame theory presented in Chapter 4, the mode of behaviour of each assembly can be determined by appropriately representing the three rigidities for the assembly.

Two simplified methods have been presented for the analysis of laterally loaded three-dimensional symmetric and asymmetric tall building structures consisting of parallel systems of wall-frame assemblies.

Based on the revised wall-frame theory and a spring supported rigid beam model, the first approximate method was presented in Chapter 5 for the analysis of complete three-dimensional symmetric or asymmetric tall wall-frame structures subjected to bending and torsional actions. The numerical studies have shown that based on only a few relatively simple formulae, the simplified method can generally produce accurate results for the deflections, the rotations, and the interactive forces between the assemblies for a relatively complicated three-dimensional tall building structure. These usually require the solution of a considerable number of equations when using other methods. The method in general has a merit in its simplicity which is most appropriate for a hand method. It could be very useful in the preliminary stage of apportioning members in a structural design, and could be appropriately used as an overall guide to examine the reasonableness of the results from other more complex methods, such as finite element analysis.

The second method is an extended and simplified version of an earlier influence coefficient analysis. It has been shown from the numerical studies that, on assuming a simple form of load distribution on each assembly, and using the area influence coefficients instead of the displacements at arbitrarily chosen height levels to achieve the horizontal deformation compatibilities, a reasonably accurate solution to the problem is generally obtained. The analysis can be carried out either by simple programming on small computers to solve large matrices, or by a hand method which requires the inversions of matrices of order three and six, by means of using a pocket calculator.

7.2 Recommendations For Future Work

In this thesis, two different approximate methods for the analysis of laterally loaded three-dimensional high-rise building structures were presented, and a number of numerical examples showed that in most cases both methods produced reasonably accurate solutions when compared with the results from the finite element analysis. Clearly neither of them is a complete solution to the general tall building analysis. Questions and problems may arise in some respects as follows, and further investigations need to be made.

1. In Chapter 5, a problem arose in determining the forces distributed into the two components of a wall-frame assembly (Eq. 5.12). As the second component involved two types of rigidities, GA and EF_f , which define its two different modes of deformation behaviour, in the absence of any more fundamental basis for distributing the second force component, it was assumed to take an average effect of the two factors (GA and EI_f). The same technique was also used when it was to determine the final force distributions in the equivalent assemblies, subjected to the 'effective' rigidities (Eqs. 5.26). Obviously, this is not the exact case. It was found in some cases that one factor was more dominant than the other. Further studies are required to investigate how the forces are truly distributed into the composite assembly involving the two different modes of deformation behaviour.

2. In the rigid beam method of calculating the effective rigidities for the interactive assemblies in a structure in Chapter 5, when the structure considered is highly asymmetric and subjected to some particular resultant lateral loads, two problem may occur: (a) a set of absurd effective rigidities of a particular assembly may be obtained from Eqs. 5.40 to 5.42, when, for example, the

effective flexural rigidity EI_{ei} may be obtained relatively much larger than the overall bending rigidity EI_{fei} due to a nearly-zero displacement δ_i (the denominator in Eq. 5.40). This will result in a relatively large value of the structural parameter k_{ei} , say, over 1.3, and usually give rise to large errors in the resulting deflections and force distributions for the particular assembly; (b) for a particular assembly, a set of effective rigidities of different signs due to one or two negative displacements resulting from the rigid beams will usually make the equations completely inapplicable. For example, the structural parameter α_{ei} for the assembly will be an imaginary value if the EI_{ei} and GA_{ei} are of different signs (Eq. 5.17), and a parameter k_{ei} of less than 1.0 (Eq. 5.18) also makes it difficult to achieve an accurate result from the equations (Eqs. 5.16 to 5.24). It should be noted that the method is applicable when the three effective rigidities are all negative values, and the results in such cases are usually quite good. Due to the above difficulties, further investigations for the refinement of the rigid beam model are desirable.

Possible further investigations for the refinement and extension of the study could also be in some other respects such as:

3. For the analysis of three-dimensional structures subjected to bending and torsion using the revised wall-frame method and the rigid beam method, further studies and comparison with the finite element method for the other two standard load cases, a triangularly distributed lateral load and a concentrated horizontal top lateral load, are required to examine comprehensively the validity of the method.
4. In the rigid beam method presented in Chapter 5, further investigations are required to take into account the effects of torsional stiffnesses of individual assemblies. This might be done, for example, by adding rotational resisting springs

into the rigid beam model. Each rotation-resisting spring, representing a torsional assembly, similar to that of a regular supporting spring, might include three types of torsional rigidities. It would then be possible to analyze structures including core assemblies which involve large torsional stiffnesses, such as stiffened open-box sections.

5. Although the area influence coefficient analysis presented in Chapter 6 gives the solution for structures involving torsional resisting assemblies, studies on the mode of torsion-twisting behaviour for such individual core assemblies are required, and numerical studies are necessary to examine the accuracy of the method when such torsional resisting assemblies are involved.

6. The methods presented in the thesis concerned only structures which are uniform throughout the height. An extension of the studies for approximate method for irregular structures, which are commonly found in practice, are highly desirable.

7. Studies of the modes of deformation behaviour of other types of bents should be included, such as braced frames and other types of perforated shear walls which are also commonly employed in high-rise building structures.

8. The methods of analysis developed have concerned structures consisting of parallel assemblies only. It would be desirable to extend the analysis to include assemblies in two orthogonal directions, especially when torsional actions are involved.

REFERENCES

1. Khan, F. R., "Structural Design of Tall Buildings" Proc. of National Conf. On Tall Buildings, New Delhi, India, 1973, pp. 106-128.
2. — "Steel Designers' Manual", Crosby Lockwood, Third Ed., 1966, Chapter 31.
3. Macleod, I. A., "Simplified Equations for Deflection of Multistory Frames" Build. Sci., Vol. 6, 1971, pp. 25-31.
4. Chan, P. C. K., Heidebrecht, A. C. and Tso, W. K., "Approximate Analysis of Multistory Multibay Frames" Jnl. Struct. Div., ASCE, Vol. 101, No. St5, 1975, pp. 1021-1035.
5. Macleod, I. A., "Lateral Stiffness of Shear Walls With Openings" Tall Buildings, Pergamon Press, London, 1967, pp. 233-244.
6. Macleod, I. A., "Analysis of Shear Wall Buildings by the Frame Method" Proc. Ins. Civ. Engrs, London, Vol. 55, 1973, pp. 593-603.
7. Kratky, R. J. and Puri, S. P. S., "Discussion of Modified Beam Method for Analysis of Symmetrical Inter-Connected Shear Walls", By B. Stafford Smith, ACI Jnl., Vol. 68, 1971, pp. 472-474.
8. Schwaighofer, J. and Microys, H. F., "Analysis of Shear Wall Structures Using Standard Computer Programs", ACI Jnl., Vol. 66, 1969, pp. 1005-1008.

9. Heidebrecht, A. C. and Stafford Smith, B., "Approximate Analysis of Tall Wall-Frame Structures", Jnl. of the Struct. Div., ASCE, Vol. 99, No. ST2, 1973, pp. 199-221.
10. Beck, H., "Contribution to the Analysis of Coupled Shear Walls, ACI Jnl., Vol. 59, 1962, pp. 1055-1069.
11. Rosman, R., "Approximate Analysis of Shear Walls Subjected to Lateral Loads", ACI Jnl., Vol. 61, 1964 pp. 717-732.
12. Coull, A., "Contribution to the Continuum Theory of Coupled Shear Walls" Res. Mechanica, Vol. 26, 1989, pp. 353-370.
13. Coull, A., "Interactions Between Coupled Shear Walls and Cantilevered Cores in Three-Dimensional Regular Symmetric Cross-Wall Structures", Proc. ICE, Vol. 55, 1973, pp. 827-840.
14. Stafford Smith B. and Abergel, D.P., "Approximate Analysis of High-Rise Structures Comprising Coupled Walls and Shear Walls", Building and Environment, Vol. 18, No. 1/2, 1983, pp. 91-96.
15. Arvidsson, K., "Interaction Between Coupled Shear Walls and Frames" Proc. ICE, Vol. 67, Part 2, 1976, pp. 589-596.
16. Khachatorian, H., "Distribution of Lateral Forces In Structures Consisting of Cores, Coupled Shear Walls and Rigidly Jointed Frames" Proc. Instn Civ. Engrs, Vol. 73, Part 2, 1982, pp. 731-745.

17. Stafford Smith, B., Kuster, M. and Hoenderkamp, J. C. D., "A generalized Approach to the Deflection Analysis of Braced Frames, Rigid Frames, and Coupled Wall Structures" *Can. Jnl. Civ. Engr.*, 1981 pp. 230–240
18. Stafford Smith, B., Kuster, M. and Hoenderkamp, J. C. D., "Generalized Method For Estimating Drift In High–Rise Structures" *Jnl. Struct. Div. Proc. ASCE*, Vol. 110, July 1984, pp. 1549–1562.
19. Hoenderkamp, J. C. D. and Stafford Smith, B., "Simplified Analysis of Symmetric Tall Building Structures Subject to Lateral Loads" *Proceeding, Third International Conference on Tall Buildings, Hong Kong and Guangzhou, Dec. 1984*, pp. 28–36.
20. Coull, A. and Adams, N. W., "A simplified Method of Analysis of the Load Distribution in Multistorey Shear Wall Structures", "Response of Multistorey Concrete Structures to Lateral Forces", *Publication SP–36, ACI Jnl.*, 1973, pp. 187–216.
21. Coull, A. and Mohammed, T. H., "Simplified Analysis of Lateral Load Distribution In Structures Consisting of Frames, Coupled Shear Walls, and Cores", *Struct. Engr. Vol. 61b*, 1983, pp. 1–8.
22. Stafford Smith, B., "Modified Beam Method for Analyzing Symmetrical Interconnected Shear Walls", *ACI Jnl.*, Vol. 67, Dec. 1970, pp. 977–980.

APPENDIX 1

SIMPLE WALL-FRAME THEORY

SOLUTIONS FOR OTHER TWO STANDARD LATERAL LOAD CASES

1. Concentrated Horizontal Load P_0 at the TopDeflection y :

$$y = \frac{P_0 H^3}{EI} \left\{ \frac{\xi}{(\alpha H)^2} - \frac{\sinh \alpha H - \sinh \alpha H (1-\xi)}{(\alpha H)^3 \cosh \alpha H} \right\} \quad (1)$$

Moments on the flexural and shear cantilevers, M_b and M_s :

$$M_b = P_0 H \frac{\sinh \alpha H (1-\xi)}{\alpha H \cosh \alpha H} \quad (2)$$

$$M_s = P_0 H \left\{ (1-\xi) - \frac{\sinh \alpha H (1-\xi)}{\alpha H \cosh \alpha H} \right\} \quad (3)$$

Shears in the flexural and shear cantilevers, S_b and S_s :

$$S_b = P_0 \frac{\cosh \alpha H (1-\xi)}{\cosh \alpha H} \quad (4)$$

$$S_s = P_0 \left\{ (1-\xi) - \frac{\cosh \alpha H (1-\xi)}{\cosh \alpha H} \right\} \quad (5)$$

Distributed loads on the flexural and shear cantilevers, w_b and w_s :

$$w_b = -w_s = \frac{P_0}{H} \frac{\alpha H \sinh \alpha H (1-\xi)}{\cosh \alpha H} \quad (6)$$

2. Triangularly Distributed Lateral Load of Maximum Intensity q_0 at the TopDeflection y :

$$y = \frac{q_0 H^4}{EI} \left\{ \frac{1}{2(\alpha H)^2} \left(\xi - \frac{\xi^3}{3} \right) - \frac{\xi}{(\alpha H)^4} \right. \\ \left. + \frac{\cosh \alpha H \xi + (\alpha H/2 - 1/\alpha H) [\sinh \alpha H (1-\xi) - \sinh \alpha H] - 1}{(\alpha H)^4 \cosh \alpha H} \right\} \quad (7)$$

Moments in the flexural and shear cantilevers, M_b and M_s :

$$M_b = q_0 H^2 \left\{ -\frac{\xi}{(\alpha H)^2} + \frac{\cosh \alpha H + (\alpha H/2 - 1/\alpha H) \sinh \alpha H (1-\xi)}{(\alpha H)^2 \cosh \alpha H} \right\} \quad (8)$$

$$M_s = q_0 H^2 \left\{ \frac{\xi^3 - 3\xi + 2}{6} + \frac{\xi}{(\alpha H)^2} - \frac{\cosh \alpha H + (\alpha H/2 - 1/\alpha H) \sinh \alpha H (1-\xi)}{(\alpha H)^2 \cosh \alpha H} \right\} \quad (9)$$

Shears in the flexural and shear cantilevers, S_b and S_s :

$$S_b = q_0 H \left\{ \frac{1}{(\alpha H)^2} - \frac{\sinh \alpha H - (\alpha H/2 - 1/\alpha H) \cosh \alpha H (1-\xi)}{\alpha H \cosh \alpha H} \right\} \quad (10)$$

$$S_s = q_0 H \left\{ \frac{1-\xi^2}{2} - \frac{\xi}{(\alpha H)^2} + \frac{\sinh \alpha H - (\alpha H/2 - 1/\alpha H) \cosh \alpha H (1-\xi)}{\alpha H \cosh \alpha H} \right\} \quad (11)$$

Distributed loads on the flexural and shear cantilevers, w_b and w_s :

$$w_b = q_0 \frac{\cosh \alpha H + (\alpha H/2 - 1/\alpha H) \sinh \alpha H (1-\xi)}{\cosh \alpha H} \quad (12)$$

$$w_s = \left\{ \xi - \frac{\cosh \alpha H + (\alpha H/2 - 1/\alpha H) \sinh \alpha H (1-\xi)}{\cosh \alpha H} \right\} \quad (13)$$

APPENDIX 2

CONTINUUM THEORY OF COUPLED SHEAR WALLS
SOLUTIONS FOR OTHER TWO STANDARD LATERAL LOAD CASES

1. Concentrated Horizontal Load P_0 at the TopDeflection y :

$$y = \frac{P_0 H^3}{EI} \left\{ \frac{k^2-1}{6k^2} (3\xi^2 - \xi^3) + \frac{\xi}{k^2(\alpha H)^2} - \frac{\sinh \alpha H - \sinh \alpha H(1-\xi)}{k^2(\alpha H)^3 \cosh \alpha H} \right\} \quad (14)$$

Axial forces in the walls N :

$$N = \frac{P_0 H}{lk^2} \left\{ (1 - \xi) - \frac{\sinh \alpha H(1-\xi)}{\alpha H \cosh \alpha H} \right\} \quad (15)$$

Shear flow in the connecting medium q :

$$q = \frac{P_0}{lk^2} \left\{ 1 - \frac{\cosh \alpha H(1-\xi)}{\cosh \alpha H} \right\} \quad (16)$$

Axial force flow in the connecting medium n :

$$n = - \frac{P_0}{k^2 H} \left[\frac{b/2+d_2}{l} - \frac{EI_2}{EI} \right] \frac{\alpha H \sinh \alpha H(1-\xi)}{\cosh \alpha H} \quad (17)$$

Moments in the two walls, M_1 and M_2 :

$$M_1 = \frac{EI_1}{EI l} P_0 H \left\{ \frac{k^2-1}{k^2} (1-\xi) + \frac{\sinh \alpha H(1-\xi)}{k^2 \alpha H \cosh \alpha H} \right\} \quad (18)$$

$$M_2 = \frac{EI_2}{EI l} P_0 H \left\{ \frac{k^2-1}{k^2} (1-\xi) + \frac{\sinh \alpha H(1-\xi)}{k^2 \alpha H \cosh \alpha H} \right\} \quad (19)$$

Shears in the two walls, S_1 and S_2 :

$$S_1 = P_0 \left\{ \frac{EI_1}{EI} + \frac{1}{k^2} \left[\frac{b/2+d_1}{l} - \frac{EI_1}{EI} \right] \left[1 - \frac{\cosh \alpha H(1-\xi)}{\cosh \alpha H} \right] \right\} \quad (20)$$

$$S_2 = P_0 \left\{ \frac{EI_2}{EI} + \frac{1}{k^2} \left[\frac{b/2+d_2}{l} - \frac{EI_2}{EI} \right] \left[1 - \frac{\cosh \alpha H(1-\xi)}{\cosh \alpha H} \right] \right\} \quad (21)$$

2. Triangularly Distributed Lateral Load of Maximum Intensity q_0 at the Top

Deflection y :

$$y = \frac{q_0 H^4}{EI} \left\{ \frac{k^2-1}{120k^2} (\xi^5 - 10\xi^3 + 20\xi^2) + \frac{1}{2k^2(k\alpha H)^2} \left(\xi - \frac{\xi^3}{3} \right) - \frac{\xi}{k^2(k\alpha H)^4} \right. \\ \left. + \frac{\cosh k\alpha H \xi + (k\alpha H/2 - 1/k\alpha H) [\sinh k\alpha H(1-\xi) - \sinh k\alpha H] - 1}{k^2(k\alpha H)^4 \cosh k\alpha H} \right\} \quad (22)$$

Axial forces in the walls N :

$$N = \frac{q_0 H^2}{k^2 l} \left\{ \frac{\xi^3 - 3\xi + 2}{6} + \frac{\xi}{(k\alpha H)^2} \right. \\ \left. - \frac{\cosh k\alpha H + (k\alpha H/2 - 1/k\alpha H) \sinh k\alpha H(1-\xi)}{(k\alpha H)^2 \cosh k\alpha H} \right\} \quad (23)$$

Shear flow in the connecting medium q :

$$q = \frac{q_0 H}{k^2 l} \left\{ \frac{1-\xi^2}{2} - \frac{1}{(k\alpha H)^2} \right. \\ \left. + \frac{\sinh k\alpha H - (k\alpha H/2 - 1/k\alpha H) \cosh k\alpha H(1-\xi)}{k\alpha H \cosh k\alpha H} \right\} \quad (24)$$

Moments in the two walls, M_1 and M_2 :

$$M_1 = \frac{EI_1}{EI} q_0 H^2 \left\{ \frac{(k^2-1)(\xi^3 - 3\xi + 2)}{6k^2} - \frac{\xi}{k^2(k\alpha H)^2} \right. \\ \left. + \frac{\cosh k\alpha H + (k\alpha H/2 - 1/k\alpha H) \sinh k\alpha H(1-\xi)}{k^2(k\alpha H)^2 \cosh k\alpha H} \right\} \quad (25)$$

$$M_2 = \frac{EI_2}{EI} q_0 H^2 \left\{ \frac{(k^2-1)(\xi^3 - 3\xi + 2)}{6k^2} - \frac{\xi}{k^2(k\alpha H)^2} \right. \\ \left. + \frac{\cosh k\alpha H + (k\alpha H/2 - 1/k\alpha H) \sinh k\alpha H(1-\xi)}{k^2(k\alpha H)^2 \cosh k\alpha H} \right\} \quad (26)$$

Shears in the two walls, S_1 and S_2 :

$$S_1 = \frac{S}{k^2} \left[\frac{b/2+d_1}{l} + (k^2-1) \frac{EI_1}{EI} \right] - \left[\frac{b/2+d_1}{l} - \frac{EI_1}{EI} \right] f(x) \quad (27)$$

$$S_2 = \frac{S}{k^2} \left[\frac{b/2+d_2}{l} + (k^2-1) \frac{EI_2}{EI} \right] - \left[\frac{b/2+d_2}{l} - \frac{EI_2}{EI} \right] f(x) \quad (28)$$

in which,

$$S = \frac{q_0 H}{2} (1-\xi^2) \quad (29)$$

and,

$$f(x) = \frac{q_0 H}{k^2} \left\{ \frac{1}{(\kappa\alpha H)^2} - \frac{\sinh \kappa\alpha H \xi - (\kappa\alpha H/2 - 1/\kappa\alpha H) \cosh \kappa\alpha H (1-\xi)}{\kappa\alpha H \cosh \kappa\alpha H} \right\} \quad (30)$$

Axial force flow in the connecting medium n :

$$n = \frac{q_0 \xi}{k^2} \left[\frac{b/2+d_2}{l} + (k^2-1) \frac{EI_2}{EI} \right] + \left[\frac{b/2+d_2}{l} - \frac{EI_2}{EI} \right] g(x) \quad (31)$$

in which,

$$g(x) = \frac{df(x)}{dx} = -q_0 \frac{\cosh \kappa\alpha H \xi + (\kappa\alpha H/2 - 1/\kappa\alpha H) \sinh \kappa\alpha H (1-\xi)}{k^2 \cosh \kappa\alpha H} \quad (32)$$

APPENDIX 3

REVISED WALL-FRAME THEORY

SOLUTIONS FOR OTHER TWO STANDARD LATERAL LOAD CASES

1. Concentrated Horizontal Load P_0 at the TopDeflection y :

$$y = \frac{P_0 H^3}{EI} \left\{ \frac{k^2-1}{6k^2} (3\xi^2 - \xi^3) + \frac{\xi}{k^2 (\kappa\alpha H)^2} - \frac{\sinh \kappa\alpha H - \sinh \kappa\alpha H (1-\xi)}{k^2 (\kappa\alpha H)^3 \cosh \kappa\alpha H} \right\} \quad (33)$$

Interactive force flow q :

$$q = - \frac{P_0}{k^2 H} \frac{\kappa\alpha H \sinh \kappa\alpha H (1-\xi)}{\cosh \kappa\alpha H} \quad (34)$$

Moments in the flexural and shear-flexural cantilevers, M_B and M_S :

$$M_B = P_0 H \left\{ \frac{k^2-1}{k^2} (1-\xi) + \frac{\sinh \kappa\alpha H (1-\xi)}{k^2 \kappa\alpha H \cosh \kappa\alpha H} \right\} \quad (35)$$

$$M_S = \frac{P_0 H}{k^2} \left\{ (1-\xi) - \frac{\sinh \kappa\alpha H (1-\xi)}{\kappa\alpha H \cosh \kappa\alpha H} \right\} \quad (36)$$

Shears in the flexural and shear-flexural cantilevers, S_B and S_S :

$$S_B = P_0 \left\{ \frac{k^2-1}{k^2} + \frac{\cosh \kappa\alpha H (1-\xi)}{k^2 \cosh \kappa\alpha H} \right\} \quad (37)$$

$$S_S = \frac{P_0}{k^2} \left\{ 1 - \frac{\cosh \kappa\alpha H (1-\xi)}{\cosh \kappa\alpha H} \right\} \quad (38)$$

Distributed loads on the flexural and shear-flexural cantilevers, q_B and q_S :

$$q_B = -q_S = \frac{P_0}{k^2 H} \frac{\kappa\alpha H \sinh \kappa\alpha H (1-\xi)}{\cosh \kappa\alpha H} \quad (39)$$

2. **Triangularly Distributed Lateral Load of Maximum Intensity q_0 at the Top**

Deflection y :

$$y = \frac{q_0 H^4}{EI} \left\{ \frac{k^2-1}{120k^2} (\xi^5 - 10\xi^3 + 20\xi^2) + \frac{1}{2k^2(k\alpha H)^2} \left(\xi - \frac{\xi^3}{3} \right) - \frac{\xi}{k^2(k\alpha H)^4} \right. \\ \left. + \frac{\cosh k\alpha H \xi + (k\alpha H/2 - 1/k\alpha H) [\sinh k\alpha H(1-\xi) - \sinh k\alpha H] - 1}{k^2(k\alpha H)^4 \cosh k\alpha H} \right\} \quad (40)$$

Interactive force flow q :

$$q = \frac{q_0}{k^2} \left\{ \xi - \frac{\cosh k\alpha H \xi + (k\alpha H/2 - 1/k\alpha H) \sinh k\alpha H(1-\xi)}{\cosh k\alpha H} \right\} \quad (41)$$

Moments in the flexural and shear-flexural cantilevers, M_B and M_S :

$$M_B = q_0 H^2 \left\{ \frac{(k^2-1)(\xi^3 - 3\xi + 2)}{6k^2} - \frac{\xi}{k^2(k\alpha H)^2} \right. \\ \left. + \frac{\cosh k\alpha H + (k\alpha H/2 - 1/k\alpha H) \sinh k\alpha H(1-\xi)}{k^2(k\alpha H)^2 \cosh k\alpha H} \right\} \quad (42)$$

$$M_S = q_0 H^2 \left\{ \frac{\xi^3 - 3\xi + 2}{6k^2} + \frac{\xi}{k^2(k\alpha H)^2} \right. \\ \left. - \frac{\cosh k\alpha H + (k\alpha H/2 - 1/k\alpha H) \sinh k\alpha H(1-\xi)}{k^2(k\alpha H)^2 \cosh k\alpha H} \right\} \quad (43)$$

Shears in the flexural and shear-flexural cantilevers, S_B and S_S :

$$S_B = q_0 H \left\{ \frac{k^2-1}{2k^2} (1-\xi^2) + \frac{1}{k^2(k\alpha H)^2} \right. \\ \left. - \frac{\sinh k\alpha H \xi - (k\alpha H/2 - 1/k\alpha H) \cosh k\alpha H(1-\xi)}{k^2 k\alpha H \cosh k\alpha H} \right\} \quad (44)$$

$$S_S = q_0 H \left\{ \frac{1}{2k^2} (1-\xi^2) - \frac{1}{k^2(k\alpha H)^2} \right. \\ \left. + \frac{\sinh k\alpha H \xi - (k\alpha H/2 - 1/k\alpha H) \cosh k\alpha H(1-\xi)}{k^2 k\alpha H \cosh k\alpha H} \right\} \quad (45)$$

Distributed loads on the flexural and shear-flexural cantilevers, q_B and q_S :

$$q_B = \frac{q_0}{k^2} \left\{ (k^2 - 1)\xi + \frac{\cosh k\alpha H \xi + (k\alpha H/2 - 1/k\alpha H) \sinh k\alpha H (1 - \xi)}{\cosh k\alpha H} \right\} \quad (46)$$

$$q_S = \frac{q_0}{k^2} \left\{ \xi - \frac{\cosh k\alpha H \xi + (k\alpha H/2 - 1/k\alpha H) \sinh k\alpha H (1 - \xi)}{\cosh k\alpha H} \right\} \quad (47)$$

